PICES Scientific Report No. 17
2001

PICES-GLOBEC INTERNATIONAL PROGRAM ON CLIMATE CHANGE AND CARRYING CAPACITY

REPORT OF THE 2000 BASS, MODEL, MONITOR AND REX WORKSHOPS, AND THE 2001 BASS/MODEL WORKSHOP

Edited by

Gordon A. McFarlane (BASS), Bernard A. Megrey (MODEL),
Bruce A. Taft (MONITOR) and William T. Peterson (REX)

August 2001
Secretariat / Publisher
North Pacific Marine Science Organization (PICES)
c/o Institute of Ocean Sciences, P.O. Box 6000, Sidney, B.C., Canada. V8L 4B2
E-mail: secretariat@pices.int Home Page: http://www.pices.int

TABLE OF CONTENTS

EXECUTIVE SUMMARY

This volume summarizes the results of the activities in 2000 by the four Task Teams of the PICES-GLOBEC Climate Change and Carrying Capacity Program. The activities reported here include the BASS, MODEL, MONITOR and REX Workshops at the PICES Ninth Annual Meeting in Hakodate, Japan (October 2000), and the joint BASS/MODEL Workshop in Honolulu, U.S.A. (March 2001).

The BASS Workshop on "The development of a conceptual model of the Subarctic Pacific basin ecosystems" discussed the possibility of applying ECOPATH/ECOSIM to the modeling of subarctic gyre ecosystems, based on presentations, the extended abstracts of which appear in the report. The workshop participants recognized that the Program has now entered its synthesis phase and the role of modeling has become more important. They have recommended convening a joint BASS/MODEL Workshop to examine the feasibility of using ECOPATH/ECOSIM as a tool to model higher trophic level components of the subarctic gyre ecosystems. This joint workshop on "Higher trophic level modeling" was held March 2001, in Honolulu. The initial eastern- and western- subarctic gyre ecosystem models were reviewed and existing data used for each model were noted. The workshop found considerable room for improving the estimates that can be accomplished by improvement of input data quality.

The MODEL Workshop on "Strategies for coupling higher and lower trophic level marine ecosystem models" discussed the strategic considerations necessary in coupling higher and lower trophic level marine ecosystem models and the extension and improvement of the prototype lower trophic level PICES NEMURO Model. The workshop reported these strategies in the form of workshop recommendations, which can be re-organized and re-stated in the future workplan of the CCCC Program for integration. The workshop report also contains abstracts, extended abstracts, and fully prepared reports presented at the workshop.

The MONITOR Workshop on "Progress in monitoring the North Pacific" reviewed ongoing and/or planned monitoring programs in North Pacific and made a number of pertinent recommendations. The summary of the workshop is followed by extended abstracts of papers given at the meeting.

The REX Workshop on "Trends in herring populations and trophodynamics" summarized generalizations, observations and hypotheses on herring populations and identified the need to add F (fish) into the current crop of NPZ (Nutrients - Phytoplankton - Zooplankton) models that are now available.

The four Task Teams are coordinating their activities in order to reach their goal, namely to answer the scientific questions addressed to the Program and to develop the ecosystem-monitoring program as an output of the Program. The final recommendations from each of these Task Teams can be found in the PICES Annual Report 2000.

Makoto Kashiwai and David W. Welch
CCCC-IP Co-Chairmen

BASS WORKSHOP ON THE DEVELOPMENT OF A CONCEPTUAL MODEL OF THE SUBARCTIC PACIFIC BASIN ECOSYSTEMS

(Co-convenors: Gordon A. McFarlane, Richard J. Beamish, Akihiko Yatsu and Andrei S. Krovnin)

At the PICES Sixth Annual Meeting, the BASS Task Team sponsored a symposium on the Ecosystem dynamics of the eastern and western subarctic gyres. The purpose was to bring together available information on the two gyres in a comparative framework. Topics included: 1) ocean responses to climate forcing, 2) nutrients and primary production, 3) structure of the lower trophic levels, the mesozooplankton communities, and the epipelagic nekton, 4) the role of midwater fishes, and 5) the importance of these areas to marine birds and mammals. Papers presented at the meeting were published in 1999, in a Progress in Oceanography special issue entitled *Ecosystem Dynamics in the Eastern and Western gyres of the Subarctic Pacific* (Guest Editors: R.J. Beamish, S. Kim, M. Terazaki and W.S. Wooster). The following "key" research problems were pointed out during discussion at the symposium: 1) the need for information on short-term or seasonal changes in the mixed layer, 2) how climate-variation may be changing the stability of the water column, 3) the role of iron: understanding transport mechanisms, 4) community dynamics and the need for small scale diet studies, and 5) biomass estimates of some "key" species.

Members of BASS Task Team felt that the next step should be to develop a conceptual model of the subarctic Pacific basin ecosystems and begin to examine appropriate models. A 2-day BASS Workshop on this topic was convened prior to the Ninth Annual Meeting in Hakodate, Japan (October 20-21, 2000). The objective of this workshop was to identify appropriate approaches, not only modelling approaches but also how to develop studies which will answer some of the questions.

At the workshop, a number of presentations were made on ecosystem models that participants had used. These models were reviewed and discussed with respect to their utility for gyre systems. Trophodynamic linkages that were likely to be common, as well as those that were model-specific, were identified, and shortfalls were highlighted. Discussions included identifying data groups and potential data sources, incorporating climate and oceanographic change in models, and linking gyre models to coastal area models. The following section contains extended abstracts of papers given at the workshop.

Investigating ecosystem dynamics with ECOPATH/ECOSIM

Jeffrey J. Polovina
Honolulu Laboratory, SWFRC, Honolulu, HI 96822-2396, U.S.A. E-mail: Jeffrey.Polovina@noaa.gov

Two applications of the ECOPATH/ECOSIM modelling approach are presented. The first constructs an ECOPATH model of the central North Pacific pelagic ecosystem, using ECOSIM to investigate the response of the ecosystem to fishing impacts. The ECOPATH model is highly resolved at the top trophic levels including species groups for each of the principal fishery target species as well as fishery impacts of 6 types of fishing gears. The ECOPATH model was used in the dynamic ECOSIM to simulate the response of the pelagic ecosystem to an elimination of all fishing: a return of the ecosystem to the early 1900s. The ECOSIM model simulation found all the fished species increased in the absence of fishing but a number of prey species including squid, flying fish and lancet fish, decreased as their predators increased. Furthermore, for the top trophic level species, large sharks and blue marlins, their biomass increased more than all other fished species because they benefited from both an absence of fishing as well as an increase in

their prey, small tunas and billfishes, species which increased in biomass when fishing was halted.

A second application of these models was a bottom-up simulation. An eastern tropical Pacific pelagic ecosystem model was constructed and used to simulate the ecosystem response to changes in ENSO periodicity and cadence, and long-term global warming. The ENSO impacts were simulated by changing the phytoplankton availability in the ECOSIM model. An El Niño was simulated by a 30% drop in phytoplankton during one year and a La Niña was simulated with a 30% increase in phytoplankton for one year. The global warming scenario was simulated by using predicted changes in SST from a 100-year global warming modelling exercise. The predicted eastern tropical Pacific SST was converted into phytoplankton biomass with an empirical relationship between these parameters for the eastern tropical Pacific. The ECOSIM results found that bottom-up forcing propagates through the 6 trophic levels of the ecosystem with time lags and amplitude of the forcing which varies by species and can be greater or weaker than the initial forcing. Changing the ENSO period results in modest changes in trophic transfer and ecosystem structure. For example, less energy reaches the top of the ecosystem when El Niño events occur every 2 years compared to every 6 years. However, the global warming scenario which predicted warming of SST, an increased vertical stratification and hence reduced phytoplankton in the eastern tropical Pacific, was simulated by the ECOSIM model to result in a substantial decrease in the entire ecosystem biomass at all trophic levels.

These and other experiences with ECOPATH and ECOSIM suggest that these models are useful tools to investigate the responses of complex ecosystems to both top-down and bottom-up forcing. However, issues remain regarding how well the models capture the complexity of actual ecosystem dynamics. More evaluations of model results with actual ecosystem dynamics are needed. There is a considerable literature on applications of these approaches and a web site "www.ecopath.org" which serves as a source for the programs and related literature.

ECOPATH as a potential tool for modeling the North Pacific Gyre ecosystems

Kerim Y. Aydin
Alaska Fisheries Science Center, NMFS, Seattle, WA 98115 U.S.A. E-mail: Kerim.Aydin@noaa.gov

The subarctic North Pacific oceanic gyres contain highly productive pelagic ecosystems. These waters have been subject to past fisheries and are important rearing areas for Pacific salmon (*Oncorhynchus* spp.), marine mammals and commercially harvested squid. Furthermore, the species of the region responds to oceanographic signals on the order of decades, and thus they present a case study for the interactions between climate and marine ecology. However, the ecosystems of these regions are poorly understood, in part due to the difficulty of obtaining consistent data across such large systems.

Extensive biological data exist for these regions and have been gathered by PICES member countries. It would be extremely useful to assemble these data to provide a meaningful quantification of ecosystem structure and function. To this end, the software package ECOPATH may be a useful tool, as it helps researchers in modeling oceanic food webs, and provides a meaningful context for comparing estimates of biological production across species and regions.

ECOPATH is simply a tool for comparing independent estimates of biomass, production, consumption and diet, migrations, and fisheries catch of the important players in a food web. Such comparisons help determine:

- if available estimates are consistent between species;
- the relative importance of species or guilds within an ecosystem; and

- how targeting increased research effort on critical, keystone species might aid in improving our understanding of the system's structure and function.

In cases where two similar ecosystems are to be compared, such as with the eastern and western subarctic gyres, ECOPATH provides a quantitative basis for comparison.

Creating an ECOPATH model should be a strongly collaborative process among participating scientists. The framework of ECOPATH lends itself to an iterative peer-review process between the primary modelers, the data collectors, and the wider scientific community. There are five main steps in creating a model:

- determining the model framework;
- assembling and documenting the initial data;
- assessing the data in preliminary models;
- peer-review of data and preliminary models;
- use of models to test hypotheses.

Determining the model framework To set up a modeling effort, the boundaries, time period, time step, species of interest, and important hypotheses for the system must be identified. While these identifications may change as the model develops, it is important to have some preliminary framework to aid in collecting data. This stage may also identify key data sources and providers. Generally this task may be completed in a series of discussions over a short time period.

Assembling and documenting the initial data Data assembly and documentation may take from weeks to months depending on the ecosystem in question. This process may involve contacting researchers in many institutions to provide data to a central source. At the same time, the quality of the data may be assessed and adjustments made to the model framework if necessary.

Assessing the data in preliminary models The initial assembly of data for an ECOPATH model is best conducted in a workshop setting with a limited number of participants who are familiar with aspects of the data. The purpose of such a workshop is to view the pieces of data as a whole for the first time, and make preliminary judgements on the quality of the data and the usefulness of the model. At this stage, plans may be made to revisit hypotheses or attempt to refine data estimates.

Peer-review of data and preliminary models After an initial workshop, participants should be able to show the initial model to a wider community over a period of months. This process allows additional input to be gathered to improve the model. Successive iterations of data exchange during this period will substantially improve the model. In addition, the model may be used to direct further data collection.

Use of models to test hypotheses When the peer-review process has reached the larger research community, the models may be distributed and used to compare the relative roles of anthropogenic effects, predator-prey interactions, climate changes, or dynamic function of the ecosystem through a variety of modeling techniques.

ECOPATH, like all models, is a simplification of nature. However, the quantitative, iterative peer-review process has in many cases contributed to an increased understanding of the ecosystem's structure and function. Overall, ECOPATH is a powerful tool for assembling and synthesizing ecosystem data from disparate sources.

Modeling the western Bering Sea ecosystem with help of ECOPATH software

Victor V. Lapko, Elena P. Dulepova and Vladimir I. Radchenko
TINRO- Centre, Vladivostok, 690950, Russia. E-mail: interdept@tinro.wavenet.ru

The purpose of our presentation is to identify some methodological aspects substantially affecting, or even defining, the quantitative appearance of the model, and as a result the applied conclusions derived from the model. This modeling work was initiated by our colleagues from the National

Marine Fisheries Service (NOAA, U.S.A.) with the goal of constructing an ecosystem model of one of the major fishing area in the northern Pacific - Bering Sea. The co-operative project stipulated that with the help of the ECOPATH software, we should build a model of the western Bering Sea (WBS) in addition to one of the eastern Bering Sea (EBS) that had already been created by US scientists. Further they intended to combine both models into a general model describing the whole Bering Sea ecosystem.

Following accepted rules, we built a WBS ecosystem model for the 1980s. During that decade TINRO-Centre carried out large-scale investigations of marine biota and collected numerous data on diverse species and groups of pelagic and demersal taxa. Those data allowed tracing seasonal and interannual dynamics of species abundance, distribution, migrations, feeding etc. This information became a base for our model.

The entire Russian EEZ in the western Bering Sea was used as the model area. It covers a total of 702,200 km^2 and encompasses a wide range of marine habitats including shelf, slope and deep basins, but it was treated as a single homogenous region in the model. To describe the WBS ecosystem, we separated all taxa into 48 functional groups, composed of a single species or an aggregation of ecologically similar species, covering all trophic levels from phytoplankton to marine birds and mammals. The model uses annual averages, i.e. all necessary data on abundance and feeding collected in various habitats were combined proportionally to the areas of those habitats and averaged seasonally and annually to provide year-round annual average characteristics, which were entered into the two main tables (basic input and diet composition). Commercial fishery catch was also included into the model. Furthermore our model was balanced and we have compared the results obtained in the WBS and EBS (Trites *et al*. 1999). Comparison was particularly interesting because both models are composed of a very similar list of functional groups and relate to the same time period. Results are presented in Table 1.

Total biomass in the WBS ecosystem was 1.75 times higher than in the EBS, while other important ecological indices differed in even greater proportions. For example, the sum of all biological production was 4 times higher, the sum of all consumption - 2.7 times, the sum of all flows into detritus - almost by order of magnitude greater and total system throughput - 4.5 times

Table 1 Descriptive summary statistics for the eastern (EBS), western (WBS) and partially changed (WBS^1) Bering Sea ecosystem models in the 1980s.

Parameters\model	EBS	WBS	WBS^1
Sum of all consumption	3073.72	8318.623	6445.045
Sum of all exports	2.62 (?)	5194.181	699.061
Sum of all respiratory flows	1620.43	2450.86	2600.98
Sum of all flows into detritus	994.99	9593.33	2984.748
Total system throughput	5691.76	25557	12730
Sum of all production	2612.84	10234	4752
Mean trophic level of the catch	3.3	3.6	3.6
Gross efficiency (catch/net p p.)	0.0021	0.000124	0.000286
Calculated total net primary production	1920	7645	3300
Total primary production/total respiration	0.78	3.119	1.269
Net system production	356.43	5194.14	699.02
Total primary production/total biomass	4.94	17.109	7.385
Total biomass/total throughput	0.045	0.017	0.035
Total biomass (excluding detritus)	255.95	446.846	446.846
Total catches	2.62	0.945	0.945
Connectance Index	0.3	0.168	0.168
System Omnivory Index	0.157	0.203	0.209

higher in the WBS. At the same time, the WBS ecosystem was exploited much less - gross efficiency was almost 20 times lower compared to the EBS. Judging from these statistics in the 1980s, the WBS ecosystem functioned much more intensively but less efficiently compare to the EBS. However, it should be remembered that the EBS is generally warmer and shallower than the WBS, and therefore we might have expected the opposite situation. What is the reason? We assume that the main reason lies in higher average ecological characteristics, and first of all in the values of production/biomass (P/B) and consumption/biomass (Q/B) ratios, we have applied to describe some functional groups of species in the WBS ecosystem.

Table 2 P/B and Q/B values applied in the WBS (above slash) and EBS (below slash) models.

Group name	P/B	Q/B
Phytoplankton	139 / 60	-
Copepods	9.5 / 6.0	26.2 / 22.0
Euphausiids	3.13 / 5,5	17.0 / 22.0
Amphipods	2.5 / 3.5	14.0 / 22.0
Herring	0.7 / 1.0	14.6 / 3.65
Cod	0.52 / 0.40	3.3 / 2.04
Yellowfin sole	0.26 / 0.40	9.8 / 2.96
Rock sole	0.24 / 0.40	6.5 / 3.6
Halibut	0.25 / 0.40	3.5 / 2.49
Juv. pollock	2.5 / 2.5	13.0 / 8.3
Adult pollock	0.5 / 0.5	10.0 / 2.64
Steller sea lion	0.06 / 0.06	18.0 / 12.7
Toothed whales	0.02 / 0.02	17.5 / 13.11

As follows from Table 2, the annual Q/B values, which were defined for the WBS, are substantially higher in higher trophic level groups (pollock and herring are particularly indicative) and lower – in lower trophic level groups, compare to the EBS. Another important difference is in P/B ratios of phytoplankton (see Table 2). Apparently application of all these values caused the aforementioned differences between the models. To test this assumption we have entered into the WBS ecosystem model P/B and Q/B ratios from the EBS one, keeping biomass and diet composition unchanged. Although the resulting model was found to be slightly unbalanced, the descriptive statistics, as we expected, had intermediate values between both original models (Table 1, last column).

Thus, the values of the such important ecological parameters as P/B and Q/B ratios, entered into the model, are crucial for its resulted appearance, features, further simulation of commercial exploitation rate and final conclusion. It is difficult to imagine that trophic and productive characteristics of the same taxa differ by several times in the same biogeographical area. Of course, the some differences should take place due to various size-age composition of populations, food conditions, general temperature of environment, etc., however, we presume they are not so drastic.

It is quite possible that the ECOPATH software will be accepted as a standard tool for modeling of ecosystems in diverse Pacific areas. Pacific waters are inhabited by various fauna, but there are no doubt that almost everywhere predominating species and groups of species will coincide in high extent, especially for adjacent areas. Thus, it would be very useful for future modeling efforts to compare and discuss methodical approaches for determining the most important ecological parameters of common species and groups in the northern Pacific.

Changes in the Strait of Georgia ECOPATH model needed to balance the abrupt increases in productivity that occurred in 2000

Richard J. Beamish, Gordon A. McFarlane, C.M. Neville and I. Pearsall
Pacific Biological Station, Nanaimo, B.C., Canada. V9R 5K6 E-mail: beamishr@pac.dfo-mpo.gc.ca

ECOPATH is a trophic accounting model that is a practical way of studying the interactions of all species in an ecosystem. We used ECOPATH to study the dynamics of the Strait of Georgia ecosystem (area: 6,900 km^2), located between Vancouver Island and the British Columbia mainland. The Strait of Georgia is probably the most important marine ecosystem on Canada's west

Table 3 Functional groups, biomass, production/biomass and consumption/biomass values used in the Strait of Georgia model and resulting ecotrophic efficiencies.

Functional Group	Biomass (t/km^2) 1998	2001	Production/Biomass (t/year)	Consumption/Biomass (t/year)	Ecotrophic Efficiency 1998	2001
Phytoplankton	36.000	72.000	130.000		0.992	0.912
Kelp/Sea Grass	23.300	23.300	34.000		0.280	0.559
Herbiverous zooplankton	25.000	50.000	20.000	80.000	0.892	0.647
Neocalanus plumchrus	25.000	40.000	20.000	80.000	0.909	0.796
Pseudocalanus minutus	10.000	20.000	20.000	80.000	0.878	0.668
Shellfish	60.000	90.000	3.000	12.000	0.569	0.636
Crab	4.000	8.000	3.500	14.000	0.671	0.461
Grazing invertebrates	40.000	90.000	3.000	12.000	0.729	0.493
Carniverous zooplankton	40.000	50.000	5.000	20.000	0.581	0.912
Euphausiid	80.000	160.000	3.000	12.000	0.755	0.581
Predatory invertebrate	25.000	25.000	5.000	20.000	0.293	0.488
Shorebirds	0.005	0.005	0.100	5.000	0.000	0.000
Herring	9.000	13.000	3.000	12.000	0.787	0.886
Small Pelagics	15.000	40.000	2.000	8.000	0.770	0.704
Lampetra ayresi	0.020	0.020	2.000	8.000	0.782	0.782
Seabirds	0.018	0.018	0.100	5.000	0.009	0.009
Gulls	0.004	0.004	0.100	12.500	0.000	0.000
Misc. demersal fish	20.000	50.000	2.100	8.400	0.431	0.412
Chum	1.000	2.000	2.000	8.000	0.398	0.364
Coho	1.000	2.000	3.000	12.000	0.361	0.357
Chinook	1.000	2.000	2.000	8.000	0.445	0.421
Toothed Whales	0.003	0.003	0.020	0.400	0.000	0.000
Hake	10.000	14.000	0.600	2.400	0.559	0.783
Dogfish	4.500	4.500	0.100	1.000	0.052	0.052
Lingcod	0.350	0.350	0.500	2.000	0.114	0.114
Pollock	2.000	2.000	0.600	2.400	0.124	0.206
Leuroglossus	0.200	0.400	2.000	8.000	0.660	0.342
Yelloweye	0.500	0.500	0.200	2.000	0.070	0.070
English Sole	1.000	1.000	0.180	0.720	0.034	0.034
Sea Lions	0.020	0.020	0.180	21.600	0.013	0.013
Seals	0.050	0.050	0.125	15.510	0.028	0.028
Detritus	38.700	38.700			0.572	0.529

coast, as much of the population of British Columbia lives within 10 km of its shores and it is a key rearing area for Pacific salmon, herring, and other species.

Our ECOPATH model has 32 functional groups. We estimated the biomass, production/ biomass ratios, consumption/biomass rates, and diet compositions for each functional group. We used a number of references and the unpublished results of our own studies over the past 26 years to estimate these data. An important estimate for the lower trophic levels was the hydroacoustic estimate of euphausiids made in 1999 and 2000 (Pearsall *et al*. 2001). The two dominant fish species in the Strait of Georgia are Pacific hake and Pacific herring. Reliable biomass estimates existed for both of these species (McFarlane *et al*. 2000; Schweigert and Fort 2000). Pacific salmon are both abundant as juveniles and important commercially, culturally, and politically. In recent years, juvenile salmon have reared in the Strait of Georgia longer than in the past, but adult coho were virtually absent. Chinook of larger sizes and ocean ages greater than age 0 remained in the Strait but their abundance was much lower in the late 1990s than in the 1970s and 1980s.

Table 4 Diet matrix in the models.

Prey/Predator	3	4	5	6	7	8	9	10	11	12	13	14	15	16	17	18	19	20	21	22	23	24	25	26	27	28	29	30	31
Phytoplankton	0.700	0.700	0.700	0.579	0.002	0.176		0.809			0.020	0.005				0.005	0.005	0.005	0.005		0.005			0.010	0.020				
Kelp/Sea grass				0.100	0.100	0.300								0.010															
Herb. zooplankton				0.030	0.060	0.050	0.359	0.050	0.065		0.050	0.100				0.040	0.120	0.200	0.100		0.020	0.010		0.010	0.310	0.001	0.011		
N. plumchrus				0.050	0.020	0.050	0.404		0.050		0.150	0.150				0.051	0.050	0.050	0.030		0.020	0.010	0.001	0.030	0.300	0.001	0.011		
P. minutus				0.020	0.020	0.050	0.102		0.050		0.100	0.070				0.050	0.050	0.050	0.030		0.010	0.010	0.001	0.020	0.150				
Shellfish				0.010	0.150		0.030	0.001	0.055	0.115	0.001	0.030		0.350	0.150	0.172	0.020	0.020	0.040		0.030	0.050	0.038	0.001	0.001	0.001	0.030		
Crab				0.001	0.010		0.002		0.010		0.001	0.010		0.005			0.005	0.005	0.005		0.001	0.010							
Grazing invertebrates					0.200		0.003		0.100	0.500	0.010	0.050		0.090	0.020	0.090	0.095					0.150			0.056		0.130		
Carn. zooplankton							0.050				0.084	0.264		0.080		0.154	0.100	0.145	0.255		0.163	0.110		0.090	0.050				
Euphausiid									0.111		0.580	0.150		0.080		0.100	0.300	0.300	0.220		0.700	0.080	0.030	0.668	0.102				
Predatory invertebrate									0.036	0.200		0.050		0.090	0.030	0.040	0.150	0.150	0.150	0.040	0.005	0.235	0.051	0.050		0.200	0.100	0.020	
Shorebirds																													
Herring									0.022	0.020	0.001	0.020	0.640	0.050	0.069	0.030	0.030	0.030	0.135	0.252		0.020	0.243	0.050		0.100		0.300	0.231
Small pelagics									0.001	0.050	0.002	0.100	0.199	0.080	0.020	0.050	0.005	0.005	0.005	0.164	0.040	0.042	0.100	0.010	0.010	0.200	0.250	0.113	0.100
Lampetra ayresi															0.001							0.005	0.010					0.004	
Seabirds																				0.014									
Gulls																													
Misc. demersal fish														0.050		0.100				0.064		0.010	0.391			0.446	0.418	0.225	0.175
Chum										0.020		0.001	0.053	0.001	0.010	0.001		0.010	0.010	0.025	0.001	0.055	0.020					0.010	0.010
Coho													0.051			0.004		0.002	0.002	0.032	0.001	0.070	0.020					0.011	0.008
Chinook													0.051	0.003		0.003		0.001	0.002	0.158	0.001	0.070	0.005					0.005	0.005
Toothed whales																													
Hake											0.001		0.001	0.020		0.010	0.040	0.027	0.001	0.064		0.056	0.050	0.010	0.001	0.050	0.050	0.300	0.464
Dogfish																						0.005							0.001
Lingcod																							0.028					0.001	
Pollock													0.005						0.010	0.001	0.002	0.001	0.001	0.001				0.011	0.006
Leuroglossus																					0.001			0.050					
Yelloweye																							0.010						
English sole																						0.001	0.001			0.001			
Sea Lions																				0.040									
Seals																				0.146									
Detritus	0.300	0.300	0.300	0.210	0.438	0.374	0.050	0.140	0.500	0.095				0.091	0.700	0.100	0.030												
Sum	1.000	1.000	1.000	1.000	1.000	1.000	1.000	1.000	1.000	1.000	1.000	1.000	1.000	1.000	1.000	1.000	1.000	1.000	1.000	1.000	1.000	1.000	1.000	1.000	1.000	1.000	1.000	1.000	1.000

In this report, we model two ecosystem states: one in 1998 and one in 2001. We show that the increase in production that occurred in 2000 had a major impact on the dynamics of the trophic relationships in the Strait of Georgia in 2001. The increase in productivity in 2000 probably resulted from a change in the climate and a corresponding change in the oceanography.

The 1998 model (Table 3) assumed a biomass of phytoplankton of 36 t/km^2 and a production/ biomass ratio of 130. The model was balanced with 99.2% of the phytoplankton production being consumed by higher trophic levels. On average, over 90% of the production of the four herbivorous zooplankton groups (euphausiids, *P. minutus*, *N. plumchrus* and other herbivorous zooplankton) was consumed by higher trophic levels. Carnivorous zooplankton (amphipods) contributed 58.1% of its production to higher trophic levels. The biomass of Pacific hake was 10 t/km^2. The major items in the hake diet were euphausiids (70%) and carnivorous zooplankton (16%). Diet composition for the models are summarized in Table 4. Although adult hake fed on juvenile hake and herring in the past, we have not found fish remains in hake stomachs in the late 1990s. Pacific herring migrate out of the Strait of Georgia after about age 1, and return only to spawn in the winter in their third and subsequent years. We estimated that euphausiids made up 58% of their diet. Euphausiids were also an important prey for juvenile salmon, accounting for 22% to 30% of their diet. Another major fish species in the model was spiny dogfish. Dogfish are omnivorous, but grow only a few mm/year, thus their consumption is small relative to their biomass. The model balanced for 1998 indicated that 75.5% of the euphausiids were consumed by higher trophic levels.

The hydroacoustic study indicated that there was 109.7 t/km^2 and 227.5 t/km^2 of euphausiids in the Strait of Georgia in September/October 1999 and 2000, respectively. The biomass estimates in Pearsall *et al*. (2001) were modified for our ECOPATH model to approximate our interpretation of their life history. The maximum biomass of euphausiids in the Strait of Georgia occurs late in the year and the minimum biomass about June. The life span exceeds one year thus the P/B will be lower than other groups of zooplankton. Therefore, we estimated the annual biomass to be 80 t/km^2 in 1998 and 160 t/km^2 in 2001. A variety of scenarios would be possible to balance the 2001 model with the increased euphausiid production, but all scenarios would indicate a substantial increase in the biomass of a number of functional groups. The addition of the biomass of euphausiids used in the 2001 model into the 1998 model resulted in 37.8% of the production being consumed by predators and an imbalance of 115.8% of the phytoplankton production. Because euphausiids feed primarily on phytoplankton, the increase in euphausiid abundance most likely was associated with an increase primary productivity. Such an increase would also benefit larval copepod survival. We balanced the 2001 model by increasing the biomass of these and other functional groups that would benefit directly or indirectly from increases

Table 5 Changes in the abundances of functional groups from the 1998 model to 2001 model, scaled to the impact of the euphausiid biomass increase.

Functional Group	1998 Biomass t/km^2	2001 Biomass t/km^2
Euphausiid	80.00	160.00
Phytoplankton	36.00	72.0
N. plumchrus	25.00	40.00
P. minutus	10.00	20.00
Shellfish	60.00	90.00
Crab	4.00	8.00
Grazing invertebrates	40.00	90.00
Carnivorous zooplankton	40.00	50.00
Small Pelagics	15.00	40.00
Miscellaneous Demersal Fish	20.00	50.00
Chum	1.0	2.0
Coho	1.0	2.0
Chinook	1.0	2.0
Hake	10.0	14.0
Herring	9.0	13.0
Herbiverous zooplankton	25.0	50.0
Leuroglossus	0.2	0.4

in euphausiid biomass (Table 3). We adjusted the biomass of species that might be directly affected by the increased productivity in the 2001 model (Table 3), but did not change the diets used in the 1998 model.

In our 2001 model, we assigned only 58.1% of the new euphausiid production to consumers, yet there were increases in biomass of 40% for herring and hake, 50% for shellfish, 100% for crab, chum, chinook and coho, 150% for miscellaneous demersal fish, and 267% for small pelagic fishes (Table 5). It is possible that these increases might take longer to develop, however, the model increases would be indicative of the possible changes in biomass. The changes in salmon abundance would be particularly important. In another study we are testing the hypothesis that salmon survival or production is a function of both predation and summer growth. If our hypothesis is correct, the improved summer growth in 2000 will increase marine survival, and the returns of coho and pink salmon in 2001 will be larger than previous years. We note that if the primary production remains at the 2000 level, there will be continued major changes in the ecosystem as higher trophic levels increase their biomass in response to the increases in prey.

References

Pearsall, I.A., Macaulay, M., Beamish, R.J., McFarlane, G.A., and Saxby, G. 2001. An abrupt doubling of euphausiids in the Strait of Georgia, British Columbia, Canada. Fisheries Oceanography (in preparation).

McFarlane, G.A., Beamish, R.J. and Schweigert, J. 2000. Common factors have opposite impacts on Pacific herring in adjacent ecosystems. Proc. Lowell Wakefield Symposium, Anchorage, AK (in press).

Schweigert, J., and Fort, C. 2000. Stock assessment for British Columbia herring in 1999 and forecasts of the potential catch in 2000. 96 p. Series Canadian Stock Assessment Secretariat Research Document; 99/178.

Simulating historical changes in the Strait of Georgia ecosystem using ECOPATH and ECOSIM

Steven J.D. Martell, Carl J. Walters, Alasdair Beattie, Tarun Nayar and Robyn Briese
UBC Fisheries Centre, Vancouver, B.C., Canada. V6T 1Z4 E-mail: smartell@fisheries.com

The Strait of Georgia (SOG) ecosystem has been heavily exploited for the last 90 years and development in commercial fisheries has shifted the focus from top predators in the ecosystem to more abundant lower trophic level species (Wallace 1998). This phenomenon is known as "fishing down food webs" (Pauly *et al*. 1998; Pauly *et al*. 2000). Salmon fisheries were by far the most important fishery in the early years of fishing development, and by 1897, British Columbia was canning more than 1 million cases of salmon a year (Lichatowich 1999). Both chinook and coho salmon have been heavily exploited in the SOG by the commercial net and troll fisheries, and by sports fisheries (DFO 1999a; DFO 1999b). With almost all SOG coho stocks in jeopardy, a coastwide closure for all coho fisheries was implemented in 1998, with the exception of a sports fishery for hatchery fish at the mouth of the Capilano River.

As fishing technologies improved, herring fisheries and groundfish fisheries grew rapidly in the 20th century, with precipitous results. By the early 1960s, herring stocks were being harvested at unsustainable rates and the fishery collapsed in 1967 (Stocker 1993). Since this time, however, herring stocks have recovered to near historically high levels (Schweigert *et al*. 1998). Prior to 1970, herring were mainly used for fishmeal, but after the collapse, a more valuable roe fishery was developed. Groundfish such as lingcod and several rockfish species were also heavily exploited in the 1900s, and with the introduction of trawl fisheries to the SOG in 1943, exploitation rates rose dramatically (Cass *et al.* 1990; Martell

1999). Invertebrate fisheries have existed in the SOG for the last 100 years, however, until the 1950s the fisheries were mainly focused on dungeness crabs and manilla clams (an exotic species). Since the 1950s, there have been developments in shrimp fisheries, geoduck clams, sea urchin, sea cucumbers and octopus fisheries (Ketchen *et al*. 1983).

Stock assessment reports have attributed the observed declines in abundance to factors other than overfishing. In fact, more attention has been spent on trying to explain environmental processes that may have led to a reduction in marine survival rates in salmon (Beamish and Bouillon 1995), or changes in food availability associated with changes in physical properties (Robinson 1999). At this time, the occurrence of a "regime shift", or long-term changes in primary productivity in the Pacific Ocean (Beamish *et al.* 1999), is postulated as the major factor leading to abundance declines in the SOG.

An obvious, but often unresolved, issue is the role of trophic interactions in suppressing recruitment or indirectly changing natural mortality rates (generally assumed to be constant). Among fisheries scientists and academia, there is a growing consensus that we can no longer forge ahead and exploit a resource without considering trophic interactions at an ecosystem scale (Walters *et al.* 1997). The majority of data available, however, are usually restricted to species of commercial importance. In the SOG alone for example, there are more than 250 different species of fish, but fisheries statistics are collected for less than 50 species coast-wide (vertebrate and invertebrate combined). Moreover, we have even less knowledge about the specific interactions among members in an ecosystem, a problem we are now forced to face.

The objective of this paper is to carry out a retrospective analysis of the Strait of Georgia ecosystem and use data from single species stock-assessment programs to determine if the observed data suggest that changes in primary productivity have occurred in the last 50 years. We address this issue by comparing reconstructed ecosystems from 1950 to 1998 using two scenarios: 1) assume that there has been no changes in relative primary productivity, and 2) estimate relative primary productivity regimes that would better explain the observed data. Finally, we compare the estimated primary productivity regimes to environmental correlates, specifically wind speed squared (a measure of sheer stress), and the Pacific Decadal Oscillation.

Predicting biomass dynamics using ECOPATH with ECOSIM

The trophic mass-balance model used in ECOPATH uses a set of simultaneous linear equations that assumes the production of group i is equal to the consumption of group i by all predators j, plus export and non-predation losses (including fisheries landings) of group i, over a specified time period. This function is generally expressed as:

Equation 1

$$B_i \cdot (P/B)_i \cdot EE_i = Y_i + \sum_{j=1}^{n} B_j \cdot (Q/B)_j \cdot DC_{ji}$$

Where B_i is the biomass of group *i*, $(P/B)_i$ is the production biomass ratio of group *i*, $(Q/B)_j$ is the consumption biomass ratio of group *j* (predators of group *i*), and DC*ji* is the average diet fraction of prey *i* for group *j*. EE_i is the ecotrophic efficiency, or the fraction of production that is consumed within the system, including fisheries yields (Y_i).

The following differential equation is used to predict dynamic changes in biomass and is dependent on whether the group is a primary producer or a consumer in the system:

Equation 2

$$dB_i / dt = f(B) - M_o B_i - F_i B_i - \sum_{j=i}^{n} c_{ij}(B_i, B_j)$$

Here $M_o = (1 - EE_i) * (PIB)_i$ represents the fraction of production that is unaccounted for (other mortality), F_i is the fishing mortality rate, and c_{ij} is a function used to predict consumption of group *i* by predator *j*, conditional on the interactions and abundance of the two groups (see Eqn. 4). For primary producers, a simple saturating function is used to predict biomass production:

Equation 3

$$f(B_i) = r_i B_i / (1 + B_i h_i) \qquad \text{(a)}$$

Whereas if group *i* is a consumer then

$$f(B_i) = g_i \sum_{j=1}^{n} c_{ji}(B_i, B_j) \qquad \text{(b)}$$

here g_i is the growth efficiency and must satisfy the relationship $B_i(P/B)_i = g_i \sum_j Q_{ji}$. Predicting consumption in ECOSIM stems from the "Foraging Arena" concepts proposed by Walters and Juanes (I993). At equilibrium the consumption of *i* by *j* is:

Equation 4

$$c_{ij}(B_i, B_j) = \frac{a_{ij} v_{ij} B_i B_j}{(2v_{ij} + a_{ij} B_j)}$$

In Equation 4, a_{ij} is the mass action consumption rate, and vij describes the exchange rate process from "available" to "unavailable" behavioural states. Using ECOPATH estimates (Q_{ij}, B_i, and B_j) the mass action consumption rate can be estimated by re-arranging Equation 4. Therefore, the only user specified parameter is the behavioural exchange rate parameter (v_{ij}). Equation 4 is structured such that consumption is dependent on both predator and prey biomass. If predator biomass is low then consumption reduces to a mass-action flow, and if predator biomass is high then consumption approaches a "donor control" rate represented by the behavioural exchange rate process v_{ij} (Walters *et al*. 1997; Walters *et al*. 2000). As v_{ij} approaches 1, the rate of predation is dependent on the biomass of the predator (top-down control), and as *v* approaches 0, prey spend a larger fraction of their time budget hiding from predators and predation is limited by biomass of prey in the system (bottom-up or donor control).

ECOSIM uses a Marquardt non-linear search algorithm with a trust region modification for each of the Marquardt steps to estimate relative forcing inputs and v_{ij}. To evaluate the differences between predicted and observed data, ECOSIM uses a log-least-squares criterion, which we refer to as SS fit to the data. We allow the search routine to estimate v_{ij} parameters and, when we assume there have been changes in relative primary production over time, a relative forcing time series that is applied to the primary production. Estimating v_{ij} is equivalent to estimating observation errors in a single species stock assessment approach, and the relative changes in primary production is equivalent to estimating process errors.

Changes in primary productivity

The observed time series data, shown as circles in Figures 1 and 2, are better explained when we assume that there have been substantial changes in primary productivity over the 50-year time series (also see Table 6). Under the constant primary production hypothesis the log sum of squares fit to the data was 115.87, and under a fluctuating primary production hypothesis the fit to the data was 75.24 (roughly a 35% reduction). The probability of this reduction in the SS by chance alone is 0.006, i.e. the observed data do suggest a change in primary productivity must have occurred. Under the constant primary production hypothesis, model biomass predictions generally agree with the observed data. However, it fails to capture recent observations in harbour seal abundance and southern resident killer whales. Marine survival rates for coho and chinook salmon have also declined through the 1990s, and a more parsimonious explanation is that there has been a severe decline in primary production starting around 1990 (Fig. 2).

The estimated changes in relative primary productivity are shown in Figure 3, and we compared this estimated index with other environmental correlates that are linked to primary production. We were unable to find any significant correlations between primary production and Fraser River discharge, wind speed, sea surface temperature, upwelling, or the Pacific Decadal Oscillation. However the overall downward trend in primary production is very similar to the downward trend observed in average wind speed squared (Fig. 4). The square of the wind speed is a measure of sheer stress between air and the water surface, which results in vertical mixing of the water column allowing entrainment of nutrients used in photosynthesis (Blackett, 1993). A similar downward trend is also observed in the Pacific Decadal Oscillation index (PDO).

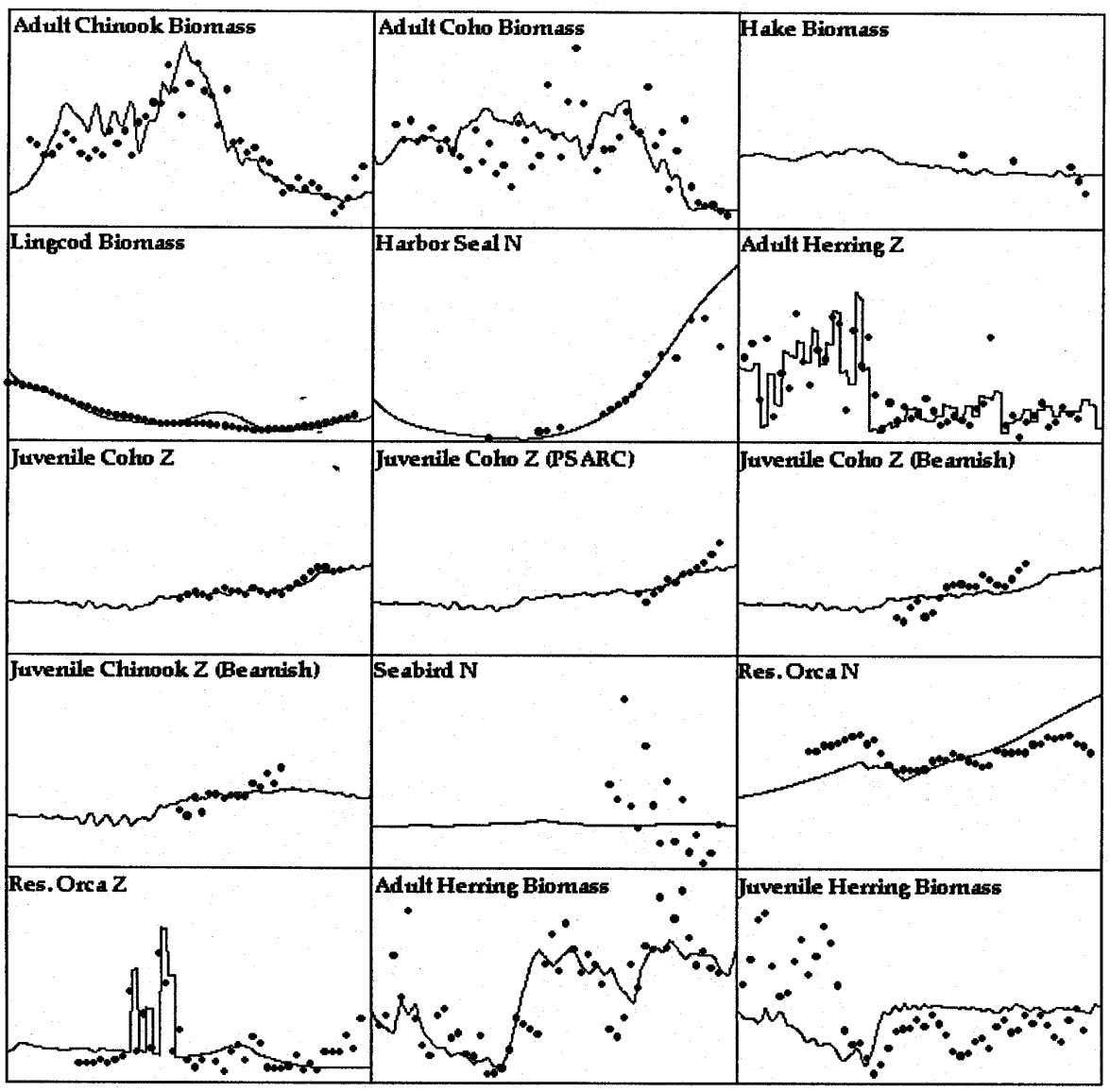

Fig. 1 Predicted and observed abundance and total mortality indices assuming the relative primary production has remained constant from 1950 to 1998. SS=115.87.

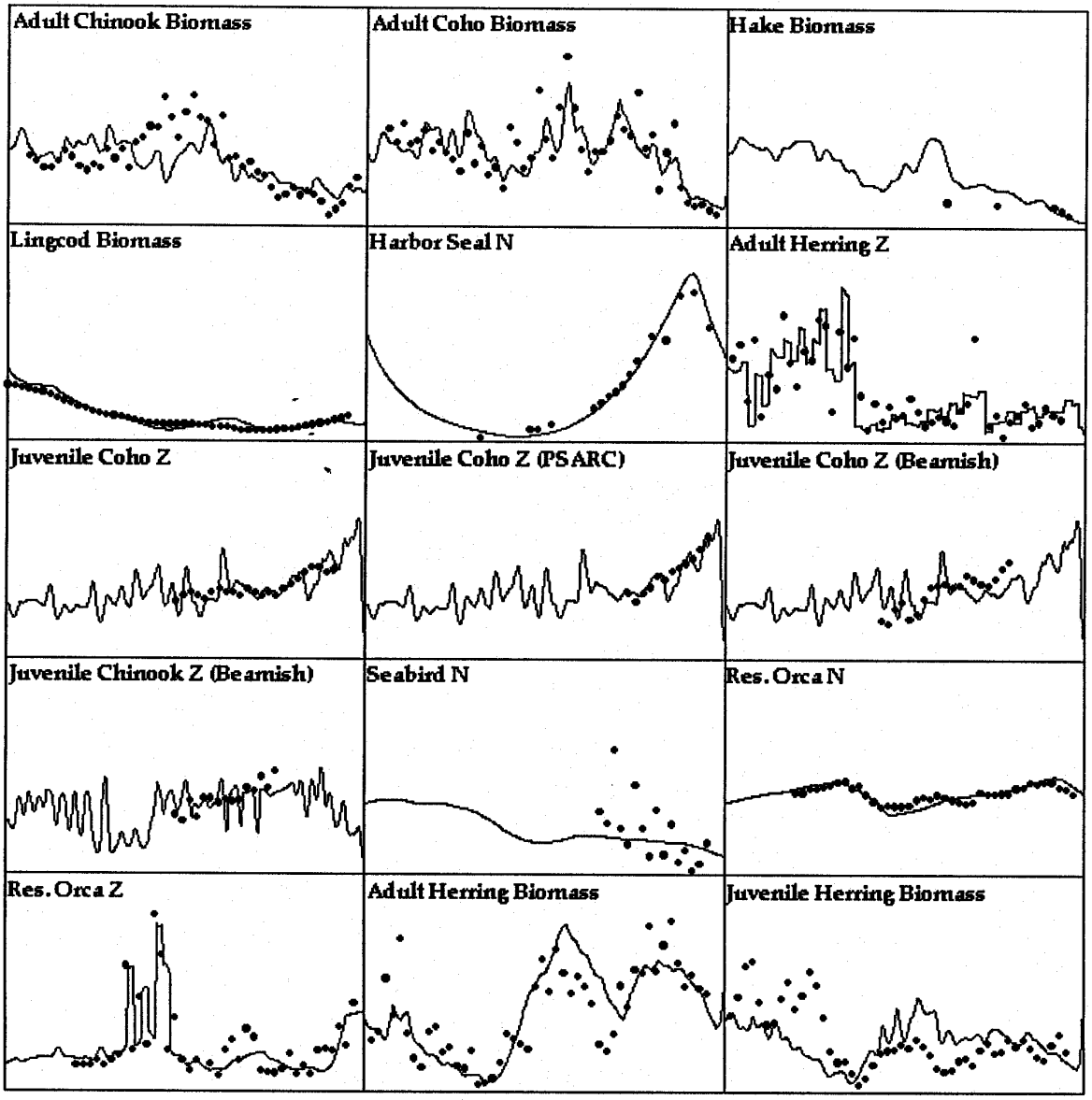

Fig. 2 Predicted and observed abundance and total mortality indices using relative primary productivity sequence shown in Figure 3. SS= 75.24.

Table 6 Sum of square deviations (SS) between model predictions and observed data for biomass and mortality. *SS no model* is equivalent to fitting a straight line through the data, and *SS no environment* assumes constant primary production.

Data Type	*SS No Model*	*SS No Trophic Interactions*	*SS No Environment*	*SS all Effects*
Adult Chinook Biomass	13.43	26.61	12.89	6.33
Adult Coho Biomass	14.34	29.68	19.69	3.83
Hake Biomass	0.38	2.97	0.19	1.53
Lingcod Biomass	11.68	72.25	9.95	2.37
Harbour Seal N	15.31	2.09	1.08	1.74
Adult Herring Z	22.79	13.76	17.71	15.91
Juvenile Coho Z	0.47	0.44	0.33	0.62
Juvenile Coho Z (PSARC)	0.56	0.55	0.58	0.13
Juvenile Coho Z (Beamish)	1.57	1.54	1.3	1.12
Juvenile Chinook Z	0.47	0.47	0.59	0.67
Seabird N	10.82	10.75	10.95	9
Res. Orca N	0.37	0.61	1.03	0.18
Res. Orca Z	13.1	6.34	5.53	4.4
Adult Herring Biomass	24.81	103.42	9.14	7.33
Juvenile Herring Biomass	15.78	122.35	24.91	20.08
Total	145.88	393.83	115.87	75.24

Discussion

The observed time series for 11 of the 15 data types (Table 6) suggest that large fluctuations in primary production must have occurred in the Strait of Georgia over the last 50 years. Declines in average wind speed, and the Pacific Decadal Oscillation index also support the decline in primary productivity hypothesis. Ideally, this study should include direct estimates of primary productivity over the entire Strait of Georgia; unfortunately, we were unable to find these data, if they exist. Nevertheless, it is clear, from our understanding of ecosystem dynamics that observed declines are better explained by assuming primary productivity has declined.

The fisheries stock assessment data used here were not made for the purposes of studying the role of climate effects on ecosystem dynamics. It is important to note that these data are limited in use, as predictors of relative changes in primary productivity. Untangling the complicated trophic interactions, climate effects, and mortality patterns in ecosystem analysis is difficult; and direct observations on each of these processes will be required to improve our understanding of ecosystem dynamics. Many physical oceanographic studies have been completed, and currently in progress, in the Strait of Georgia. Incorporating these data into the analysis will greatly improve our understanding of ecosystem responses to changing physical environments. Probably one of the more difficult tasks, however, will be to study small-scale processes of changing trophic interactions that are related to spatial and temporal abundance of animals. Predator-prey interactions play a key role in determining optimal exploitation rates in that we need to understand how reducing the abundance of one species effects mortality rates for other species in an ecosystem with variable productivity.

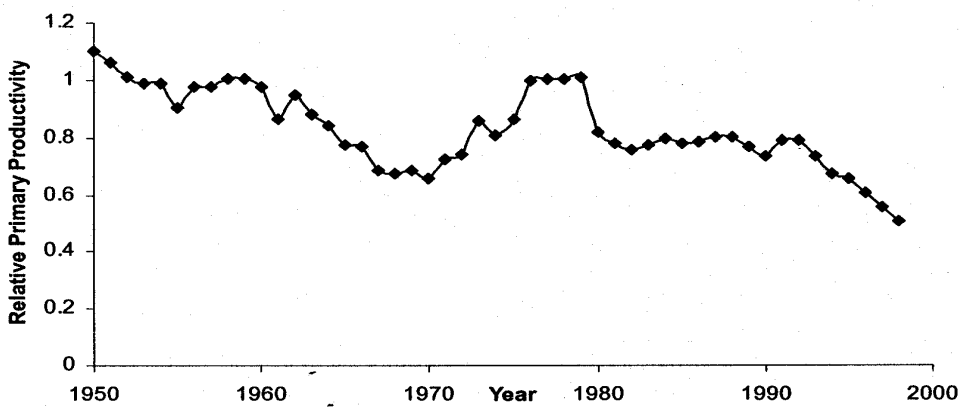

Fig. 3 Relative changes in primary productivity from 1950 to 1998.

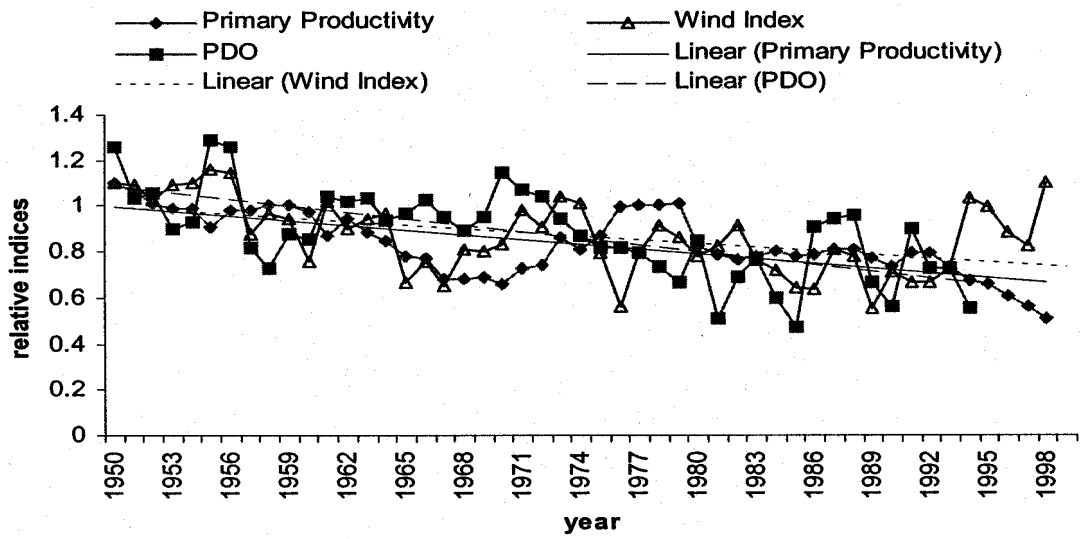

Fig. 4 Relative primary productivity, average annual wind speed squared in the Strait of Georgia (a measure of sheer stress) and the Pacific Decadal Oscillation (PDO) from 1950 to 1998. Solid lines represent linear trends line for each index.

References

Beamish, R.J., and Bouillon, D.R. 1995. Marine fish production trends off the Pacific coast of Canada and the United States. *In* Climate Change And Northern Fish Populations. *Edited by* R.J. Beamish. Can. Spec Pub. Fish. Aquat. Sci. 121 pp.585-591.

Beamish, R.J., Noakes, D.J., McFarlane, G.A., Klyashtorin, L., lvanov, V.V. and Kurashov, V. 1999. The regime concept and natural trends in the production of Pacific Salmon. Can. J. Fish. Aquat. Sci. 56: 516-526.

Blacket, A. W. 1993. Wind induced entrainment in the Strait of Georgia and the possible consequences for fish survival. M.Sc. Thesis, University of British Columbia. 82p.

Cass, A.J., Beamish, R.J. *et al*. 1990. Lingcod (*Ophiodon elongatus*). Can. Spec. Pub. Fish. Aquat. Sci. 40 p.

DFO, 1999 a. Fraser River Chinook Salmon. DFO. Science Stock Status Report D6-11 (1999).

DFO, 1999 b. Coho Salmon in the Coastal Waters of the Georgia Basin. DFO Science Stock Status Report D6-07 (1999).

Hay D. E., McCarter, P.B., and Daniel, K. 1999. Pacific herring tagging from 1936-1992: A re-evaluation of homing based on additional data. Canadian Stock Assessment Secretariat Research Document 99/176.

Ketchen, K.S., Bourne, N., and Butler, T.H. 1983. History and present status of fisheries for marine fishes and invertebrates in the Strait of Georgia, British Columbia. Can. J. Fish. Aquat. Sci. 40: 1095-1119.

Lichatowich, J. 1999. Salmon without rivers. Island Press, Washington D.C., 317p.

Martell, S.J.D. 1999. Reconstructing Lingcod Biomass in Georgia Strait and the Effect of Marine Reserves on Lingcod Populations in Howe Sound. M.Sc. Thesis, University of British Columbia. 89p.

Pauly, D., Christensen, V., Dalsgaard, J., Froese, R., and Torres, F. Jr. 1998. Fishing down marine food webs. Science 279: 860-863.

Pauly, D., Christensen, V., Froese, R., and Palomares, M.L. 2000. Fishing Down Aquatic Food Webs. American Scientist, 88: 46-51.

Robinson, C.L.K., and Ware, D.M. 1999. Simulated and observed response of the southwest Vancouver Island pelagic ecosystem to oceanic conditions in the 1990s. Can. J. Fish. Aquat. Sci. 56: 2433-2443.

Sainsbury, K. 1998. Living marine resource assessment for the 21st Century: What will be needed and how will it be provided? *In* Fisheries Stock Assessment Models. *Edited by* F. Funk, T. J. Quinn 11, J. Heifetz, J. N. lanelli, J. E. Powers, J. F. Schweigert, P. J. Sullivan, and C.I. Zhang, Alaska Sea Grant College Program Report No. AK-SK-98-01, University of Alaska Fairbanks.

Schweigert, J.F., Fort, C., and Tanasichuk, R. 1998. Stock assessments for British Columbia Herring in 1997 and forecasts for potential catch in 1998. Can. Tech. Rep. Fish. Aquat. Sci. 2217: 64 p.

Stocker, M. 1993. Recent management of the B.C. herring fishery. *In* Perspectives on Canadian Marine Resource Management. *Edited by* L. S. Parsons and W. H Lear. Can. Bull. Fish. Aguat. Sci. 226, pp. 267-293.

Wallace, S.S. 1998. Changes in Human Exploitation of Marine Resources in British Columbia (Pre-Contact to Present Day). *In* Back to the Future: Reconstructing the Strait of Georgia Ecosystem *Edited by* D. Pauly, T. Pitcher, D. Priekshot, J. Heame. Vol 6, pp. 58-64.

Walters, C.J., Christensen, C., and Pauly, D. 1997. Structuring dynamic models of exploited ecosystems from trophic mass-balance assessments. Reviews in Fish Biology and Fisheries. 7: 139-172.

Walters, C.J., Pauly, D., Christensen, V., and Kitchell, J.F. 2000. Representing density dependent consequences of life history strategies in aquatic ecosystems: Ecosim II. Ecosystems 3: 70-83.

Preliminary mass-balance ECOPATH Model in the Bohai Sea

Ling Tong[1], Qi-Sheng Tang[1] and Daniel Pauly[2]

[1] Yellow Sea Fisheries Research Institute, Qingdao 266071, P. R. China. E-mail: tongling@ysfri.ac.cn

[2] Fisheries Centre, University of British Columbia, 2204 Main Mall, Vancouver, B.C., Canada. V6T IZ4

Introduction

The Bohai Sea (Fig. 5) is a semi-closed continental water of China, which is nearly encircled by land only with a mouth about 90 km at the eastern apex that connects it to the Yellow Sea. The Bohai Sea is located in the temperate water region between 37°00'~ 41°00'N with 77,000 km^2 in area and the average depth of 18.7 m and the maximum water depth of 70 m. Water temperature changes a lot resulting from the impact of the land climate. The highest SST is 26~30°C in September and the lowest one is 1.2~4°C in February. Much of the fresh waters run into the Bohai Sea from about 20 rivers, for example the Yellow River, Liao River, Raoyang River, Ling River, Luan River, and other rivers. The runoff of fresh water was 31.4 billion m^3 per year in the 1970s and half of it came from the Yellow River. The sea is an ocean space with distinct productivity, strong fishing activity and complicated relationship of food web, and is also polluted by industry and living sewage recently.

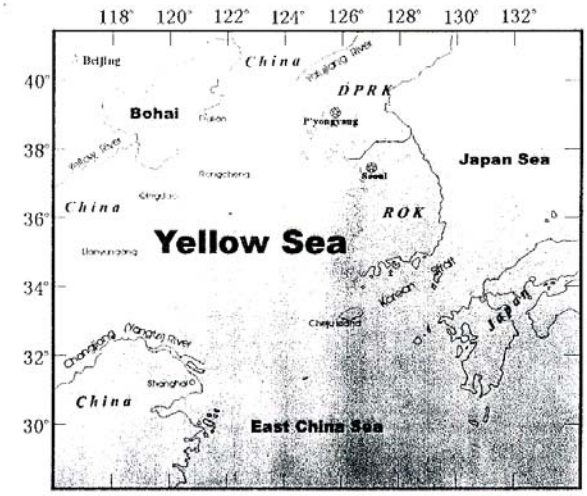

Fig. 5 Bohai Sea region.

The Bohai Sea ecosystem depends on the amount of input of solar energy and the organisms imported from several rivers. NO_3-N and PO_4-P are basic nutrients supporting the primary productivity in the Bohai Sea. The production of organic carbon of the sea is 112 gC/m^2/year. The productivity, like other marine ecosystem, is characterized by seasonal and spatial variability with high levels in spring and fall and in the southern part of the sea, but not much change between years. In the Bohai Sea, the dominant small zooplankton are neritic brackishwater species, such as *Sagitta crassa* Tokioka, *Labidocera euchaeta* Giesbrecht and *Centropages mcmurrichi* Willey. The Bohai Sea small zooplankton biomass has two seasonal peaks, in June and September, and the biomass of other individual species has only one seasonal peak (Bai *et al*. 1991). The fishing effort in the sea has been increasing more and more since 1962, and has led to a significant variation in the abundance and distribution of the most species in the area. The intensive fishing resulted in the decrease of biomass of demersal species with high economic value (large predatory species), such as *Pseudo-sciaena polyactis* and *Trichiurus haumela*, while harvesting more of smaller pelagic species, such as *Setipinna taty* and *Engraulis japonicus*.

Methodology and the ECOPATH model

The first ECOPATH model was developed to describe a coral reef ecosystem (Polovina 1984) and was further developed by Christensen and Pauly (1992) at ICLARM to make it widely available as a well-documented software running on a microcomputer. Lately the ECOPATH model has been integrated with ECOSIM for dynamic simulation modeling based on a mass-balanced model by Walter, Christensen and Pauly (1997). In an ECOPATH model it is assumed that the ecosystem modeled is in steady state for each of the living groups, which implies that input equals output, i.e. Q = P + R + U, where Q is consumption, P - production, R - respiration, and U - unassimilated food. The above equation can be structured around a system of linear equations for expressing mass-balance with the simplest form. It can be expressed for an arbitrary time period and for each element i of an ecosystem by Equation 1 (see Martell *et al*. this report). It is the simultaneous linear equations used in ECOPATH to state that the production and consumption are balance within an ecosystem.

The ECOPATH model allows rapid construction and verification of mass-balance model of ecosystem. The mass-balance model not only verifies the previously published biomass estimates, but also identifies the biomass required for assessment of marine carrying capacity. Constructing an ECOPATH model includes the following steps:

1. Identification of the area and period for which the ecosystem model will be constructed;
2. Definition of all functional groups (boxes), from primary producers to top predators, in the ecosystem to be included for the thermodynamic balance;
3. Setting parameters of production/biomass ratio (P/B), consumption/biomass ratio (Q/B), biomass (B) and ecotrophic efficiency (EE) for each function group, but only three of them are necessary as the basic input parameters in the model, and also entry of the catches to every fishing species;
4. Entry of a diet consumption matrix (DC) expressing the diet fraction of predator/prey relationship in the model;
5. Modify the entries of P/B, Q/B, EE or the biomass, to balance the ECOPATH model (repeating steps (3) and (4) above) until the mass input equals output for each box.

Structure of the Bohai Sea ECOPATH model

The resources composition in the Bohai Sea changed a lot along with the fishing effort increase to multi-species fish communities after 1962. The CPUE (catch per horse power) was 7.61 tons in 1962, but it went down to 0.88 ton in 1983. The traditional species fished in the area, such as small yellow croaker, slender shad, cutlasfish, were high valuable in the market, but the biomass of them declined then. The small pelagic fish and small crustacean species appeared more in the landings and fluctuated much more annually. The highest annual landing of *Acetes* (a sergestid shrimp) can be 100 hundred metric tons (1.3 t/km^2) in the sea. The highest catch of jellyfish reached 280 hundred tons during the 1970s. This reflects a gradual transition in catch from long-lived, high trophic level piscivorous bottom species toward short-lived, low trophic level invertebrates and planktivorous pelagic species. The Bohai Sea is an example of an overfished marine ecosystem leading to smaller, high-turn-over species. It is a peculiarity of the sea that small pelagic fish and jellyfish replace large table fish in an over-exploited ecosystem (Pitcher 1998).

The mass-balance model of the Bohai Sea is aimed at constructing a quantitative description of trophic structure and the relationship among the different groups in the whole Bohai Sea. The model is based on the data of the Bohai Sea ecosystem survey project completed during April 1982 to May 1983. The project collected the data monthly by the bottom trawling and mainly made assessment of the commercial important species and their biological characteristics study. As this is the first ECOPATH model of the Bohai Sea, it only presents a preliminary revelation of the trophic structure and flow in the sea between different functional groups. The functional groups in the model covered the main trophic flows among the living marine species and detritus, but the group definition is very rough because of the limited type of survey data available in the region. The functional group determination is based on the species distribution in the water and their feeding behaviour after inspecting the stomach contents of 54 species from 1863 samples. Considering the limited data and no existing mass-balance model in the Bohai Sea, the model only has 13 function groups.

One primary producer of phytoplankton was identified. Zooplankton was split into two groups, microzooplankton and macrozooplankton. The former includes small herbivorous and carnivorous zooplankton and the latter mainly consists of jellyfish and *Acetes*. Benthic invertebrates were divided into small mollusca, large mollusca, small crustacean and large crustacean, most species of which were commercial harvest in the sea but the landing data were not readily available. There were no biomass data for some species in the small invertebrate groups so their biomass were estimated by the model using the fixed ecotrophic efficiency (EE=0.95). Biomass for the two large groups were obtained by summing up the biomass data from the survey. Five fish function groups were identified in the model on the basis of 31 fish species which hold about 90% of total biomass for the fish community in the Bohai Sea. The herbivorous feeders group includes mainly *Mugil cephalus* and *Liza haematocheila*. The other four groups were small pelagic fish, demersal fish, benthic feeders and top pelagic feeders, which were important commercial fishing targets. The details of 13 function groups (box) in the Bohai Sea ECOPATH model are summarized in Table 7. Many species are included in one box of the model so it is hard to find P/B and Q/B from one species for the whole group. The P/B and Q/B parameters were based on the parameters from similar function groups in the models of the Strait of Georgia (Dalsgaard 1998), the Brunei Darussalam, South China Sea (Silvestre 1993) and the Georges Bank (Sissenwine 1984).

The basic parameters of biomass (wet weight t/km^2), P/B, Q/B, EE and harvest for the 1982-83 ECOPATH model of the Bohai Sea ecosystem are presented in Table 8. Detritus is estimated from primary production of carbon by equation A5 of the empirical relationship method (Pauly, D., M.L.Soriano-Bartz *et al*. 1993). Phytoplankton was estimated from Bohai Sea primary productivity of 112 gC/m^2/year converted to g wet weight phytoplankton m^{-2}year^{-1} by a wet weight:carbon ratio of 10:1.

Table 7 Functional groups in the model.

1. Microzooplankton	2. Macrozooplankton
3. Small mollusca	4. Large mollusca
5. Small crustacea	6. Large crustacea
7. Herbivorous feeders	8. Small pelagic fish
9. Demersal fish	10. Benthic feeders
11. Top pelagic feeders	12. Phytoplankton
13. Detritus	

Results and discussion

To balance import to and export out from every box, the EE values are leading check parameters for equilibration of a model when running the ECOPATH 3.0 software. The EE value should be between 0 and 1. Here, a value of 0 indicates that the group is not consumed by any other groups in the system, nor is it exported. Conversely, a value near or equal to 1 indicates that the group is being heavily preyed or fished, leaving no individuals to die of old age. Some of the original biomass inputs from the Bohai Sea trawling survey in 1982-83 are considered too low, and as aresult equilibrium cannot be reached in the model with the high value of EE. This is because the survey data connecting commercial species from bottom trawling and the function groups in the model cover a wide range of living marine species. According to the results obtained by different resource assessment methods (Fig. 7.5; Laevatsu and Alverson 1996), biomass value estimated by bottom trawling survey is much lower than the ones from other stock assessment methods. It is necessary to modify the biomass data to equilibrate the model. The biomass of small pelagic fish group is estimated from 1.2 to 2.14 ton/km^2, and the benthic fish group from 0.32 to 0.68 ton/km^2.

The model estimated the biomass density of commercially utilized species to be at 12.33 ton/km^2 and the density of all fish species at only 4.4 ton/km^2. A flow chart showing trophic interactions and energy flow in the Bohai Sea is presented in Figure 6. It shows the estimated trophic level of the 13 functional groups and the relative amounts of energy that flow in and out of each box. The trophic flow to detritus, respiration and catch are also represented. Two food paths, a plankton path and a benthic path, are shown, which are the food webs characteristic of the Bohai Sea. The lower trophic level groups have a strong influence on the Bohai Sea ecosystem. High fishing effort leads to decline of high value living marine resources, which can be seen by the negative impacts to the ecosystem from fishery.

No common information is available for the biomass comparison with other ECOPATH models in the Bohai Sea. The values in our model are low compared with densities in other ecosystems, such as the Caribbean coral reef and

Table 8 Parameter estimation for the group from the mass-balance model of the Bohai Sea. Values in brackets were calculated by the ECOPATH program, and dashes mean no entry.

Group	Catch (t/km^2)	Biomass (t/km^2)	P/B (year)	Q/B (year)	EE
Microzooplankton	-	4.40	36.0	186.0	(0.961)
Macrozooplankton	1.40	2.80	3.00	12.0	(0.964)
Small mollusca	0.78	(2.76)	6.85	27.4	0.950
Large mollusca	1.50	0.24	2.00	7.0	(0.890)
Small crustacea	0.20	(2.01)	8.00	30.0	0.950
Large crustacea	0.20	0.37	1.50	11.60	(0.823)
Herbivorous feeders	0.10	0.56	3.00	15.0	(0.903)
Small pelagic fish	0.50	2.14	2.37	7.9	(0.927)
Demersal fish	0.22	0.62	2.10	8.7	(0.808)
Benthic feeders	0.10	0.68	0.80	4.6	(0.902)
Top pelagic feeders	0.15	0.59	0.46	4.1	(0.553)
Phytoplankton	-	15.70	71.20	-	(0.457)
Detritus	-	43.00	-	-	(0.386)

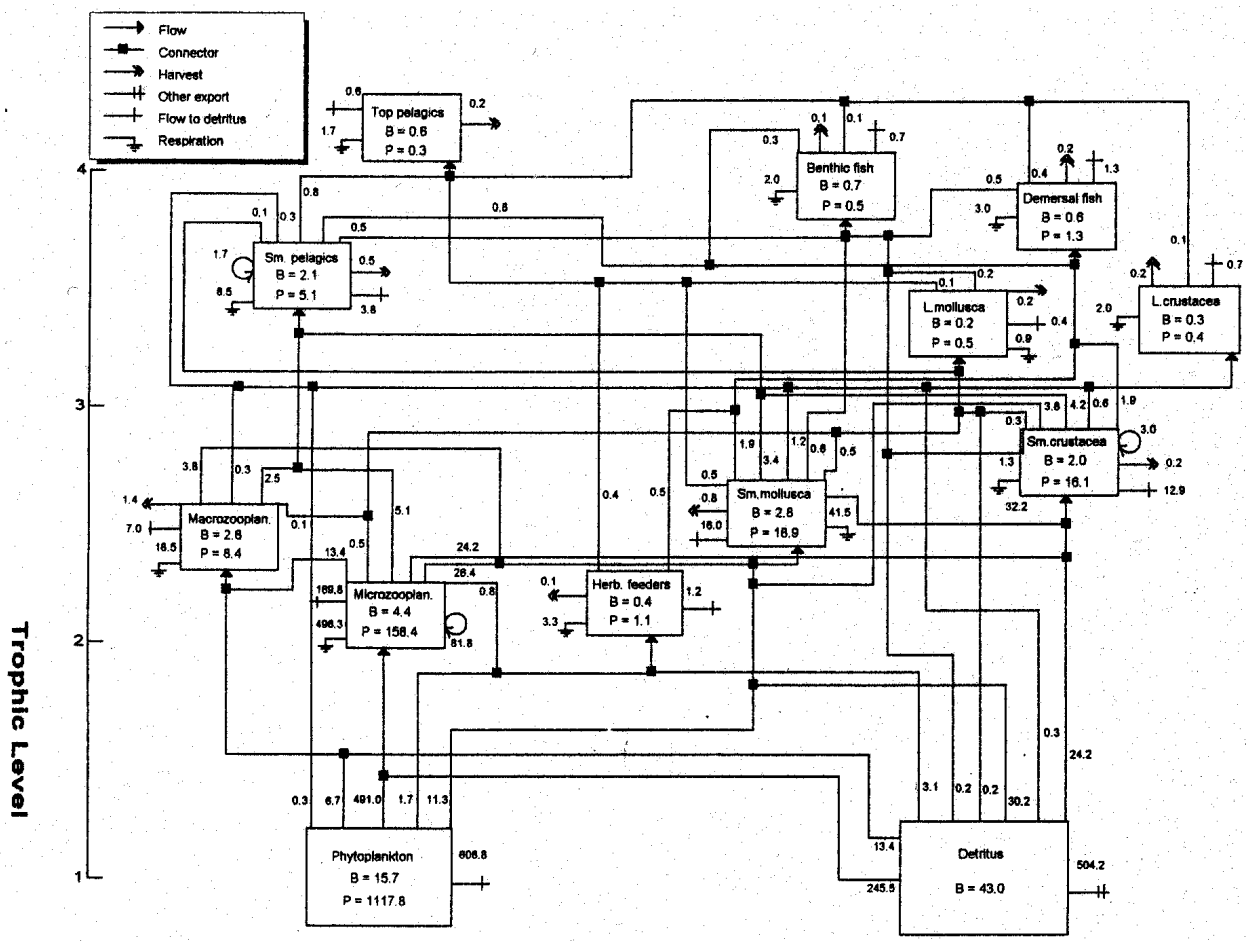

Fig. 6 Flow chart of trophic interactions in the Bohai Sea ECOPATH model.

the southern B.C. shelf, but it is higher than that reported in other models of the Bohai Sea. The output from the ECOPATH model looks more reasonable. We conclude that the total biomass of commercially fished species in the sea is 950,000 t and 338,000 t are fish species of value.

Ecosystem statistic and trophic flow of the Bohai Sea ecosystem model (1982-1983) could be considered as reasonable value, but some problem concerned with the input data have to be taken into account. First the function groups should be split further to estimate more precisely input parameters, like P/B and Q/B, for each box. Then the diet data for some species is also needed to be modified slightly to let all EEs be reasonable. Thirdly, it is better to consider the habitat for different species in the ECOPATH model developed in the future.

References

Christensen, V., and Pauly, D. 1992. ECOPATH II - software for balancing steady-state ecosystem models and calculating network characteristics. Ecological Modelling 61: 169-185.

Christensen, V., and Pauly. D. 1993. ECOPATH for Windows - A users guide. ICLARM. 71p.

Bai, X., and Zhuang. Z. 1991. Studies on the fluctuation of zooplankton biomass and its main species number in the Bohai Sea. Marine Fish. Research No. 12:71-92 (in Chinese with English abstract).

Dalsgaard J.S, Wallace, S., *et al*. Mass-balance model of the Strait of Georgia: today, one hundred and five hundred years ago. (pers. comm.)

Deng, J. 1988. Ecological bases of marine ranching and management in the Bohai Sea.

Marine Fish. Research No. 9: 1-10 (in Chinese with English abstract).
Deng, J., Meng, T., *et al*. 1988. The fish species composition, abundance and distribution in the Bohai Sea. Marine Fish. Research No.9: 11-90 (in Chinese with English abstract).
Deng, J., Meng, T., and Ren, S. 1988. Food web of fishes in the Bohai Sea. Marine Fish. Research No.9: 151-172 (in Chinese with English abstract).
Deng, J., Zhu, J., and Cheng, J. 1988. Main invertebrates and their fishery biology in the Bohai Sea. Marine Fish. Research No.9: 91-120 (in Chinese with English abstract).
Laevatsu T., Alverson, D.L., and Marasco, R.J. 1996. Exploitable marine ecosystem: Their behaviour and management. Fishing News Books, Blackwell Science Ltd. 321p.
Pauly, D., Soriano-Bartz, M.L., *et al*. 1993. Improved construction, parametrization and interpretation of steady-state ecosystem models. *In* Trophic models of aquatic ecosystems. *Edited by* V. Christensen and D. Pauly. ICLAM Conf. Proc. 26, pp. 1-13.
Pauly, D., Christensen, V., *et al*. 1998. Fishing down marine food webs. Science 279: 860-863.
Pitcher, T.J., and Pauly, D. 1998. Rebuilding ecosystem, not sustainability, as the proper goal of fishery management. *In* Reinventing Fisheries Management. *Edited by* T.J. Pitcher *et al*. Chapman & Hall, London. pp. 312-328.
Polovina, J.J. 1984. Model of a coral reef ecosystem, Part I: the ECOPATH model and its application to French Frigate Shoals. Coral Reefs 3: 1-11.
Purcell, J. 1996. Lower trophic levels for Alaska Gyre model. Mass-balance model of North-Eastern Pacific Ecosystem. Fisheries Centre Research Report 4(1), University of British Columbia, Vancouver BC. Canada
Okey, T. A., and Pauly, D. 1998. A mass-balanced model of trophic flow in Prince William Sound: De-compartmentalizing ecosystem knowledge. Presented at the 16th Lowell Wakefield Fisheries Symposium, Ecosystem Consideration in Fisheries Management, Anchorage, Alaska.
Sissenwine M.P., Cohen, E.B. and Grosslein, M.D. 1984. Structure of the Georges Bank Ecosystem. Rapp. P. Reun.Cons. int. Explor. Mer. 183: 243-254.
Silvestre, G., Selvanathan, S., and Salleh, A.H.M. 1993. Preliminary trophic model of the coastal fisheries resources of Brunei Darussalam, South China Sea. *In* Trophic Models of Aquatic Ecosystems. *Edited by* V.Christensen and D.Pauly. ICLARM, Conf. Proc. 26, pp. 300-306.
Walters, C.J., Christensen, V., and Pauly, D. 1997. Structuring dynamic model of exploited ecosystems from trophic mass-balance assessments. Rev. Fish Biology and Fisheries 7: 139-192.
Yang, J., Yang, W., *et al*. 1990. The fish species biomass assessment in the Bohai Sea. Act Oceanology Sinica 12: 359-365.

Ecosystem modeling, monitoring, and Japanese studies relevant to the Western Subarctic Gyre and Kuroshio-Oyashio transition zone ecosystems

Akihiko Yatsu
National Research Institute of Fisheries Science, Fisheries Agency of Japan, Yokohama, Japan. 236-8648

Current Japanese programs on ecosystem studies in the oceanic waters of the northern North Pacific have been carried out mainly by Hokkaido University (HU- Faculty of Fisheries) and Fisheries Research Institutes belonging to the Fisheries Agency of Japan (FAJ). The Western Subarctic Gyre (WSAG) and the Kuroshio-Oyashio Transition Zone (TZ) are of major interests to Japan because of the fisheries resources available there. For example, Wada *et al*. (1998) adapted a trophodynamics model to sardine and walleye pollock populations in the Oyashio Current Region using STELLA-II software. Modeling of the entire ecosystem for WSAG and TZ, however, has not been established.

Aydin (this workshop) raised four discussion points on WSAG ecosystem study: (1) the appropriate boundaries and species groupings of the model; (2) the issues involves with scaling seasonal models of lower trophic levels up to a model with an annual time scale; (3) sources for data and parameterization methods, and (4) the appropriate methods for the inclusion of highly migratory species, specifically Pacific salmon (*Oncorhynchus* spp.) and marine mammals. These are also true for TZ.

In this report I will briefly introduce ecosystem study projects, monitoring activities and major published reports relevant to this workshop. BIOCOSMOS results are summarized in Oozeki (2000).

Recent ecosystem projects

HUBEC (Hokkaido University SuBarctic Ecosystem dynamics and Climate) is a research program organized by oceanographers and fisheries scientists in the Faculty of Fisheries to address the question of how climate change and dynamics may affect the abundance and production of animals in the sea.

ORI-GLOBEC is a project established by the Ocean Research Institute, University of Tokyo, to study response of plankton, micronekton and fish population to climate regime-shift in the Kuroshio-Oyashio region. Progress of ORI-GLOBEC and HUBEC by 1998 was reported in Terasaki *et al*. (1999), where ecosystem-physical modeling of a warm-core ring was presented.

VENFISH (Variation of the oceanic ENvironment and FISH populations in the northwestern Pacific) is a comprehensive study supported by the Tohoku National Fisheries Research Institute (TNFRI-FAJ) and Hokkaido National Fisheries Research Institute (HNFRI-FAJ), etc. in 1997-2002. Study components are:

- Development of a forecasting method for the variation of phytoplankton biomass;
- Development of a forecasting method for the variation of zooplankton biomass;
- Observation and modelling of the variation of resources abundance of saury and Alaska pollock;
- Clarification of response of saury and pollock to the oceanic environmental variation; and
- Development of the forecasting ecosystem model for saury and Alaska pollock abundance (including population dynamics and trophodynamics models).

Only bottom-up processes from physical forcing to saury and pollock populations are considered. Predations on saury and pollock and competition among each trophic level will be treated in the next stage of the project.

High Trophic Ecosystem (1999-200?) is a consecutive project of VENFISH organized by the National Research Institute of Far Seas Fisheries (NRIFSF- FAJ). Study components:

- Monitoring distribution and abundance of species with driftnet and midwater trawl;
- Stomach content analysis of small cetaceans, sea birds, albacore, skipjack, sharks and squids;
- Trophic level analysis with stable isotope techniques;
- Energetic demand estimation of large predators;
- Input of results on dynamics of lower trophic level ecosystem from VENFISH project; and
- Ecosystem modeling.

Monitoring data

- HU: Oceanography and driftnet surveys along 155°E, 170°E, 175°E, etc., from 1979-present;
- TNFRI: Oceanography, primary production, zooplankton, driftnet surveys, etc.;
- HNFRI: Oceanography and driftnet surveys along 165°E;
- Other routine observations by FAJ, prefectural governments, etc.

Discussion points

Boundaries and species groupings of the model

From oceanographic features, WSAG and TZ have been treated separately. From biological point of view, however, the two ecosystems are interdependent. Small pelagics, squids and predatory animals (sharks, salmons, tunas, birds, marine mammals) migrate across the Subarctic

Front (the boundary between WSAG and TZ) although this front acts as a barrier or a selective filter for some species or species size. Some species such as Pacific salmon migrate in an east-west direction, e.g. between WSAG and the Okhotsk Sea. Minor species components with similar ecological features may be grouped. On the contrary, size (or biologically) segregated migration as in Pacific pomfret may be treated separately.

Scaling seasonal models of lower trophic levels up to a model with an annual time scale

Because of seasonality in primary production and migrations of zooplankton, nekton, mammals and seabirds, models must be constructed season by season at a first step, then to be combined to include interannual variability. A general problem is the availability of data other than in summer. Seasonal and vertical variations in zooplankton biomass have been monitored in Kuroshio, Oyashio and TZ. Modeling effort of Oyashio region including the effect of the vertical migration of *Calanus*/*Neocalanus* spp. has been continued by the MODEL Task Team and Hokkaido University's group (see PICES Sci. Report 15: 1-77, 137-139; Kishi *et al*. 2000).

Sources for data and parameterization methods

Primary and secondary productions have been studied primarily by HUBEC and VENFISH. Biomass estimations are obtained from the routine stock assessment for commercially important species (sardine, mackerel, common squid, etc.). For other species, driftnet and midwater trawl surveys would be useful. Russian surveys are of course important in this aspect (e.g., Shuntov *et al*. 1996). Estimations for production and consumption rates need to be thoroughly examined, since transfer efficiencies from primary production to zooplankton and from zooplankton to fishes in Oyashio were different from those in California Current (Wada *et al*. 1998).

Methods for the inclusion of highly migratory species

This is the notorious problem that needs monitoring for all seasons. Monitoring activities have been concentrated in summer season, although some information on seasonal migration of predatory animals is available.

References

Beamish, R.J. 1999. An introduction to the PICES symposium on the ecosystem dynamics in the Eastern and Western Gyres of the Subarctic Pacific. Prog. Oceanogr. 43: 157-161.

Belyaev, V.A., and Shatilina, T.A. 1995. Variations in abundance of pelagic fishes in the Kuroshio zone as related to climatic changes. Can. Spec. Publ. Fish. Aquat. Sci. 121: 553-559.

Brodeur, R.D. 1988. Zoogeography and trophic ecology of the dominant epipelagic fishes in the northern North Pacific. Bull. Ocean Res. Inst. Univ. Tokyo, (26/2): 1-27.

Eslinger, D.L. *et al*. (eds.) 2000. Final report of the international workshop to develop a prototype lower trophic level ecosystem model for comparison of different marine ecosystems in the N. Pacific. PICES Sci. Rep. 15: 1-77.

Fisheries Agency of Japan. 1985-1992. Research reports for improvement of fisheries stock assessment systems. (in Japanese)

Hokkaido University. 1980-2000. Data record of oceanographic observations and exploratory fishing. Fac. Fish. Nos. 22-43.

Hunt, G.L., Kato, H., and McKinnell, S. 2000. Predation by marine birds and mammals in the Subarctic North Pacific Ocean. PICES Sci. Rep., 14: 1-165.

Ishida, Y, Zaumaya, T., and Fukuwaka, M. 1999. Summer distribution of fishes and squids caught by surface gillnets in the western North Pacific Ocean. Bull. Hokkaido Nat. Fish. Res. Inst. 63: 1-18.

Kishi, M.J., Motono, H., Kashiwai, M., and Tsuda, A. 2000. Ecological-physical coupled model with ontogenic vertical migration of zooplankton in the northwestern Pacific. Journal of Oceanography, submitted

Pearcy, W.G. 1991. Biology of the transition region. NOAA Tech. Rep., NMFS 105: 39-55.

Noto, M., and Yasuda, I. 1999. Population decline of the Japanese sardine, *Sardinops melanostictus*, in relation to sea surface

temperature in the Kuroshio Extension. Can. J. Fish. Aquat. Sci. 56: 973-983.

Oozeki, Y. 2000. Mechanism causing the variability of the Japanese sardine population: Achievements of the Bio-Cosmos Project in Japan. PICES Press 8: 20-23.

Shuntov, V.P., Dulepova, E.P., Radchenko, V.I., and Lapko, V.V. 1996. New data about communities of plankton and nekton of the far-eastern seas in connection with climate-oceanological reorganization. Fish. Oceanogr. 5: 38-44.

Sugimoto, T., and Tadokoro, K. 1998. Interdecadal variation of plankton biomass and physical environment in the North Pacific. Fish. Oceanogr. 7: 289-299.

Terazaki, K., Ohtani, T., Sugimoto, T., and Watanabe, Y. (editors). 1999. Ecosystem dynamics of the Kuroshio-Oyashio Transition Region (Proceedings of Japan GLOBEC Symposium in 1998). Japan Marine Science Foundation, Tokyo, 273p.

Wada, T., Ware, D.M., Kashiwai, M., Yamamura, O., and Robinson, C.L.K. 1998. Response of plankton and fish production dynamics to sardine abundance regime shifts in the Oyashio Current Region. Mem. Fac. Fish. Hokkaido Univ. 45: 123-130.

BASS Workshop recommendations

As the PICES CCCC Program enters its synthesis phase, modelling will play a more prominent role in CCCC activity. Participants recommended the BASS and MODEL Task Teams to convene a joint workshop to examine the feasibility of using the ECOPATH/ ECOSYSTEM modelling approach as a means to organize our understanding of the marine ecosystems of the subarctic gyres. Specific objectives include to: (a) synthesize all trophic level data in a common format; (b) examine trophic relations in both gyres using ECOPATH/ ECOSIM/ECOSPAC; and (c) examine methods of incorporating the PICES NEMURO lower trophic level model into the analysis.

Participants recommended that collaboration and synthesis of the data into a common format take place prior to the workshop. G. McFarlane will co-ordinate this issue for North America and A. Krovnin and A. Yatsu for Asia. K. Aydin will synthesize the data into the ECOPATH format. If possible, the workshop should be held in conjunction with the PICES Census of Marine Life Workshop to be held March 7-9, 2001, in Honolulu. Locating the venue in Hawaii at this time is seen as a cost-effective way to involve workshop participants from both sides of the Pacific and would lead to a more balanced scientific representation from the nations of the North Pacific.

BASS Endnote 1

Participation List

Canada
- Gordon A. McFarlane
- Richard J. Beamish
- Jacquelynne R. King
- James Irvine
- Steven J.D. Martell

China
- Ling Tong

Japan
- Akihiko Yatsu
- Masahide Kaeriyama
- Yukimasa Ishida
- Takashige Sugimoto

Russia
- Andrei S. Krovnin
- Victor Tsiger

U.S.A.
- Jeffrey J. Polovina
- Kerim Y. Aydin
- Albert J. Hermann
- Dale B. Haidvogel

MODEL WORKSHOP ON STRATEGIES FOR COUPLING HIGHER AND LOWER TROPHIC LEVEL MARINE ECOSYSTEM MODELS

(Co-convenors: Michio J. Kishi and Bernard A. Megrey)

Introduction

A variety of models have been used to describe lower trophic level (LTL) and higher trophic level (HTL) components of North Pacific ecosystems. In order to facilitate comparisons of model results among areas, the goal of the MODEL Task Team for the next few years is to adapt a prototype LTL model developed at the workshop held in Nemuro, Japan, in January 2000, and to apply it to basin and regional scale ecosystems in the North Pacific. These activities will require coordination with BASS, REX, and MONITOR Task Teams. The Nemuro Workshop focused on the development and parameterization of a LTL model to PICES regional ecosystems, and began discussions about ways to link HTL models to LTL models. The follow-up Hakodate Workshop described in this report was intended to extend the initial discussion that began in Nemuro, and to develop viable strategies for this important linkage.

The following summary of the Task Team discussions from the Hakodate Workshop outlines some important factors which determine how LTL production flows to HTL predators, and how much of this energy is transformed into HTL production. Many of the factors and processes mentioned below should be included, either explicitly or implicitly, in an HTL model. The output of the coupled model should also be analyzed to ensure that it is able to reproduce reasonable production/biomass and consumption/biomass ratios, and ecotrophic efficiencies.

Goals and objectives of the workshop

The goals of the workshop were to:

1. Collectively identify viable strategies for linking the NEMURO LTL (Fig. 1) model to HTL models of the North Pacific ecosystem at the regional and basin scales of interest to BASS and REX.
2. Develop strategies for integrating different time/space scales and size spectra from various models.
3. Find areas of mutual interest where MODEL could interact with other CCCC Task Teams, especially REX and BASS.
4. Achieve broad synthesis through modeling which will lead to global understanding of the response of marine ecosystems to global climate change.
5. Discuss strategies for simulating variability in populations of fish and zooplankton, to evaluate the cause of this variability, and to identify approaches that will ultimately permit the development of a predictive capability.
6. Discuss how to best link LTL and HTL marine ecosystem models, regional circulation models, and how to best incorporate these unified models into JGOFS models and the CCCC Program.

Participants, venue and schedule

The workshop was held at the Future University in Hakodate, Japan, during the PICES Ninth Annual Meeting in October 2000. Participants (MODEL Endnote 1) consisted of LTL and HTL modelers and individuals with knowledge about key data sets in each selected region and activity within that region.

The workshop schedule (MODEL Endnote 2) consisted of a half-day CCCC plenary session held jointly with other CCCC Task Teams. This was followed by a full-day MODEL Workshop. The final afternoon consisted of a wrap-up CCCC plenary session. During PICES X there were several impromptu meetings between MODEL and BASS, and between MODEL and REX.

The following section contains abstracts, extended abstracts, and fully prepared reports presented at the workshop. The reports are organized by author according to the workshop schedule. The author in bold font made the presentation. Model versions referenced in these reports are described in Megrey *et al.* (2000).

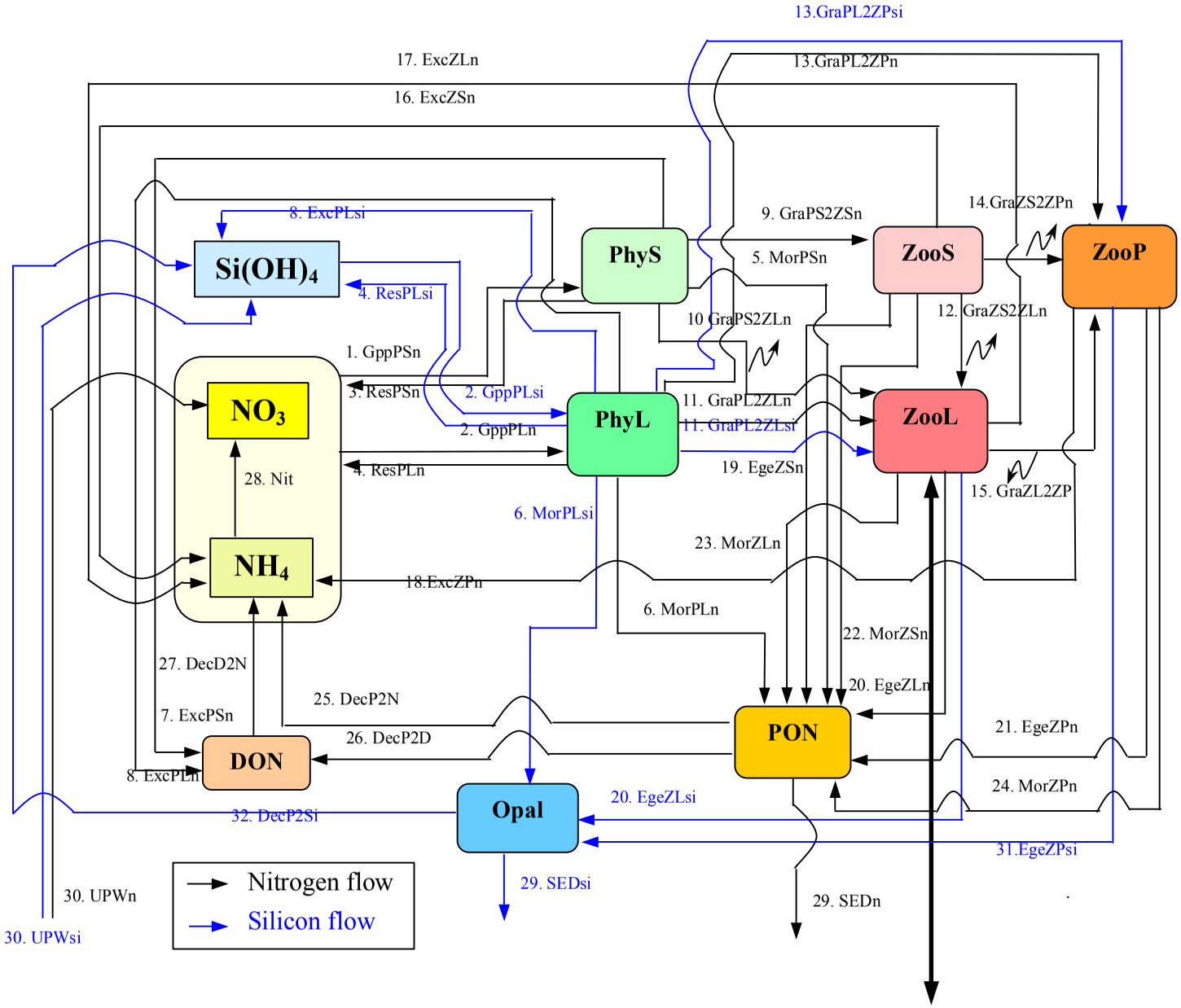

Fig. 1 NEMURO – A PICES/CCCC prototype lower trophic level marine ecosystem model of the North Pacific Ocean. The dark arrow indicates diel vertical migration by large zooplankton (ZooL).

Strategies for coupling upper and lower trophic levels in ecosystem models

Kenneth A. Rose
Coastal Fisheries Institute & Department of Oceanography and Coastal Sciences, Louisiana State University, Baton Rouge, LA 70803, U.S.A. E-mail: karose@lsu.edu

Ecological issues have become complex, with increasing emphasis being placed on ecosystem considerations. Anthropogenic stresses on the ecosystem, such as global climate change, require a whole-system approach to adequately account for both the direct and indirect effects. Yet, despite great effort, we have had great difficulty in quantitatively understanding the relationships between habitat and fish population dynamics (Rose 2000). Previous efforts of the PICES MODEL Task Team have involved development of a lower trophic level simulation model (NEMURO) that tracks nitrogen, phytoplankton, and zooplankton (NPZ). In my presentation, I focus on the issues and strategies related to coupling upper trophic levels to lower trophic models, such as the NEMURO NPZ model. I also present three examples that illustrate these issues and strategies. I conclude with some general comments related to coupling upper and trophic levels in dynamic models.

There are five general issues that must be considered when coupling upper and lower trophic levels. These issues are: (1) spatial and temporal scales, (2) biological scale, (3) site-specificity, (4) feedbacks, and (5) specification of the question. Good models are properly scaled to address the question of interest.

The temporal scale is defined by the time step of the model and the duration of the simulations. The spatial scale is defined by the grain (finest grid size) and extent (geographic area being modeled). The processes controlling nitrogen, phytoplankton and zooplankton operate on different time and space scales than those important to fish, birds and mammals. Most everyone would agree that a 90-second timestep on cm-scale spatial grid is not appropriate to simulate long-term fish population dynamics. The optimal temporal and spatial scales in a model are determined by the properties of the important processes, the availability of data, and the questions to be addressed. Unfortunately, there are no general rules for knowing whether the optimal scales are being represented in a particular model.

The second issue of specifying the biological scale is related to determining the optimal temporal and spatial scales. When modeling upper trophic levels, a fundamental decision is whether the question can be addressed with partial or full life cycle predictions. Partial life cycle predictions might be survival and growth during a particular life stage or period of time. Full life cycle simulations allow for multiple generations to be simulated and for long-term predictions. Developing models that permit full life cycle simulations is a much more difficult and labor-intensive effort. New issues, such as long-term population stability, become important. Population models that do not include negative feedbacks (density-dependence) have only two possible solutions, either extinction or populations going to infinity. Neither of these ultimate solutions is realistic for full life cycle situations; yet, the most difficult aspect of full life cycle modeling is specifying the density-dependent (negative feedback) relationships.

The third issue of site-specificity also greatly influences the effort involved with model development and validation, and the appropriate way to interpret predictions. Models can be developed that attempt to simulate the population in an actual geographic area for specific time periods. Such models require extensive data to account for the nuances of the particular population and location and are more involved to develop, but result in higher confidence in site-specific predictions and results that are easy to relate to resource management. The alternative approach is to develop models that do not claim to simulate a particular location and time period, but rather, simulate a taxa like the species of interest in environments representative of the area of interest. Such models are usually easier to

configure because data can be borrowed from related species and from nearby or similar geographic areas. The disadvantages to such representative models are that we have low confidence in their site-specific predictions and their interpretation focuses on patterns rather than magnitude. The relative merits of the site-specific versus representative models depend on the resolution required to address the question of interest.

The fourth issue is how to represent feedbacks in coupled lower and upper trophic level models. Model coupling is simplified if the effects between trophic levels can be assumed to be bottom-up. This allows the lower trophic model to be run separately from the upper trophic level model. If the dynamics of the upper trophic levels affect the dynamics of the lower trophic levels, then simultaneous solution of both levels are required. Another type of important feedback is the negative feedbacks that act to stabilize population dynamics. Accurate prediction of the dynamics of upper trophic levels requires understanding of the density-dependent feedbacks that operate to keep populations within certain numerical bounds. Representing these feedbacks in upper trophic models can be difficult and, at times, controversial. The shape of spawner-recruit curves assumed in fish population dynamics models is a good example. Such feedbacks determine the response of populations and communities to stressors, and ultimately determine the resilience of the population and the magnitude of harvest that is sustainable.

The fifth, and perhaps most important, issue related to coupling upper and trophic level models is the specification of the question to be addressed. The question of interest must be clearly specified, preferably stated as an hypothesis or family of hypotheses. Otherwise, one is assured of developing an improperly scaled model with the wrong structure, inputs, and outputs. Treating the modeling effort as an experiment with hypotheses and experimental design can avoid many of the problems with inappropriate models. A saying with some merit is that "there are no bad models, just bad model applications".

Two commonly used modeling approaches for upper trophic levels are matrix projection modeling and individual-based modeling. Matrix projection modeling has the advantages of using readily available data on growth, mortality, and reproduction, and well-known mathematical solution (eigenvalue analysis) methods. The disadvantages to the matrix approach are that adding stochasticity and density-dependence often limits the ability for mathematical analysis; density-dependence is represented with aggregate, difficult-to-measure, relationships; all individuals in a life stage are treated as identical; and only a few discrete spatial regions can be represented.

Two general approaches to individual-based modeling are the p-state and i-state methods. The *p*-state approach follows probability distributions of individuals with partial differential equations. The *i*-state approach simulates individuals as discrete units, following thousands of such individuals in simulations. DeAngelis *et al*. (1993) showed that both approaches yield very similar predictions when formulated from the same information. The *p*-state approach is mathematically elegant, while the *i*-state approach is more flexible allowing for greater biological realism. I focus on the *i*-state approach in this presentation. The *i*-state approach is conceptually appealing. The individual is the evolutionary unit in nature, and summing over individuals yields population level behavior. The *i*-state individual-based approach addresses some of the disadvantages of the matrix projection approach. Representation of episodic effects, local interactions, and movement of individuals is relatively easy. Also, the difficult-to-specify density-dependent relation-ships inherent in the matrix approach become emergent properties of the rules imposed on individuals. The disadvantages to the *i*-state individual-based approach are that it is data hungry, computationally intensive, sometimes difficult to validate at the individual level, and due to lack of data, individuals are often assigned the same average values.

I use three examples of upper trophic levels being coupled to lower trophic level or physical models

to illustrate these five issues, and to also illustrate the use of matrix and individual-based modeling. These examples are: walleye pollock, striped bass, and northern anchovy. Hinckley (1999) embedded individual fish as particles into a 3-D hydrodynamics model, and then allowed the individuals to encounter prey via a coupled NPZ model. The model was site-specific, focused on young-of-the-year (YOY) life stages, and was designed to understand recruitment variability. Model results illustrated the benefits of a Lagrangian approach for modeling of upper trophic levels in spatially-explicit grids.

The second example is a model of striped bass population dynamics (Rose *et al.* in prep.), and illustrates a hard-coupling between upper and lower trophic levels. YOY striped bass were simulated using a detailed, individual-based model. This process-based YOY model was coupled to an age-structured matrix projection model for ages 1 to 17 to permit multigenerational simulations. For the YOY model, San Francisco Bay was divided in four coarse spatial boxes. A spatially-detailed hydrodynamics model was used to simulate particle transport for typical low flow and average flow years. Movement of individuals among the four coarse spatial boxes in the YOY model was based on probability transitions estimated from the hydrodynamic simulations. Predicted spatial distributions of YOY in the four boxes agreed with observed spatial distributions. A set of 30-year simulations showed that no single factor could explain the decline in striped bass, but that the combined effects of the multiple factors resulted in a realistic rate of population decline. One of the most controversial aspects of the entire modeling exercise was the density-dependent survival from age-1 to age-3 assumed in the adult matrix model.

The third example is an individual-based, full life cycle model of northern anchovy in the California Bight (Wang *et al.* 1998). This example illustrates a soft-coupling. Individuals were followed from birth to death in a two box model. Movement was simulated using a set of simple rules that were qualitatively based on measured distributions and transport considerations. Typical zooplankton densities for normal and ENSO years were determined from long-term monitoring data, but could also be thought of spatially-averaged output of a NPZ model. Climate change was simulated by increasing the intensity assumed for ENSO conditions, by increasing the frequency of ENSO years, and both combined. While predicted northern anchovy population abundance in 200-year simulations was generally lower under more intense and more frequent ENSO conditions, there were also periods of 10 or more years in which predicted abundances were similar to baseline conditions.

In summary, I presented a brief (and biased) view of how to couple upper trophic levels to lower trophic levels in ecosystem models. The *lessons learned* were:

(1) Highly site-specific models allow easy interpretation of predictions but require a large effort and have questionable generality;

(2) Avoid reliance on intuition, as responses are often not proportional to the magnitude of changes imposed and interactive effects among multiple, time-varying factors are the norm rather than the exception;

(3) Maintain a keen awareness of the capabilities of the model to ensure the formulations are appropriate for addressing the specific questions of interest,

(4) Be flexible and willing to use a suite of models, with each tailored to a particular problem and realize that the obvious way to couple trophic levels may not be the optimal approach; and

(5) Clearly define the question of interest as a hypothesis and then tailor the model or models to the particular problem.

Summary of Nemuro 2000: An international workshop to develop a prototype lower trophic level ecosystem model for comparison of different marine ecosystems in the North Pacific

Bernard A. Megrey[1], Michio J. Kishi[2], Daniel M. Ware[3] and Makoto Kashiwai[4]

[1] National Marine Fisheries Service, Alaska Fisheries Science Center, 7600 Sand Point Way NE, Seattle, WA 98115, U.S.A. E-mail: bern.megrey@noaa.gov
[2] Hokkaido University, Graduate School of Fisheries Sciences, Hakodate, Hokkaido, Japan. 041-8611 E-mail: kishi@coast0.fish.hokudai.ac.jp
[3] Adjunct-Professor, Department of Earth and Ocean Sciences, University of British Columbia. Mailing Address: 3674 Planta Road, Nanaimo, B.C., Canada. V9T 1M2 E-mail: mandd@island.net
[4] Hokkaido National Fisheries Research Institute, Katsurakoi 116, Kushiro, Hokkaido, Japan. 085-0802 E-mail: kashiwai@hnf.affrc.go.jp

An ecosystem model with 11 compartments was developed in order to describe primary and secondary production in the Northern Pacific Ocean. This model was made by the request of the PICES/GLOBEC CCCC Program. Model equations describe the interactions of nitrate, ammonium, silicate, two phytoplankton size fractions (tentatively, these are diatoms and flagellates), three zooplankton size fractions (tentatively, microzooplankton, copepods, and predatory zooplankton), as well as nutrient kinetics. Formulations for the biological processes are based primarily upon process equations presented in Kawamiya *et al.* (1995). A 1-D physical-biological coupled model including a mixed layer closure model (1-D NPZ model) is used to simulate time dependent features of the ecosystem at three locations: Ocean Station P, Station A7 of the Akkeshi line off Hokkaido Island, Japan, and a region in the southeast Bering Sea. Time series of biological dynamics from the biological model as well as time-depth distributions of nutrient and plankton obtained from the 1-D NPZ model for three regions in the North Pacific are compared. This presentation summarized the work and accomplishments of the PICES CCCC/MODEL Task Team Workshop, held in Nemuro, Japan, in January 2000 (see PICES Scientific Report No. 15, and Megrey *et al*. 2000, and for details).

Sensitivity analysis on NEMURO

Michio J. Kishi and Hiroshi Kuroda
Graduate School of Fisheries Sciences, Hokkaido University, Hakodate, Hokkaido, Japan. 041-8611 E-mail: kishi@coast0.fish.hokudai.ac.jp

A sensitivity analysis was performed on the NEMURO/FORTRAN Box model using the Monte Carlo analysis. The ecological parts of the model were run to calculate the nitrogen-based biomass of each compartment until steady state solutions were obtained. Values of each compartment and ecological parameters were stored to be used as the baseline values around which random perturbations were generated and put into the Monte Carlo error analysis. A Monte Carlo error analysis with 600 individual calculations was made with input parameters and initial values perturbed independently over random error distribution with limits of ± 10% of base line values. Principal component analysis (PCA) was used to reduce the 600 sets of output of biological parameters and initial values. The PCA indicated four factors, which together, explained 22% of the variance in the data space. The first principal component, which was clearly related to photosynthesis of PL, accounted for 10% of the data space variance and included the variables

V_{maxS}, V_{maxL}, and PL, $N0_3$, NH_4. The second principal component was related to the zooplankton state variables, ZL and ZS. Based on this sensitivity analysis, we selected five biological parameters to estimate using data from the A-line (off Hokkaido, Japan - outside Oyashio region) and guessed parameter values. We used the conjugate gradient method (FR method) to get the local minimum of the cost function, which is defined by the squared difference between observed and simulated chlorophyll and NO_3.

The cost function is:

$$f = \sum_{i=1}^{N_1} M_1 (PhySn(i) + PhyLn(i) - chla(i))^2 + \sum_{i=1}^{N_2} M_2 (NO_3(i) - NO_3 dat(i))^2 + \sum_{k=1}^{11} M_k^{/} (C_k(1440) - C_k(0))^2$$

The parameters to be estimated were V_{maxS}, V_{maxL}, λ_P, Mor_{ZP0} and $VD2_{N0}$, and the initial values were:

Group A

V_{maxS} = 0.500	(day^{-1})
V_{maxL} = 0.200	(day^{-1})
λ_P = 1.50E+06	(molN/l)
Mor_{ZP0} = 5.00E+04	(day^{-1})
$VD2_{N0}$ = 2.20E-02	(day^{-1})

However, we were unable to find a stable local minimum with the above first guess. Consequently the following values were used as the first guess:

Group B

V_{maxS} = 1.50	(day^{-1})
V_{maxL} = 0.20	(day^{-1})
λ_P = 1.00E+06	(molN/l)
Mor_{ZP0} = 5.85E+04	(day^{-1})
$VD2_{N0}$ = 5.00E-02	(day^{-1})

The parameter values that minimized the cost function were:

Group C

V_{maxS} = 0.206	(day^{-1})
V_{maxL} = 0.184	(day^{-1})
λ_P = 0.668E+06	(molN/l)
Mor_{ZP0} = 5.224E+04	(day^{-1})
$VD2_{N0}$ = 2.151E-02	(day^{-1})

With these values, we calculated the time dependent features of each compartment of the NEMURO/FORTRAN Box model. Two specific examples are presented in Figures 2 and 3. It is clear the results seem much better if the new assimilated parameter values are used. A more detailed analysis will be done in the future.

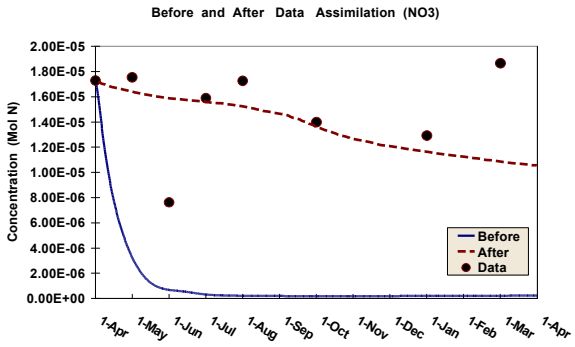

Fig. 2 The time dependent features of NO_3 by the NEMURO/FORTRAN Box model. The blue line shows results with parameter set Group B and the pink line with Group C (assimilated parameters). Dots indicate the mean averaged observed value of the upper 100 m at station A7.

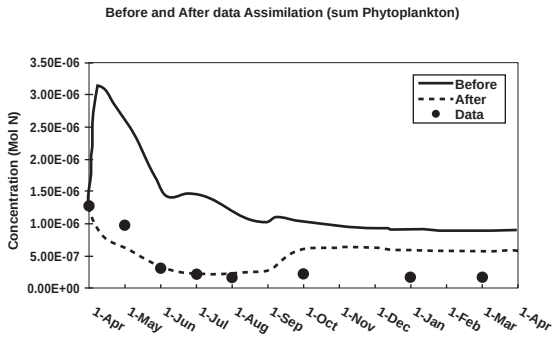

Fig. 3 The time dependent features of PS + PL by the NEMURO/FORTRAN Box model. The blue line shows results with parameter set Group B and the pink line with Group C (assimilated parameters). Dots indicate the mean averaged observed value of the upper 100 m at station A7.

To the physical forcing and the ways of improvements in the NEMURO Model

Vadim V. Navrotsky
Pacific Oceanological Institute, Vladivostok, Russia. 690041 E-mail: navr@online.vladivostok.ru

Supposing we know the behavior of the biological part of an ecosystem with stationary physical conditions, the problem is to define the main physical parameters and the ways of their influence on the ecosystem behavior. In the NEMURO model, the main physical parameter entering almost all equations is temperature, which is calculated with the use of a mixed layer model. Many observations (examples for the northwestern Pacific and Okhotsk Sea are given) show that small-scale fluctuations of the temperature gradient vertical structure (fine-structure FS and microstructure MS) are important as for vertical distribution of plankton, and for its integral biomass. Mechanisms of FS and MS influence on phytoplankton and zooplankton production may be different, but as a first approximation we propose to use an additional coefficient proportional to *rms* of the vertical temperature fluctuations in the layer studied (0-330 m) in all temperature-dependent terms. The values of *rms* can easily be obtained from observations (XBT, for example), and a model is proposed that helps to evaluate them.

Some additional improvements in the model are discussed, including: 1) time-lag in the dependence between zooplankton and phytoplankton concentrations; 2) adjusting averaging scales to the intrinsic (biological) and forced (physical) time scales; 3) interdependence between input parameters; and 4) criteria for comparisons between models and observations.

Summary of extensions to the NEMURO/MATLAB Box Model developed at the Hakodate PICES Meeting

David L. Eslinger[1], Daniel M. Ware[2], **Francisco E. Werner[3]** and Bernard A. Megrey[4]

[1] Coastal Remote Sensing Program, NOAA Coastal Services Center, 2234 South Hobson Avenue, Charleston, SC 29405-2413, U.S.A. E-mail: dave.eslinger@noaa.gov

[2] Adjunct-Professor, Department of Earth and Ocean Sciences, University of British Columbia. Mailing address: 3674 Planta Road, Nanaimo, B.C., Canada. V9T 1M2 E-mail: mandd@island.net

[3] Marine Sciences Department, CB# 3300, University of North Carolina, Chapel Hill, NC 27599-3300, U.S.A. E-mail: cisco@email.unc.edu

[4] National Marine Fisheries Service, Alaska Fisheries Science Center, 7600 Sand Point Way NE, Seattle, WA 98115, U.S.A. E-mail: bern.megrey@noaa.gov

Discussion and extensions to the NEMURO/ MATLAB Box model at the Hakodate Workshop and the months that followed included three main components: development of diagnostics and comparison to observed and literature values, effect of vertical migration by large zooplankton, and the inclusion of an approximation to a microbial loop formulation. Results of these experiments, which are summarized below, are presented for the Station P location.

Diagnostics of NEMURO at Station P

To quantify the results of the NEMURO/ MATLAB Box model at Station P, we developed a series of diagnostic measures including daily production/biomass ratios (P/B) for phytoplankton and zooplankton, and food consumption/biomass ratios (C/B) for small, large and predatory zooplankton and the ecotrophic efficiency (EE), a measure of how much primary production transfers to the zooplankton species. A brief description of the procedures and results is given below.

1. Output for the 8th year from the model was post-processed to calculate a number of variables: daily P/B ratios for phytoplankton and zooplankton, and C/B ratios for small, large and predatory zooplankton and the ecotrophic efficiency.
2. The P/B, C/B and EE are calculated as follows:

NPPS=GppPSn-ResPSn – Net Primary Production for small phytoplankton
NPPL=GppPLn-ResPLn – Net Primary Production for large phytoplankton
NCZS=GraPS2ZSn+GraPL2ZSn – Net Consumption for small zooplankton
NCZL=GraPS2ZLn+GraPL2ZLn+GraZS2ZLn – Net Consumption for large zooplankton
NCZP=GraPL2ZPn+GraZS2ZPn+GraZL2ZPn – Net Consumption for predatory zooplankton
TNPP=NPPS+NPPL – Total Net Primary Production
TGPP=GraPS2ZSn+GraPS2ZLn+GraPL2ZLn+GraPL2ZPn – Total Gross Primary Production
NPZS=NCZS-ExcZSn-EgeZSn – Net Production for small zooplankton
NPZL=NCZL-ExcZLn-EgeZLn – Net Production for large zooplankton
NPZP=NCZP-ExcZPn-EgeZPn – Net Production for predatory zooplankton
P2BPS=NPPS/PS – Production/Biomass Ratio for small phytoplankton
P2BPL=NPPL/PL – Production/Biomass Ratio for large phytoplankton
P2BZS=NPZS/ZS – Production/Biomass Ratio for small zooplankton
P2BZL=NPZL/ZL – Production/Biomass Ratio for large zooplankton
P2BZP=NPZP/ZP – Production/Biomass Ratio for predatory zooplankton
C2BZS=NCZS/ZS – Consumption/Biomass Ratio for small zooplankton
C2BZL=NCZL/ZL – Consumption/Biomass Ratio for large zooplankton
C2BZP=NCZP/ZP – Consumption/Biomass Ratio for predatory zooplankton
EE=TGPP/TNPP – Ecotrophic Efficiency (all zooplankton)
EEZLZP=(TGPP-GraPS2Zsn)/TNPP – EE for large and predatory zooplankton only

Table 1 Results of NEMURO/MATLAB Box model simulations.

Variable	Group	Model Value	Empirical Value	Source
P/B daily P/B annual B mean	PS	0.108-0.636 /d mean = 0.355/d ~ 0.12		
P/B daily P/B annual B mean	PL	0.032-0.212/d mean = 0.116/d ~0.11		
P/B daily P/B annual B mean	ZS	0.081-0.222/d mean = 0.134/d ~0.055		
P/B daily P/B annual B mean	ZL	0.026-0.127/d mean = 0.065/d ~0.055		
P/B daily P/B annual B mean	ZP	0.001-0.015/d mean = 0.007/d ~0.08		
C/B	ZS	0.387-1.06/d mean = 0.639/d		
C/B	ZL	0.124-0.604/d mean = 0.308/d		
C/B	ZP	0.004-0.070/d mean = 0.033/d		

Table 2 Comparison of NEMURO/MATLAB Box model results to empirical estimates.

Variable	Group	P/C	Empirical	Source
P/C	ZS	0.21	0.2-0.3	Straile 1997
P/C	ZL	0.21	0.2-0.3	Straile 1997
P/C	ZP	0.21		

Results

Simulation results (Fig. 4) show that there is a small spring bloom of large phytoplankton (PL) (which peaked at a level of about 3× the average biomass around time year 8.2 (or day 73 or March 13)). This bloom is an artifact of the "box" nature of the model. The addition of a process to "activate" grazing by the large zooplankton (ZL) when the large phytoplankton begin to bloom is discussed later in this report.

Figure 5 shows the P/B, C/B, and P/C (production/ consumption) ratios. Additional model result summaries are presented in Tables 1 and 2 from the model output for year 8. In this case, the P/B ratio= specific growth rate (daily), the P/C ratio= growth efficiency, and B= annual mean biomass (μmolN/l).

Recently, several methods have been used to estimate the annual primary production (Annual PP) around Station P. The bold values in Table 3 are based on direct measurements and therefore are probably more accurate. Calculated values from NEMURO are given in Tables 4 and 5 using conversion factors from Table 6. A comparison of model output and diagnostics to field measurements can be summarized as follows:

1. The C/B and P/C ratios are reasonable (Tables 1 and 2).
2. The annual primary production in the model (128 $gC/m^2/yr$) is only 8% lower than the best current estimate (Table 3 - 140 $gC/m^2/yr$).
3. The average chlorophyll concentration at Station P in the model (Table 5 - 0.36 mg/m^3 is only 10% lower than the long-term value (0.4 mg/m^3) measured by Wong *et al.* (1995) (Table 7).
4. An approximate f-ratio can be estimated from the annual productivity of PL / Total primary production (Table 7). This estimate assumes that the production of the large phytoplankton (PL) is primarily fuelled by "new" nitrogen (NO_3) with "f-ratio"= 29.5/128 = 0.23. Wong *et al.* (1995) estimated an f-ratio of 0.25. So the agreement is good.

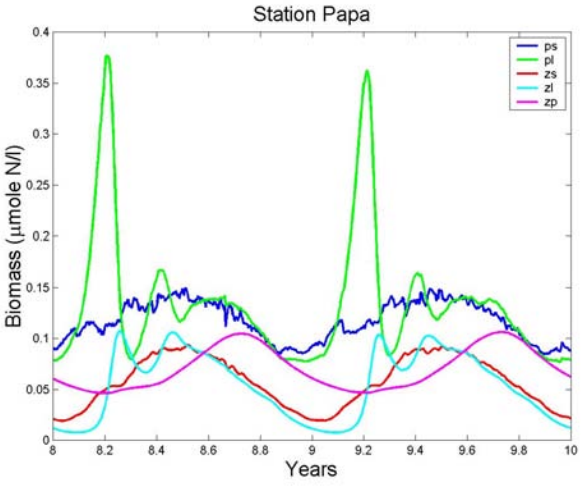

Fig. 4 NEMURO model base-case solution at Ocean Station Papa.

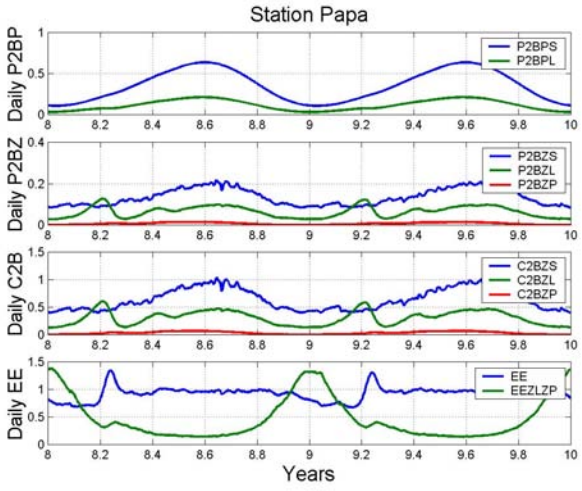

Fig. 5 P/B (production / biomass), C/B (consumption / biomass), P/C (production / consumption) ratios and Ecotrophic Efficiency.

Table 3 Estimates of Station P primary production.

Method	Average Daily PP ($gC/m^2/d$)	Annual PP ($gC/m^2/yr$)	Source
C14		**140**	Wong *et al.* 1995
Nitrate depletion		**133**	Wong *et al.* 1995
Particle flux		**120**	Wong *et al.* 1995
Chl *a*	0.55	199	Longhurst *et al.* 1995
Secchi disc data		167	Falkowski and Wilson 1992

Table 4 Average annual biomass (B1-B4), P/B, and annual primary production (PP) for PS and PL.

Group	B1 µmolN/l	B2 µmolC/l	B3 gC/m^3	B4 gC/m^2	P/B d^{-1}	PP $gC/m^2/yr$
PS	0.12	0.792	0.0095	0.760	0.355	98.5
PL	0.11	0.726	0.0087	0.697	0.116	29.5
PS + PL	0.23	1.518	0.0182	1.457		128

Calculations:

1. B2 = 6.6 (Redfield ratio) × B1
2. B3 = 0.012 × B2 (Table 6)
3. B4 = 80 m × B3 (Table 7)
4. PP = P/B × B4 × 365 d

Table 5 Average chlorophyll-*a* concentration of PS and PL.

Group	B3 gC/m^3	C/Chl *a*	Chl *a* mg/m^3
PS	0.0095	50	0.19
PL	0.0087	50	0.17
PS + PL	0.0182	50	0.36

Table 6 Conversion factors.

Variable	Value	Source
C/N (Redfield)	6.6	Wong *et al.* 1995
C/N	7.8	Kawamiya *et al.* 1997
N/Chl *a*	7.5	Kawamiya *et al.* 1997
C/Chl *a*	50	Kawamiya *et al.* 1997

Table 7 Station P Characteristics.

Variable	Value	Source
Euphotic zone	80 m	Wong *et al.* 1995
Average Chl *a* (annual)	0.4 mg/m^3 (µg/L)	Wong *et al.* 1995
f-ratio	0.25	Wong *et al.* 1995
f-ratio (summer)	0.25-0.52	Wong *et al.* 1998

Inclusion of microbial loop: sensitivity studies to climate change

Under certain scenarios, it is possible that changes in climate could lead to differences in the amount of primary production passing through the microbial loop. For example, an increase in stratification – due to increased freshwater inputs or higher temperatures – may reduce the nutrient entrainment to the euphotic zone, shifting the pelagic foodweb toward smaller species. We have modified the NEMURO/MATLAB Box model to include an approximation to a microbial loop as described in Megrey *et al.* (2000) and its possible effects on higher trophic levels. Using the same variable names as in Megrey *et al.* (2000), our simplified paramaterization of the microbial food web, which is included in the variable BetaZS is:

$$BetaZS = 0.3^{(1+\ PhySn/(PhySn+PhyLn))}$$

This means that the gross growth efficiency of the small zooplankton can vary between 0.3 and 0.09, and will probably average about 0.16 over the year at Station P. For the base model run, a constant BetaZS=0.3 was used. We found (Fig. 6) that the inclusion of a microbial loop has only a small impact on the standing stocks of small and large zooplankton, but reduces predatory zooplankton standing stocks by about one half. These differences are due to the decreased net trophic efficiency of the system when a large portion of the primary production passes through a microbial community before entering the zooplankton community. With the decreased predatory zooplankton biomass, there is only half as much biomass potentially available for fisheries production.

Vertical migration by large zooplankton: sensitivity studies

At Station P, during spring, the large zooplankton component (ZP) should be dominated by *Calanus/Neocalanus* spp. These species exhibit a strong ontogenetic migration: they arrive in the upper layers in early spring at C1 (and older) copepodites and feed for about 60 days until descending from the surface layer as C5's. Therefore, the model population should increase in

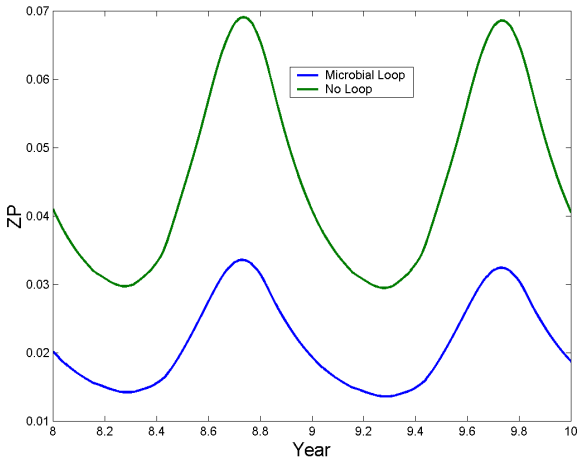

Fig. 6 Predatory zooplankton biomass (in µM N/m^3) for two years with (blue line) and without (green line) the inclusion of a microbial loop.

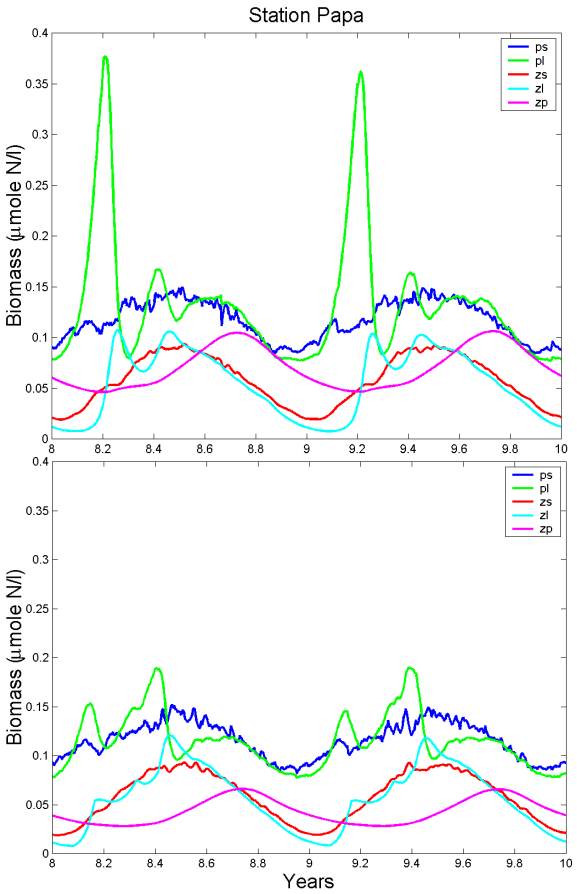

Fig. 7 Sensitivity at Station P to migration of large zooplankton (ZP). Without migration of ZP (top panel) the diatom bloom (PL) is close to twice as large as in the presence of ZP migration (bottom panel).

biomass in the early spring independent of food availability/grazing. Later in the year, the population should decrease by some amount to simulate the descent of the C5's. To explore this effect, we modified the model as follows. Over a certain time (between days-of-the-year 30 and 60), we increased the large zooplankton population five-fold. The increased population would be available to graze on the diatoms. Other dynamics occur as normal. After 60 more days, we begin decreasing the large zooplankton population by one half over 30 days (between days 120 and 150). Again, other dynamics are unchanged. Figure 7 shows results with and without migration. In the case of migration, the diatom (PL-large phytoplankton) bloom is much reduced. The estimates of Ecotropic Efficiency (not shown) are not significantly affected.

NEMURO Model follow up

Yasuhiro Yamanaka[1, 2]

[1] Graduate School of Environmental Earth Science, Hokkaido University, N10W5 Kita-Ku, Sapporo, Japan. 060-0810 E-mail: galapen@ees.hokudai.ac.jp

[2] Global Warming Research Program, Frontier Research System for Global Change, Shibaura 1-2-1, Minato-Ku, Tokyo, Japan. 105-6791

The model presented is based on the NEMURO / 1-D Yamanaka Model described in Megrey *et al.* (2000), but it is extended to 15 compartments including silica and carbon cycles. The extended model is applied to Station A7 offshore of Hokkaido Island (41°30' N, 145°30' E), in the northwestern Pacific, which is one of the stations along the A-line where the Hokkaido National Fisheries Research Institute has been conducting surveys 5-7 times each year from 1987 to 2000. The model successfully simulates the observed spring diatom blooms and large annual variation of chlorophyll-*a*. A comparison between cases with/without silicate limitation shows that the silicate limitation causes the decease of primary production by diatoms in the summer and the transition of phytoplankton species between diatoms and others.

Model description

The model and boundary conditions in this study are exactly the same as the NEMURO/1-D Yamanaka model or that in Kishi *et al.* (2001), except the original 11 compartments describing the biological processes where changed into 15. Figure 8 shows interactions among the 15 compartments in the biological processes. We divide phytoplankton and zooplankton into two categories, respectively: large phytoplankton (PL) and small phytoplankton (PS), large zooplankton (ZL) and small zooplankton (ZS). ZL represents copepods with seasonal vertical migration, i.e., coming up to upper layer in spring, becoming adults and grazing on other plankton, and then returning to the deep layer in fall. This treatment is similar to that in Kishi *et al.* (2001). ZS represents the others. PL is diatoms which make siliceous shells from silicate in the water. Therefore, the nutrient limitations for photosynthesis by PL are not only nitrogen but also silicate in the water, which are not taken into account in Kishi *et al.* (2001). PS represents the other phytoplankton, non-diatom and flagellate. Some of PS and ZS are regarded as coccolith and foraminifera, which have calcarious shells, respectively. Predatory zooplankton (ZP) represents something like euphausiids grazing on other plankton, which connect the lower trophic level food chain to the higher trophic levels such as fishes, following discussions at the PICES MODEL Workshop in Nemuro. The model also has three nutrients, nitrate (NO_3), ammonium (NH_4), and silicate ($Si(OH)_4$), particulate organic matter (POM), dissolved organic matter (DOM), Opal, calcium carbonate ($CaCO_3$). Calcium (Ca) in the sea water is taken into account, in order to calculate total alkalinity (TAlk) using the concentrations of NO_3, $Si(OH)_4$, Ca following the TAlk definition. Total carbon (TCO_2) is obtained with assumption that all plankton have the same C/N stoichiometry as classical Redfield ratio, 106/16.

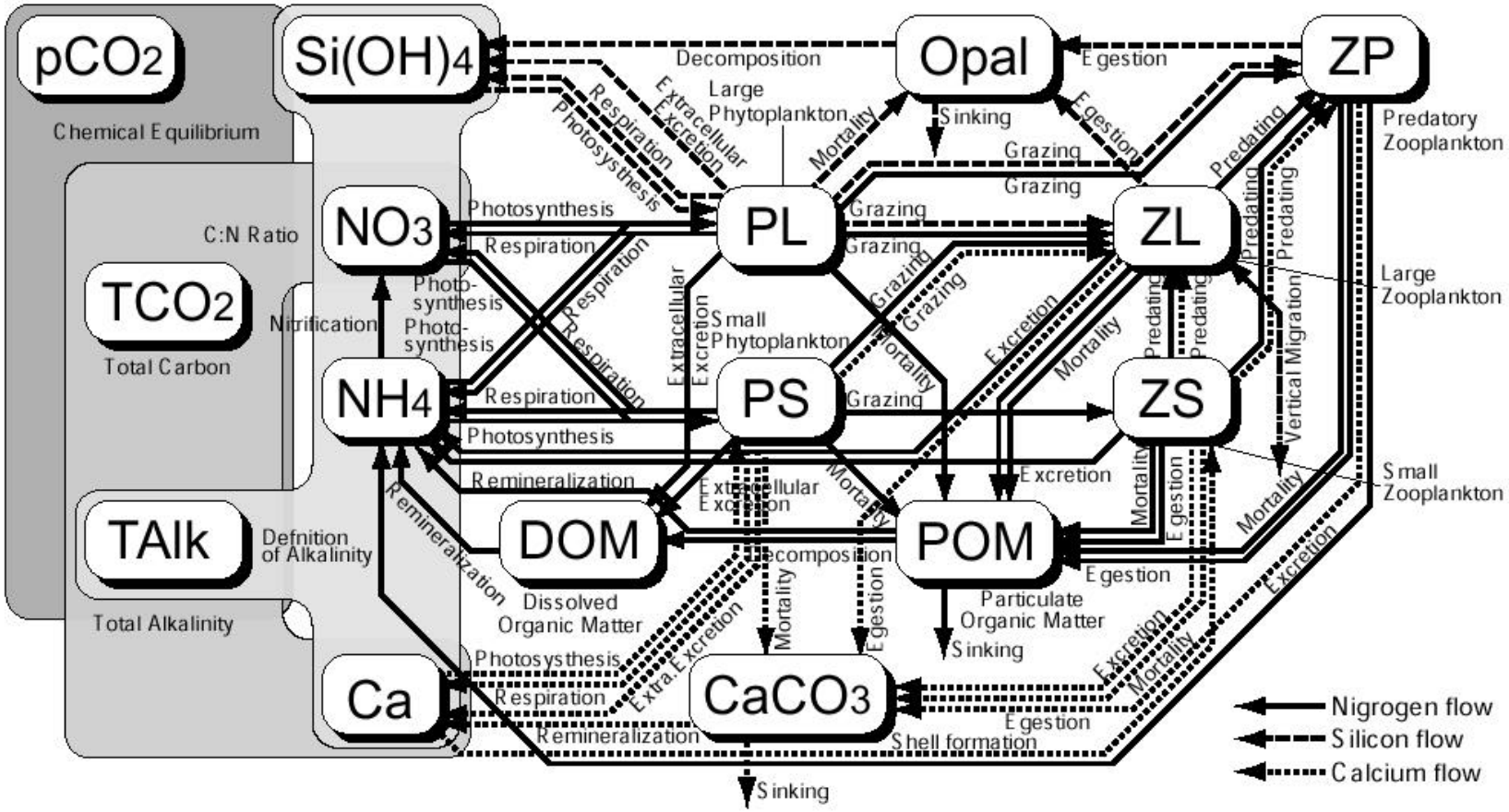

Fig. 8 Interactions among 15 compartments for a modification of the NEMURO/1-D Yamanaka Model.

Table 8 Biological parameters used in the model.

V_{maxS}	Small Phytoplankton Maxium Photosynthetic Rate at 0°C	0.4	/day
$K_{\mathrm{NO_3S}}$	Small Phytoplankton Half Saturation Constant for Nitrate	1.0	μmolN/l
$K_{\mathrm{NH_4S}}$	Small Phytoplankton Half Saturation Constant for Ammonium	0.1	μmolN/l
Ψ_{S}	Small Phytoplankton Ammonium Inhibition Coefficient	1.5	l/μmolN
k_{S}	Small Phytoplankton Temperature Coefficient for Photosynthetic Rate	0.0693	/°C
I_{optS}	Small Phytoplankton Optimum Light Intensity	104.7	W/m^2
M_{PS0}	Small Phytoplankton Mortality Rate at 0°C	0.0585	l/μmolN day
k_{MPS}	Small Phytoplankton Temperature Coefficient for Mortality	0.0693	/°C
R_{PS0}	Small Phytoplankton Respiration Rate at 0°C	0.03	/day
k_{RS}	Small Phytoplankton Temperature Coefficient for Respiration	0.0519	/°C
γ_{S}	Small Phytoplankton Ratio of Extracellular Excretion to Photosynthesis	0.135	(Nodim)
V_{maxL}	Large Phytoplankton Maxium Photosynthetic Rate at 0°C	0.8	/day
$K_{\mathrm{NO_3L}}$	Large Phytoplankton Half Saturation Constant for Nitrate	3.0	μmolN/l
$K_{\mathrm{NH_4L}}$	Large Phytoplankton Half Saturation Constant for Ammonium	0.3	μmolN/l
K_{SiL}	Large Phytoplankton Half Saturation Constant for Silicate	6.0	μmolSi/l
Ψ_{L}	Large Phytoplankton Ammonium Inhibition Coefficient	1.5	l/μmolN
k_{L}	Large Phytoplankton Temperature Coefficient for Photosynthetic Rate	0.0693	/°C
I_{optL}	Large Phytoplankton Optimum Light Intensity	104.7	W/m^2
M_{PL0}	Large Phytoplankton Mortality Rate at 0°C	0.029	l/μmolN day
k_{MPL}	Large Phytoplankton Temperature Coefficient for Mortality	0.0693	/°C
R_{PL0}	Large Phytoplankton Respiration Rate at 0°C	0.03	/day
k_{RL}	Large Phytoplankton Temperature Coefficient for Respiration	0.0519	/°C
γ_{L}	Large Phytoplankton Ratio of Extracellular Excretion to Photosynthesis	0.135	(Nodim)
G_{RmaxS}	Small Zooplankton Maxium Grazing Rate at 0°C	0.4	/day
k_{GS}	Small Zooplankton Temperature Coefficient for Grazing	0.0693	/°C
λ_{S}	Small Zooplankton Ivlev Constant	1.4	l/μmolN
$\mathrm{PS}^*_{\mathrm{ZS}}$	Small Zooplankton Threshold Value for Grazing Small Phytoplankton	0.043	μmolN/l
α_{ZS}	Small Zooplankton Assimilation Efficiency	0.7	(Nodim)
β_{ZS}	Small Zooplankton Growth Efficiency	0.3	(Nodim)
M_{ZS0}	Small Zooplankton Mortality Rate at 0°C	0.0585	l/μmolN day
k_{ZS}	Small Zooplankton Temperature Coefficient for Mortality	0.0693	/°C
$G_{\mathrm{RmaxL,PS}}$	Large Zooplankton Maxium Rate of Grazing Small Phytoplankton at 0°C	0.1	/day
$G_{\mathrm{RmaxL,PL}}$	Large Zooplankton Maxium Rate of Grazing Large Phytoplankton at 0°C	0.4	/day
$G_{\mathrm{RmaxL,ZS}}$	Large Zooplankton Maxium Rate of Predating Small Zooplankton at 0°C	0.4	/day
k_{GL}	Large Zooplankton Temperature Coefficient for Grazing	0.0693	/°C
λ_{L}	Large Zooplankton Ivlev Constant	1.4	l/μmolN
$\mathrm{PS}^*_{\mathrm{ZL}}$	Large Zooplankton Threshold Value for Grazing Small Phytoplankton	0.04	μmolN/l
$\mathrm{PL}^*_{\mathrm{ZL}}$	Large Zooplankton Threshold Value for Grazing Large Phytoplankton	0.04	μmolN/l
$\mathrm{ZS}^*_{\mathrm{ZL}}$	Large Zooplankton Threshold Value for Predating Small Zooplankton	0.04	μmolN/l
α_{ZL}	Large Zooplankton Assimilation Efficiency	0.7	(Nodim)
β_{ZL}	Large Zooplankton Growth Efficiency	0.3	(Nodim)
M_{ZL0}	Large Zooplankton Mortality Rate at 0°C	0.0585	l/μmolN day
k_{ZL}	Large Zooplankton Temperature Coefficient for Mortality	0.0693	/°C

Table 8 (*continued*)

$G_{\mathrm{RmaxP,PL}}$	Predatory Zooplankton Maxium Rate of Grazing Large Phytoplankton at 0°C	0.2	/day
$G_{\mathrm{RmaxP,ZS}}$	Predatory Zooplankton Maxium Rate of Predating Small Zooplankton at 0°C	0.2	/day
$G_{\mathrm{RmaxP,ZL}}$	Predatory Zooplankton Maxium Rate of Predating Large Zooplankton at 0°C	0.2	/day
k_{GP}	Predatory Zooplankton Temperature Coefficient for Grazing	0.0693	/°C
λ_{P}	Predatory Zooplankton Ivlev Constant	1.4	l/μmolN
$\mathrm{PL}^{*}_{\mathrm{ZP}}$	Predatory Zooplankton Threshold Value for Grazing Large Phytoplankton	0.04	μmolN/l
$\mathrm{ZS}^{*}_{\mathrm{ZP}}$	Predatory Zooplankton Threshold Value for Predating Small Zooplankton	0.04	μmolN/l
$\mathrm{ZL}^{*}_{\mathrm{ZP}}$	Predatory Zooplankton Threshold Value for Predating Large Zooplankton	0.04	μmolN/l
Ψ_{PL}	Predatory Zooplankton Preference Coefficient for Large Phytoplankton	4.605	l/μmolN
Ψ_{ZS}	Predatory Zooplankton Preference Coefficient for Small Zooplankton	3.010	l/μmolN
α_{ZP}	Predatory Zooplankton Assimilation Efficiency	0.7	(Nodim)
β_{ZP}	Predatory Zooplankton Growth Efficiency	0.3	(Nodim)
M_{ZP0}	Predatory Zooplankton Mortality Rate at 0°C	0.0585	l/μmolN day
k_{ZP}	Predatory Zooplankton Temperature Coefficient for Mortality	0.0693	/°C
α_1	Light Dissipation Coefficient of Sea Water	0.04	/m
α_2	Self Shading Coefficient	0.04	l/μmolN m
N_{Nit0}	Nitrification Rate at 0°C	0.03	/day
k_{Nit}	Temperature Coefficient for Nitrification	0.0693	/°C
S_{POM}	POM Sinking Velocity	40.0	m/day
V_{PA0}	Decomposition Rate of POM to Ammonium at 0°C	0.100	/day
k_{PA}	Temperature Coefficient for POM Decomposition to Ammonium	0.0693	/°C
V_{PD0}	Decomposition Rate of POM to DOM at 0°C	0.100	/day
k_{PD}	Temperature Coefficient for POM Decomposition to DOM	0.0693	/°C
V_{DA0}	Decomposition Rate of DOM at 0°C	0.200	/day
k_{DA}	Temperature Coefficient for DOM Decomposition	0.0693	/°C
S_{Opal}	Opal Sinking Velocity	40.0	m/day
V_{Opal}	Decomposition Rate of Opal at 0°C	0.100	/day
k_{Opal}	Temperature Coefficient for Opal Decomposition	0.0693	/°C
$S_{\mathrm{CaCO_3}}$	Calcium Carbonate Sinking Velocity	40.0	m/day
$V_{\mathrm{CaCO_3}}$	Decomposition Rate of Calcium Carbonate at 0°C	0.050	/day
$k_{\mathrm{CaCO_3}}$	Temperature Coefficient for Calcium Carbonate Decomposition	0.0693	/°C
R_{CN}	Stoichiometry of Carbon to Nitrogen	6.625	(Nodim)
R_{SiN}	Large Plankton Stoichiometry of Silicon to Nitrogen	2.0	(Nodim)
R_{coco}	Ratio of Cocolithophorids to Small Phytoplankton	0.1	(Nodim)
R_{fora}	Ratio of Foraminifera to Small Zooplankton	0.1	(Nodim)
R_{Cco}	Ratio of Inorganic Carbon to Total Carbon in Cocolithophorids	0.5	(Nodim)
R_{Cfo}	Ratio of Inorganic Carbon to Total Carbon in Foraminifera	0.5	(Nodim)

The 15 compartments described above, PL, PS, ZL, ZS, ZP, NO_3, NH_4, $Si(OH)_4$, POM, DOM, Opal, $CaCO_3$, Ca, TAlk, and TCO_2, are calculated as prognostic variables. The partial pressure of carbon dioxide (pCO_2) in the ocean surface is obtained from the TAlk and TCO_2 under the chemical equilibrium at each time step. The silica cycle coupled with the nitrogen cycle accounted for in the photosynthesis process by PL affects the ecosystem dynamics. On the other hand, carbon and calcium cycles do not affect ecosystem dynamics because carbon and calcium are plentiful in the water and do not limit primary production. Parameters used in this study are shown in Table 8. Most parameters are based on Kishi *et al.* (2001) and NEMURO, although some parameters, V_{maxL}, K_{NH4L}, K_{SiL}, V_{maxS}, and K_{NO3S}, are tuned to reproduce the observed data, as discussed in parameter studies (Yoshie *et al.* in preparation).

We use the coupled ecosystem model mentioned above with physical model, vertical one-dimensional model with mixed layer closure scheme, used in Kishi *et al.* (2001). Boundary conditions, SST, SSS, wind stress, solar radiation, are the same as described in Kishi *et al.* (2001). Time integration is performed for ten years using data of 1991, and after that actual forcing from 1991 to 1996.

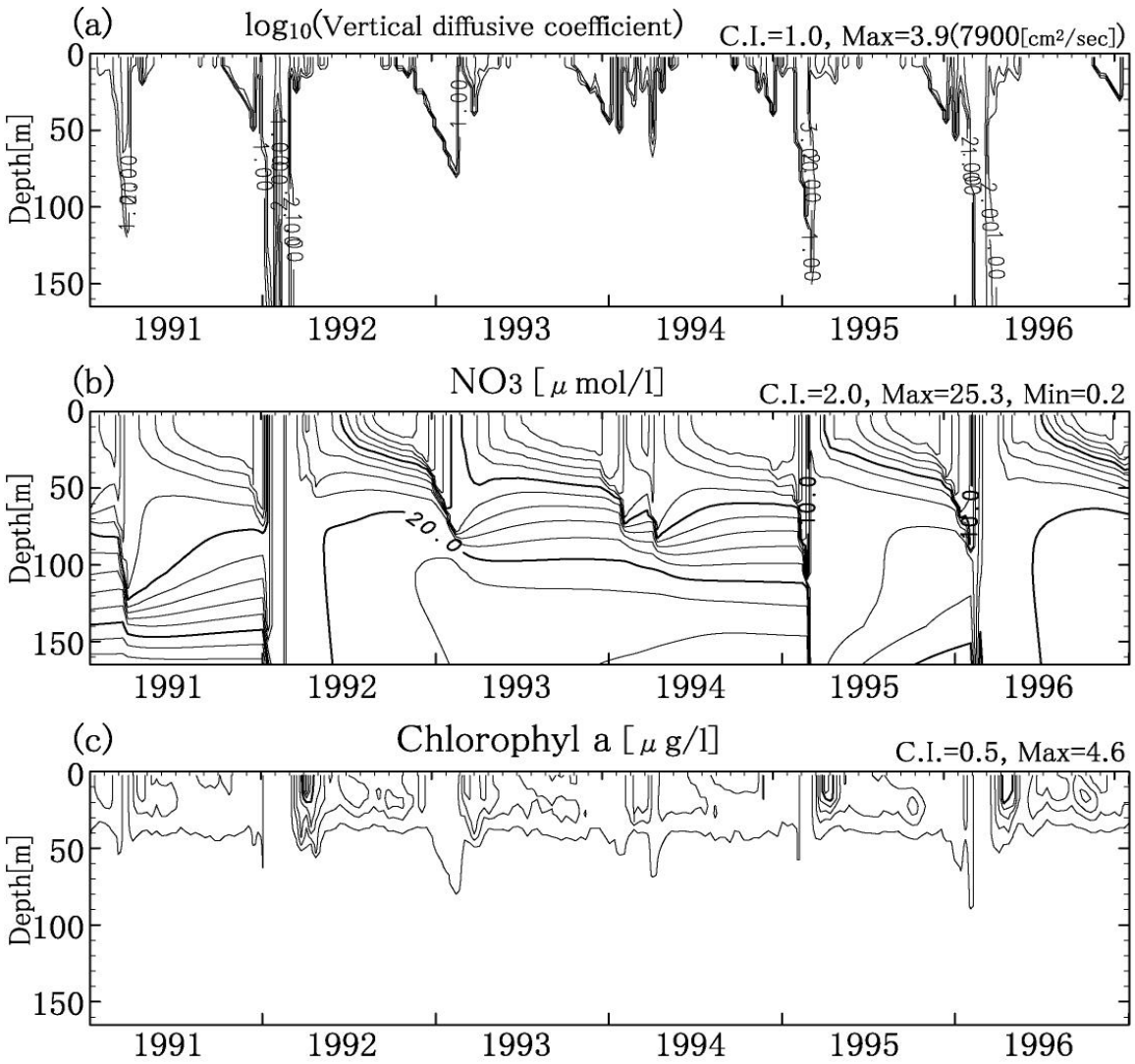

Fig. 9 Vertical distributions of (a) vertical diffusive coefficient, (b) nitrate concentration, and (c) chlorophyll-*a* concentration from 1991 to 1996.

Results

Figure 9 shows vertical distributions of vertical diffusive coefficient A_{HV}, nitrate concentration, and chlorophyll-*a* concentration from 1991 to 1996. Areas of high A_{HV} represent the mixed layer with seasonal changes. Deep convections in winter penetrated deeper than 160 m depths in 1992 and 1996. The nitrate-laden waters of almost 20 $x10^{-6}$ mol/l are supplied to the ocean surface associated with winter convections and cause a strong spring bloom by diatoms after winter. In 1992, the maximum value of chlorophyll-*a* concentration reaches $4.6x10^{-6}$ mol/l, which compares well with observed values during the spring bloom period. On the other hand, in 1993 or 1994, winter convections penetrated to around 70 m and the spring bloom was very weak. In summer, nutrients in the surface are exhausted and the maximum layer of chlorophyll-*a* concentration is located around 30 m. The model successfully reproduces the observed seasonal variations of nitrate, silicate, and chlorophyll-*a*, although the model cannot reproduce effects of horizontal advection/diffusion due to meso-scale eddy effects on nutrient and chlorophyll-*a* concentrations.

Figure 10a shows primary production by PL and PS and partial pressure of CO_2. The light solid line, primary production by diatoms, has highest

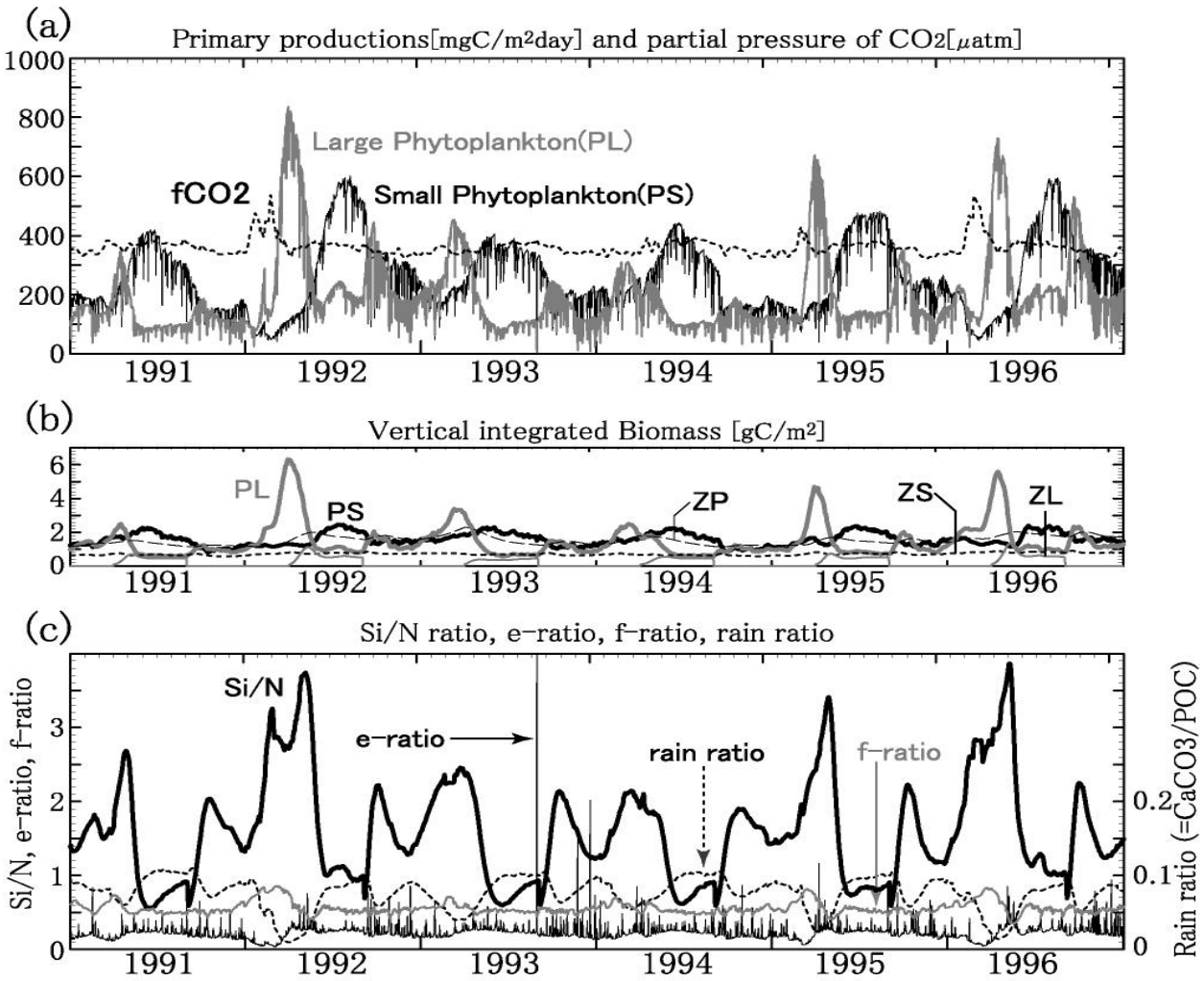

Fig. 10 Primary production by PL and PS, and partial pressure of CO_2 (a), vertically integrated biomasses of PS, PL, ZS, ZL, and ZP (b), and f-ratio, e-ratio, Si/N ratio, rain ratio (c) from 1991 to 1996.

peak in spring and the second highest peak in the fall. The spring bloom reaches 600 to 800 mg C/m^{2}day in 1992, 1995, and 1996, which compares well with observed levels. The spring bloom of diatoms has large annual variation, and the spring bloom in 1991 and 1994 is weak. The cessation of the spring bloom of diatoms is associated with increasing grazing pressure by copepods, although both nitrate and silicate in the surface water still remain over 10 x10^{-6} mol/l at the end of bloom. After the diatom bloom, primary production by PS increases, an often observed transition of species from diatoms to flagellates, and nitrate in the surface water is exhausted at the end of summer. Many frequent downward spikes of primary production's lines in Figure 10a can be seen. These represent decreases of primary production due to decreasing solar radiation on rainy or cloudy days. The partial pressure of carbon dioxide has a maximum associated with winter convection, rapidly decreases due to the spring bloom, and is kept almost constant, canceling out the temperature effect and biological production effect.

A dark thick line in Figure 10c shows Si/N ratio obtained from downward fluxes of opal and POM at depth of 100 m. The water supplied from the deep layer has a Si/N ratio of 1.7. Si/N ratios have large seasonal variations: about 3.0 in winter and spring, and about 1.0 in summer, although the total time average of the Si/N ratio in total settling particles is equal to 1.7. It looks inconsistent that a Si/N ratio of 3.0 is greater than the stoichiometry

of diatoms, i.e., Si/N ratio of 2.0. However, when copepods (ZL) and euphausiids (ZP) graze on diatoms, shells of diatoms are quickly discarded as settling opal and exported out of the euphotic layer. On the other hand, the soft tissue of diatoms become some of their bodies or DOM and nitrogen is recycled in the euphotic layer. Therefore, Si/N ratio takes a higher value than the stoichiometry of diatoms.

A light thin line in Figure 10c shows f-ratio, ratio of nitrate uptake to nitrogen uptake in the photosynthetic processes of PL and PS. The f-ratio is highest, 0.8, at the start of spring bloom, which is due to nitrate supply from the deep water associated with the winter deep convection, then decreases rapidly due to increase of ammonium and a decrease of nitrate as a result of the spring bloom, and takes a minimum of 0.3 (see f-ratio in 1996). In the other season, the f-ratio is kept almost constant at about 0.5. The e-ratio (a thin solid line), which is the ratio of downward flux due to POM to primary production, is smaller than 0.3, except for spikes due to small primary productions on bad weather days. The e-ratio is smaller by the factor of 2-3 than f-ratio, because POM is dissolved in the euphotic layer, and because organic matters directly returns to ammonium and nitrate by extracellular excretion and is quickly recycled. The rain ratio (a broken line in Fig. 10c), ratio of calcium carbonate flux to POC's at 100 m depths, is 0.01 to 0.11, which has the maximum in summer and minimum during the spring bloom.

A new approach to the modeling of marine ecosystems

Vladimir I. Zvalinsky
Pacific Oceanological Institute, 43 Baltiyskaya Street, Vladivostok, Russia. 690041 E-mail: biomar@mail.ru

The existing approaches to mathematical modeling of marine ecosystems are undergoing a crisis. This situation was evident to some extent in all reports concerning descriptions of the ecosystem function. At the MODEL Workshop in Nemuro this was also evident: it has left unsolved problems such as the limitation by additional environmental factors into the primary link (except light, nitrogen, and silicon), in particular, by Fe; as well as including the microbial link into the ecosystem. The problem of including higher trophic levels into the ecosystem has not been solved. The practical workers have proposed new questions such as splitting some trophic links into age groups, the behavior of which differs greatly.

The MODEL Task Team has done a lot of work. It has developed the Prototype Lower Trophic Level Ecosystem Model (NEMURO, Eslinger *et al.* 2000), which is a generalization of practically all of the most important developments on modeling marine ecosystems available in the published literature (Fasham *et al.* 1995; Kawamiya *et al.* 1997; Oguz *et al.* 1999). Due to this, the NEMURO model possesses both advantages and deficiencies typical of such models. That is why, in our opinion, the NEMURO model has significant difficulties in solving the problems described above.

The main problem in modern modeling of marine ecosystems is related to the fact that the approach to modeling is based on empirical models of each biological process, and, consequently, the ecosystem as a whole. The existing models do not involve the mechanisms of the biological processes.

From a strictly mathematical point of view, it is not important by which functions, empirical or those based on mechanism, to describe different processes. It is important that these functions reflect the real processes quite well. Still it is known that the empirical approaches are not only limited in application, but they do not make it possible to understand real processes, and, consequently, they do not possess the perspectives for the development of modeling.

The 20th century, especially the second half, is marked by the greatest discoveries in biophysics, biochemistry and physiology of organisms in general, and plants in particular. For example, in the field of primary production, being discovered were the carbon Calvin's cycle, two photosystems of photosynthesis, the water splitting system, photosynthetic and respiration electron-transport chains, cyclic and non-cyclic photo-phosphorylation, and photorespiration, (Edwards and Walker 1983; Goodwin and Mercer 1983). The peculiarities of carbon and nitrogen, phosphorus metabolism, and their interrelation were investigated; and the role of macro- and microelements in formation of primary production has been stated. An important achievement is establishing the fact that the biological processes present themselves as the chains and nets of coupling cyclic (in particular, enzymatic) interactions (Goodwin and Mercer 1983). These non-disputable facts are not presented in the most recent models of marine ecosystems.

The difficulties of analysis of mass fluxes for modeling of ecosystems are conditioned by non-homogeneity of the processes and structures forming the hierarchy of the ecosystem levels, starting from a cell up to the complicated assemblages of populations. With this, the necessity arises to couple the phenomena different in nature and temporal scales - physical-chemical ones, biochemical, physiological, and those of population. A unique approach to the description of such sort of systems is possible if the system is considered as the interaction of mass fluxes which is in accordance with the common laws of nature for the whole system.

Below an attempt is made to develop an approach to modeling marine ecosystems, starting from descriptions of separate biological processes and ending with the ecosystem as a whole.

Primary link of ecosystem

Primary production, i.e. the creation of organic matter, is central in the turnover of substances of the ecosystem. This link predetermines the volume of fluxes through all the other links. Understanding the processes of primary production and their adequate quantitative description is a determining one for the flow description in the ecosystem as a whole.

The processes of matter transformation into various trophic links of the ecosystem are based on general biochemical (enzymatic) mechanisms. Along with this, the primary production link differs from heterotrophic links, at least, in two ways: (1) the process rate depends on several substrate factors simultaneously, and (2) one of "substrates" of the process is the light energy. Matter flux through the heterotrophic link depends just on one substrate factor - food concentration, where the biogenous elements are relatively balanced.

Just these two circumstances create serious difficulties with quantitative modeling of the dependence of the primary production rate on the environmental factors which have not been coped with yet.

Photosynthesis scheme

Photosynthesis is the basis of primary production. A large number of generalized schemes of the process can be found in scientific literature (Edwards and Walker 1983; Goodwin and Mercer 1983). Figure 11 presents a simplified variant of "Z-scheme" of photosynthesis after Goodwin and Mercer (1983) in accordance with the modern notions. Even such a simplified scheme is a chain of 13 consecutive coupled cyclical reactions.

Two of them are cyclical transformations of oxidation-reduction of reaction centers PSII and PSI, coupled by an electron-transport chain consisting of five electron carriers. PSII receives an electron from water via a water-splitting system (Z) (cycle 1), and via an electron transport chain (cycles 3-7) transfers it to PSI. In its turn, PSI transfers an electron to acceptor (X), which via the carrier (cycle 10) reduces NADP to $NADH_2$ (cycle 11). $NADH_2$ is involved in poli-enzyme pentose-phosphate reduction cycle (Calvin's cycle), where CO_2 reduces to hydrocarbon (cycles 11-13).

An approach for the mathematical description of such kind of chains of cyclic coupled processes has been developed earlier (Zvalinsky and Litvin 1986). It has been shown that a linear chain of

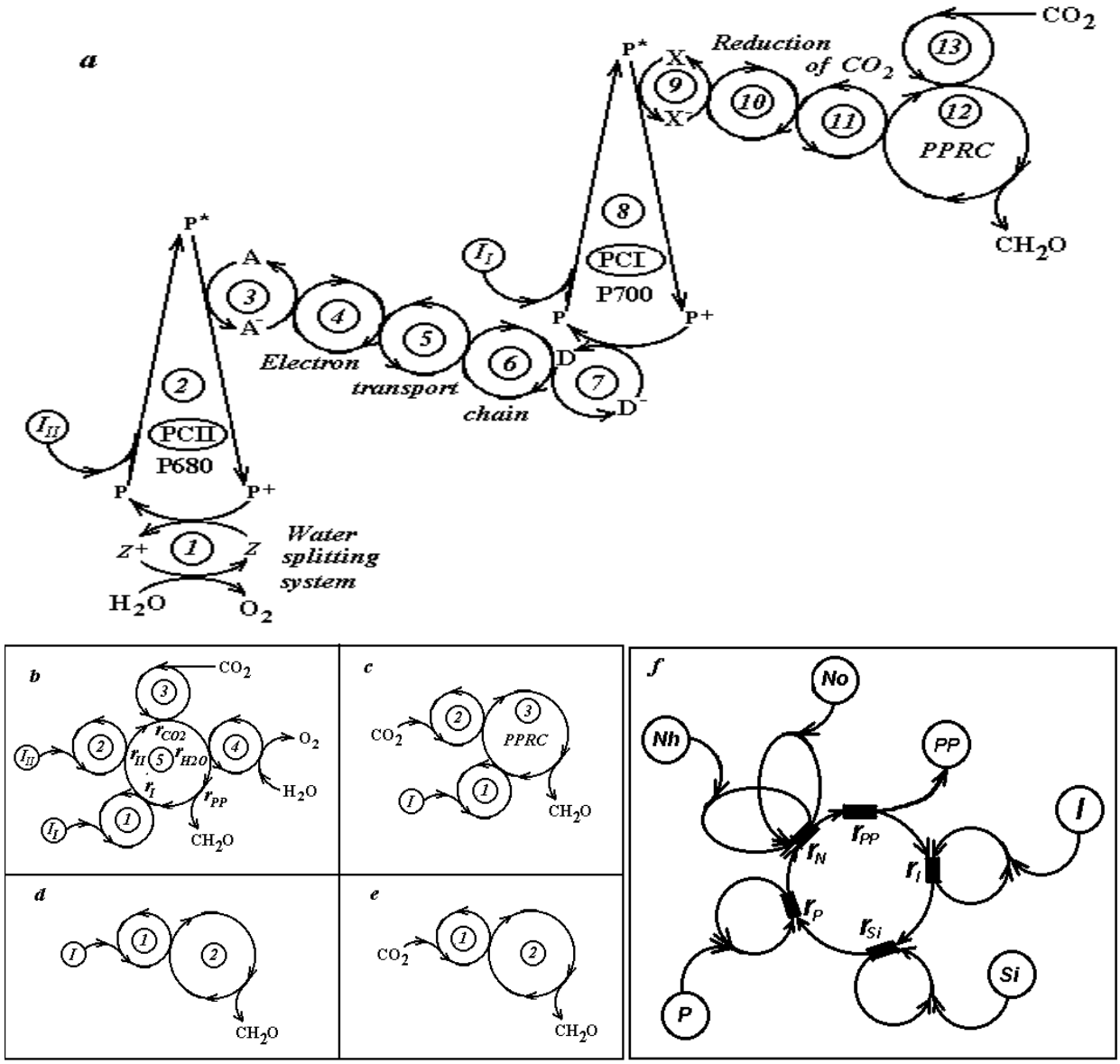

Fig. 11 Photosynthesis modeling by chains of coupling cyclical reactions of different complexity. (a) "Z-scheme" of photosynthesis – a chain of 13 consecutive coupling cyclical reactions; (b) a simplified model of photosynthesis for description of rate dependence on four substrates; (c) a simplified model for description of rate dependence on two substrates; (d) and (e) models for description of rate dependence on one substrate (light and CO_2); (f) a generalized model for description of primary production rate dependence on any number of substrates. For details see text.

coupled reactions is described by a linear chain fraction. For instance, for the scheme in Figure 11a, an equation for the description of the process rate with relation to the parameters of coupled reactions and values of the environmental factors - light intensity (I), CO_2 and H_2O substrate concentrations, will be as follows (to economize the space a fraction is divided into two parts):

Equation 1

$$\frac{r_{56}*V}{1-\frac{r_{45}*V}{1-\frac{r_{34}*V}{1-\frac{r_{23}*V}{1-\frac{V}{b*I_{II}}-\frac{r_{12}*V}{1-V/H_2O}}}}}+\frac{r_{67}*V}{1-\frac{r_{78}*V}{1-\frac{V}{a*I_I}-\frac{r_{89}*V}{1-\frac{r_{9,10}*V}{1-\frac{r_{10,11}'*V}{1-\frac{r_{11,12}'*V}{1-r_{PP}'*V-\frac{r_{12,13}*V}{1-V/CO_2}}}}}}}=1$$

Here: $V = P/P^m$ is the relative rate of the process with P and P^m as the rate and maximal rate of the process; $I_I = [I]/K_I$ and $I_{II} = [I]/K_{II}$ are the relative intensity of light in corresponding substrate constants PSI and PSII; α and β are the portions of the light absorbed by photo-systems I and II respectively; $H_2O = [H_2O]/K_{H2O}$ and $CO_2 = [CO_2]/K_{CO2}$ are the concentrations of water and carbon dioxide in the corresponding substrate constants; $K_{Si} = P^m/(k_{si}*[E_i^0])$ is a substrate constant with dimensions of concentration (k_{si} is a constant of incorporation rate of the i^{th} substrate; $[E_i^0]$ is the concentration of the component assimilating the i^{th} substrate); $r_{i,i+1} = P^m/\{k_{i,i+1}*[E_i^0]*[E_i+1^0]\} = P^m/P^m_{i,i+1}$ is a dimensionless generalized kinetic parameter marked as the 'resistance' of coupling reaction of the i^{th} and $i+1^{th}$ cycles and proportional to the time of the reaction progress ($k_{i,i+1}$ is a rate constant; E_i^0 and E_{i+1}^0 are total concentrations of reaction components; $P^m_{i,i+1} = k_{i,i+1}*[E_i^0]*[E_{i+1}^0]$ is the maximal rate of reaction of a corresponding link). The meaning of the $r_{i,i+1}$ parameter is analogous to that of diffusion 'resistance' or to the 'resistance' of carboxylation at photosynthesis (Edwards and Walker 1983). The inverse of resistance is the maximal relative link capacity or its conductivity

$$1/r_{i,i+1} = P^m_{i,i+1}/P^m.$$

We studied the kinetic characteristics of the chain fraction similar to Equation 1 (Zvalinsky and Litvin 1988a, b). The analysis has shown that if we do not consider oxidizing-reducing transformations of the components of the reaction chain, but just describe the dependence of the process rate on the substrates concentration, then the conceptual model and the corresponding mathematical model can be significantly simplified without considerable damage to the quality of the quantitative description. A five-cycle scheme presents a conceptual model of a four-substrate process (Fig. 11b). Mathematically, this model is described by:

Equation 2

$$\frac{r_I*V}{1-\frac{V}{a\times I}}+\frac{r_{II}*V}{1-\frac{V}{b\times I}}+\frac{r_{CO_2}*V}{1-\frac{V}{CO_2}}+\frac{r_{H_2O}*V}{1-\frac{V}{H_2O}}=1-r_{PP}*V$$

Here r_I, r_{II}, r_{CO2} and r_{H2O} are the relative coupling resistances of corresponding substrate cycles with the other reactions; r_{PP} is the total equivalent resistance of all cyclical reactions beyond the bounds of substrate cycles, and the rest are as in Equation 1. We see that in a simplified variant the dependence of rate on any substrate is described similarly, with no regard to its location in the chain of reactions (Fig. 11a): mathematically, the equation is relatively symmetric to any substrate (Eqn. 2).

In the case when the concentration of one of substrates is large ($H_2O \rightarrow \infty$, the value $[V/H_2O] \rightarrow 0$) and the limiting one is one of the photo-systems, the conceptual model of the process becomes three-cyclical (Fig. 11c), and Equation 2 becomes dependent on two factors:

Equation 3

$$\frac{r_I*V}{1-\frac{V}{a*I}}+\frac{r_c*V}{1-\frac{V}{CO_2}}=1-r_{PP}*V$$

Similarly, when one of two factors reaches saturation or is constant, the process model turns into a two-cycle one (Fig. 11d, e), and the dependence is reduced to a one-factor equation:

Equation 4

$$\frac{r_I * V}{1 - \frac{V}{a * I}} = 1 - r_{PP} * V$$

Equation 5

$$\frac{rc * V}{1 - \frac{V}{CO_2}} = 1 - r_{PP} * V$$

The relationships (4) and (5) are non-rectangular hyperbolas, the equations (2) and (3) are two-dimensional and four-dimensional non-rectangular hyperbolic surfaces correspondingly; and the equation (1) is the surface of higher order. The ratio between the kinetic parameters r_I can be found from the condition that at saturating values of concentrations, the process rate reaches its maximal value: at $I \rightarrow \infty$, $CO_2 \rightarrow \infty$ $P \rightarrow P^m$, $V \rightarrow 1$. For Equations 4 and 5, such condition is: $r_I + r_{PP} = 1$; $r_C + r_{PP} = 1$. Considering the above, Equations 4 and 5 can be rewritten in a more simple form:

Equation 6

$$[I] = K_I * \frac{V}{(1-V)} * (1 - r'_{PP} * V) \qquad \text{(a)}$$

$$[CO_2] = K_c * \frac{V}{(1-V)} * (1 - r''_{PP} * V) \qquad \text{(b)}$$

Dividing the first part of Equation 6a by V/(1 - V) gives a ratio important for the kinetics analysis:

Equation 7

$$[I] * \frac{1-V}{V} = K_I * (1 - r_{PP} * V)$$

It is seen from Equation 7 that in coordinates {[I]*(1 - V)/V} and V, that the whole hyperbolic family, rectangular and non-rectangular ones, possesses the form of a straight line with slope equal to $-r_{PP}$. With this, the continuation of the straight line cuts off the segment V_0 at the X-axis which is numerically equal to the reverse value of resistance $V_0 = 1/r_{PP}$, and at the Y-axis, the segment is equal to a substrate constant K_I (Fig. 12). The straight line parallel to the abscissa corresponds to the rectangular hyperbola of Michaelis-Menten. Analysis of experimental kinetic curves in these coordinates enables us to ascertain the character of dependence and to solve the problem of adequacy of the proposed models to the real biological processes. Moreover, such analysis allows to determine the values of parameters K_I and r_{PP} by modeling the process as a two-cyclical scheme (Fig. 11d-e, Fig. 12).

It is noteworthy that the maximal simplification of the reaction chain in Figure 11a is possible up to a one-substrate two-cyclic coupled reaction (Fig. 11e). In such 'minimal' two-cyclic model, the substrate incorporation and substrate processing take place in different systems of cyclical reactions. Further simplification up to one-cycle model is quite coarse and non-adequate, and it is possible in the only particular case when $r_{PP} \cong 0 << r_I \cong r_C \cong 1$, i.e. when ratios (Eqns. 4 and 5) pass into equations of rectangular hyperbola of Michaelis-Menten for the one-cyclical one-enzymatic reaction.

Comparison to the experiment

We have carried out a great number of experiments to measure the light and CO_2 dependence of the rate of marine alga photosynthesis. The data testify that the real dependencies are described by the equation of non-rectangular hyperbola (4) and (5) with a sufficiently high accuracy (Zvalinsky and Litvin 1988a, 1988b). The values $r_{PP} \cong 0.95$, and $r_I \cong r_C \cong 0.05$ have been determined experimentally both for the light and CO_2 curves of photosynthesis. Non-rectangular hyperbola with such parameters is the most similar to the hyperbolic tangent (Platt *et al.* 1977). It means that the rate of substrate incorporation (may) as a rule exceed the rate of substrate processing by not less than ~20 times. Also, the tests have shown high accuracy in describing photosynthesis rate by Equation 3 using two factors at a time (light intensity and CO_2 concentration, Fig. 12).

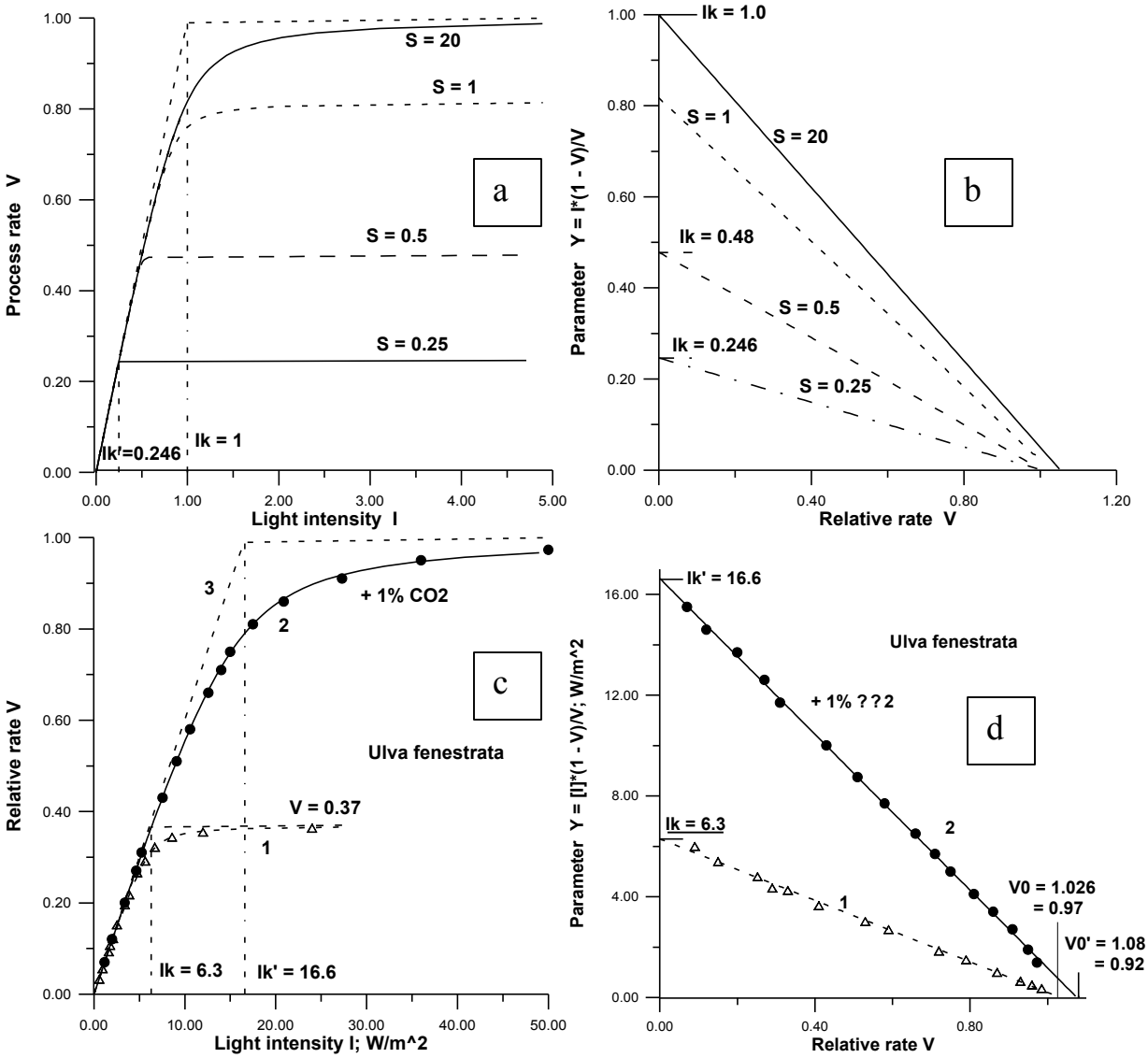

Fig. 12 The comparison of theoretical and experimental dependencies of process rate on two substrates in usual (a, c) and special (I*(1-V)/V against V, band d) coordinates. (a) the two-substrate (I - S) model as a chain of three coupled cyclical (enzymatic) reactions, the light-saturation curves are given for the different levels of other substrate 'S'; (b) the same curves in special coordinates; (c) the experimental dependence of seaweed photosynthesis on light in seawater (1), and in seawater saturated by air with 1% of CO_2 (2); (d) the same curves in special coordinates. The experimental dependencies are in a good agreement with the theoretical non-rectangular hyperbola.

Michaelis-Menten equation or non-rectangular hyperbola

In the NEMURO model, the dependence of the primary production rate on the concentration of nutrients is described by equations of rectangular hyperbola (Eqns. 1 and 2 in Eslinger *et al.* 2000). As it was noted above, all substrates are incorporated into the reaction chain via the corresponding enzymes (components, Fig. 11a) in the same manner, so conceptually and mathematically the process dependence on substrates should be described by a similar type of functions, non-rectangular hyperbola (Eqns. 2 and 5). Usage of Michaelis-Menten equation is not correct and can lead to quite low accuracy and non-adequacy of the description.

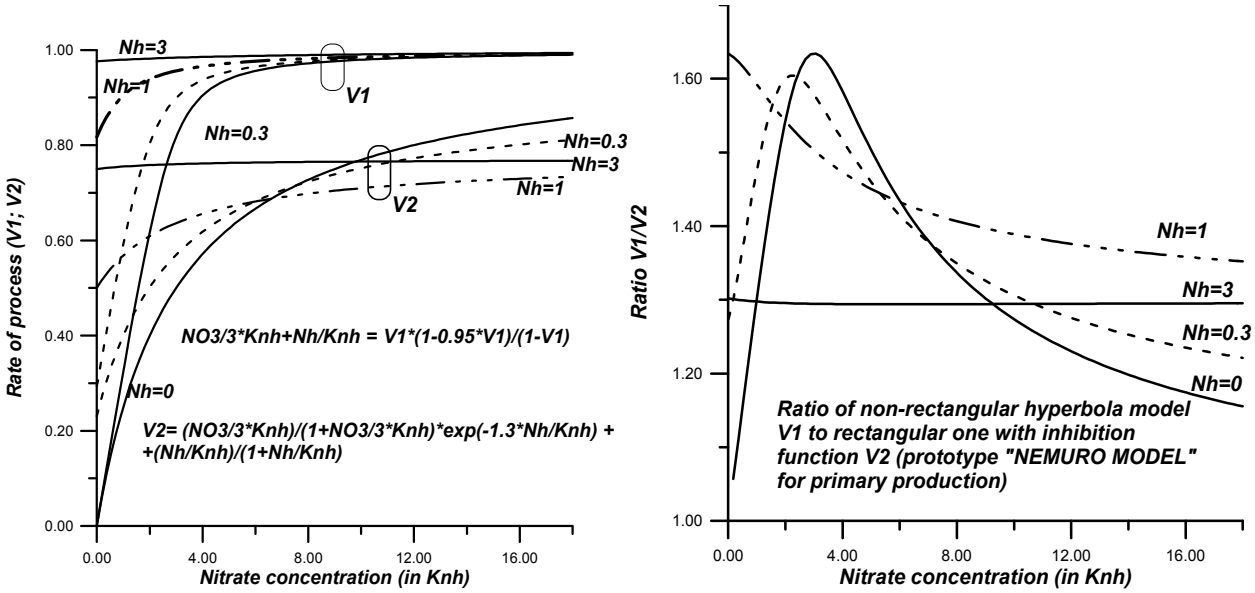

Fig. 13 Left panel: A comparison of non-rectangular hyperbola PP model with two competition substrate (nitrate and ammonium) V_1 with the NEMURO Model prototype V_2. Right panel: The ratio of these two type curves. The PP dependence curves on one of substrates (nitrate) are presented for different values of other (ammonium: Nh = 0.0; 0.3; 1.0 and 3.0 K_{nh}). The NEMURO Model results 1.2 – 1.6 times lower than non-rectangular model ones.

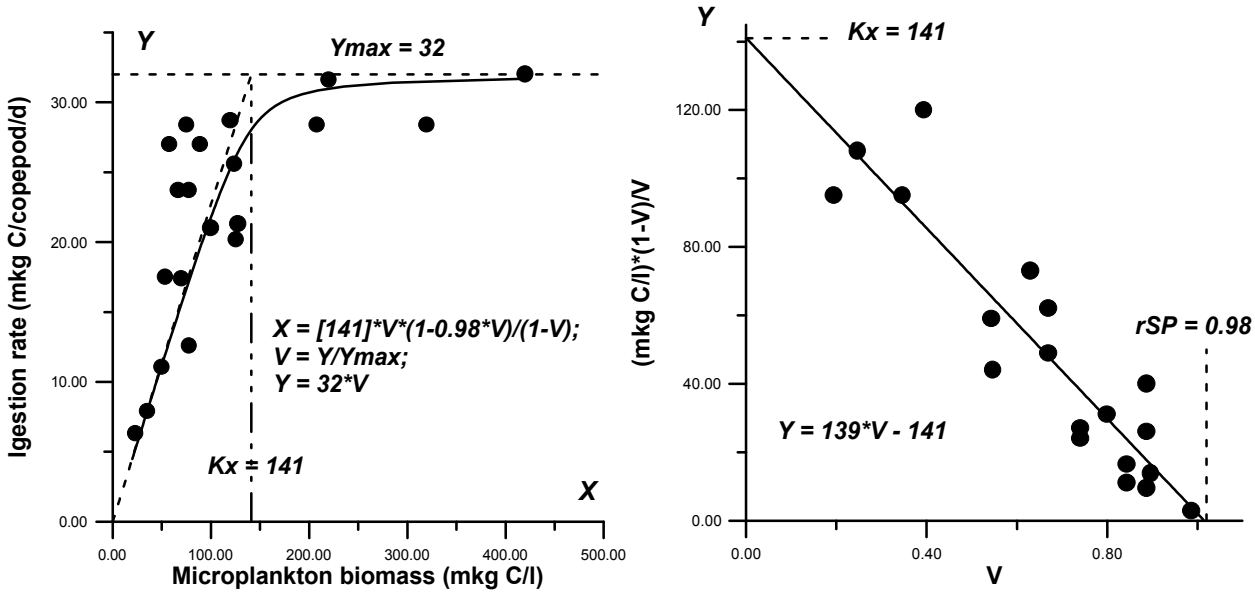

Fig. 14 Left panel: The ingestion rate of *Calanus sinicus* in relation to microplankton food supply (circles) using a theoretical curve of non-rectangular hyperbola with parameters found from data in the right panel. It is seen that K_X is not equal to substrate concentration, where rate Y = Ymax/2. Right panel: The same experimental points in linear space; Experimental points from Shiotani and Uye (2000). The regression equation and parameters of non-rectangular hyperbola are as follows: rSP = 0.98; substrate constant K_X = 141).

Inhibition or preference?

In the NEMURO model the competitive ratios of ammonium nitrogen and nitrate nitrogen consumption and also the grazing rates of large-phytoplankton and small-zooplankton to predator-zooplankton are described by introducing the inhibition function (Eqns. 1-2 and 13-14 in Eslinger *et al.* 2000). With this, inhibition takes place at quite a low concentration of substrate (food) comparable to the value of the Michaelis constant. Still, in physiology it is considered that inhibition takes place only at the highest values of substrate concentrations (many times exceeding the Michaelis constant, Edwards and Walker 1983). At low values, it is more expedient to speak not about the inhibition, but about the 'preference'. So, for two forms of nitrogen the equation of non-rectangular hyperbola (4) looks like:

Equation 8

$$\frac{r_N * V}{1 - V/(N_1 + N_2)} = 1 - r_{PP} * V$$

Concentrations of nitrogen and ammonium are expressed in the corresponding substrate constants $N_1 = [NO_3^-]/K_1$ and $N_2 = [NH_4^+]/K_2$.

Analysis has shown that the equation with inhibition (Eqns. 1-2 in Eslinger *et al.* 2000) gives values that are significantly lower than those calculated from to the equation of non-rectangular hyperbola with the light preference (Eqn. 8, Fig. 13). This distinction is especially high in the region of low and moderate concentrations (up to 60%), which is the most widespread situation in nature. As far as the tests confirm the adequacy of description of kinetics of the production process by the equation of non-rectangular hyperbola, the usage of Equation 8 with 'preference', from our point of view, should describe the process with higher precision than the function with inhibition.

General model of primary production

By analogy with the scheme of photosynthesis (Fig. 11a), a conceptual model of primary production of any complexity, incorporating any quantity of substrates (light, nutrients) can be made. The model can be maximally simplified with the aim of describing the primary production rate in relation to the environmental factors. For four factors - light intensity and concentration of main nutrients (two forms of nitrogen, phosphorus, and silicon) the model is given in Figure 11f.

The production rate *P* will be described by a system of two equations:

Equation 9

$$P = P^m * V$$

$$\frac{r_I * V}{1 - V/I} + \frac{r_N * V}{1 - V/(N_1 + N_2)} + \frac{r_P * V}{1 - V/P} + \frac{r_S * V}{1 - V/S} = 1 - r_{PP} * V$$

Here, the environmental factors are expressed in units of substrate constants: light intensity -$I = [I]/I_k$; concentration of nitrogen and ammonium - $N_1 = [NO_3^-]/K_1$ and $N_2 = [NH_4^+]/K_2$; phosphates - $P = [PO_4^{3+}]/K_P$; silicates -$S = [Si_{O3}^{2+}]/K_S$. The relative rate is $V = P/P^m$. Parameters r_I, r_N, r_P and r_S - relative coupling resistance of corresponding substrate cyclical process with the extra-substrate cyclic processes; parameter r_{PP} is the relative resistance of an assemblage of the extra-substrate reactions.

If the factor is not limiting (for instance, silicates; $S \to \infty$, $V/S \to 0$), then the denominator of the corresponding term (Eqn. 9) turns into 1.0 and this term can be incorporated into the last member of the right part. Equation 9 is transformed into a three-substrate one with $r_{PP}' = (r_{PP} + r_S)$. Similarly, it can be simplified until the level of two- and one-substrate equation (Eqns. 3 and 4). One of the terms of Equation 9 can be replaced by the other one, or a term can be included with the other limiting factor (for example, CO_2 or iron).

Thus, a system of equations (Eqn. 9) involves practically all possible variants of models for the primary production rate. This model, in our opinion, possesses a series of advantages compared to models published elsewher, as well as to NEMURO (Eqns. 1-2 in Eslinger *et al.* 2000). First of all, and this is the most important thing, the model has been developed on the basis of modern notions of the mechanism of the primary

production process. It includes parameters with clear biological meaning, and has quite a simple mathematical presentation. The model adequately describes the interrelationship of the factors, including competitive ones, the change of limitation from one factor to another without any additional conditions. The model can be naturally simplified or extended, with regard to the needs of the experiment or new knowledge (for instance, incorporation of limitation by iron or some other elements). It is naturally incorporated into the ecosystem model.

Photo-inhibition and photo-adaptation

The NEMURO model considers that the rate of primary production is inhibited by high light intensity (Steele 1962; Eqns. 1-2 in Eslinger *et al.* 2000). In plant physiology, it is usually assumed that instant light-saturation curves are measured in such a way that during the period of measurements the parameters of the production system do not change (i.e., when the processes of the light adaptation or inhibition do not manifest themselves). Just for this case, the model of primary production has been obtained. If a plant cell is in the light for a long time then the cell changes its parameters according to this light intensity, and an adaptation takes place. Our approach considers this process and allows a light curve of any form (Zvalinsky and Litvin 1991).

Heterotrophic links

Microbial link

Incorporation and metabolism of organic and mineral matters in a microbial cell is analogous to similar processes in a plant cell. That is why our one-, two-, and more-substrate models (Eqns. 1-9) can also be used to describe even bacterial cell growth rates.

Heterotrophic links of LTL

Grazing is also a chain of coupled cyclical processes: periodic food capture and the stomach filling in with its subsequent clearing due to the polyenzymatic food processing (Fasham 1995). Food processing needs one more substrate - oxygen. Consequently, in the simplest case grazing can be presented by a two-substrate (food and oxygen) three-cycle model (Fig. 11c, Eqn. 3) or as a one-substrate two-cycle model with the dependence on food concentration (the process is not limited by oxygen) (Fig. 11e, Eqn. 6b).

The grazing rate *G* for any trophic level and for any number of food types *Fn* with different preferences can be described by non-rectangular hyperbola:

Equation 10

$$\frac{r_G * V}{1 - V/(F_1 + F_2 + \ldots + F_n)} = 1 - r_{HP} * V;\ G = G^m * V$$

Here: G and G^m are the grazing rate and maximum grazing rate; V is the relative grazing rate; $F_1 = [F_1]/K_1$; $F_2 = [F_2]/K_2$; …, $F_n = [S_n]/K_n$ are the food concentrations in units of their substrate constants; ($[F_1]$, $[F_2]$, …, $[F_n]$ are concentrations of different food types, with K_1, K_2, …, K_n as their substrate constants). The substrate constants reflect the 'preference' factor. Values of r_G and r_{HP} are the parameters of the non-rectangular hyperbola. Values of r_G and r_{HP} reflect the resistances of capture and processing, respectively. The analysis of experimental data show that the ingestion rate of *Calanus sinicus* in relation to microplankton food supply describes well by Equation 10 with $r_{HP} = 0.98$ and $r_G = 0.02$ (Fig. 14).

As the rate of food capture exceeds by many times the rate of its processing, then, as in case of primary production $r_{HP} >> r_G$ ($r_G \approx 0.02$ - 0.05 and $r_{HP} \approx 0.95 - 0.98$). Non-rectangular hyperbola with such parameters is very similar to the hyperbolic tangent, i.e. it has longer initial segment and reaches the saturation sooner as compared to the exponent (Platt *et al.* 1977). As with the case of several forms of nitrogen, using the current grazing function in NEMURO to describe grazing in the presence of several kinds of food is not sufficiently grounded (Eqns. 13-14 in Eslinger *et al.* 2000). It is difficult to imagine a mechanism of such 'inhibition', especially, if we take into account that it persists at low food concentration. Non-rectangular hyperbola (Eqn. 10) with different 'preference' to different kinds of food is closer to the real processes.

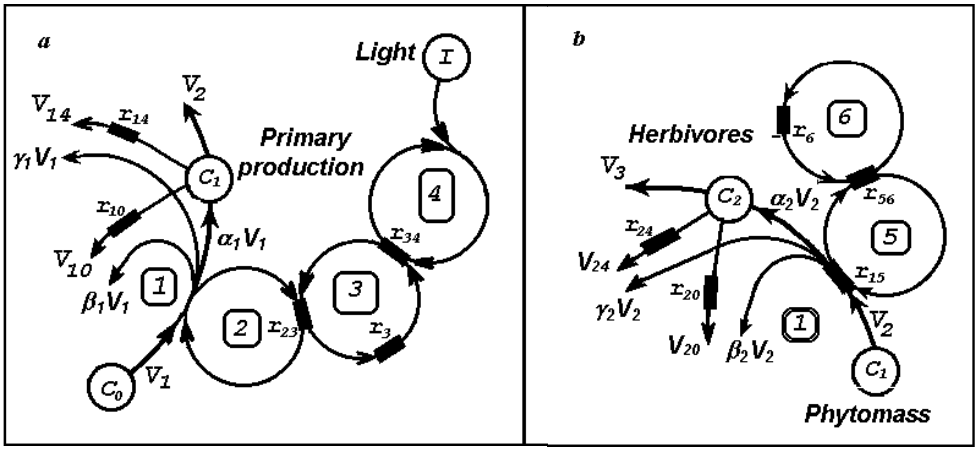

Fig. 15 The conceptual models of two-substrate primary production (a), and unisubstrate secondary production (b), with input and output (spending) fluxes of matter. Input fluxes: V_1 – incorporation of inorganic matter C_0 and V_2 – grazing rate of phytomass to herbivore (α_1 and α_2 – ecotrophic coefficients). Output fluxes: β_1V_1 and β_2V_2 – biosynthesis respiration; γ_1V_1 and γ_2V_2 – excretion and egestion; V_{10} and V_{20} – maintenance respiration expenses of C_1 or C_2; V_{14} and V_{24} – mortality; V_2 and V_3 – grazing phytoplankton and zooplankton to next trophic links.

Higher trophic levels

Grazing in the HTL and LTL do not differ considerably. HTL animals must first capture then process the food (polycyclical polyenzymatic food processing). Dependence of the HTL grazing rate in relation to the food supply can be described by the same function as for the LTL (Eqn. 10).

Inputs and outputs of different trophic links

The models described above refer to the input fluxes of different trophic links. Besides the input fluxes there are several output fluxes in each link. Figure 15a presents a primary link with 1 input flux (incorporating inorganic matter C_0 in the primary link) and 5 types of output fluxes: biosynthesis respiration, excretion, maintenance respiration expenses of phytoplankton biomass c_1, mortality, and phytoplankton grazing to the next trophic link.

Figure 15b presents fluxes for the secondary link - an input flux (grazing rate of phytomass to herbivore) and 5 output fluxes: biosynthesis respiration, egestion, maintenance respiration expenses of herbivore biomass c_2, mortality, and herbivorous zooplankton grazing to next trophic link. Unlike in the NEMURO model, respiration in each line is divided into two parts - biosynthesis respiration and maintenance respiration. They differ in the following. Biosynthesis respiration occurs at the expense of the eaten food and is proportional to the biomass of this food, when there is no food, this type of respiration is absent. Maintenance respiration takes place at the expense of the individual's biomass and does not depend on the volume of food eaten. This type of respiration predetermines the threshold of an organism's existence: if the volume of food eaten does not compensate the expenses of maintenance respiration, the organism dies (Edwards and Walker 1983). Just the maintenance respiration of the phytoplankton predetermines the boundary of the photic layer.

Ecosystem modeling

Conceptual model of any complicity ecosystem can be constructed by the consecutive and parallel linking of its different compartments (Fig. 15) with each other in accordance with direction of matter flows.

Figure 16 presents one version of this type of model consisting of six compartments. Four of these compartments are the biological ones (primary link, herbivores, carnivores and bacteria)

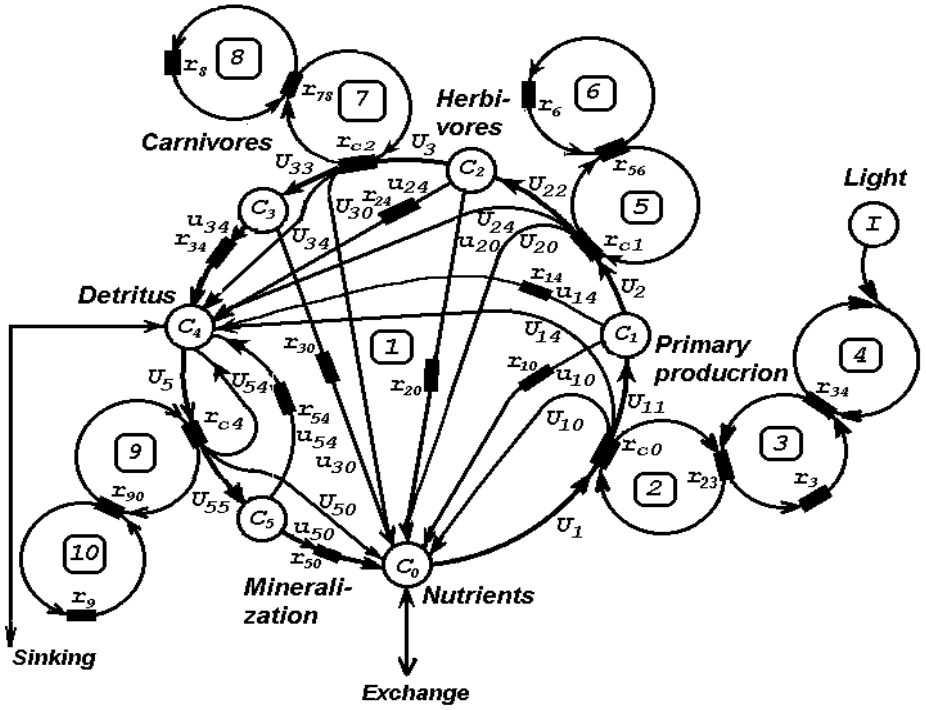

Fig. 16 The conceptual model of six-compartment ecosystem. The masses Ci of different trophic levels are drawn by circles. The arrows show the direction of matter flow between compartments. The kinetic parameters r_{ij} reflect types of interactions and determine the value of fluxes. For explanation and designation see the relevant sections in the text and in the Tables.

and two of them are non-living compartments (nutrients and detritus). All ecosystem fluxes of matter are closed. All fluxes and kinetic parameters are expressed in terms of main primary production flow P_1^m, all matter concentrations – in terms of total ecosystem concentrations of corresponding elements. Such ecosystem presentation is very convenient because it gives the possibility to write the equation system similar to graph method. This model is described by a system of 26 algebraic and differential equations (Tables 9 and 11). The parameters of the first three links are close to parameters of "average phytoplankton", "average herbivorous zooplankton" and "average carnivorous zooplankton" of NEMURO model (Eslinger *et al.* 2000). It is seen that the value of total resistance of link is inversely related to its maximum grazing (uptake) rate.

Figure 17 shows the time-dependence dynamics of ecosystem component concentrations that were calculated using equations of Table 9 and parameters of Table 11. The calculations were carried out using a specially developed program in TURBO PASCAL 7. The comparison of Figure 17a-f shows high sensitivity to changes of parameters. So, a relatively small increase of carnivore biomass spending (from 7% to 16% of maximum grazing) leads to a chain of changes: noticeable decreasing its own biomass, increasing of biomass of previous link and decreasing of primary link (compare Fig. 17a, b). The drastic shifts in biomasses are observed when the substrate constants (the analogue of half-saturation constants) change (compare Fig. 17b with c and d). The great decrease in herbivore substrate constant leads to drastic decreases in primary link biomass. The bulk of total mass exists in non-living forms (detritus and inorganic matter; compare Fig. 17d and e). There is revealed the tendency toward oscillations in this case. Using the Michaelis-Menten rectangular hyperbola for nutrient uptake instead of the non-rectangular hyperbola, is equivalent to decreasing the substrate constant which leads to corresponding declines in the primary link biomass (Fig. 17f). The tendency toward oscillations increases.

Table 9 Simultaneous equations for description of a six-compartment ecosystem.

No.	Equations for specific fluxes and mass compartment balance	Equations for full fluxes	Notes
	1. Primary production		
1.1.	$C_0 = \dfrac{r_{c0} * V_1}{1 - \dfrac{r_{23} * V_1}{1 - r_3 * V_1 - \dfrac{r_{34} * V_1}{1 - V_1 / I}}}$	$U_1 = C_1 * V_1$ $U_{11} = \alpha_1 * C_1 * V_1$	Incorporation of nutrients Phytomass accumulation
1.2.	$V_{10} = \beta_1 * V_1$	$U_{10} = \beta_1 * C_1 * V_1$	Biosynthesis respiration
1.3.	$v_{10} = 1/r_{10}$	$u_{10} = C_1 * v_{10}$	Maintenance respiration at the expense of c_1-biomass
1.4.	$V_{14} = \gamma_1 * V_1$	$U_{14} = \gamma_1 * C_1 * V_1$	Excretion
1.5.	$v_{14} = 1/r_{14}$	$u_{14} = C_1 * v_{14}$	Mortality
1.6.	$dC_1/dt = U_{11} - (u_{10} + u_{14} + U_2)$		Balance of c_1 biomass
	2. Herbivore link		
2.1.	$C_1 = \dfrac{r_{c1} * V_2}{1 - \dfrac{r_{56} * V_2}{1 - r_6 * V_2}}$	$U_2 = C_2 * V_2$ $U_{22} = \alpha_2 * C_2 * V_2$	Grazing rate of phytomass to herbivore Accumulation of c_2-biomass
2.2.	$V_{20} = \beta_2 * V_2$	$U_{20} = \beta_2 * C_2 * V_2$	Biosynthesis respiration
2.3.	$v_{20} = 1/r_{20}$	$u_{20} = C_2 * v_{20}$	Maintenance respiration at the expense of c_2-biomass
2.4.	$V_{24} = \gamma_2 * V_2$	$U_{24} = \gamma_2 * C_2 * V_2$	Excretion (egestion)
2.5.	$v_{24} = 1/r_{24}$	$u_{24} = C_2 * v_{24}$	Mortality
2.6.	$dC_2/dt = U_{22} - (u_{20} + u_{24} + U_3)$		Balance of c_2 biomass
	3. Carnivore link		
3.1.	$C_2 = \dfrac{r_{c2} * V_3}{1 - \dfrac{r_{78} * V_3}{1 - r_8 * V_3}}$	$U_3 = C_3 * V_{3+}$ $U_{33} = \alpha_3 * C_3 * V_3$	Grazing rate herbivore to carnivore Accumulation of c_3-biomass
3.2.	$V_{30} = \beta_3 * V_3$	$U_{30} = \beta_3 * C_3 * V_3$	Biosynthesis respiration
3.3.	$v_{30} = 1/r_{30}$	$u_{30} = C_3 * v_{30}$	Maintenance respiration at the expense of c_3-biomass
3.4.	$V_{34} = \gamma_3 * V_3$	$U_{34} = \gamma_3 * C_3 * V_3$	Excretion (egestion)
3.5.	$v_{34} = 1/r_{34}$	$u_{34} = C_3 * v_{34}$	Mortality
3.6.	$dC_3/dt = U_{33} - (u_{30} + u_{34})$		Balance of c_3 biomass
	4. Bacterial link		
4.1.	$C_4 = \dfrac{r_{19} * V_5}{1 - \dfrac{r_{90} * V_5}{1 - r_9 * V_5}}$	$U_5 = C_5 * V_5$ $U_{55} = \alpha_5 * C_5 * V_5$	Utilization rate detritus to bacteria Accumulation of c_5-biomass
4.2.	$V_{50} = \beta_5 * V_5$	$U_{50} = \beta_5 * C_5 * V_5$	Biosynthesis respiration
4.3.	$V_{50} = 1/r_{50}$	$u_{50} = C_5 * v_{50}$	Maintenance respiration at the expense of c_5-biomass
4.4.	$V_{54} = \gamma_5 * V_5$	$U_{54} = \gamma_5 * C_5 * V_5$	Excretion
4.5.	$V_{54} = 1/r_{54}$	$u_{54} = C_5 * v_{54}$	Mortality
4.6.	$dC_5/dt = U_{55} - (u_{50} + u_{54})$		Balance of c_5 biomass

Table 9 (*continued*)

	5. Equations of continuity	***Notes***
5.1.	$dC_4/dt = (U_{14} + u_{14} + U_{24} + u_{24} + U_{34} + + u_{34} + U_{54} + u_{54}) — U_5$	Balance of c_4 biomass
5.2.	$C_0 = 1 — (C_1 + C_2 + C_3 + C_4 + C_5)$	Balance of c_0 biomass

Table 10 List of designations.

No.	Designation	**Notes**
	1. Fluxes	
1	$[I]; I = [I]/ K^I$	Absolute and relative (in units of K^I) light (energy) flux
2	P_1^m	Absolute maximum specific rate of primary link
3	$V_1^m = P_1^m/P_1^m = 1/(r_{23} + r_3 + r_{34}) = 1$	Relative maximum specific rate of primary link
	$V_2^m = P_2^m/P_1^m = 1/(r_{56} + r_6) = 1/R_2$	Relative maximum specific rate of herbivore link
	$V_3^m = P_3^m/P_1^m = 1/(r_{78} + r_8) = 1/R_3$	Relative maximum specific rate of carnivore link
	$V_5^m = P_5^m/P_1^m = 1/(r_{90} + r_9) = 1/R_5$	Relative maximum specific rate of bacterial link
3	V_i, V_{ij}	Relative (to P_1^m) specific fluxes of ecosystem
4	$U_i = C_i * V_i; U_{ij} = C_i * V_{ij}; u_{ij} = C_i*v_{ij}$	Relative (to P_1^m) full fluxes of ecosystem
5	$P_i = V_i*P_1^m; P_{ij} = V_{ij}*P_1^m; p_{ij} = v_{ij}*P_1^m$	Absolute specific rate of i-th link
	2. Relative resistance **(*for specific fluxes*)**	
5	$r_{ci} = K^{Ci}/\Sigma[C_i]$	Incorporation or grazing of c_i-substrate (biomass) to (i+1)–th trophic link
6	$r_{ij} = P_1^m/\{k_{ij}*[E_i^0]*[E_j^0]\} = P_1^m/P^m_{ij}$	Coupling of substrate cycles with another cyclic reactions of link (capture resistance)
7	$r_i = P_i^m/(k_i*[E_i^0])$	Resistance substrate (food) processing of i-th link
8	$r_{i0} = P_1^m/k_{i0}$	Specific maintenance respiration of the expense of c_i-biomass
9	$r_{i4} = P_1^m/k_{i4};$	Specific rate of mortality
	3. Concentrations	
10	$[C_i];$ $\Sigma[C_i]$	Absolute concentration of i-th component (link) Total concentration of all components (links)
11	$C_i = [C_i]/\Sigma[C_i]$	Relative component concentrations
	4. Constants	
12	$K^I = P_1^m/(A*\varphi)$	Substrate constant for light energy
13	$K^{Ci} = P_i^m/(k_{ci}*[E_{ci}^0])$	Substrate constant for i-th substrate (biomass)
14	k_{i0}	Specific constant of maintenance respiration
15	$k_{i4}; k'_{i4}$	Specific constant of mortality 0-th and 1-th order respectively
	5. Coefficients	
16	α_i	Ecotrophic coefficient (food utilization efficiency) of i-th link
17	$\beta_i,$	Portion of captured food, using for biosynthesis respiration
18	γ_i	Portion of non-using food (excretion and egestion)

Table 11 Parameter values of six compartment ecosystem (Fig. 16, Table 9) which, to a considerable extent, correspond to parameter values for NEMURO Model (Eslinger *et al.* 2000).

No.	Parameter	Value	Notes
	1. Primary link		
1.1	$I = [I]/ K^I$	10	Relative (in units of K^I) light intensity
1.2	r_{c0}	0.2	Resistance of substrate uptake by primary link
1.3	P_1^m,	1,0 (1/day)	Absolute maximum specific rate of primary link
1.4	$V_1^m = P_1^m/P_1^m = 1/(r_{23} + r_3 + r_{34})$	1,0	Relative maximum specific rate of primary link
1.5	$r_{23} = r_{34}$	0.05	Resistance of reaction of coupling of substrate cycles with cycle of processing reactions
1.6	r3	0.9	Resistance of reactions of processing cycle
1.7	$R_1 = r_{23} + r_3 + r_{34}$	1.0	Total resistance of primary link
1.8	r_{10}	30	Resistance of specific maintenance respiration
1.9	r_{14}	100	Mortality
1.10	α	0.7	Growth efficiency
1.11	$\beta = \gamma$	0.15	Excretion and biosynthesis respiration
	2. Herbivorous (secondary) link		
2.1	r_{c1}	0.5	Resistance of substrate uptake (food grazing)
2.2	$V_2^m = P_2^m/P_1^m = 1/(r_{56} + r_6)$	1.0	Relative maximum specific rate of herbivore link
2.3	r_{56}	0.05	Resistance of coupling reaction of substrate (food) cycle with cycle of processing reactions
2.4	r_6	0.95	Resistance of reactions of processing cycle
2.5	$R_2 = r_{56} + r_6$	1.0	Total resistance of secondary link
2.6	r_{20}	25	Resistance of specific maintenance respiration
2.7	r_{24}	30	Mortality
2.8	$\alpha = \beta$	0.3	Growth efficiency and biosynthesis respiration
2.9	γ	0.4	Egestion
	3. Carnivorous link		
3.1	r_{c2}	1.0	Resistance of substrate uptake (food grazing)
3.2	$V_3^m = P_3^m/P_1^m = 1/(r_{78} + r_8)$	0.25	Relative maximum specific rate
3.3	r_{78}	0.2	Resistance of coupling reaction of substrate (food) cycle with cycle of processing reactions
3.4	r_8	3.8	Resistance of reactions of processing cycle
3.5	$R_3 = r_{78} + r_8$	4.0	Total resistance of carnivorous link
3.6	r_{30}	140	Resistance of specific maintenance respiration
3.7	r_{34}	100	Mortality
3.8	$\alpha = \beta$	0.3	Growth efficiency and biosynthesis respiration
3.9	γ	0.4	Egestion
	4. Bacterial link		
4.1	r_{c4}	0.08	Resistance of substrate uptake
4.2	$V_5^m = P_5^m/P_1^m = 1/(r_{90} + r_9)$	4.0	Relative maximum specific rate of bacterial link
4.3	r_{90}	0.0125	Resistance of coupling reaction of substrate cycle with cycle of processing reactions
4.4	r_9	0.2375	Resistance of reactions of processing cycle
4.5	$R_5 = r_{90} + r_{09}$	0.25	Total resistance of bacterial link
4.6	r_{50}	3.0	Resistance of specific maintenance respiration
4.7	r_{54}	10	Mortality
4.8	$\alpha = \beta$	0.3	Growth efficiency and biosynthesis respiration
4.9	γ	0.4	Egestion

	5. Concentrations		
5.1	$[C_i]$; $\Sigma[C_i]$	Not used	Absolute concentration of i-th component (link) Total concentration of all components (links)
5.2	$c_i = [C_i]/\Sigma[C_i]$	To be calculated	Relative component concentrations
5.3	$c_0 + c_1 + c_2 + c_3 + c_4 + c_5 = \Sigma\, c_i$	1.0	Total relative component concentrations

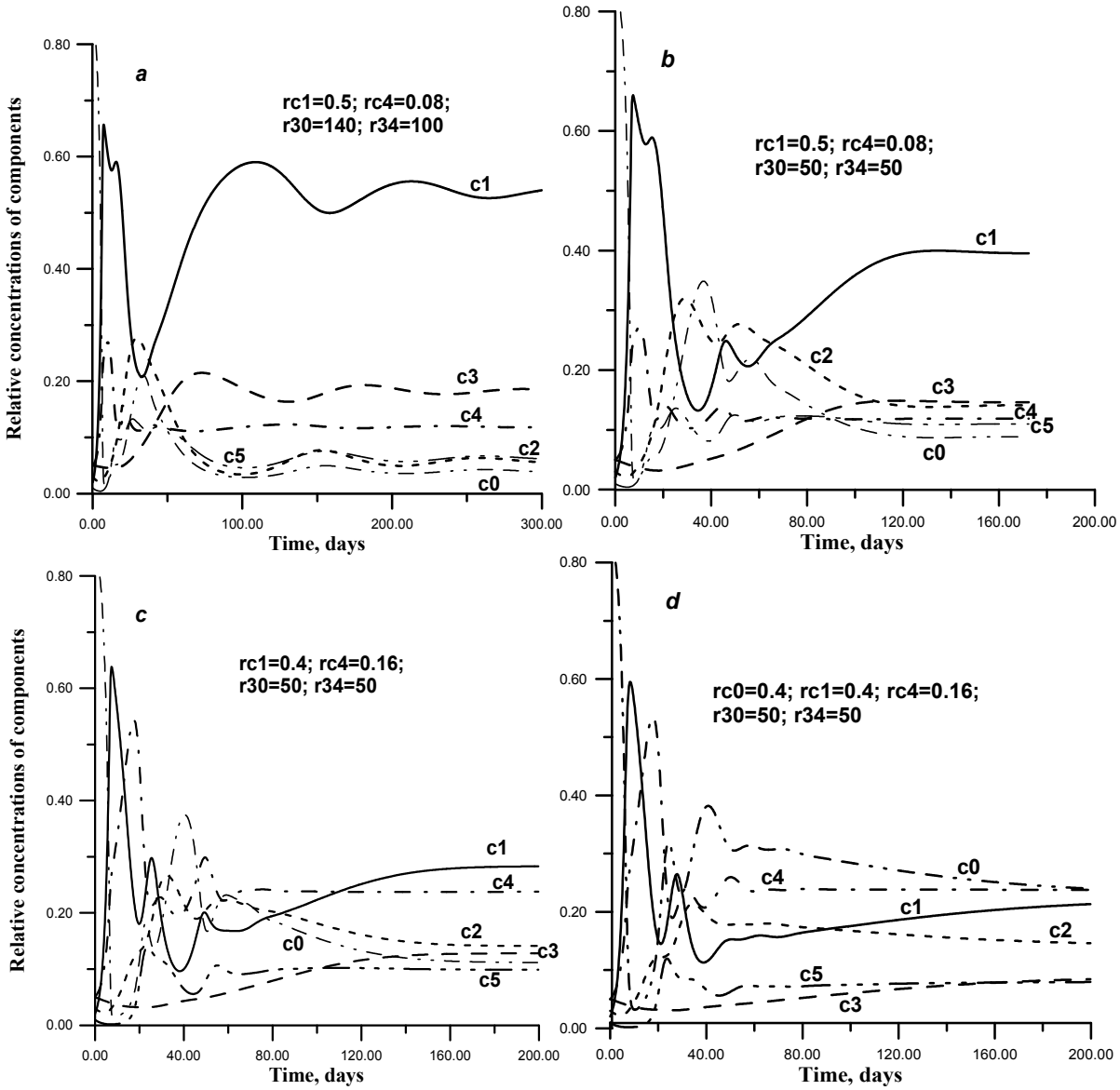

Fig. 17 Six compartment ecosystem model (Table 9)/TURBO PASCAL 7 output showing the time-dependence dynamics of concentrations of ecosystem components (link masses). The initial concentrations are: c1 = 0.02; c2 = 0.03; c3 = 0.05; c4 = 0.05; c5 = 0.01; c0 = 0.84 (phytoplankton, herbivores, carnivores, detritus, bacteria and inorganic matter correspondingly). a – parameters of Table 1; b – r30 and r34 decreased (spending of c3 increased); c – rc1 decreased and rc4 increased (substrate constant of c2 grazing to c1 increased and substrate constant uptake of c4 by c5 decreased); d – rc0 increased (substrate constant uptake of c0 by c1 decreased); and following on the next page, e – rc1 decreased (substrate constant of c2 grazing to c1 in addition); f – r23 increased and r3 decreased (in primary link), the dependence of primary production on nutrients is closed to Michaelis-Menten equation.

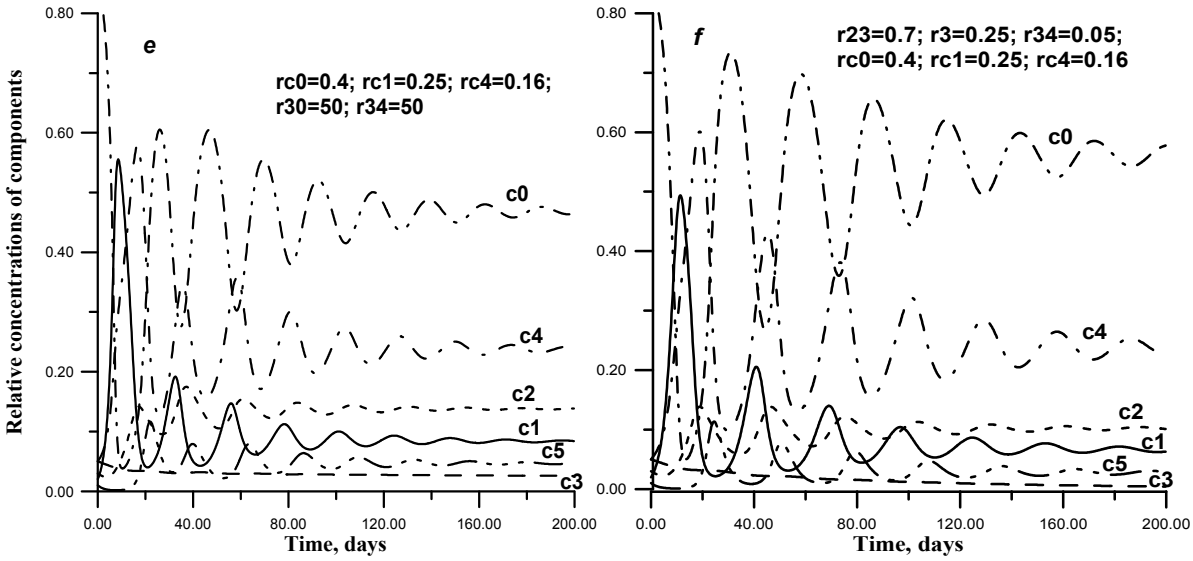

Fig. 17 (continued from the previous page)

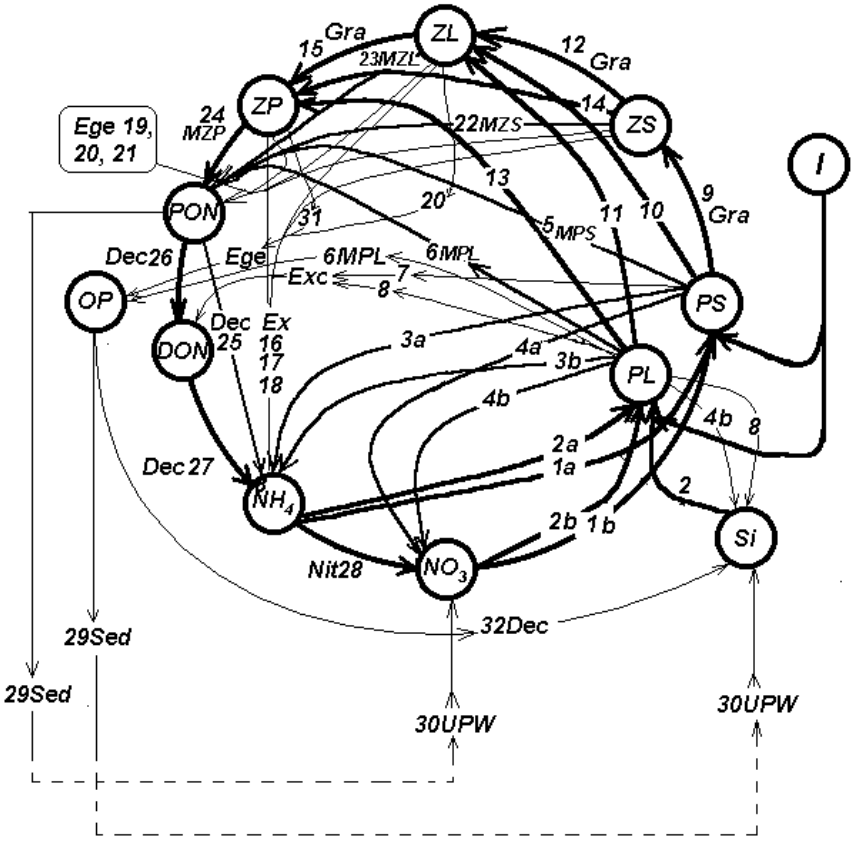

Fig. 18 NEMURO Model 2000, PICES CCCC prototype LTL marine ecosystem model. Ecosystem is represented as ecological cycle of limited nutrient. It is seen that cyclical flows of matter are the main attribute of ecosystem. Sedimentation and upwelling are the parts of the cyclical fluxes. Designation see in the original (Eslinger *et al.* 2000).

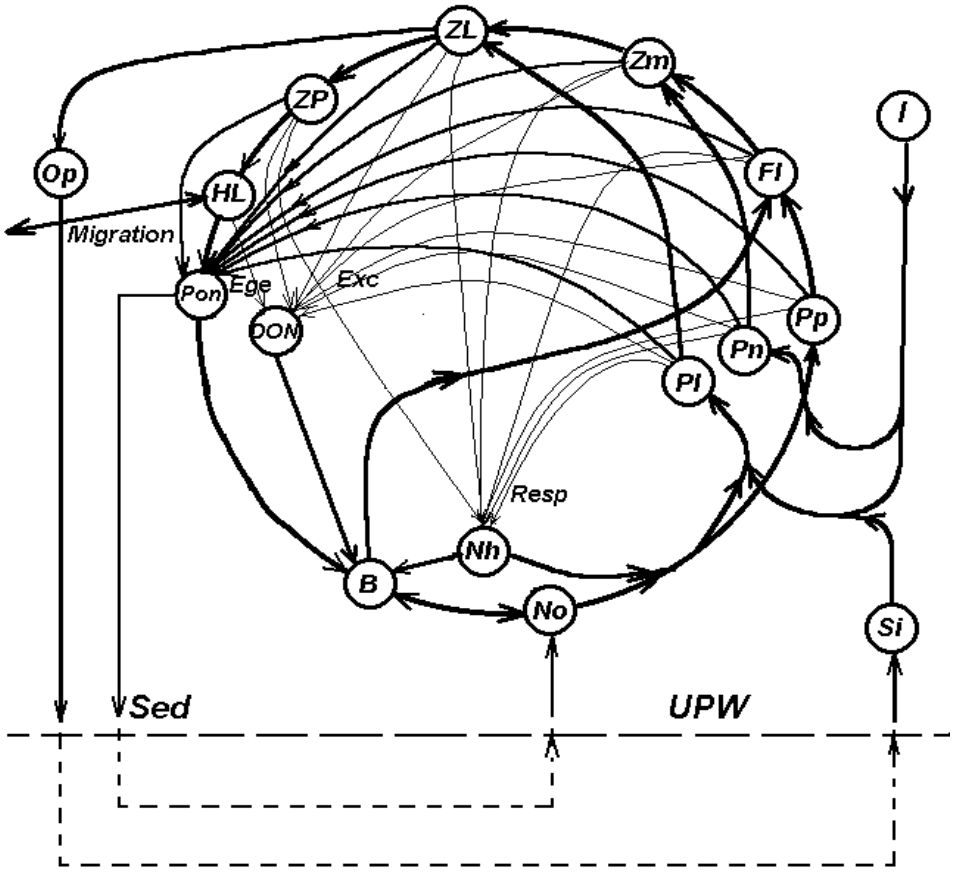

Fig. 19 The complicated NEMURO Model 2000. Model includes the microbial food web and higher trophic level (HTL). Such a model consists of 15 compartments. PON and DON are the food of bacteria with different preference; ammonium and nitrate are the sources of nitrogen. Bacteria in turn are the food to Flagellates (Fl). This model is describing by about of 60 algebraic and differential simultaneous equations. HTL can migrate in and off the ecosystem. Designation the same as in Figure 18.

Such relatively simple model as Figure 16 can be very convenient for investigation of ecosystem operation and its sensitivity to parameter changes. This model is the step to development and investigation of more complex ecosystem with including in it the bacterial and higher trophic levels (such as Fig. 19).

Figure 18 presents the NEMURO Model. This model can be complicated by way of including in it the bacterial food web and link of higher trophic level. Figure 19 presents the simplified variance of such a 15-compartment model. This model is described by a system of about 60 equations.

So the main difficulties lie in constructing the correct (close to reality) conceptual and mathematical models and in understanding its behavior. Which of the factors have a strong effect on ecosystem behavior and what other ones have a low influence on the system behavior needs to be established.

The unique approach, the possibility of composing the quantitative description of the schemes of arbitrary complexity gives the opportunity to apply it to all the processes in which the biological systems play significant part. We are sure that the proposed approach, based on the mechanism of biological processes, will allow us to describe and to understand both the functioning of each processes of the ecosystem, and the ecosystem as a whole. The results of our preliminary studies confirm such possibilities.

Coupling lower and higher trophic level models in marine ecosystems: Some considerations

Daniel M. Ware[1], Bernard A. Megrey[2], Francisco E. Werner[3] and Kenneth A. Rose[4]

[1] Adjunct-Professor, Department of Earth and Ocean Sciences, University of British Columbia. Mailing address: 3674 Planta Road, Nanaimo, B.C., Canada. V9T 1M2 E-mail: mandd@island.net

[2] National Marine Fisheries Service, Alaska Fisheries Science Center, 7600 Sand Point Way NE, Seattle, WA 98115, U.S.A. E-mail: bern.megrey@noaa.gov

[3] Marine Sciences Department, CB# 3300, University of North Carolina, Chapel Hill, NC 27599-3300, U.S.A. E-mail: cisco@email.unc.edu

[4] Coastal Fisheries Institute & Department of Oceanography and Coastal Sciences, Wetlands Resources Building, Louisiana State University, Baton Rouge, LA 70803, U.S.A. E-mail: karose@lsu.edu

The development of a coupled lower and higher trophic level model can be guided by asking five basic questions:

How many key functional groups link the lower and higher trophic levels?

Real food webs are very complex. Diet information can be used to determine the number of significant pathways linking LTL organisms to HTL predators. Seasonal changes in the diet also need to be considered. The model should have at least two pathways linking the lower and higher trophic levels; three is probably better and is certainly more realistic. Alternate pathways are important because they allow LTL production to flow at different rates, to different HTL predators, under different environmental conditions. Three globally important LTL linking groups are: copepods, euphausiids and predatory zooplankton. The order of importance of each of these groups can be expected to vary from place to place, and probably over time in response to climate regime shifts and anthropogenic impacts.

- Copepods are eaten by the larvae and juveniles of most higher trophic level fish species, and by all sizes of small pelagic fishes like herring, anchovy, sardine and sand lance.
- Euphausiids and predatory zooplankton are also eaten by a wide range of small and medium sized pelagic species (including mackerel and small hake).

For these reasons, the Task Team noted that consideration should be given to dividing the large zooplankton (ZL) component in the PICES NEMURO Model into separate copepod and euphausiid components.

What HTL response do we want to model and why?

Typically, the objective is to model the time-varying daily nutrient flux, and the biomass and production rates of key HTL predators, which are of commercial and societal importance, so the current state of these organisms and the resource management implications can be evaluated. Computationally, and also because of limited knowledge of some of the important biological processes, it is difficult to handle more than ten HTL species (or functional groups) in most dynamic models. An important exception to this is ECOSIM, which, because of the way it is structured, has the capability of handling up to fifty species. The number of species (or functional groups) that need to be included depends on the purpose of the model. A number of models of different complexity may be required to answer a range of species-specific questions.

How should each species or functional group of species be represented in the model?

The simplest arrangement is to have a single aggregated group (for example "small zooplankton" or "small pelagic fish"). In other cases, it may be more appropriate to structure the model so some of the key species are represented as a population of multiple size, or age groups. In all likelihood, the model will be structured with a mixture of simple, pooled functional groups, and one or more size or age structured species groups.

For example, the HTL model could contain a detailed age-specific sub-model of herring, with the other HTL predators aggregated into one or more functional groups, similar to the European Regional Sea Ecosystem Model (ERSEM).

How do HTL predators consume LTL production, or, what is the most likely functional response?

If predators and prey tend to be distributed uniformly in space then it is appropriate to use a simple prey-dependent type II functional response to model the feeding rate (I). Numerous short-term experiments have found that a type II functional response appears to characterize the feeding response of a variety of predators (e.g. Valiela 1995). However, experimental research has also shown that turbulent mixing, temperature, predator behaviour, and predator density can modify the functional response.

Mixing The rate of food consumption by fish larvae increases with the amount of turbulent mixing, because it increases the rate of prey contact (e.g. Sundby and Fossum 1990). Theoretically feeding rate increases with increasing turbulence, achieves a maximum at some intermediate turbulent mixing rate, after which feeding tapers off with increasing turbulence (Rothschild and Osborne 1988). This phenomenon is most important for small zooplankton and fish larvae, and perhaps some juvenile fish.

Temperature The rate of prey consumption and hence the maximum daily ration are dome-shaped functions of temperature (e.g. Brett and Groves 1979).

Predator behaviour Although rarer, there are examples of an S-shaped type III functional response (e.g. Valiela 1995). It may arise from changes in predator behaviour, like prey switching, or searching image formation.

Predator density If predators form dense schools, the resulting functional response will depend on both the predator (P) and prey (N) densities, in a manner that reflects feeding interference between the predators (Cosner *et al.* 1999). Accordingly, some of the more probable functional responses formulations include:

Holling Type II: Prey (N) dependent functional response (I is the ingestion rate) when the predator is uniformly distributed (Fig. 20).

$$I = eN / (1 + ehN)$$

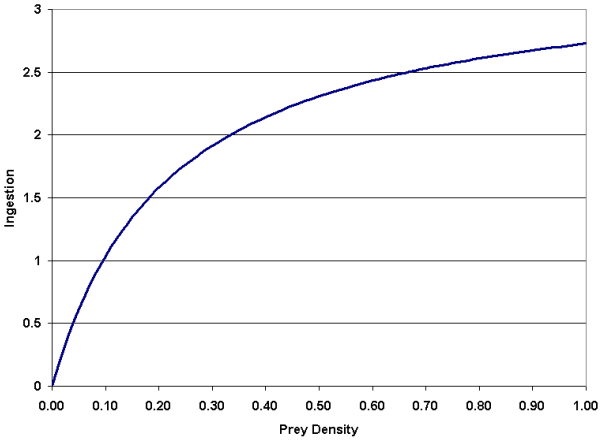

Fig. 20 Relationship between prey density and ingestion rate using a Holling II type functional response. Parameters used are e=15.0, h=0.3.

Holling Type III: S-shaped prey-dependent functional response (Fig. 21).

$$I = k / [1 + a \exp(-bN)]$$

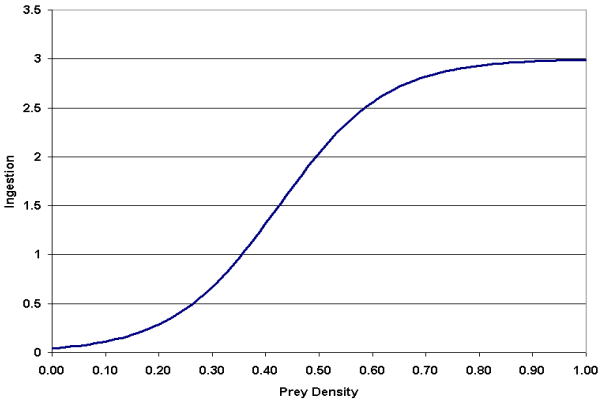

Fig. 21 Relationship between prey density and ingestion rate using a Holling III type functional response. Parameters used are k=3.0, a=70.0, and b=10.0.

Hassell-Varley Type: Functional response depends on both prey (N) and predator (P)

densities. For a school of predators foraging in 3 dimensions (Fig. 22):

$$I = ecN / (P^{1/3} + ehcN)$$

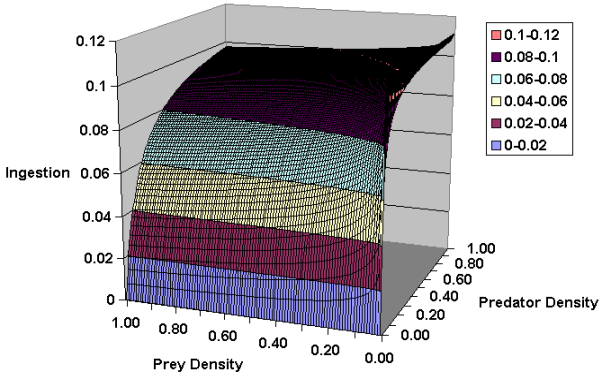

Fig. 22 Relationship between predator and prey density and ingestion rate using a Hassel-Varley type functional response. Parameters used are e=0.4, h=9.0, and c=2.0.

DeAngelis-Beddington Type: With feeding interference among predators (Fig. 23):

$$I = eP_oN / (P_o + P + ehP_oN)$$

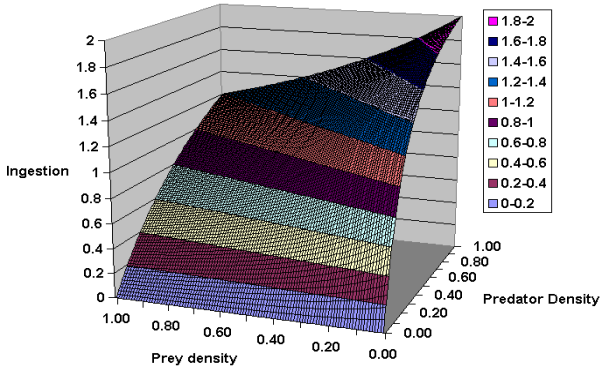

Fig. 23 Relationship between predator and prey density and ingestion rate using a De-Angelis-Beddington type functional response. Parameters used are e=10.0, h=0.4 and P_0=0.3.

How much consumed energy is converted into HTL predator production?

Three important factors affecting HTL predator growth rates are the size of the food ration, the metabolic rate, and water temperature.

The master bioenergetics equation is:

$$I = E + M + G$$

where I = ingested energy, E = excretion, M = metabolism, and G = growth (and reproduction). For well-fed carnivorous fish in the laboratory Brett and Groves (1979) found:

$$(100)I = (27)E + (44)M + (29)G$$

In natural ecosystems, E will probably be similar, but M will be much higher because of the additional metabolic costs incurred by finding food and avoiding predators, and because natural foods are not as digestible as the man-made foods that were used in these experiments. Hence G will be much lower, probably around 10% to 15% of the ingested ration.

- The growth rate is usually a saturating function of ration size (Brett *et al.* 1969), but in some cases it may be weakly dome-shaped at very high rations.
- The growth efficiency tends to be highest at intermediate sized rations (Brett *et al.* 1969).
- For any given ration, the resulting growth rate is a dome-shaped function of temperature (Brett *et al.* 1969). In Figure 24, note how the highest growth rate occurs at a lower temperature when the prey density, and hence the ration, are reduced. This is an important phenomenon, which the HTL component of the model should be able to reproduce.

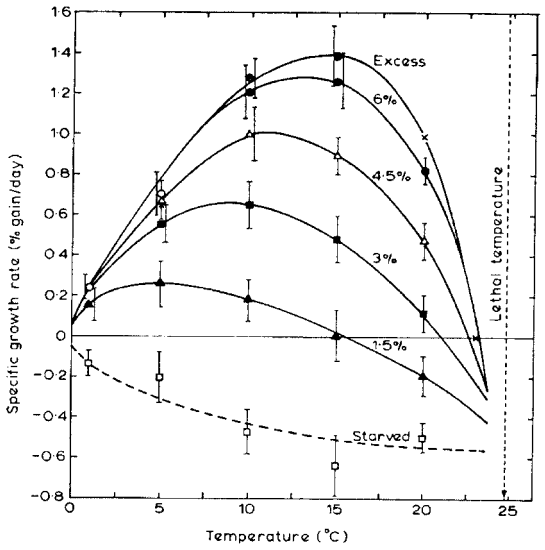

Fig. 24 Relation between temperature and specific growth rate (± 2 S.E.) of young *Orcorhynchus nerka* when fed various rations as percentage of body dry weight. Points marked (X) and (O) are separate experiments using excess ration (after Brett *et al*. 1969).

Are seasonal migrations by HTL predators important?

Large biomasses of fish, birds and marine mammals migrate into or through most subarctic marine ecosystems in the summer to feed.

- The arrival time and the biomass of these migrants can have a significant impact on the biomass and production of LTL prey species. (e.g. Robinson and Ware 1994).
- The largest fish tend to migrate further north (e.g. sardine and hake in the NE Pacific).
- Presumably the movements of migrating species are also affected by other factors like: temperature, food supply, predators, reproductive state, etc. Much more needs to be learned about this.

Diagnostic analysis

Once the coupled model has been constructed and the output has passed a "reasonableness" test the model can be used as a tool to diagnose the current productivity of the system. Time series measurements of important physical variables, like radiation, temperature, and wind speeds, and the estimated biomass of important fish species (from stock assessment analyses), can be input to the model to estimate the *current lower trophic level productivity* of the system, and the productivity of some key HTL organisms. The results will enable fisheries managers to determine if the target harvest rates are sustainable. This information will be very useful, because it will enable the manager to adjust the harvest rate annually, in response to model estimates of the current productivity of the system.

Prognostic analysis

Prognostic analysis is very difficult because it involves predicting the future state of complex ecosystems. For successful long-range forecasting we need to be able to estimate how the future growth, mortality and recruitment rates of each key species in the model will respond to both "bottom-up" forced and "top-down" forced changes in the state of the system. These changes are caused by natural variations in the physical forcing variables and by anthropogenic forcing, through global warming, habitat destruction and over-fishing. Given our current, limited knowledge about many of the complex processes involved here, long-range productivity forecasting cannot be done with any precision at this time. Accordingly, the production of most HTL species should not be forecast more than a few years ahead, until the models improve.

An overview of ECOPATH/ ECOSIM

Steven J.D. Martell
Fisheries Centre, University of British Columbia, Vancouver, B.C., Canada. V6T 1Z4 E-mail: smartell@fisheries.com

A brief overview of the ECOPATH/ECOSIM modeling approach was provided in request of the potential need to couple the NEMURO model to another higher trophic level modeling paradigm.

A tool for visualizing ecosystem model output

Kerim Y. Aydin
National Marine Fisheries Service, Alaska Fisheries Science Center, 7600 Sand Point Way NE, Seattle, WA 98115, U.S.A. E-mail: kerim.aydin@noaa.gov

A demonstration was given of a custom software that assists visualizing ecosystem model output. The tool organizes output information by trophic level and plots fluxes as a ration of production to biomass. Figure 25 shows an example screen shot from an eastern tropical Pacific tuna fishery.

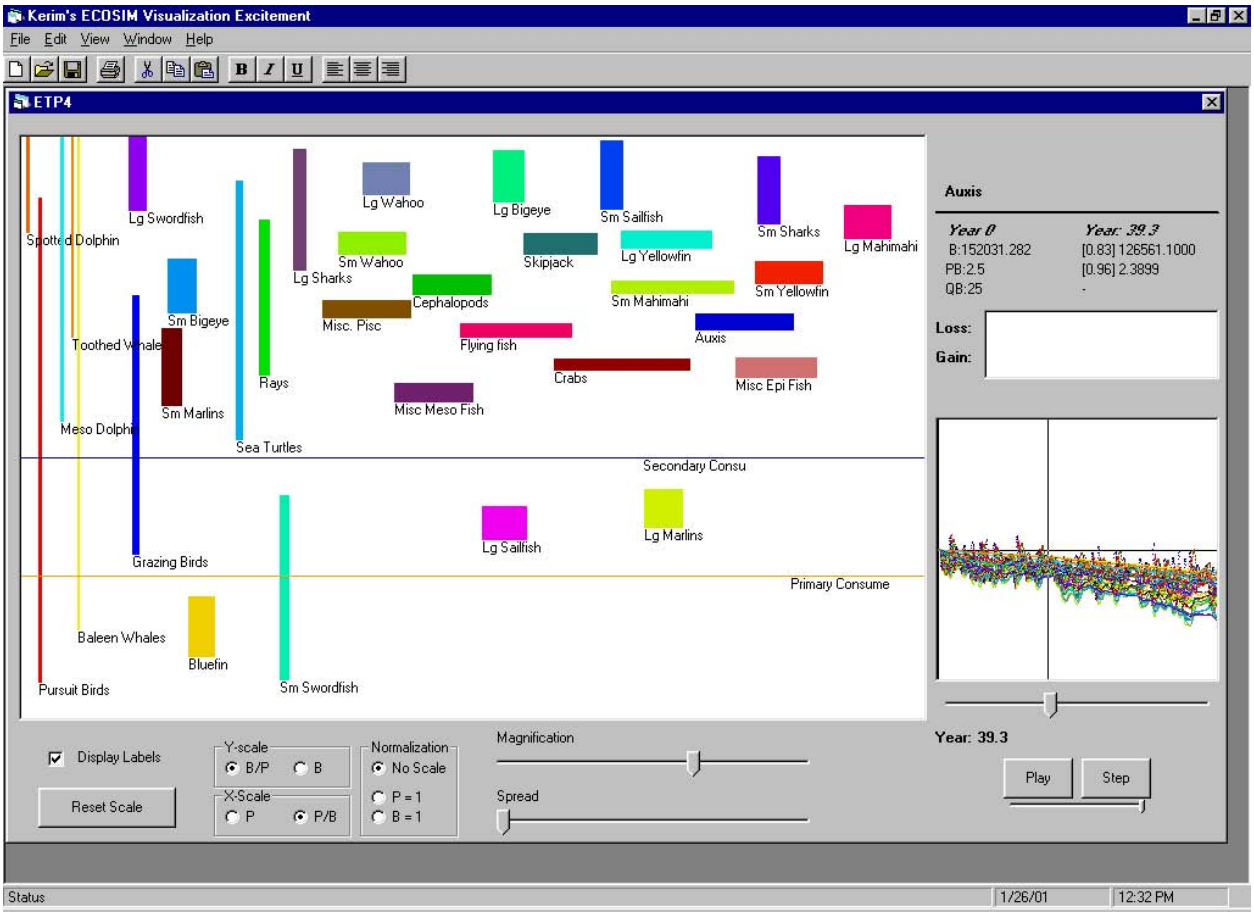

Fig. 25 Example of prototype NEMURO visualization software. Example presented is a simulation of the eastern tropical Pacific tuna fishery, showing the relative Biomass (Y-dimension of each box) and P/B ratio (X-dimension of each box) during a period of high production. R-selected species have long horizontal direction, while K-selected species have a long vertical direction.

MODEL Workshop Summary

At the Hakodate Workshop, the MODEL Task Team discussed some of the processes that need to be considered for representing LTL coupled to HTL trophodynamics in marine ecosystems. The Task Team noted that significant advances in modeling the dynamics of LTL in aquatic systems (i.e. the microbial food web, and large phytoplankton and zooplankton) have occurred in the last decade. Progress has also been made in linking the production of HTL organisms (e.g. squid, fish, seabirds, and marine mammals) to LTL production models. Problems still exist when scaling process information and data to the scales required for marine ecosystem models. Figure 26 (ICES Study Group 1993) summarizes the relationship between observed species composition, state variables in modeling approaches that build from the "bottom up" with increasing complexity (and numbers of species). The suggested approach is to focus on the target species with links to lower and higher trophic levels by aggregating/sub grid-scale representation rather than including the full complexity of the neighboring trophic components.

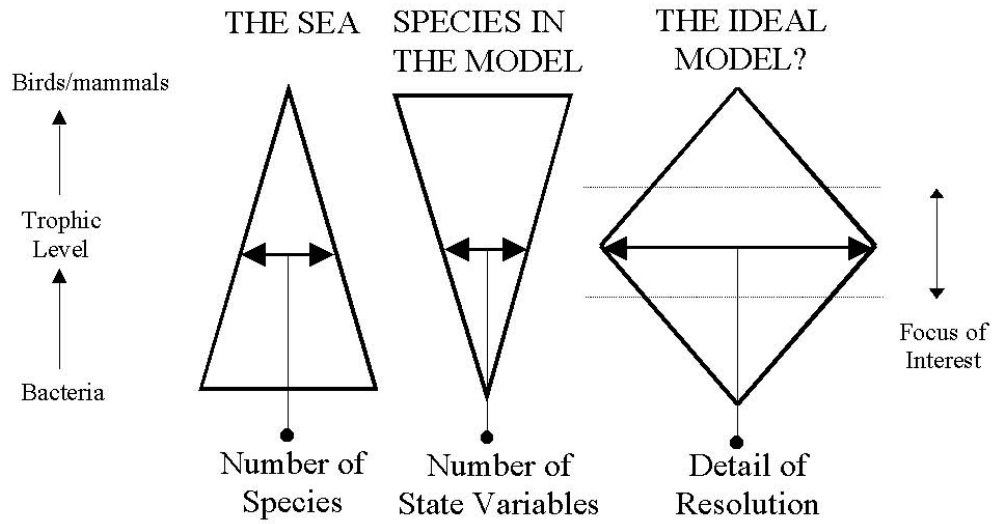

Fig. 26 Cartoon depicting tradeoffs between spatial and temporal scales of model resolution and model integration as they relate to modeling ecosystems. After ICES Study Group on Spatial and Temporal Integration, Glasgow, 1993 (ICES C.M. 1993/L:9).

Since LTL and HTL organisms function on different time and spatial scales within the ecosystem, successful coupling requires getting a number of things right -- or just about right. In this context, information about the diet, the functional response, growth efficiencies, large-scale seasonal movements of migratory species, and the impact of climate variability on these processes are required. For some marine ecosystems in the PICES area, enough biological, ecological, and stock assessment knowledge exists to begin using coupled models as primitive diagnostic tools to assess the current productivity and impacts of climate change on the ecosystem, and the effects on the dynamics of the key organisms within it. The development of a successful prognostic capability is a more challenging, longer-term problem, which requires getting a number of other things right, such as recruitment dynamics, dispersal and migratory behavior, and behavioral changes in predator-prey interactions.

Recommendations

- Convene a MODEL Workshop to implement improvements to the PICES NEMURO model.
- Increase interaction with BASS and REX to support their modeling initiatives through cooperative modeling workshops.
- The CCCC Co-Chairmen should present these workshop proposals to the Science Board as a coordinated package of integrated activity underscoring the cooperation and interdependencies.
- Facilitate joint planning; time needs to be allocated at the next PICES Annual Meetings for joint CCCC inter-sessional meetings.
- Encourage opportunities for more CCCC Task Team interaction, joint CCCC Task Team meetings are needed to coordinate and implement Task Team plans. In Victoria, the Task Team meetings should be at non-overlapping times and places.
- Request that the PICES Secretariat provide assistance to help MODEL build a web page to present NEMURO code, data and results.
- Issues related to model management need to be addressed so as to better control the increasing number of different versions of a model, including process equations, parameter files, physical forcing data files, and post processing programs. We propose to examine the ICES/GLOBEC experience to obtain guidance as to how best to proceed.
- Develop "NEMURO/Stella" Box Model using the Stella software package.
- Make progress on preparing an executable version of the prototype model available on the WWW.

- Develop a means of staying in contact to continue unfinished work.

Achievements and future steps

- Link with high trophic level model.
- The LTL model needs to include fishes, marine mammal, marine birds, and also micro-nekton.
- Perform basic model validation studies.
- Develop model validation protocols.
- Compare physical factors with direct observations.
- Compare model biomass predictions with direct observations at Stations A7 and the Bering Sea.
- Identify scientific questions for comparison.
- Communication and cooperation with the REX and BASS Task Teams is needed.
- Perform listed experiments.
- NEMURO extensions:
  - add Fe limitation to phytoplankton production;
  - add microbial food web;
  - split ZL into copepods and euphausiids;
  - add sinking rate of phytoplankton to detritus pool;
  - parameterize NEMURO to a coastal region.
- NEMURO diagnostics:
  - code diagnostic and performance measures into NEMURO such as P/B, C/B ratios and ecotrophic efficiency calculations;
  - validate model output against data fro each regional location;
  - perform side-by-side comparison of NEMURO Box and NEMURO MATLAB models to same equations and data.
- Spatially explicit approach:
  - extend 1-D coupled model per above;
  - work toward eventually embedding NEMURO into larger scale 3-D ocean model similar to Kawamiya *et al.* (2000a, 2000b).
- Linkages with other CCCC components:
  - modify NEMURO per needs of REX and convene joint workshop to achieve extension of NEMURO to include higher trophic levels;
  - devise scheme to link NEMURO with ECOPATH/ECOSIM with the aim towards meeting the objectives of BASS.
- Establish links with other programs such as GODAE, WCRP, CLIVAR.
- Modifications as required to accommodate BASS and REX needs.

References

Brett, J.R., Shelbourn, J.E., and Shoop, C.T. 1969. Growth rate and body composition of fingerling sockeye salmon, *Oncorhynchus nerka* , in relation to temperature and ration size. Journal of the Fisheries Research Board of Canada 26: 2363-2394.

Brett, J.R., and Groves, T.D. 1979. Physiological energetics. *In* Fish Physiology Vol. VIII. Academic Press. P. 280-352.

Cosner, C., DeAngelis, D.L., Ault, J.S., and Olson, D.B. 1999. Effects of spatial grouping on the functional response of predators. Theoretical Population Biology 56: 65-75.

DeAngelis, D.L., Rose, K.A., Crowder, L., Marschall, E., and Lika, D. 1993. Fish cohort dynamics: application of complementary modeling approaches. American Naturalist 142: 604-622.

Edwards, G., and Walker, D. 1983. C3, C4 : mechanisms, and cellular and environmental regulation, of photosynthesis. Oxford, Blackwell Scientific Publications: 598 p.

Eslinger, D.L., Kashiwai, M.B., Kishi, M.J., Megrey, B.A., Ware, D.M., and Werner, F.E. 2000. Final report of the International Workshop to Develop a prototype lower trophic level ecosystem model for comparison of different marine ecosystems in the North Pacific. *In* PICES-GLOBEC International Program on Climate and Change and Carrying Capacity Report on the 1999 MONITOR and REX Workshops, and the 2000 MODEL Workshop on Lower Trophic Level Modeling. *Edited by* B.A. Megrey, B.A. Taft, and W.T. Peterson. PICES Scientific Report No. 15, 285p.

Falkowski, P.G., and Wilson, C. 1992. Phytoplankton productivity in the North Pacific since 1900 and implications for absorption of anthropogenic CO2. Nature. 358: 741-743.

Fasham M.J.R. 1995. Variations in the seasonal cycle of biological production in subarctic oceans: a model sensitivity analysis. Deep-Sea Research I. 42: 1111-1149.

Fasham, M.J.R., Ducklow, H.W., and McKelvie, D.S. 1990. A nitrogen-based model of plankton dynamics in the oceanic mixed layer. Journal of Marine Research 48: 591-639.

Goodwin, T.W., and Mercer, E.I. 1983. Introduction to Plant Biochemistry. Oxford, Pergamon Press, Vol. 1: 392p.

Hinckley, S. 1999. Biophysical mechanisms underlying the recruitment process in walleye pollock (*Theragra chalcogramma*). Ph.D. Dissertation. University of Washington, Seattle. 259p.

ICES Study Group on Spatial and Temporal Inte-gration, Glasgow, 1993 (ICES.C.M. 1993/L:9)

Kawamiya, M, Kishi, M.J., Yamanaka, Y., and Suginohara, N. 1995. An ecological-physical coupled model applied to Station P. Journal of Oceanography 51: 635-664.

Kawamiya, M., Kishi, M.J., Yamanaka, Y., and Suginorhara, N. 1997. Obtaining reasonable results in different oceanic regimes with the same ecological-physical coupled model. Journal of Oceanography 53: 397-402.

Kawamiya, M., Kishi, M.J., and Suginohara, N. 2000a. An ecosystem model for the North Pacific embedded in a general circulation model. Part I: Model description and characteristics of spatial distributions of biological variables. Journal of Marine Systems 25: 129-157.

Kawamiya, M., Kishi, M.J., and Suginohara, N. 2000b. An ecosystem model for the North Pacific embedded in a general circulation model. Part II: Mechanisms forming seasonal variations of chlorophyll. Journal of Marine Systems 25: 159-178.

Kishi, M.J., Motono, H., Kashiwai, M., and Tsuda, A. 2001. An ecological-physical coupled model with ontogenetic vertical migration of zooplankton in the northwestern Pacific. Journal of Oceanography (submitted).

Longhurst, A., Sathyendranath, A., Platt, T., and Caverhill, C. 1995. An estimate of global primary production in the ocean from satellite radiometer data. Journal of Plankton Research 17: 1245-1271.

Megrey, B.A., Kishi, M.J., Kashawai, M.B., Ware, D., Werner, F.E., and Eslinger, D.L. 2000. PICES Lower Trophic Level Modeling Workshop, Nemuro 2000. PICES Press 8: 18-22.

Oguz, T., Ducklow, H.W., Malanotte-Rizzoli, P., Murray, J., Shushkina, E.A., Vedernikov, V.I., and Unluata, U. 1999. A physical-biochemical model of plankton productivity and nitrogen cycling in the Black Sea. Deep-Sea Research 46: 597-636.

Platt T., Denman, K.L., and Jassby, A.D. 1977. Modelling the productivity of phytoplankton. *In* The sea: ideas and observations of progress in the study of the seas, Vol. 6. *Edited by* E.D.Goldberg, I.N.McCave, J.J.O'Brien and J.H.Steele. New York, N.Y., John Wiley & Sons pp. 807-856.

Robinson, C.L.K., and Ware, D.M. 1994. Modeling pelagic fish and plankton trophodynamics off southwestern Vancouver Island, British Columbia. Can. J. Fisheries and Aquatic Sciences 51: 1737-1751.

Rose, K.A. 2000. Why are quantitative relationships between environmental quality and fish populations so elusive? Ecological Applications 10: 367-385.

Rothschild, B.R., and Osborn, T.R. 1988. Small-scale turbulence and plankton contact rates. Journal of Plankton Research 10: 465-474.

Straile, D. 1997. Gross growth efficiencies of protozoan and metazoan zooplankton and their dependence on food concentration, predator-prey weight ratios, and taxonomic group. Limnol. Oceanogr. 42: 1375-1385.

Shiotani, T., and Uye, S. 2000. Selective feeding of the calanoid copepod *Calanus sinicus* on the natural microplankton assemblage, with special reference to microzooplankton. Abstracts. PICES Ninth Annual Meeting. Hakodate. pp. 133-134.

Sundby, S., and Fossum, P. 1990. Feeding conditions of Arctro-norwegian cod larvae compared with the Rothschild-Osborn theory on small-scale turbulence and plankton contact rates. J. Plankton Res. 12: 1153-1162.

Steele, J.H. 1962. Environmental control of photosynthesis in the sea. Limnol. Oceanogr. 7: 137-150.

Valiela, I. 1995. Marine ecological processes. Springer-Verlag New York. 686p.

Wang, S-B. 1998. Comparative studies of the life history and production potential of bay anchovy *Anchoa mitchilli* and northern anchovy *Engraulis mordax*: an individual-based modeling approach. Ph.D. Dissertation. University of South Alabama, Mobile.

Wong, C.S., Whitney, F.A., Iseki, K., Page, J.S., and Zeng, J. 1995. Analysis of trends in primary productivity and chlorophyll-a over two decades at Ocean Station P (50° N 145° W) in the Subarctic Northeast Pacific Ocean. *In* Climate Change and Northern Fish Populations. *Edited by* R.J. Beamish. Canadian Special Publication in Fisheries and Aquatic Sciences 121: 107-117.

Zvalinsky, V.I., and Litvin, F.F. 1986. Steady-state kinetics of chains of coupled cyclic reactions. Biochimiya (Rus.) 51: 1741-1755.

Zvalinsky, V.I., and Litvin, F.F. 1988a. Modelling of photosynthesis and its coupled processes. Biofisika (Rus.) 33: 169-182.

Zvalinsky, V.I., and Litvin, F.F. 1988b. The photosynthesis dependence on carbon concentration, intensity and spectral composition of light. Fisiologiya rastenii (Rus.) 35: 444-457.

Zvalinsky, V.I., and Litvin, F.F. 1991. Quantitative analysis of photosynthesis adaptation to light. Fisiologiya rastenii (Rus.) 38: 431-442.

MODEL Endnote 1

Participation List

Canada
- Kenneth L. Denman
- Steven J. Martell
- Daniel M. Ware

Japan
- Michio J. Kishi
- Hiroshi Kuroda
- Maki Noguchi
- Masako Saitoh
- Lan S. Smith
- Yasuhiro Yamanaka

Korea
- Sukyung Kang

Russia
- Gennady A. Kantakov
- Vladimir I. Zvalinsky

U.S.A.
- Kerim Y. Aydin
- Andrew W. Leising
- Sarah Hinckley
- Bernard A. Megrey
- Kenneth A. Rose
- Francisco E. Werner

Other
- Sergio Hernandez (Mexico)

MODEL Endnote 2

Meeting Schedule

Friday, October 20, 2000

CCCC First Plenary Session

09:25-09:35 Overview of MODEL workshop and activities (Kishi & Megrey)

11:00-11:30 Kenneth A. Rose. (keynote speaker) A review of the use of individual-based models as upper trophic level modelling tools.

MODEL Workshop

13:30-13:45 Opening remarks (Kishi)

13:45-14:15 Bernard A. Megrey, M.J. Kishi, D.M. Ware and M. Kashiwai. Summary of NEMURO 2000: An international workshop to develop a prototype lower trophic level ecosystem model for comparison of different marine ecosystems in the North Pacific.

14:15-14:35 Michio J. Kishi and H. Kuroda. Sensitivity analysis on NEMURO.

14:35-14:55 Vadim V. Navrotsky. To the physical forcing and the ways of improvements in the NEMURO model.

14:55-15:15 Francisco E. Werner and D.L. Eslinger. Lower trophic level models in oceanic ecosystems: status of the NEMURO LTL model and suggested extensions.

15:15-15:35 Yasuhiro Yamanaka, N. Yoshie, M. Fujii and M.J. Kishi. NEMURO model follow up.

15:35-15:55 Coffee/tea Break

15:55-16:15 Vladimir I. Zvalinsky. Coupling of different trophic levels in marine ecosystem models.

16:15-16:35 Daniel M. Ware. Coupling lower and higher trophic level models in marine ecosystems: an overview.

16:35-17:30 Discussion

Saturday, October 21, 2000

MODEL Workshop

09:00-09:30 Steven J. Martell. Review on ECOPATH modeling.

09:30-09:50 Fransisco E. Werner. Report from GLOBEC Focus 3 WG.

09:50-10:40 Discussion how to connect lower trophic and higher trophic level models (Discussion leaders: Kishi & Megrey)

10:40-11:00 Coffee/tea Break

11:00-12:00 Discussion how to connect lower trophic and higher trophic level models (Discussion leaders: Megrey & Kishi)

12:00-13:00 Future work and recommendations

CCCC Second Plenary Session

14:15-14:30 Report of MODEL Workshop and recommendations (Megrey)

MONITOR WORKSHOP ON PROGRESS IN MONITORING THE NORTH PACIFIC

(Co-convenors: Bruce A. Taft and Yasunori Sakurai)

A 2-day MONITOR Workshop on "Progress in monitoring the North Pacific" was convened prior to the Ninth Annual Meeting in Hakodate, Japan (October 20-21, 2000). The workshop reviewed ongoing and/or planned monitoring programs in North Pacific, and the section below contains extended abstracts of papers given at the meeting. As a result of the workshop discussions, the following recommendations were made:

Continuous plankton recorder field program

PICES should strongly support the principal investigators in their efforts to find long-term funding support for this important monitoring program. It was pointed out that interpretation of the zooplankton data would be enhanced if ancillary environmental data were collected. Specific suggestions were: (a) the collection of sea-chest temperature data; (b) collection of sea-chest water samples for salinity determination; and (c) underway measurement of fluorescence.

Ocean tracking network for the coastal ocean

Participants recognize the potential scientific benefits of the acoustic monitoring array and urge that PICES promote the timely evaluation of this proposal within the community to establish proof of concept.

Preservation of existing North Pacific monitoring programs

a. A biophysical mooring (designated station #2) has been maintained for the last five years southwest of the Pribyloff Is. This time series data set has been used extensively to describe the variability of environmental conditions in this region. It is slated to be terminated this year. The Workshop recommends that PICES lobby in the scientific community for the continuance of this valuable time series.
b. The Japanese shipboard program in the North Pacific is in transition. The *R/V Oshoro-Maru* will not continue to occupy the Bering Sea section at 180º, and the Japan Fishery Agency (JFA) will take over this section. The 180º section is a key section with a long tradition of state-of-the-art observations. The participants recommend that PICES urge that every effort is made by JFA to provide a data set comparable in quality to the *R/V Oshoro-Maru* measurements.
c. For the last 40 years JFA has supported a prefectural monitoring program in the coastal seas of Japan. Shipboard measurements are made from the coast out to 60 nautical miles. The data are used for forecasting of coastal fishing conditions, and in addition constitutess very valuable climate data set. JFA has proposed a 50% cut in funds for this program. The Workshop recommends that PICES call for an assessment of the effects of this proposed action on climate studies in this critical region.

PICES/GOOS interaction

The Workshop recommends that PICES set up a Steering Group to define the direction that PICES should take in integrating their regional interests with GOOS. This Group would consider issues such as the identification of existing observing systems in the North Pacific which could contribute toward a regional PICES GOOS, new observations required to complete the system, and possible eventual establishment of a Regional Analysis Center (RAC), along the lines suggested by LMR-GOOS. The Steering Group would also comment on the possible benefits to PICES countries of providing an annual ecological assessment of the state of the North Pacific.

NEAR-GOOS Planning Workshop

A NEAR-GOOS Forecasting Workshop is planned to consider the future strategy for the program. In order to better serve the climate community NEAR-GOOS need to expand the types of data that they collect and archive by including chemical and biological data. It was recommended that PICES work with the workshop planners to ensure that they have the necessary expertise for a successful workshop.

Gulf Ecological Monitoring (GEM) program

It was recommended that the MONITOR Task Team always include a scientist representing GEM, as this program is a major contribution to monitoring in the PICES region.

Continuous Plankton Recorder measurements in Subarctic Pacific

Sonia D. Batten
Sir Alister Hardy Foundation for Ocean Science, 1, Walker Terrace, Plymouth, UK. PL1 3BN Email: soba@wpo.nerc.ac.uk

Continuous Plankton Recorder (CPR) tows in the North Pacific were begun in March 2000, and a series of seven tows were completed in the March-August time period. The data return was apparently high and it is expected that 450 samples will be analyzed for the year. Processing of the March-May 2000 samples has been completed and preliminary analyses of these data have been carried out.

Neocalanus plumchrus is one of the dominant copepods of the subarctic North Pacific. It was present in the March samples from just outside Prince William Sound (PWS) south to about 41° N but with no obvious peaks. The majority of the individuals were stage 2 copepodites. April abundances were generally higher, with maximum densities between 44° - 54°N. There was a clear gradient in the apparent duration of development with most of the northern individuals still present as stage 2 copepodites whilst over 60% had reached stage 5 in the southern samples. Such a gradient might be expected, since the duration of development probably depends on temperature. These data are the first to show such a pattern in development. Preliminary analyses of the zooplankton community structure reveal distinct differences along the length of these two tows. The more "coastal" samples off PWS and California showed some similarities to each other and were clearly distinct from the more oceanic samples, however, samples within the oceanic region also showed some clustering. Further analyses will reveal the species contributing to these differences, but the fact that communities can already be identified demonstrates that the sampling resolution will be adequate to characterize regional community composition.

Comparisons of zooplankton sampling gear

Jeffrey M. Napp
Alaska Fisheries Science Center, NMFS, Seattle, WA 98115-0070, U.S.A. E-mail: Jeff.Napp@noaa.gov

Zooplankton collection devices cannot be calibrated - there are no absolute standards to compare the *in situ* capture or counting efficiency of various collection devices. However, comparisons of efficiency among samplers, for example total biomass or size frequency captured and retained, are useful. There are at least four types of situations where sampling equipment have been compared:

1. Multiple collection devices were used on the same project and there is a scientific need to combine the data to form indices (example - Georges Bank GLOBEC).
2. Collection devices were changed during a time series and there is a need to compare the catch before and after the change (example - Ocean Station P).
3. A collection device is being used which is based on new technology and it is important to know how it performs relative to a more traditional device (example - compare acoustic estimates with net sample collections).
4. International cooperative monitoring is undertaken and a comparison of sampling procedures used by various countries must be carried out (example- PICES CCCC Program).

Reports were presented at the workshop by S. McKinnell (Canada) and K. Nakata (Japan), dealing with problems associated with adjusting time series to account for changes in method of measurement. At Station P early measurements were made with a NORPAC net and after 10 years of sampling, a SCOR net was used. McKinnell reported the results of over 50 comparisons of the two types of gear. These collections spanned the range of zooplankton biomass observed at Station P. He concluded that the NORPAC biomass estimates must be multiplied by approximately 1.2 to be comparable to the SCOR net when flowmeter estimates of volume filtered are unavailable (e.g. Station P 1956-1981). Another aspect of the study was that more than 40 paired comparisons were needed for adequate precision of the intercalibration. Similar problems were reported by Nakata who identified significant differences between collections made with the NORPAC, Marutoku and Long NORPAC nets - particularly at high biomass levels. Biomass was lowest with the Long NorPac net and the interpretation is that greater clogging of the Long NorPac net produced a systematic error.

The ICES Working Group on Zooplankton Ecology held a "Workshop at Sea" in 1993 to make comparisons among different zooplankton samplers. Thirty-eight scientists from eight ICES countries used two ships (*Johann Hjort* and *A.V. Humboldt*) to make simultaneous collections in a Norwegian Fjord. Net systems compared were: WP2 net, CALCOFI net, Gulf III net, Bongo net, Multi-net, LHPR, BIONESS, and MOCNESS. The data are being examined for relative efficiency for estimation of total zooplankton biomass, zooplankton size-frequency distribution and depth distribution. Manuscripts (Skjodal *et al*. unpublished) and a data CD are in preparation to describe the workshop results. Note that the workshop did not receive designated funding. All investigators participated using their own research funds.

Recommendations

1. PICES scientists are strongly encouraged to make their zooplankton time series internally consistent. If collection equipment changed during the time-series, then sufficient repeated paired collections should be made using the different devices so that there is a statistical basis for quantitative adjustment of the various estimates of zooplankton biomass and size frequency distribution.
2. Institutions holding long time-series should develop a strategy for dealing with anticipated instrumental changes. Changes should not be introduced until an adequate relative comparison of the sampling characteristics of the new and old instruments has been carried out.

Monitoring zooplankton production in the Subarctic Pacific

William T. Peterson
Hatfield Marine Science Center, National Marine Fisheries Service, 2030 S. Marine Science Drive, Newport, OR 97365, U.S.A. E-mail: bill.peterson@noaa.gov

Most monitoring work on zooplankton involves the collection of zooplankton with a plankton net, then preserving the sample with formaldelhyde or alcohol for later analysis of biomass and/or species composition and abundance. In this note, I suggest that such efforts could easily be supplemented with experimental work on living zooplankton and with a small amount of training, experimental work could become routine and could be included in any shipboard monitoring program. By following the methods given below, one can easily estimate growth and production of adult copepods (very easy to do) and growth and production of juvenile copepods (possible but more difficult). The suggested methods can also be adapted for measurement of growth of euphausiids.

One good reason for including production measurements is as follows: analyzing a long time-series of zooplankton biomass and production, we would be able to determine if the

interannual and decadal scale changes in biomass are due to changes in growth rate (i.e., production) or to other factors. For example, subarctic Pacific experienced a two-fold change in zooplankton biomass after 1977. Was this due to an overall increase in production of the subarctic or a two-fold decline in predation on zooplankton?

Methods

To estimate production, one must incubate animals for 24 hours in ambient seawater at some constant temperature. Female copepods are maintained in clean bottles of 500 mL or 1-liter capacity, 1 or 2 females per container for large species (such as *Calanus*) and 5-10 for small species (such as *Paracalanus*) for 24 h, during which time they will produce eggs. Adult female copepods in most cases do not grow, rather channel all energy for growth into egg production. Therefore egg production is a measure of growth. Juvenile copepods grow by moulting from one copepodite stage into another. If you know the moulting rates of a given copepodite stage, you can calculate growth, using the equations given below. Moulting rates are measured by incubating a number of juveniles of a given stage (30 or more animals per experiment) in a 1-L or 2-L container. A small number of those individuals will moult during the 24 h incubation period and those are the data used to calculate moulting rate in the equations below. If such measurements are made along with measurements of chlorophyll concentration, one will, in time, build up an understanding of relationships between secondary production that, with luck, will allow calculation of copepod production from knowledge solely of copepod biomass and chlorophyll concentration.

The basic equation used to calculate production (P) is

$$P = gB$$

where g is growth rate and B the biomass. The growth rate of juveniles is given by

$$g_i = \ln (W_i+1 / W_i) * MR$$

where W is the weight of copepodite stages and MR the moulting rate. The growth rate of adults is given by

$$gf = W_{eggs} / W_{female}$$

and total production is the sum of the two

$$P = (g_i B_i) + gf Bf$$

References below give more details on methods.

References

Kimmerer, W.J., and McKinnon, A.D. 1987. Growth, mortality, and secondary production of the copepod *Acartia tranteri* in Westernport Bay, Australia. Limnol. Oceanogr. 32: 14-28.

Peterson, W.T., Tiselius, P., and Kiorboe, T. 1991. Copepod egg production, smolting and growth rates and secondary production in the Skagerrak in August 1988. J. Plankton Res. 13: 131-154.

Report on standardization of plankton sampling by the national institutes of the Japan Fisheries Agency

Kaoru Nakata

National Research Institute of Fisheries Science, 2-12-4 Fukuura, Kanazawa-ku, Yokohama, Japan. 236-8648 E-mail: may31@nrifs.affrc.go.jp

Since 1964, national institutes of the Japan Fisheries Agency and prefectural fisheries experimental stations have conducted cooperative surveys for forecasting fishing and ocean conditions. These surveys were primarily designed to measure the distribution and abundance of eggs and larvae of pelagic fish. Plankton biomass was also a variable of interest. The measurements were made with a variety of sampling nets (Marutoku, Marunaka, NORPAC nets) so there was concern about the possibility of systematic errors in the survey results. The sampling nets differed in mesh shape and size, type of gauze material, and in the ratio of filtering area to mouth area. A working group was formed in 1993 to consider implementation of procedures

to standardize the survey measurements. The working group identified the primary target organism to be fish eggs. A requirement in the standardization of the plankton sampling was that the data from the new net should be comparable to that collected in the past. They chose the Long NORPAC net for the standard net to be used in the furure, which has a ratio of the filtering area to the mouth size of 5.12 and consists of monofilament and plain weave gauze. Measurements of the collection efficiency for total biomass have shown that the Long NORPAC net values are lower compare to the Marutoku and NORPAC nets. Therefore the old measurements with the Marutoku net must be adjusted downward to be comparable to the Long NORPAC net data. Further work is needed to compare the Marunaka net with the Long NORPAC net. Further inter-comparisons for the biomass sampling efficiency of all the devices in the size range will allow a uniform time series to be constructed incorporating the old data with the new data.

Optimal measuring conditions for plankton counters

Tadafumi Ichikawa
National Research Institute of Fisheries Science, Kochi, Japan. 780-8010 E-mail: wamusi@affrc.go.jp

In marine ecological studies, one of the critical needs is the development of an accurate and automatic device which will measure the size distribution of zooplankton. Present microscope techniques are very labor intensive and often impractical. Optical plankton counters are a possible solution to this problem. Zooplankton biomass, zooplankton abundance and zooplankton biomass density have been measured by three methods and compared with those made by manual measurement under a microscope. The three automatic methods are: *in situ* optical (OPC) and electrical (EPC) plankton counters and a laboratory optical plankton counter (OPC-L). Both zooplankton abundance and biomass density measurements with OPC-L were highly correlated ($P<0.001$), when particle concentration was less than 5 counts/sec. However, there is a significant difference between samples from the Oyashio and Kuroshio regions: the relation was more variable in the Kuroshio than in the Oyashio. The plankton counter is capable of accurately reflecting differences in zooplankton abundance and biomass density and can be used under these conditions in zooplankton monitoring. Particle size distributions measured by the OPC-L are similar to those obtained by manual measurement in the size range larger than 0.5 mm under the conditions that the particle concentration passing through the OPC-L is less than 5 counts/sec, and the samples were stained. Identical samples were provided to the Scripps Institution of Oceanography (SIO) so that they could make analogous OPC-L measurements with their counter. Below 0.5 mm the SIO counts are consistently lower than the

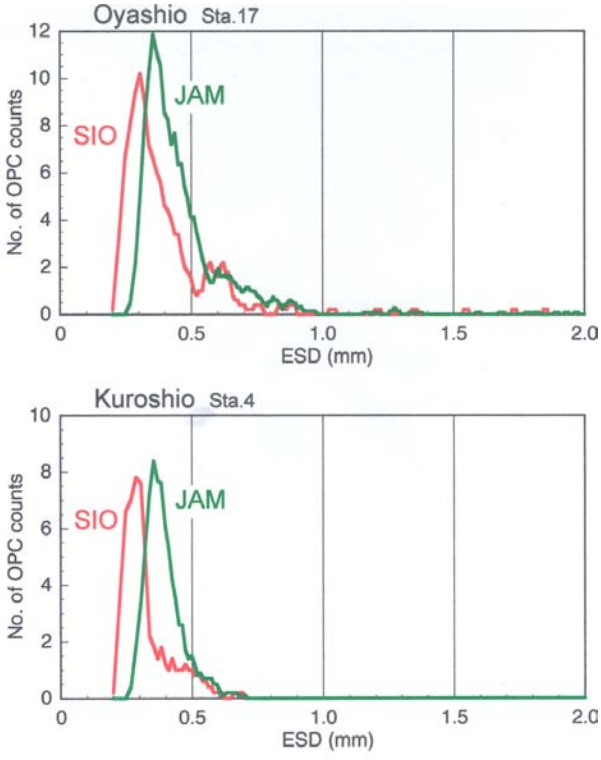

Fig. 1 Comparison of size frequencies of the same plankton samples obtained from circulation systems equipped with OPC-L (Scripps Institution of Oceanography) and OPC-L (JAM).

Japan National Research Institute of Fisheries Science counts (Fig. 1). The source of this discrepancy is not understood. In the area of low abundance of gelatinous plankton and/or *Noctiluca*, abundance and biomass density of zooplankton measured with OPC and EPC are strongly correlated ($P<0.01$) with manual measurements, under the condition that concentrations are less than 100 particles per liter.

Design and testing of an underwater microscope and image processing system for the study of zooplankton

Tatsuro Akiba
Life Electronics Research Center, Amagasaki, Hyogo, Japan. 661-0974 E-mail takiba@etl.go.jp

Oceanic ecosystem research needs a method to monitor the density of zooplankton at appropriate space-time scales. In order to address this need, a submersible microscope was equipped with a non-interlacing CCD camera. The target plankton for this method of measurement included Copepoda, Ploima, and Ciliata, which are the dominant species in the coastal waters around Japan. The key issues investigated for their possible influence on system performance were lens selection, camera selection, and method of illumination. Higher order local autocorrelation (HLAC) masks are used to extract features from images. Combining these with multivariate analysis, which is a two-step feature extraction method, results in a powerful tool for deriving general information from images. In our procedures a set of these features provides a 33-dimensional vector. To identify and count zooplankton, canonical correlation and discrimination analysis are performed. These procedures allow zooplankton to be counted and classified into taxonomic units. Another canonical correlation analysis is made for the sizing of the plankton. Proof of the principle experiment was obtained by using images of both preserved and living Copepoda. At this stage the limitations on the performance of the HLAC features are not clear because the number of images and the number of species is small. In the near future, a large number of plankton images will be collected, which will lead to improved algorithms for identification and counting. Future improvements in image processing may also increase the accuracy of identification because the quality of the obtained images is expected to be very high.

Status of the Census of Marine Life Program

Vera Alexander
University of Alaska Fairbanks, AK 99775-7220, U.S.A. E-mail: vera@ims.alaska.edu

The Census of Marine Life is an international research program that seeks to assess and explain changes in diversity, distribution and abundance of life in the oceans. Development of the program was fostered through a series of workshops and is currently guided by an international Scientific Steering Committee (SSC) and managed by a Secretariat. The SSC is preparing a draft scientific strategy document for review by the scientific community: the overall program will be developed in cooperation with marine scientists and funding agencies from around the world. Regional assessments of marine life will address specific questions related to ocean biogeography. Ecosystems supporting extensive fishing, mid-ocean ridges, seamounts, and open-ocean pelagic environments are under consideration. An Ocean Biogeographical Information System is being developed, with several exploratory projects supported through the National Ocean Partnership Program. Other areas of interest include the History of Marine Animal Populations (HMAP) and the application of novel sampling technologies for marine populations.

Plan to monitor migrations of key species in the North Pacific

David W. Welch
Fisheries & Oceans Canada, Pacific Biological Station, Nanaimo, B.C., Canada. V9R 5K6 E-mail: welchd@pac.dfo-mpo.gc.ca

Many marine animals are confined to the continental shelf ecosystem for much or all of their life. For example, after entering the ocean from freshwater, Pacific salmon smolts generally move along the west coast of North America following the continental shelf (Fig. 2). Earlier work had suggested that juvenile salmon began to move off the shelf by early fall and move directly into the Gulf of Alaska (e.g. Hartt and Dell 1986). However, subsequent studies (Welch *et al.* 1998) involving an extensive sampling period, have shown that all juvenile salmon remained along the continental shelf until reaching the Aleutian archipelago (note the location of the head of the final arrow in Figure 2).

Because the continental shelf is narrow along the west coast of North America (shown in light blue), the migration corridor is restricted to a long thin region that can be monitored at many locations at relatively low cost. Marked juveniles captured during surveys indicate that most salmon swim rapidly along the continental shelf (Fig. 3). Some coho and chinook smolts remain as year-round residents of the coastal zone, while others migrate at least as far as the Aleutians islands before moving offshore.

There are some populations of Pacific salmon which move southward along the continental shelf, opposite to the general pattern of movement (Weitkamp *et al*. 1995); at present, it is not clear why they do so or which groups are involved. Identifying which groups do so is an important management issue because this may partially determine which groups experience poor marine survival. Newly developed acoustic technology is the basis of the proposed tracking program. The miniature pingers to be placed on the individual fish (body length in excess of 15 cm) are 24 mm long and have an operational life of about four months (Eveson and Welch 2000). Field tests of the acoustic receivers to be mounted on the bottom indicate that pingers can be detected at distances of perhaps 0.6-1.0 km. The receivers have a life-time of one year. Because the shelf is usually less than 20 km wide, 20-30 receivers strung across the shelf and down the slope to a depth of 0.5 km should be capable of detecting all tagged animals crossing the line (Fig. 4).

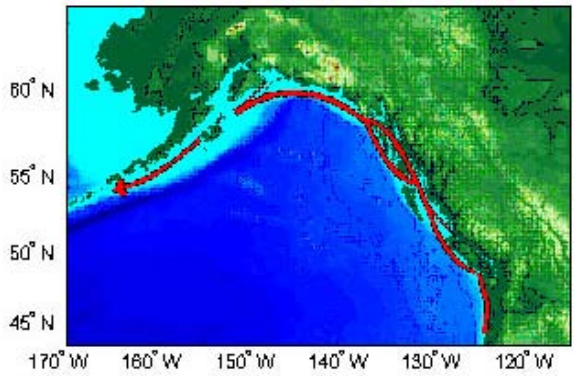

Fig. 2 Migration path of juvenile Pacific salmon. All species (excluding steelhead) were found to remain strictly over the continental shelf (depths<200 m, shown in light blue). The only juveniles we have found off the shelf were at the far end of the Alaskan Peninsula on Dec 7th, at the start of the Aleutian Islands.

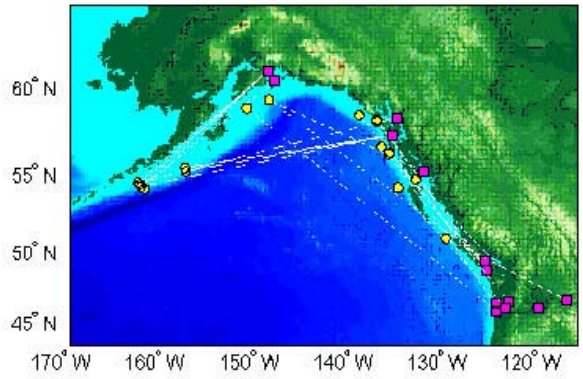

Fig. 3 Release (squares) and recovery (circles) locations for tagged juveniles. Many of these animals travelled continuously at 1-2 BL/sec to reach the recapture points, and thus moved very rapidly out of the estuary or coastal zone around their rivers of origin.

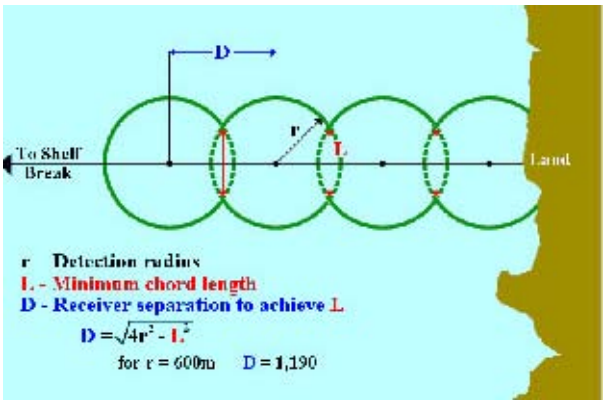

Fig. 4 Conceptual example of a cross-shelf acoustic monitoring system. The dots indicate the location of a series of linearly aligned receivers placed on the seabed, each capable of detecting an acoustically tagged animal at a distance of r meters. The receivers would be placed D meters apart, chosen so that an animal swimming perpendicular to the array would remain within the detection area long enough to ensure reliable detection of at least one signal. For example, if the detection radius was 600 m and this minimum path length was chosen to be 150 m, the receivers could be spaced 1.2 kms apart.

The approximate cost of a single acoustic monitoring line is on the order of $50 K so that for roughly $2 M a network of 20 acoustic listening lines could be deployed that would stretch from California to the Aleutian Is. The acoustic array would provide the basis for reconstructing the movements of any animal that was tagged with a uniquely identifiable sonic tag. If initial design phase studies indicate that a credible observational program can be developed, the scientific objectives that a full-scale research program could address are listed below:

1. Determine the ocean migration pathways of multiple species of animals and their rates of migration;
2. Establish which stocks of salmon move to the offshore open Pacific or remain as coastal residents;
3. Establish the shelf feeding grounds of the shelf-resident animals;
4. Determine the period of time animals remain as residents of various sections of the coastal regime which are expected to be significantly affected by climate change; and
5. Establish movement patterns for mature and immature salmon by tagging these animals in the ocean one or more years prior to return to their natal rivers. Their movements up-river could also be tracked by placing receivers at various points in the rivers.

Seabird monitoring and North Pacific ecosystem dynamics

William Sydeman
Point Reyes Bird Observatory, Stinson Beach, CA 94970, U.S.A. E-mail: wjsydeman@prbo.org

Seabirds are important constituents of marine ecosystems. Worldwide, nine families of marine birds, totaling over 300 species, are full-time participants in marine energy and nutrient cycles, deriving all their food from the sea, voiding feces in the sea, and dying at sea. Some seabirds feed almost exclusively on macro-zooplankton (e.g., auklets), while others have diets based primarily on nektonic fishes and cephalopods (e.g., murres, shearwaters and albatross).

Monitoring seabirds is important because they are sensitive biological indicators of ecosystem state, providing information on environmental change on multiple temporal and spatial scales. In addition, seabirds enjoy tremendous public support and are relatively inexpensive to study. Moreover, because marine birds are conspicuous, widespread and abundant, seabird monitoring studies yield powerful and robust numerical information to test hypotheses concerning climate change and ecosystem response. Interactions with fisheries, some positive and others negative, also provide impetus to monitor seabird populations and trophic dynamics.

There are many types of seabird monitoring strategies depending on the methodology (e.g., colony-based, wildlife telemetry, and vessel-

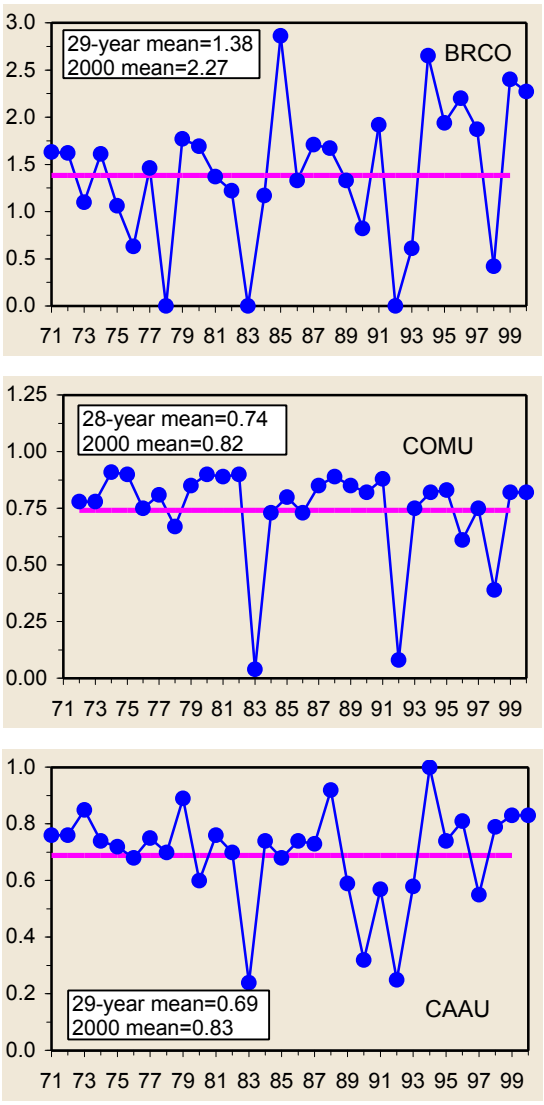

Fig. 5 Productivity of three species of seabirds on Southeast Farallon Is., 1971-2000. Productivity is measured as the average number of chicks fledged per breeding pair.

based) and the temporal/spatial scales under consideration (e.g., short-term and long-term). Colony-based studies provide information on distribution and abundance, reproductive chronology and performance, and food habits. Similarly, shipboard monitoring of seabirds at sea provides information on distribution and abundance, and prey and oceanic habitat selection. Remote (e.g., telemetric) monitoring of seabirds at sea is a developing field that promises to reveal more information about oceanic habitat selection and predator-prey relationships on large spatial scales (e.g., basin wide). Short-term studies often provide a brief, intensive snapshot of marine bird ecology (e.g., duration / destination of a foraging trip, marine bird aggregation at a specific hydrographic feature) ideal to discern the mechanistic linkages between seabirds and their environment.

Long-term seabird monitoring provides information useful to place these short-term intensive studies in perspective by interpreting their findings in a climatic context. Studies spanning several decades are ideal to detect and understand climatic change, including the phasing, intensity, and periodicity of climate change events (Fig. 5). Examples include ecosystem response to inter-annual variability, as exemplified by the El Niño/Southern Oscillation cycle, and ecosystem response to inter-decadal variability in climate, as demonstrated by changes in state of the Pacific Decadal Oscillation.

As secondary and tertiary consumers in marine ecosystems, monitoring marine bird trophic relationships provides a means of assessing major shifts in food web composition, the relative abundance of food web components, inshore and offshore movements of prey species, and bio-physical relationships for many midtrophic-level organisms. Studies have demonstrated how seabird productivity is related to inter-annual variability in coastal pelagic fish biomass, and how changes in the timing and intensity of mesoscale oceanographic events affects the apparent availability of prey to seabirds and other predators. Other important, yet difficult to obtain information concerning the age, size, and sexual characteristics of forage fishes, cephalopods, and macrozooplankton (particularly euphausiids and large copepods) may be provided by coupling studies of marine bird food habits with direct ship-board studies of these mid-trophic level organisms. Importantly, many marine birds and large predatory fishes (e.g., salmonids) occupy the same trophic positions, and may respond to changes in climate and local oceanographic factors similarly. Like predatory fishes, birds are sensitive to gradients in water characteristics (e.g., SST, thermocline depth, etc.) which promote primary productivity and aggregate prey.

Seabird monitoring has important applications for the assessment of human interactions with marine ecosystems, for example, changes in chemical and petroleum pollutants. Repeated measurements of contaminant levels in seabird tissues and eggs have revealed long-term changes in persistent organochlorine pesticides, trace metals, and petroleum products, and the introduction of new contaminants in marine ecosystems. Monitoring contaminants has highlighted the need to investigate confounding factors (e.g., oil pollution, climate change, and fisheries interactions) in relation to goals of understanding and predicting the population dynamics of many marine organisms.

As part of the Living Marine Resources (LMR) module of the Global Ocean Observing System (GOOS), one could envisage a Seabird Observation System (SOS) devised to complement other oceanographic monitoring systems and sources of information. One approach would be to augment existing marine bird time-series in both the western and eastern North Pacific Ocean, especially those longer than a decade, or those using new technologies (e.g., remote monitoring via satellite telemetry). Advantages of this approach would be the enhanced spatial and temporal coverage of well-defined large marine ecosystems at a reduced cost. There are a number of pre-existing cooperative research teams and infrastructures that could be used to promote information exchange. For example, the Seabird Monitoring Database of the Pacific Seabird Group has summarized seabird monitoring data from colonies for most of the past 30 years. This database will soon be available to the oceanographic community via the World Wide Web.

Potential new directions for seabird monitoring programs are also required. In particular, while seabirds provide an integrated and inexpensive means of monitoring both physical and biological oceanographic attributes, research is needed to calibrate the information provided by marine bird monitoring of ecosystem state and food web dynamics. We must assume that seabirds are not unbiased samplers of marine ecosystems. Research designed to couple colony, at-sea, and remote seabird monitoring with oceanographic information based on traditional shipboard sampling and remote sensing would provide information needed to calibrate marine bird datasets. Seabird observations on new research programs are also necessary to provide complementary information. For example, because seabirds forage on sub-surface prey, marine bird observations in conjunction with the PICES/Continuous Plankton Recorder (CPR) project would serve to help identify oceanographic changes that might influence variability in the plankton data. Finally, a system to monitor global contaminant levels through non-destructive predator tissue sampling would provide the oceanographic community with new information about anthropogenic impacts on marine ecosystems.

Role of regional organizations in the design of GOOS

Ned Cyr
Global Ocean Observing System, IOC/UNESCO, Paris, France. 75015 E-mail: n.cyr@unesco.org

Although the basic operational units for GOOS implementation are national observing systems, several regional GOOS activities have been initiated; these include EuroGOOS, MedGOOS, Africa-GOOS, Pacific-GOOS, Near-GOOS, ICES-GOOS, IOCARIBE-GOOS and Black Sea-GOOS. These regional activities have been created for various reasons: conduct ecosystem assessments, existence of common economic interests, economies of scale in operating observing systems and decentralization of GOOS administration. Groups of countries can initiate regional GOOS activities as long as they adhere to the published GOOS principles.

One model for a regional GOOS activity relevant to PICES is ICES, another intergovernmental marine science organization. In 1997, ICES

recognized the opportunity to establish a regional GOOS for the North Atlantic and accordingly set up an ICES-IOC Steering Group for GOOS with the following term of reference: "prepare an action plan for how ICES should take an active role in the further development and implementation of GOOS at a North Atlantic regional level with special emphasis on fisheries oceanography".

After reviewing options for an ICES-GOOS, it was recommended that an observing system be developed with two elements: (1) an Atlantic component focused on climate; and (2) a regional component focused on ecosystem dynamics of the North Sea with emphasis on the need to improve management of fish stocks. ICES is moving toward the implementation of both components.

Provisional terms of reference of a GOOS/PICES Scientific Steering Group (SSG) could be:

1. Determine the ways in which PICES can assist in the implementation of GOOS and advance its own interests.
2. GOOS (LMR module report) has proposed that ecosystem monitoring be designed and carried out by scientific groups familiar with particular ecosystems. The SSG should consider the desirability of PICES assuming the responsibility for reporting on the state of the North Pacific ecosystem.
3. In support of GOOS, a number of scientists in PICES have suggested setting up a Regional Analysis Center (RAC) for the North Pacific. The RAC would issue periodic assessments of the state of the North Pacific ecosystem. The SSG should make a recommendation to the Science Board as to whether or not the design of a RAC should be undertaken.
4. If the recommendation is made to proceed toward setting up a PICES RAC, the SSG should make specific recommendations on its structure, e.g. distributed (virtual) center or physical center with dedicated personnel, centers in the western and eastern Pacific or a single center, etc.
5. The SSG should report to the Science Board at PICES X.
6. Suggested membership of the SSG is David W. Welch (Canada), Warren S. Wooster (U.S.A.), Takashige Sugimoto (Japan) and Vyacheslav B. Lobanov (Russia), with Ned Cyr (GOOS) as a liaison member.

Long-term plans of NEAR-GOOS

Maarten Kuijper
IOC/WESTPAC, c/o National Research Council, Bangkok, Thailand. E-mail: westpac@samart.co.th

NEAR-GOOS is one of the regional GOOS bodies focusing its efforts on the Northeast Asia region. Its member states are Japan, the People's Republic of China, the Republic of Korea, and Russia. These countries have agreed to a common data exchange policy under the NEAR-GOOS framework. During the last few years, the major emphasis of NEAR-GOOS has been on solving problems of data processing, archiving and creation of data products. A limited set of physical parameters has been addressed: temperature, salinity, ocean currents, winds and ocean waves. In the long term, it is expected that the NEAR-GOOS system will expand to better serve the overall goal of global ocean and climate monitoring and forecasting.

The NEAR-GOOS system operates through two different modes: a (near) real-time database and a delayed mode database. Data are kept in the real-time database for 30 days and then transferred to the delayed mode database and added to the long-term records. The databases are maintained by different agencies. The Japan Meteorological Agency (JMA) and the Japan Oceanographic Data Center (JODC) carry out the respective data aggregation at the regional level. There are a number of future developments that are envisioned:

1. At the present time other data sets are being considered for inclusion and archival: sea level, dissolved oxygen and inorganic nutrients. In addition, NEAR-GOOS will undertake to access remotely sensed variables

such as satellite altimeter sea-height, ocean-color and scatterometer wind measurements.
2. Another concern is the application of data quality standards to the submitted data. Up to the present time it has been understood that data quality has been the responsibility of the data provider. NEAR-GOOS recognizes that they must be able to provide users a statement of data quality and will begin to address ways of doing this routinely.
3. Potential users of the archived data set often have needs for specific data products. NEAR-GOOS will consider adding products based on assimilation of data into models (including forecasting models). The choices will be made in such a way that they do not compete with existing specialized agencies that support similar or more advanced systems.
4. Cooperation should not be limited to the NEAR-GOOS area. Participation in global research programs (GODAE, CLIVAR, etc.) offers valuable opportunities for the development of data applications in the NEAR-GOOS system.

NEAR-GOOS will hold a three-day workshop in August 2001, in conjunction with the Fifth IOC/WESTPAC Scientific Symposium in the Republic of Korea. The focus of the workshop will be the current status and need of ocean forecasting capacity in the NEAR-GOOS area. PICES will be asked to participate.

Argo: Progress toward implementation

Nobuyuki Shikama
Meteorological Research Institute, Japan Meteorological Agency, Tsukuba, Japan. 305-0052 E-mail: nshikama@mri-jma.go.jp

The Argo program proposes to deploy globally an array of 3,000 profiling floats to provide real-time observations of the temperature and salinity structure of the upper layer of the ocean. The floats are designed to drift at a depth of 2,000 m and rise to the surface every 10-14 days to measure the vertical profiles of temperature and salinity. After relaying the profile data to shore via satellite, the floats will descend to 2,000 m to begin another cycle. The lifetime of a float is expected to be four years.

Argo is being planned under the auspices of the World Meteorological Organization (WMO) and Intergovernmental Oceanographic Commission (IOC). The February 7, 2000, joint IOC-WMO Circular Letter JCOMM No.00-2 states that "... it is an important component of the operational ocean observing system, as well as a major contribution to scientific research programs". International support for Argo has increased greatly over the past year. As of August 23, 2000, 11 countries (Australia, Canada, France, Germany, India, Japan, New Zealand, Korea, Spain, U.K., U.S.A.) and the European Union have proposals on file to fund 2,324 floats. Proposals for 425 floats have already been funded. In addition to these nations, China and Norway have expressed interest in providing floats.

All Argo data - both real-time and delayed-mode - will be available to anyone, with no period of exclusive use. Real-time data will be put on to the Global Telecommunications System within 12 hours of collection for use by operational forecasting agencies. Delayed-mode data, which have been scientifically quality controlled, will be accessible via the Internet within 90 days of collection. Locations and functions of Argo data centers and data exchange formats are under discussion by an Argo data-system task team.

Performance of Argo sensors has been under evaluation for several years. Provisional standards for instrument accuracy are 0.005°C for temperature, 0.01 psu for salinity and 5 db for pressure. Tests of deployment of floats from commercial vessels at full speed indicate no adverse problems, and the U.S. Navy is evaluating aircraft deployment of floats.

Since Argo floats are untethered freely drifting objects, some floats may enter the EEZs of non-participating countries. This is a particular concern of Pacific island nations. In order to address these concerns, IOC Resolution XX-6 was adopted that "...concerned coastal states must be informed in advance ….of all deployments of profiling (Argo) floats which might drift into waters under their jurisdiction (i.e. EEZs)".

The International Argo Science Team (IAST) was created to review national plans and commitments in order to formulate a strategy for global coverage for the benefit of all nations. Current members of the Team are U.S.A., Japan, Canada, Korea, China, Australia, New Zealand, E.U., Germany, France, U.K. and India. The third IAST meeting will take place at the Institute of Ocean Sciences, Sidney, Canada, in March 2001.

Regional model of a long-term marine science program: Gulf of Alaska Monitoring (GEM)

Phillip Mundy
Gulf Ecosystem Monitoring, Exxon Valdez Restoration Office, Anchorage, AK 99501-3451, U.S.A.
E-mail: phil_mundy@oilspil.state.ak.us

In 1999, the Exxon Valdez Trustee Council dedicated a fund, expected to be $120 M by October 2002, to support a program of research and monitoring in the northern Gulf of Alaska in perpetuity. The goal of the program is to promote use of living marine resources through increased understanding of the ways in which natural and human factors cause changes in these resources. The Trustee Council invites the scientific community of PICES to participate in planning and implementing the program.

The entry point for those who wish to participate is the draft GEM program document that describes the policies of the Trustee Council, and the scientific background for the northern Gulf of Alaska and related ecosystems (available on the web at www.oilspill.state.ak.us). Drawing on the expertise of many concerned scientists and the scientific literature, the draft program provides the scientific basis for regional monitoring in terms of North Pacific and global climate and oceanographic processes. The program document advances a conceptual foundation of how geophysical and human factors cause changes in the abundances of living marine resources through impacts on availability of food, amount of habitat and extent of removals by activities such as fishing. Long-term monitoring is expected to be a large part of the program, based on experience and research on a large-scale ecological disaster - the 1989 Exxon Valdez oil spill. Lessons learned during the decade following the oil spill point out that understanding the sources of changes in living marine resources, whether natural or influenced by human activities, requires a solid historical context. Comments on the program document and suggestions for monitoring activities are open until October 2001, which is the target date for completion of the review now underway by the USA National Research Council's Polar Research Board. The NRC review and other peer-review comments will be used to produce the first call for proposals under GEM in late winter 2002. Initial implementation is expected in October 2002, with further consideration of proposals for funding at regular intervals thereafter.

It is emphasized that the process of developing the scientific basis for GEM is now ongoing. For example, as part of the process of encouraging cross-disciplinary cooperation in the design of GEM, a workshop was held in Anchorage in October 2000, to exchange ideas on monitoring and research in the northern Gulf of Alaska. Teams of scientists from geophysical and biological sciences met with policymakers and stakeholders to develop responses to specific examples for monitoring and research in the region. Results from the workshop indicate broad support among scientists for long-term monitoring of physical and biological processes in order to understand and evaluate change in living marine resources. Specific recommendations from the

workshop will be incorporated into the process of developing the first invitation for proposals in 2002. To receive a summary of the workshop sessions or to be put on the mailing list for future information and activities, please contact gem@oilspill.state.ak.us.

The proper development of the regional GEM program has important consequences for PICES, and for other international marine scientific organizations. An important lesson learned in the aftermath of the oil spill was that coordination among researchers, integration of data acquisition operations, and synthesis of results across disciplines are essential to make cost-effective progress in understanding change. PICES has been established to promote international cooperation, integration and synthesis for the same purposes. The Trustee Council has studied national and international scientific programs to find additional models essential to the development of a regional monitoring program. The approaches of the Global Ocean Observing System (GOOS) and the Global Ocean Ecosystem Dynamics (GLOBEC) have been found to be fully consistent with the policies established by the Trustee Council for GEM. GOOS seeks to define a core set of physical and biological variables essential to understanding changes that can be adapted to local user needs. GLOBEC has focused on understanding physical forcing of primary and secondary productivities in relation to production of higher trophic level organisms such as fish. These aspects of GOOS and GLOBEC are to be incorporated into the development of the GEM program.

Seasonal variability of temperature/salinity structure on repeated sections in the Okhotsk Sea

Nikolay Rykov
Far Eastern Regional Hydrometeorological Research Institute, Vladivostok, Russia. 690600

Physical processes in the Okhotsk Sea have a strong influence on regional climate. In order to understand the role of external factors on water mass structure, measurements of water characteristics on a variety of space and time scales are needed. Seasonal variations of water properties on two quasi-zonal hydrographic sections (central and southern Okhotsk Sea) have been estimated for three periods: spring (May-June), summer (July-September) and autumn (October-November).

The temperature structure is characterized by a thermocline (strongest in summer and weakest in fall) in the surface layer, a temperature minimum layer at about 100 m (coolest in summer) and warmer temperatures at depth. Seasonal temperature variability is strongest near the Sakhalin and Kamchatka coasts. On the southern section, the depth of the core layer thermocline is 75-100 m, and deeper off Kamchatka than off Sakhalin. Negative temperatures at the core are confined to west of 151°E, 150°E and 148°E respectively, in spring, summer and fall. Under the cold layer seasonal temperature variations are small.

Salinity increases monotonically with depth. On the sections the largest seasonal variation of salinity in both surface and subsurface waters occurs near the two boundaries. On the northern section, the freshest water, due to Amur River runoff and melting, is found in the spring off Sakhalin (21-24 psu). In summer, on the northern section the salinity off Sakhalin increases to 23-24 psu and the low salinities spread to 150 m and to the east. Off Kamchatka salinity varies from 31.6 to 32.0 psu over the three seasons. In the southern Okhotsk Sea, close to the Sakhalin coast, the average surface salinity varies from 32.0-32.3 psu in spring, to 31.1-31.9 psu in summer and to 30.0-30.5 psu in fall.

These results might be considered as the first approximation to the seasonal variation of temperature and salinity in the central and southern Okhotsk Sea and could serve as a baseline for future monitoring in the region.

REX WORKSHOP ON TRENDS IN HERRING POPULATIONS AND TROPHODYNAMICS

Co-convenors: Douglas E. Hay, Tokimasa Kobayashi, William T. Peterson and Vladimir I. Radchenko

A 2-day REX Workshop on "Trends in herring populations and trophodynamics" was convened prior to the Ninth Annual Meeting in Hakodate, Japan (October 20-21, 2000). Papers were presented by 8 speakers from among 25-30 participants. At the workshop, we learned that there are long time series (80+ years) of data for herring populations related to catch, size-at-age, length and weight, spawning time, distribution and age composition. Shorter time series are available for biomass estimates, age-structured abundances, survival index, production and instantaneous growth rates. Process studies have examined food habits and energetics, vertical distribution, timing of migration, age-specific habitat requirements, larval survival and distribution, juvenile abundance and distribution, genetic structure of populations, densities of herring aggregations, gonad weight and fecundity and key competitors and predators.

As a result of the workshop discussions, the following generalizations, observations and hypotheses were generated:

1. Herring populations are broadly distributed but geographically discrete.
2. The effects of fish community dynamics on herring size at age merit further study.
3. There are striking patterns in size-at-age including a pronounced decline since the 1970's for recruited herring adults.
4. There is some coherence in year-class strength among regions necessitating further analysis.
5. The frequency of year-class strength varies along a latitudinal cline.
6. There are recognizable types of herring. *Lagoon* herring are confined to Japan, Sakhalin Island and southeast Kamchatka. *Coastal* herring are small-sized and short-distance migrators found ubiquitously but especially along the eastern Pacific Ocean. *Oceanic* herring are large, fast growing and long distance migrating fish confined to Hokkaido-Sakhalin, Okhotsk, Kamchatsky and the Bering Sea.
7. Herring is an indicator species to investigate bottom-up response to climatic variability at various time scales.
8. Where data exist, there are strong links between zooplankton biomass and herring dynamics.
9. Numerical modeling suggests that environmental impacts on herring and zooplankton dynamics exceed those imposed by herring predation.

Those interested in more information and/or references to any of the above statements should contact William Peterson (bill.peterson@noaa.gov).

Another topic of discussion was the need for REX herring scientists to work with the MODEL Task Team on incorporating "fish" into the NEMURO model. At the present time, the NEMURO model is primarily an NPZ (Nutrients-Phytoplankton-Zooplankton) model. Both REX and MODEL scientists felt strongly that the time is right for MODEL to explore the ways and means of adding F (fish) to the NPZ formulations, and that herring would be an excellent model organism. We felt that herring would be a great choice because much is known about herring ecology, herring growth and feeding rates as well as trophodynamics in general. To facilitate this interaction, interested members of REX will work together to summarize herring population dynamics and trophodynamics parameters that are needed to model herring growth. Thus, as an inter-session topic, REX members will work (using e-mail) to complete a matrix of life history parameters, growth parameters in relation to environmental variables (seasonal cycles of temperature, nutrients, and biomass of phytoplankton and zooplankton) for one or two herring stocks. Since such data will likely be variable among years and may be showing long-term trends, we may find it instructive to produce matrices for various decades (1970s, 1980s etc.).

A final discussion topic concerned the nature of future REX sessions. For PICES X we decided to focus on size-at-age for fish species other than herring within the PICES study region. We will look for patterns in size-at-age among genera and relate these to climate variables where possible. We will discuss environmental factors that may affect size-at-age and consider density-dependence and zooplankton biomass where possible. Fish species for which we expect to find considerable amounts of data include salmonids, whiting, halibut, mackerels, sardines and anchovies. A proposal was also received to consider a topic session on "Phytoplankton, zooplankton and nekton synchrony in the use of the spring bloom event in the North Pacific". The idea stems from an observation of several PICES scientists that there have been shifts in the timing of the seasonal peaks in zooplankton biomass. If a workshop focused on this topic, we would produce a review of the timing of spawning of herring stocks around the Pacific Rim in relation to the timing of the spring bloom and timing in peaks in zooplankton biomass. The first steps would be to make an inventory of herring spawning times, phytoplantkon biomass and copepod biomass.

Abundance, biology, and historical trends of Pacific herring, *Clupea pallasi,* in Alaskan waters

Fritz Funk
Alaska Department of Fish and Game, Division of Commercial Fisheries, P.O. Box 25526, Juneau, AK 99802-5526, U.S.A. E-mail: fritz_funk@fishgame.state.ak.us

Introduction

Alaska occupies the northeast corner of the range of Pacific herring, *Clupea pallasi*. Within this range the growth and recruitment patterns of Pacific herring are quite plastic, yet spatial and temporal patterns on differing scales link the biology of Pacific herring to the underlying physical oceanography and the biological elements of the ecosystem. The spatial and temporal patterns in growth and recruitment within Alaska provide linkages to herring biology at adjoining corners of the North Pacific. Much of what we have learned about herring biology has been motivated by the long history of commercial exploitation of herring. This paper describes the biology of herring in Alaska, the history of Alaskan herring fisheries, a sampling of the rich amount of information that can be mined from commercial catch records, and notes some new remote sensing technologies that may further increase our understanding of herring biology.

Biology of Pacific herring in Alaska

Pacific herring spawn at discrete locations from Dixon Entrance in Southeast Alaska to Norton Sound (Fig. 1). Spawning occurs on intertidal and subtidal vegetation in late spring. The exact timing of spawning is closely related to temperature, and progresses around the Alaska coast from March in Southeast Alaska, to June in Norton Sound. In warmer years, herring spawning occurs coherently earlier throughout Alaska. However, there are some patterns in the time series of herring spawning that do not appear to be explained just by temperature variability. For example, at Sitka Sound, herring spawning has occurred three weeks earlier than in recorded history since 1993. The changes in spawn timing can be biologically significant, affecting seabirds, shorebirds, marine mammals, and piscivores that are focused on herring spawning in the spring.

The life history strategy of Pacific herring is distinctly different in the Gulf of Alaska compared to the Bering Sea. Bering Sea herring attain large body size (to 500 g), whereas Gulf of Alaska herring are approximately half that size. The eastern Bering Sea herring are long-distance migrators. The largest population spawns along the north shore of Bristol Bay, near the village of Togiak. Following spawning, these herring migrate in a clockwise direction down along the Alaska Peninsula, reaching the Unimak Pass area in early July (Funk 1990).

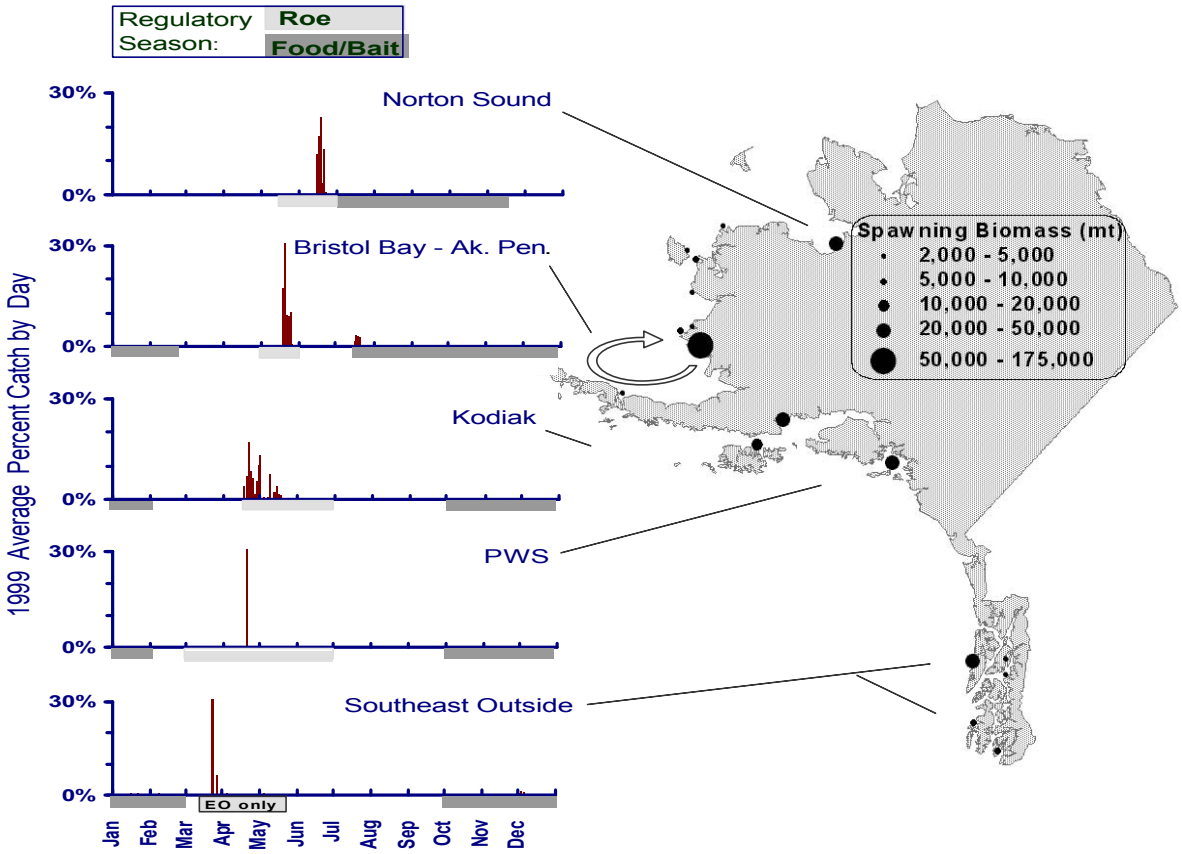

Fig. 1 Location of Alaska herring spawning populations, and timing of fisheries that targeted spawning herring in 1999, illustrating the south to north gradient in run timing, and the clockwise migration of Togiak-spawning herring around the eastern Bering Sea.

They feed along the continental shelf edge, slowly moving northward to overwinter near the Pribilof Islands. The Bering Sea herring life history strategy appears to be an adaptation to take advantage of the distant rich feeding grounds and benign overwintering areas on the continental shelf edge, while utilizing the protected inshore bays for summer larval nurseries. In contrast, Gulf of Alaska herring are smaller, have shorter lifespans, more frequent recruitment events and do not undergo long-distance migrations. In the Gulf of Alaska, recruitment events tend to occur synchronously over fairly broad areas which contain otherwise discrete spawning aggregations. Gulf of Alaska herring have some genetic distinction from Bering Sea herring (Grant and Utter 1984).

In addition to the spatial plasticity in body size, Fig. 2, top), successive age classes of herring undergo very large and biologically significant (up to 30%) changes in body size. These anomalies in growth are strongly autocorrelated, and appear almost cyclic in size-at-age time series that date back to the reduction fisheries of the early 1920s (Fig. 2, bottom). The cause of these apparent cycles in body size is not known, but the anomalies have been correlated to a time series of zooplankton abundance measured at Prince William Sound salmon hatcheries, and also to the Pacific Decadal Oscillation (Evelyn Brown, University of Alaska Fairbanks, pers. comm.). There is only a mild effect of density dependence seen in adult herring at studied locations in Alaska, such as Prince William Sound (Fig. 3). However, density dependence could be an important mechanism affecting larval and juvenile herring growth, for which little time series data exists.

Recruitment also shows signs of periodic autocorrelated anomalies. In the Gulf of Alaska recruitment time series, a four-year cycle of strong

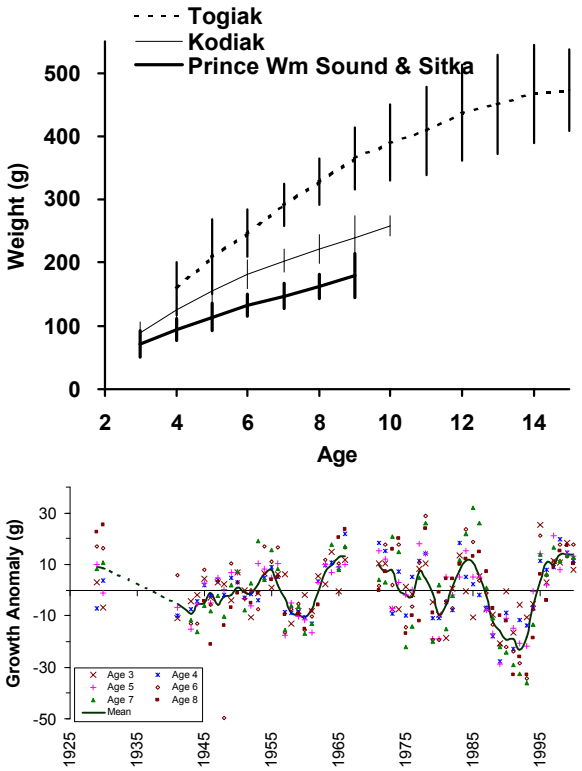

Fig. 2 Spatial plasticity in size at age in Alaska herring (top) and temporal plasticity in body size in Sitka Sound herring, 1929-1999 (bottom), illustrating apparent decadal-scale cycles in growth anomalies. 1925-66 data are from Reid (1971).

year classes is apparent, although that pattern has changed recently (Fig. 4). Recruitment events occur more frequently in the Gulf of Alaska (typically averaging every fourth year), whereas in the Bering Sea, strong recruitment events occur much less frequently, typically averaging every tenth year. Most areas experienced a positive response in recruitment associated with the 1977 regime shift.

These recruitment indices were derived from routine agency stock assessments in support of fishery management. Year class abundance is quantified at a recruiting age of three in the Gulf of Alaska, and age four in the Bering Sea. Adult survival rate is usually treated as constant for stock assessment purposes. When this holds, the recruitment time series provide an excellent measure of abundance for comparison to long-term climate indices, particularly because herring

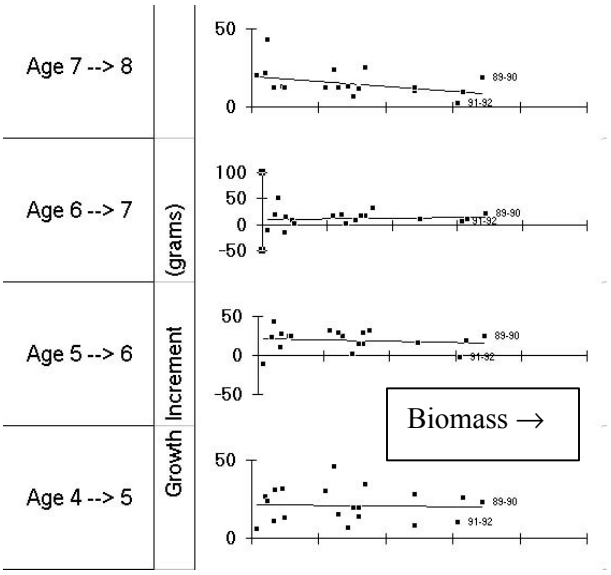

Fig. 3 Relationship of biomass to growth increment in grams for Prince William Sound herring, illustrating the occasional very weak density dependent effect.

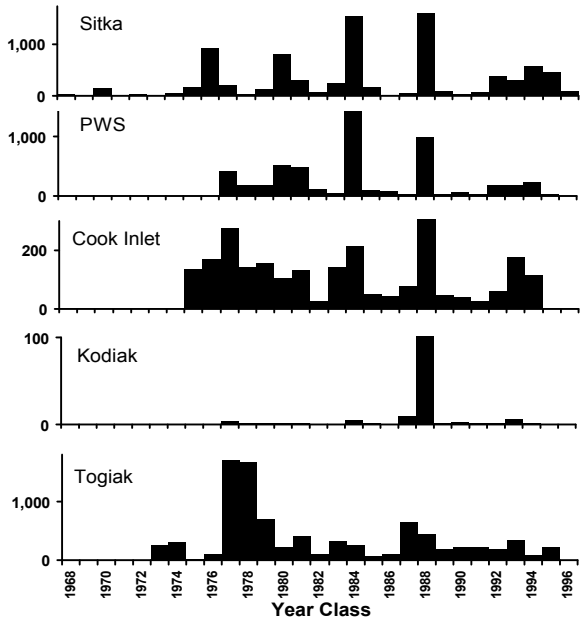

Fig. 4 Year class size (millions) for Alaska herring stocks, illustrating the regional coherence and higher frequency of strong recruitment events among Gulf of Alaska stocks (Sitka to Kodiak), compared to the Bering Sea (Togiak).

early life history is fine-tuned to ocean processes with low tolerance for changing conditions. However, occasional adult herring epizootics have

been observed in Prince William Sound, which can drastically alter adult survival rates. When adult survival rate changes substantially, the recruitment time series will not provide a good measure of adult abundance. Thus far, substantial changes in adult survival appear to be relatively rare, so that the recruitment indices typically provide a reliable index of abundance for both juveniles and adults.

Based on patterns in size-at-age and recruitment, Williams (1999) grouped Alaska herring into three categories: Bering Sea, Outer Gulf of Alaska, and Inner Gulf of Alaska. The spatial scale of these groupings reflect the spatial scale of oceanographic processes underlying herring productivity, as well as the different Bering Sea and Gulf of Alaska life history strategies. Fishery managers need to understand finer spatial scales of herring stock structure than these large groupings based on coherence in growth and recruitment anomalies. Because herring milt can be readily observed from aircraft and precisely defines spawning locations, fishery managers use maps of herring milt locations to define discrete groups of herring appropriately sized for management units.

Trends in herring abundance and historical catch in Alaska

Pacific herring have been commercially harvested in Alaska for over a century, beginning with fisheries for salt-cured and reduction products in Southeast Alaska. During the last two decades herring have been taken primarily for sac roe, with lesser amounts taken for bait. Harvest policies have become more conservative, resulting in more stable stock levels and overall catches. Herring fisheries provide an important contribution to the income of many Alaskan fishermen, with most of the harvest concentrated during the brief spring herring-spawning period.

Fishery history

Herring have supported some of Alaska's oldest commercial fisheries, and subsistence fisheries for herring in Alaska predate recorded history. The spring harvest of herring eggs on kelp has always been an important subsistence resource in coastal communities throughout Alaska. Traditional dried herring remains a major staple of the diet in Bering Sea villages near Nelson Island (Pete 1990), where salmon are not readily available.

Alaska's commercial herring industry began in 1878, when 30,000 pounds of salt-cured product were prepared for human consumption. By 1882, a reduction plant at Killisnoo in Chatham Strait was producing 30,000 gallons of herring oil annually. The herring reduction industry expanded slowly through the early 20th century reaching a peak harvest of 142,000 mt in 1934 (Fig. 5). Exploitation rates were quite high during the reduction fishery era, with large fluctuations in stock levels and annual harvests. As Peruvian anchovetta reduction fisheries developed, Alaska herring reduction fisheries declined, so that by 1967, herring were no longer harvested for reduction products in Alaska.

A Japanese and Russian trawl fishery for herring began in the central and eastern Bering Sea in the late 1950s, reaching a peak harvest of 146,000 mt in 1970. Much of the herring taken in these fisheries were from western Alaska coastal spawning stocks. These high harvests were likely not sustainable and the foreign fishery declined until it was eventually phased out with the passage of the Magnuson Fishery Conservation and Management Act in 1976.

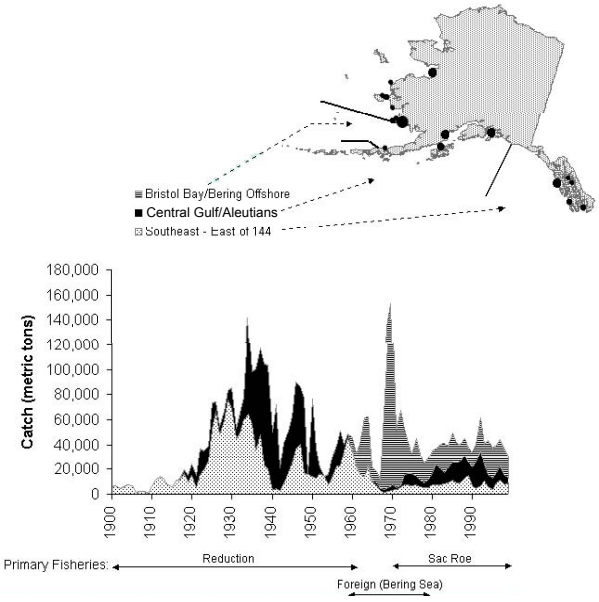

Fig. 5 Harvests of Pacific herring in Alaska.

Contemporary fisheries

Substantial catches of herring for sac roe began in the 1970s as market demand increased in Japan, where herring harvests had declined dramatically. Presently, herring are harvested primarily for sac roe, still destined for Japanese markets. Statewide herring harvests have averaged approximately 45,000 mt in recent years, with a value of approximately $30 million. In addition, about 400 mt of eggs on kelp, worth approximately 3 million, are harvested annually by commercial fisheries.

Approximately 25 distinct fisheries for Pacific herring occur in Alaskan waters (Table 1). Almost all of these herring fisheries are closely linked to a specific spawning population of herring. There are three general types of herring fisheries in Alaska, identified by season, product, gear and BOF regulations.

Most of the herring harvest currently occurs during sac roe fisheries, which targets herring just before their spring spawning period. Both males and females are harvested, although the sac roe fisheries target the much higher-valued roe-bearing females. Alaska statutes require that the males also be retained and processed and not discarded as bycatch. Herring fisheries usually incorporate spotter aircraft and are extremely efficient. On occasion the entire allowable harvest has been taken in less than one hour. However, most sac roe fisheries occur during a series of short openings of a few hours each, spanning approximately one week. Fishing is not allowed between these short openings to allow processors time to process the catch, and for managers to locate additional herring of marketable quality.

Spawn-on-kelp fisheries harvest intertidal and subtidal macroalgae with freshly deposited herring eggs. Both of these fisheries produce products for consumption primarily in Japanese domestic markets. Smaller amounts of herring are harvested from late July through February in herring food/bait fisheries, largely to provide bait in Alaskan longline and pot fisheries for groundfish and shellfish. Smaller amounts are used for bait in salmon troll fisheries, with occasional utilization for human or zoo food.

Harvest policies used for herring in Alaska set the maximum exploitation rate at 20% of the exploitable or mature biomass, consistent with other herring fisheries on the west coast of North America. The 20% exploitation rate is lower than commonly used biological reference points (Funk 1991) for species with similar life history characteristics (Fig. 6). In some areas, such as Southeast Alaska, a formal policy exists for reducing the exploitation rate as the biomass drops to low levels. In other areas, managers similarly reduce the exploitation rate as abundance drops, without the more formal exploitation rate framework. In addition to exploitation rate constraints, minimum threshold biomass levels are set for most Alaskan herring fisheries. If the spawning biomass is estimated to be below the threshold level, no commercial fishing is allowed. Threshold levels are generally set at 25% of the long-term average of unfished biomass (Funk and Rowell 1995).

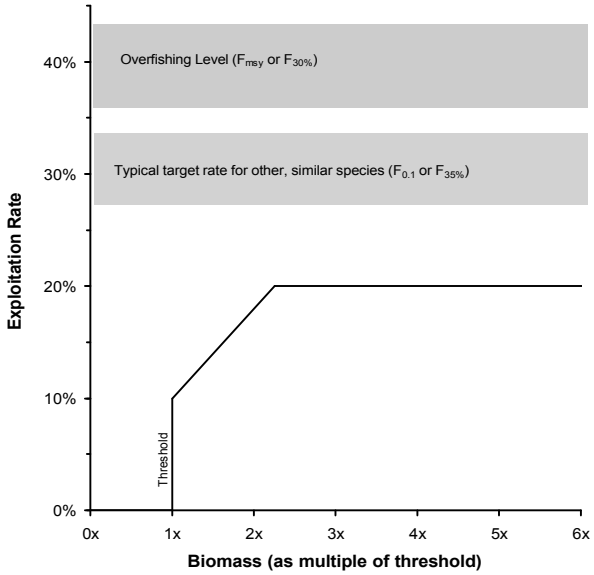

Fig. 6 Generalized exploitation rate/threshold harvest policy for herring fisheries in Alaska, illustrating the reduction in exploitation rate when abundance is near threshold, and showing biological reference points for exploitation rates.

Stock assessment technology

Spawn deposition surveys, acoustic surveys, and aerial school surface-area observations have

Table 1 Status of Alaska herring fisheries in 1999.

							Harvest Policy			1999 Fishery	
					Stock Status		Exploitation Rate		Threshold		
Fishery Area	Season	Gear [1]	Assessment Method [2]	Biomass [3] (mt)	Level	Trend	Framework	1999	(mt)	Duration	Catch (mt)
Southeastern											
Kah Shakes/Cat I.	Sac Roe	Gn	ASA	7,370	Moderate	Stable	0-20%	0%	5,443	-	0
Sitka Sound	Sac Roe	PS	ASA	39,553	High	Stable	0-20%	19%	18,144	1.3 hrs	7,711
Seymour Canal	Sac Roe	Gn	ASA	4,706	Moderate	Stable	0-20%	11%	2,722	11 hrs.	649
Hobart/Houghton	Food/Bait	PS,Gn	ASA	3,417	Moderate	Stable	0-20%	12%	1,814	2 hrs.	499
Craig, Tenakee	Food/Bait, Pd	PS, Pd	ASA	8,165	Moderate	Stable	0-20%	10%	7,257	5 days	1,238
Hoonah Sound	Spawn on Kelp	Pd	ASA	2,722	Moderate	Stable	0-20%	10%	1,814	20 days	115
Prince William Sound		PS,Gn,Pd,Hp	ASA	35,886	Low	Increasing	0-20%	15%	19,958	-	0
Cook Inlet (Kamishak)	Sac Roe	PS	ASA	5,443-11,79	Low	Stable	0-20%	0%	7,257	-	0
Kodiak	Sac Roe/Fd. Bait	PS,Gn,Tr	Catch, age comp.	Uncertain	Moderate	Stable	0-20%			30 days	1,488
Alaska Peninsula	Food/Bait	PS	*(Harvest policy specified as 7% allocation of Bristol Bay allowable catch)*							13 hrs.	2,175
Bristol Bay (Togiak)	Sac Roe	PS,Gn,Hp	ASA	81,647	Moderate	Declining	20% max.	20%	31,752	32 hrs.	17,190
Kuskokwim Area											
Security Cove	Sac Roe	Gn	Annual Survey	2,776	Moderate	Declining	20% max.	20%	1,089	9 hrs.	973
Goodnews Bay	Sac Roe	Gn	Annual Survey	2,730	Moderate	Declining	20% max.	20%	1,089	49 hrs.	1,239
Cape Avinof	Sac Roe	Gn	Annual Survey	3,225	High	Stable	15% max.	15%	454	51 hrs.	484
Nelson Island	Sac Roe	Gn	Annual Survey	5,285	High	Declining	20% max.	17%	2,722	22 hrs.	1,239
Nunivak Island	Sac Roe	Gn	Annual Survey	3,011	Moderate	Declining	20% max.	20%	1,361	-	0
Cape Romanzof	Sac Roe	Gn	Annual Survey	Uncertain	Moderate	Declining	20% max.	20%	1,361	13.5 hrs.	485
Norton Sound	Sac Roe	Gn, BS, Pd	Annual Survey	37,348	High	Stable	20% max.	20%	6,350	101 hrs.	2,357

[1] Gears: Gillnet (Gn), purse seine (PS), pound spawn-on-kelp (Pd), hand-picked spawn-on-kelp (Hp), beach seine (BS), trawl (Tr).

[2] Assessment methods: Age-structured assessment models (ASA), synthesize several sources of abundance information.

[3] Run biomass is defined as the proportion of the population which will return to spawn.

provided the primary stock assessment observations since the beginning of the sac roe fisheries in the 1970s. In most areas of Alaska, these observations are integrated with a time series of age composition and catch in stock assessment models for estimating abundance. In recent years we have been exploring remote sensing tools to augment the existing programs and to provide more synoptic coverage of herring stocks and fisheries.

A compact airborne spectrographic imager (CASI) has been successfully used to assess herring school surface areas when herring are in shallow coastal waters prior to spawning (Funk *et al*. 1995). Herring are color-adapted for a pelagic existence, so that they are readily discriminated from background water by multispectral methods using the green band of the reflected light spectrum. LIDAR, a scanning laser sensor, has also been successfully used to assess pelagic fish species (Churnside *et al*. 1997, Lo *et al*. 2000), including herring in Alaska. LIDAR provided acoustic-like information down to 50 m in the Gulf of Alaska during the summer of 2000 Oscillation (Evelyn Brown, University of Alaska Fairbanks, personal communication). LIDAR provides information about other light-reflecting targets in the water column in addition to fish, and may be particularly informative about the distribution of deeper scattering zooplankton layers near the limits of its attenuation. LIDAR information is acquired from aircraft that can synoptically survey large areas of the continental shelf, thus capturing "snapshots" of processes that are too dynamic to sample using conventional tools. Although the resolution of satellite multispectral sensors is getting sufficiently fine to discriminate herring schools, the frequent cloud cover over Alaskan coastal areas during the herring spring spawning period severely limits their application. Synthetic aperture radar (SAR) has been successfully used to describe the distribution of fishing fleets in Alaska, including Bering Sea crab and herring fisheries (Clemente-Colon *et al*. 1998). SAR uses microwave radiation and is not affected by cloud cover. In addition, SAR can discriminate ocean surface structures such as fronts and eddies, which provide meaningful augmentation to the distribution of fishing effort for determining the distribution of fishery target species.

Conclusions

Commercial fisheries provided motivation for collecting and archiving several long time series of basic biological information. "Data mining" from these time series may help elucidate important basin-wide ocean productivity mechanisms and may be helpful for understanding climate change. In particular, Pacific herring in Alaska display patterns of biologically significant, autocorrelated anomalies in body size, recruitment, and time of spawning. Examining these dramatic spatial and temporal patterns over broader geographical areas can help to generate hypotheses about productivity mechanisms to efficiently guide future research.

References

Clemente-Colon, P., Montgomery, D., Pichel, W., and Friedman, K. 1998. The use of synthetic aperture radar observations as indicators of fishing activity in the Bering Sea. Journal of Advanced Marine Science and Technology Society, 4: 249-258.

Churnside, J.H., Wilson, J.J., and Tatarskii, V.V. 1997. Lidar profiles of fish schools. Applied Optics 36: 6011-6020.

Funk, F. 1990. Migration of Pacific herring in the eastern Bering Sea as inferred from 1983-88 joint venture and foreign observer information. Division of Commercial Fisheries, Alaska Department of Fish and Game, Regional Information Report 5J90-04, Juneau.

Funk, F. 1991. Harvest policy implications of yield per recruit models for Pacific herring in Alaska. *In* Proceedings of the International Herring Symposium, Alaska Sea Grant Report AK-SG-91-01, Fairbanks, Alaska. pp. 453-462.

Funk, F.C., Borstad, G.A., and Akenhead, S.A. 1995. Imaging spectrometer detects and measures the surface area of Pacific herring schools in the Bering Sea. Pages II-833-844. *In* Proceedings of the Third Thematic Conference on Remote Sensing for Marine and Coastal Environments, Seattle, Washington, 18-20 September, 1995.

Funk, F. and Rowell, K. A. 1995. Population model suggests new threshold for managing Alaska's Togiak fishery for Pacific herring in

Bristol Bay. Alaska Fishery Research Bulletin 2:125-136.

Grant, W.S., and Utter, F.M. 1984. Biochemical population genetics of Pacific herring (*Clupea pallasi*). Canadian Journal of Fisheries and Aquatic Sciences 41: 856-864.

Lo, N.C.H., Hunter, J.R., and Churnside, J.H. 2000. Modeling statistical performance of an airborne lidar system for anchovy. Fish. Bull. 98: 264-282.

Pete, M.C. 1990. Subsistence herring fishing in the Nelson Island and Nunivak Island districts, 1990. Technical Paper No. 196, Division of Subsistence, Alaska Department of Fish and Game, Juneau.

Reid, G.M. 1971. Age composition, weight, length, and sex of herring, *Clupea pallasii*, used for reduction in Alaska, 1929-66. NOAA Technical Report NMFS SSRF 634.

Williams, E.H. 1999. Interrelationships of Pacific herring, *Clupea pallasi*, populations and their relation to large-scale environmental and oceanographic variables. Ph.D. Dissertation, School of Fisheries and Ocean Sciences, University of Alaska Fairbanks, Juneau.

Historical trends of herring in Russian waters of the North Pacific

Nikolai I. Naumenko
Kamchatka Research Institute of Fisheries & Oceanography, 18 Naberezhnaya St., Petropavlovsk-Kamchatsky, 683600, Russia. E-mail: NNaumenko@kamniro.kamchatka.ru]

Three ecological forms of Pacific herring (*Clupea pallasii*) are found in the Far-Eastern Seas: marine, coastal, and lake-lagoon. Marine herring spend their entire life in salt-water or the ocean and it undertakes extensive migrations. When foraging, its natural habitat includes both shelf and bathypelagic waters. Lake-lagoon herring spend most of their life cycle in freshwater reservoirs and move to the neighboring waters to forage. Coastal herring inhabits the shelf zone of separate gulfs or big bays exclusively and does not migrate considerably. Russian waters of the Northwest Pacific are inhabited by 6 populations of sea herring and 20 populations of coastal and lake-lagoon forms (Fig. 7). This ecological variety allows the species to obtain food resources of this area of water, and is responsible for its high abundance and wide distribution.

Marine herring are characterized by a pulsing natural habitat. During the growth of biomass it increases in abundance, but it also happens at the expense of bathypelagic waters and the populations in neighboring territories. Reduced abundance is usually associated with warm water masses, and is accompanied by a gradual cessation of reproduction in the southern parts of the range and a shifting of reproduction centers to the north.

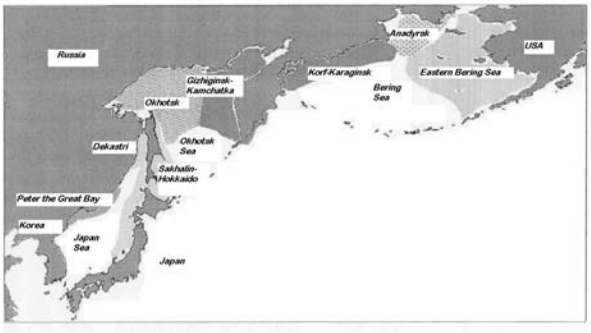

Fig. 7 Distribution of marine herring in the Far Eastern Seas.

A remarkable peculiarity of the Pacific herring is considerable change in abundance and biomass of populations in different years. Fluctuations of the stock-size are conditioned by different productivity of generations. For the years of observation in large Far-Eastern populations of marine herring, generations have differed in number by one hundred times, and adjacent generations by 8 to 60 times. Often, year-class strength fluctuates with a definite periodicity, but in some intervals of time this cyclic pattern is broken.

Distinctions in abundance are evident in both year-classes and populations in the northern and the southern herring groups. Southern populations

(Peter the Great Bay, Sakhalin-Hokkaido and Dekastri) have no stable high frequency cycles of strong and poor year-classes. The difference in productivity between adjacent year-classes is relatively small. A five-year cycle of abundance is usual in the northern group of populations (Okhotsk, Gizhiginsk-Kamchatka, Korf-Karaginsk, Anadyrsk) and the distinction in productivity rate between year-classes is the highest. The abundant offspring in the northern populations occurs more often than once in 5 years, whereas in the southern populations it may be from 3-6 years, one after another. For a long time, strong year-classes have coincided in two populations: Okhotsk and Eastern-Bering Sea (Fig. 8) while Gizhiginsk-Kamchatka has experienced a long depression. During the last years a number of the species in the Japan Sea have approached historical minima and are in need of various protection measures.

The dynamics of the northern populations stock-size was different. The highest number of herring in the northern part of the Okhotsk Sea and the western part of Bering Sea was achieved in the 1950s and early 1960s, i.e. at the epoch of the maximum solar activity of the last secular cycle (Fig. 9).

The second half of the 1970s and the 1980s were characterized by a shift in the climate of the Northwest Pacific that badly influenced herring reproduction. During this period, all the northern populations were at a low level and universally, fishery activities were limited to a sparing mode. In the 1990s, spawning stocks of the Okhotsk, Gizhigisk-Kamchatka and Korf-Karaginsk herring experienced a series of average and relatively strong year-classes and the number of spawners greatly increased. These populations have now passed the crisis. The sparing mode of fisheries has ended and renewed intensive exploitation of the species occurs in the northern part of the Okhotsk Sea and western part of the Bering Sea.

Russian herring catches in the Far-Eastern Seas have experienced considerable fluctuations in different years. The catch peak occurred in the late 1920s to early 1930s (Fig. 10).

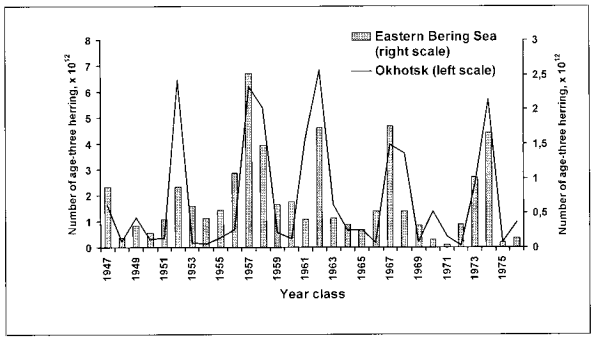

Fig. 8 Abundance of age 3 herring in the Eastern Bering Sea and Okhotsk populations.

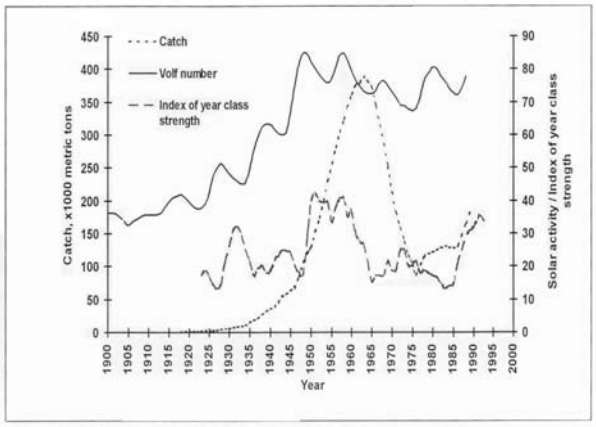

Fig. 9 Historical trends of solar activity and the abundance of the northern herring group.

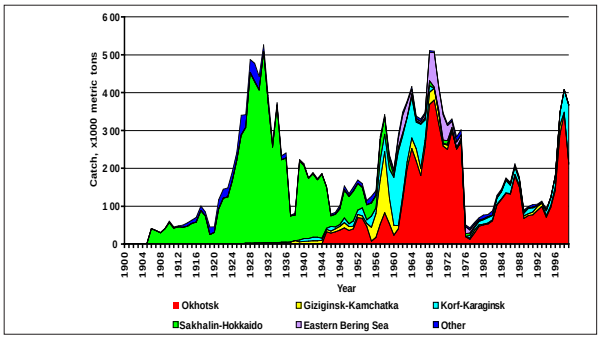

Fig. 10 Russian catches in different herring populations.

At that time the Sakhalin-Hokkaido population was intensively fished, providing an annual catch of 300,000-450,000 t. At the same time maximum catches of two Japan Sea populations were achieved – Peter the Great Bay (about 28,000 t in 1928) and Dekatstri (25,000 t in 1926). By the end of the 1930s the abundance of these two

populations, and also the Sakhalin-Hokkaido population by the mid-1940s, were considerably depleted and the catches appreciably reduced. Exploration of the previously discovered stocks of herring being in the northern half of Okhotsk Sea and the western half of Bering Sea.

The Gizhiginsk-Kamchatka and Korf-Karaginsk herring have been the object of intensive fisheries since the late 1930s, and the Okhotsk herring since the mid-1940s. By the late 1950s to early 1960s, the catches of the first two populations had reached a historical maximum: 120,000-160,000 t and 100,000-260,000 t, respectively. Starting in the 1960s, the Okhotsk population held a leading position in herring catch. During some years (1963-1975) the whole volume of catch by the Soviet fishing companies exceeded 200,000 t. At the end of the 1960s, a regular peak of catches of the Pacific herring was noticed – somewhat more than 500,000 t – which was achieved mainly by an intensive catch of the Okhotsk foraging herring.

Since the mid-1970s, i.e. during last two decades, the herring catch in the Far East underwent a deep crisis. The abundance of all large marine herring populations was depleted. For each population they went to extremes in regulating the fishery – it was completely prohibited. At the West Bering Sea (the Korf-Karaginsk herring) and the North-East Okhotsk Sea (the Gizhiginsk-Kamchatka herring) the prohibition persisted for more than 10 years, 1970-1986 and 1974-1990 respectively. Nevertheless, in spite of the extreme management actions undertaken, the abundance of these populations increased only slowly during the early 1990s, and only during the last several years has a considerable increase in abundance been observed. In 1997-1999, Russian fishermen alone caught more than 300,000 t (in 1998 – over 400,000 t) of herring. In the near future they expect the species resources to be satisfactory.

The total catch of Pacific herring in Russia (USSR) since 1904 is 18,600,000 t, an average annual catch of 192,000 t. By population, the catch is distributed as follows: the Sakhalin-Hokkaido population – 7,372,000 t, the Okhotsk population – 6,987,000 t, the Korf-Karaginsk population – 1,865,000 t, the Gizhiginsk-Kamchatka population – 1,014,000 t, other (Peter the Great Bay, Dekastri, all coastal and lake-lagoon population) – 1,407,000 t.

Trends in Pacific herring populations of British Columbia

Jake Schweigert
Fisheries & Oceans Canada, Pacific Biological Station, Nanaimo, B.C., Canada. V9R 5K6 E-mail: schweigertj@pac.dfo-mpo.gc.ca

Introduction

Herring have been one of the most important components of the British Columbia commercial fishery over the past century with catch records dating from 1877. The fishery has evolved from a dry salted product in the early 1900s, to a reduction fishery in the 1930s that collapsed in the late 1960s. After a four-year closure the current roe fishery began in 1972. Roe fisheries occur just prior to spawning when the fish are highly aggregated and very vulnerable to exploitation. Since 1983, herring roe fisheries have been managed with a fixed quota system. Under this system harvest levels are determined prior to the season based on a fixed percentage (20%) of forecast stock size. In addition, threshold biomass or cutoff levels were introduced in 1985 to restrict harvest during periods of reduced abundance.

In this report, long-term trends in several biological characteristics of British Columbia herring stocks are presented based on stock assessments from two analytical models. An escapement model reconstructs population abundance from surveys of the spawning beds and egg deposition. In addition, a catch-age or age-structured model is used to reconstruct stock abundance for the period 1951-2000. Trends in recruitment, harvest rate, total production,

population growth rate, survival rate, size at age, and condition factor are also presented for each of the five major herring populations found within British Columbia.

Methods

Pacific herring abundance in most of North America is assessed annually through some form of spawn assessment survey since the eggs are adhesive to algae and remain attached intertidally until hatching. Within British Columbia five major migratory herring populations are recognized and assessed annually (Queen Charlotte Islands, Prince Rupert District, Central Coast, Georgia Strait, west coast of Vancouver Island). Annual estimates to total stock abundance and other biological characteristics for each herring stock were determined from the egg assessment surveys using the escapement model (Schweigert and Stocker 1988). Annual harvest rate for each stock was determined as the proportion of the estimated mature or spawning population removed by the fishery. Abundance of the year-classes in each stock was determined from the catch-age model and is the estimate of the number of 3 year old herring which recruit to the fishery.

Population production was determined as the growth in total biomass from year to year summed across ages following (Chapman 1968):

$$P_{at} = g_{at} \bullet \overline{B}_{at}$$

where

P_{at} = Production of new biomass from age a to a+1 in year t to t+1;

g_{at} = instantaneous growth rate in weight from age a to a+1 in year t to t+1;

$\overline{B}_{at} = \frac{B_{at} + B_{a+1,t+1}}{2}$ = average biomass at age a to a+1 in year t to t+1.

The estimated average biomass also includes a component due to the annual production and loss of gonadal products. Weight of the gonad production was determined from the weight of individual fish at each age in each population using relationships developed by Ware (1985) for females. Gonad production of males was assumed to follow the relationship for females.

An annual survival index was also estimated for each stock based on the return of the spawning run in year t+1 relative to the escapement the previous season:

$$SI_{at} = \frac{E_{a+1,t+1} + C_{a+1,t+1}}{E_{at}}$$

where

SI_{at} = survival index of fish age a to a+1 in year t to t+1;

E_{at} = estimated number of spawning fish at age a in year t;

$C_{a+1,t+1}$ = estimated number of age a+1 fish caught in year t+1.

To investigate any long-term trends in population fitness that may be linked to food supply and ocean productivity, the average size at age was determined for each stock in each year. Unfortunately, no herring were aged during the period of the population crash from 1965-1970, so no information is available during this period. In addition, the average condition factor was calculated for each stock, each year, as:

$$CF_t = \frac{Weight_{at}}{Length_{at}^{3}}.$$

Results and discussion

Pacific herring were fished extensively for reduction from the early 1930s through the late 1960s when the stocks collapsed. During this period harvest rates frequently reached 70-80 % of the total available stock in each area. Much more conservative harvest rates occurred during the roe fishery of the past 30 years. Nevertheless, population abundance has fluctuated dramatically throughout both periods (Fig. 11) due to the recruitment of good or poor year-classes in each area (Fig. 12). Population production has also fluctuated markedly throughout this period. Production had generally been high in the 1950s and early 1960s reaching a minimum in the late 1960s as the stocks collapsed (Fig. 13). In all areas production increased rapidly in the early 1970s as stocks rebuilt, particularly in the south. In the 1980s and 1990s, stock production in the

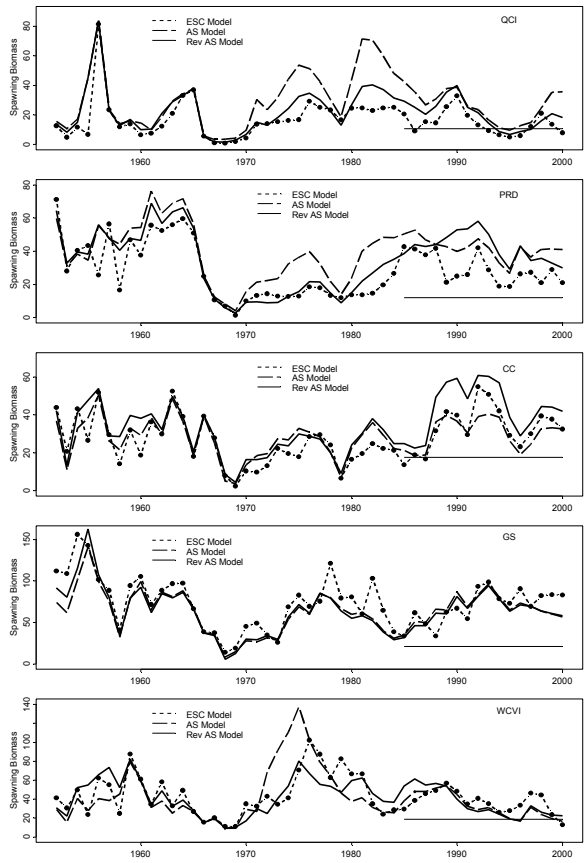

Fig. 11 Trends in abundance of Pacific herring in B.C. from 1951-2000.

QCI, PRD, and WCVI has remained low whereas in the other two areas production has approached the levels of the 1950s. Total production has varied markedly between stocks averaging 5000 t in QCI, 5-10,000 t in PRD, 10-15,000 t in CC, 25-30,000 t in GS, and 15-20,000 t in WCVI. Population production of herring appears to be related largely to recruitment rather than changing growth patterns. Estimates of instantaneous population growth or the P/B ratio indicates higher levels of population turnover in the 1950s and 60s, when harvest rates were very high and the biomass was concentrated in the younger faster growing age classes. Since the early 1970s, population growth has been stable in all areas but population production as a whole has continued to fluctuate.

The survival index was variable particularly during the early part of the time series which may be due to poorer data quality. There is no indication that survival was better or worse during

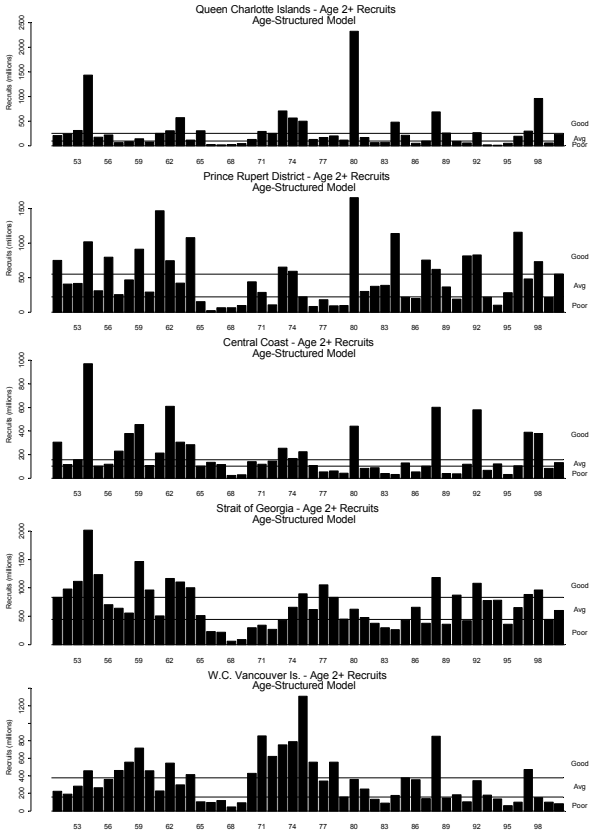

Fig. 12 Recruitment trends in Pacific herring stocks of B.C. since 1951.

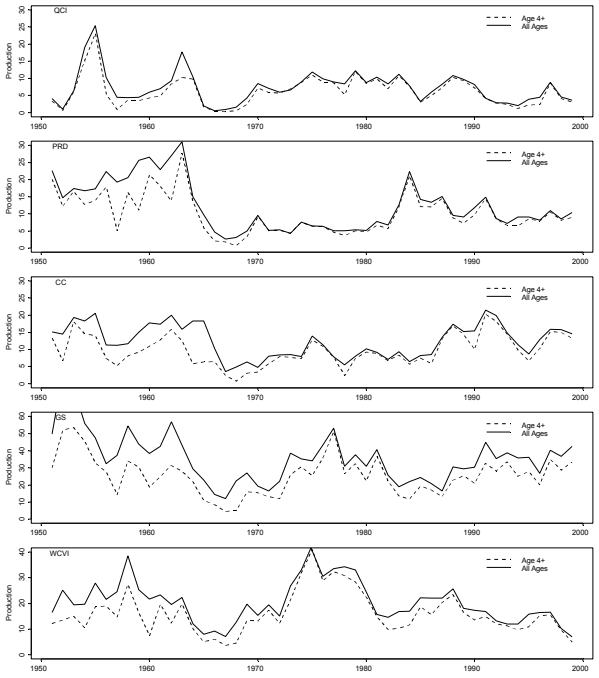

Fig. 13 Estimated population production for B.C. herring stocks from 1951-2000.

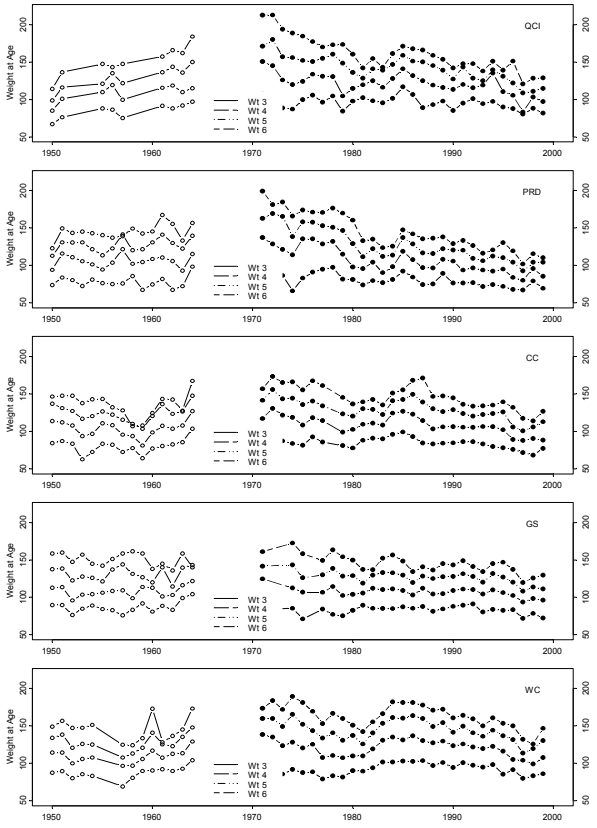

Fig. 14 Trends in estimated size-at-ages 3-6 for B.C. herring stocks since 1951.

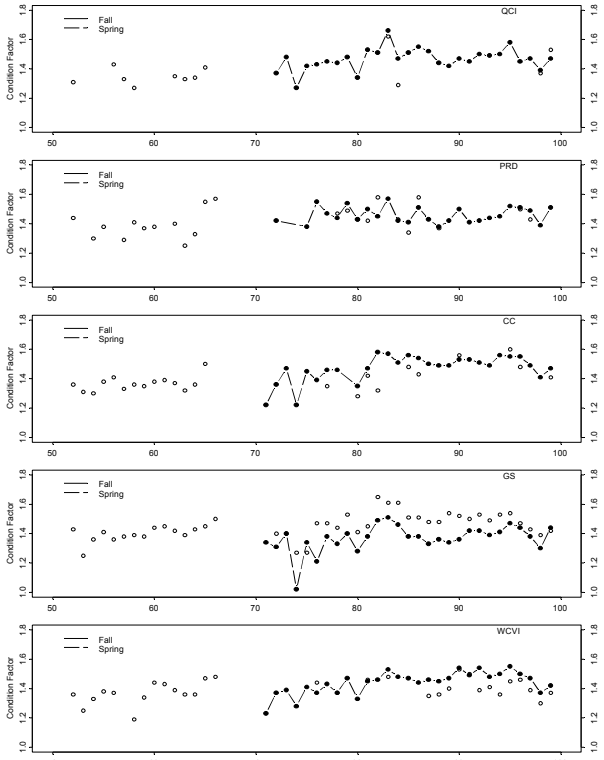

Fig. 15 Trends in condition factor for B.C. herring stocks since 1951.

periods of good recruitment. This suggests that factors affecting adult survival differ from those leading to enhanced survival and recruitment at juvenile stages. Further support for this hypothesis comes from an examination of the long-term trend in both size-at-age and condition factor.

The population characteristics investigated here do not indicate any long-term trends that might be associated with environmental effects on herring production. There appears to be some support for density dependent changes in growth rate. Size at age increased from the early 1960s through the mid-1970s, when coastwide herring abundance was greatly diminished (Fig. 14). Subsequently, size at age has declined in all areas although there is some evidence of a recent increase in some areas. Interestingly there is no evidence of any coincident changes in condition factor for these stocks (Fig. 15). The data suggest a slight increase in condition through the 1970s, but it has been stable over the past two decades.

The most important component of the total annual production of herring stocks is the recruitment of young fish into the adult population. A better understanding of the effects of environmental conditions on the survival of juvenile herring is necessary to establish the links between herring production and the ocean environment.

References

Chapman, D.W. 1988. Production. *In* Methods of assessment of fish production in fresh waters. *Edited by* W.E. Ricker. IBP Handbook No. 3. Blackwell Scientific Publications, Oxford pp. 182-196

Schweigert, J.F., and Stocker, M. 1988. Escapement model for estimating Pacific herring stock size from spawn survey data and its management implications. N. Am. J. Fish. Management 8: 63-84.

Ware, D.M. 1985. Life history characteristics, reproductive value, and resilience of Pacific herring (*Clupea harengus pallasi*). Can. J. Fish. Aquat. Sci. 42: 127-137.

Diet and feeding of juvenile Pacific herring

R. J. Foy[1] and Brenda L. Norcross[2]

[1] Fishery Industrial Technology Center, University of Alaska Fairbanks, 118 Trident Way, Kodiak, AK 99615-7401, U.S.A. E-mail: foy@sfos.alaska.edu

[2] Institute of Marine Science, University of Alaska Fairbanks, P.O. Box 757220, Fairbanks, AK 99775-7220, U.S.A. E-mail: norcross@ims.alaska.edu

Introduction

Herring are zooplanktivorous fish and depend on seasonal availability of prey for growth and energy storage (Blaxter and Holliday 1963). Herring are vertical migrators, so diel differences in spatial overlap with prey items are important for feeding (Blaxter and Holliday 1963). The diets of juvenile herring in Prince William Sound (PWS) vary on multiple spatial and temporal scales (Foy and Norcross 1999a). Feeding intensity is highest in May and June, when zooplankton biomass and energy density peaks (Foy and Norcross 1999a, b). Feeding in winter is below levels required for general maintenance (Foy and Paul 1999). Near-shore zooplankton abundance, diversity, and species composition in PWS have been linked to seasonal and annual trends in temperature and salinity (Foy 2000). Environmental variables influence fish condition directly by affecting growth rates and indirectly by altering the community structure of the prey. Juvenile herring growth rates in PWS were significantly correlated to average water temperatures in 1996 and 1997 (Stokesbury *et al*. 1999). Zooplankton species composition and abundance were significantly correlated to temperature and salinity in the same time period (Foy 2000). The objective of this study was to examine the response of juvenile herring feeding behavior to zooplankton availability and environmental conditions in PWS. To accomplish this, we establish trends in the herring diet composition and prey preference.

Methods

PWS is a large, fjord-type estuarine system consisting of numerous shallow bays, fjords, and tidewater glaciers located on the southern coast of Alaska (Niebauer *et al*. 1994; Fig. 16). We sampled fifteen times between March 1996 and

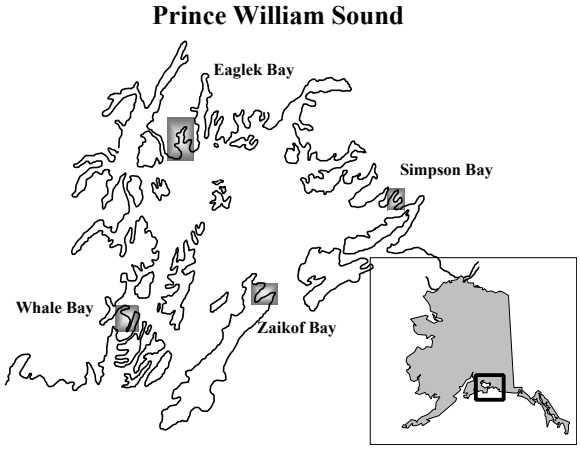

Fig. 16 Location of study sites in Prince William Sound, Alaska. Simpson, Eaglek, Whale and Zaikof Bays were sampled from 1996 until 1998.

March 1998, in two fjords with depths >250 m (Eaglek and Whale Bays), and two estuaries with depths <100 m (Simpson and Zaikof Bays). Within 7 days, each bay was sampled during the day: 0800-1559h, evening: 1600-2359h, morning: 0000-0759h. Data from the four bays were pooled for this study due to consistent interannual trends among bays.

Multiple samples were collected and processed from each sample site. Temperature loggers were deployed at a central location in each of the four bays at a depth of 5 m. Vertical zooplankton tows were made with a 0.5 m 300 μm mesh ring net from multiple sites within the four bays.

Juvenile herring (<250 mm) schools (n=194) caught using a purse seine vessel with a 250 m x 34 m or 250 m x 20 m, 150 mm stretch mesh anchovy net or a trawl vessel with a 40 m x 28 m, 150 mm mesh mid-water wing trawl net. Depth of the tow was dependent on fish depth, determined by hydroacoustics. Fish were blotted dry, weighed to the nearest 0.01 g, and standard length (SL)

measured to the nearest 1.0 mm. Stomach content was reported as % body weight (%BW) by dividing the stomach content weight by total fish weight. Taxa from each stomach were enumerated and identified to the lowest possible taxonomic level. Post-processing analyses included determining taxa richness (number of taxa) and prey selectivity using Chesson's selectivity (a) index (Chesson 1978; 1983) (see Foy and Norcross 1999a and Foy 2000). For selection information of particular prey species see Foy (2000). Life history stages of prey were identified when possible and were limited mostly to egg, nauplius, larva, juvenile and adult male/female.

Results

Temperature in the nearshore surface waters ranged from 4.3 to 13.3° C in 1996, 3.5 to 14.8°C in 1997, and was 5.0°C in March 1998 (Fig. 17). Temperatures at 5 m were significantly different among months (F=155.4, df=14, P<0.01). Temperatures were coolest in March in 1997 and 1998, and warmest in August in 1996 and 1997. The fall of 1997 and the spring of 1998 were significantly warmer than those of the previous year.

The zooplankton density in the upper 30 meters was seasonally and interannually variable. Zooplankton density was highest in June 1996 at 3166 zooplankters per m^3 (Fig. 18, top). Zooplankton abundance decreased in the winter of 1996-1997 to less than 90 zooplankters per m^3. Zooplankton densities were significantly higher in May 1997 than May 1996 (F=27.2, df=94, P<0.01). Zooplankton densities in July, August, and October 1997 were all significantly lower than in the same months in 1996 (P<0.01). No sampling occurred in June 1997 to compare to 1996. The zooplankton species richness was highest in May of both 1996 (41 taxa) and 1997 (34 taxa) and lowest in October 1996 (28 taxa) and 1997 (23 taxa) (Fig. 19). There was an overall decreasing trend in the number of zooplankton taxa between May of 1996 and October 1997.

The number and diversity of prey taxa in the herring diets per fish varied among months and between 1996 and 1997. The number of prey per herring stomach in 1996 increased from 91 in March to a peak of 1209 in July, and then declined to 3 in December (Fig. 18, bottom). Zooplankton density significantly accounted for variation in the density of prey in juvenile herring diets (F = 22.39, P = 0.0003, df = 15, R^2 = 0.62; Fig. 20). Species composition consisted mostly of small calanoid copepods and Cirripedia from March to June, while Cladocera and Larvacea became important between June and October. In 1997 the

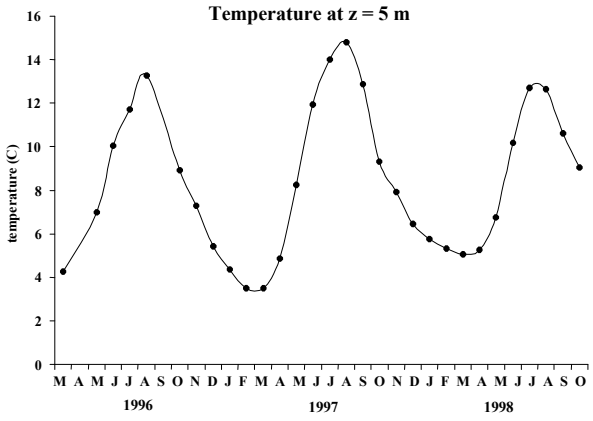

Fig. 17 Average 5 m temperature from fixed temperature loggers and CTD casts in four Prince William Sound bays.

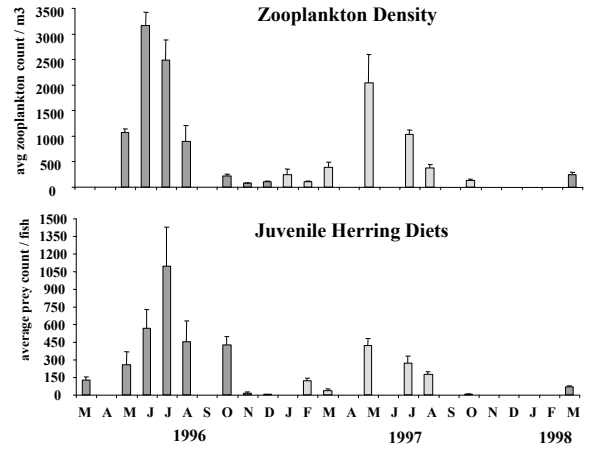

Fig. 18 Average (with standard errors) zooplankton density (count/m^3) for each month (top), and average (with standard error) prey density (count/fish) in juvenile herring diets (bottom) from March 1996 to March 1998, in four Prince William Sound bays. Blank spaces represent months that were not sampled.

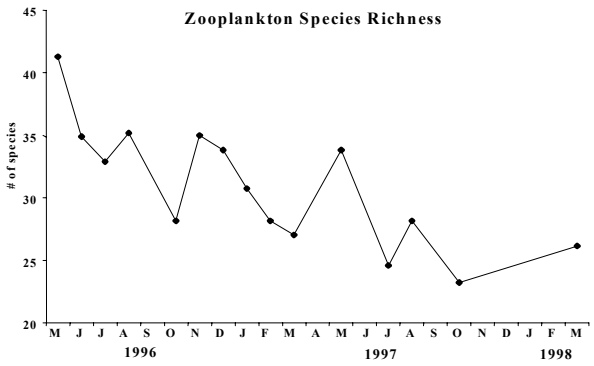

Fig. 19 The number of zooplankton taxa collected each month from March 1996 to March 1998, in four Prince William Sound bays. Blank spaces represent months that were not sampled.

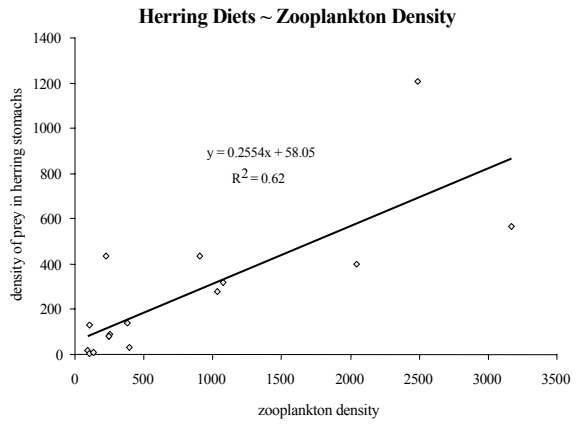

Fig. 20 The density of prey in the herring stomachs regressed as a function of zooplankton density in the water column. Each point represents an average of data for a month.

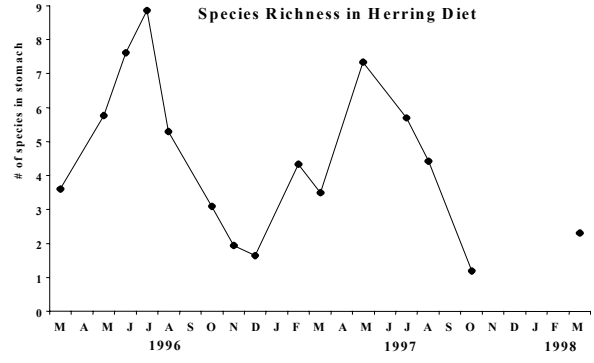

Fig. 21 The number of prey taxa from juvenile herring diets collected from March 1996 to March 1998, in four Prince William Sound bays. Blank spaces represent months that were not sampled.

average number of prey was larger in May (398 prey per fish) than July (278 prey per fish). The dominant species in the diets varied between small copepods, large copepods, Cirripedia, Euphausiacea and Larvacea in 1997.

Juvenile herring had significantly more prey per fish in May 1997 than in 1996, corresponding to the increased availability of prey in May 1997 ($F=12.3$, $df=354$, $P<0.01$). The number of prey per fish for every other month in 1997 was significantly lower than in 1996 ($P<0.01$). The number of taxa in the diets of the herring was highest in July 1996 (9 taxa) and May 1997 (7 taxa) (Fig. 21). The lowest number of taxa in the diets occurred in December 1996 (2 taxa) and October 1997 (1 taxon). All 1997 months except May had fewer taxa in the diets than in 1996. The number of empty stomachs was highest in winter (November to March) and lowest from June to August (Fig. 22, bottom). The percentage of empty stomachs in October 1997 was three times greater than in October 1996.

Juvenile herring were more selective during the winter months when prey was scarce than in the summer months when prey was abundant ($F=4.79$, $df=13$, $P<0.01$; Fig. 22, top). Selectivity index values ranged from 0.17 to 0.65 in 1996 (monthly neutral value range = 0.06 to 0.14) and from 0.22 to 0.77 in 1997 (monthly neutral value range was from 0.04 to 0.22). Juvenile herring were signifi cantly more selective in October 1997 than in October 1996 ($P<0.01$).

Diet taxa richness, evenness, composition and prey selectivity differed with time of day. The number of taxa in the diets was significantly higher from 1600 to 2359h than 0000 to 0759h or 0800 to 1559h. Evenness of prey taxa in herring diets was significantly higher from 0800 to 1559h (confidence interval: 0.64 ± 0.3), when diversity was low, than from 0000 to 0759h (confidence interval: 0.60 ± 0.3) or 1600 to 2359h (confidence interval: 0.60 ± 0.3). The diel difference in diet composition was due to the presence of large calanoid copepods from 0000 to 0759h. From 0800 to 1559h, invertebrate eggs, *Oikopleura* sp., and small calanoids dominated the diets. In the evening category (1600h to 2359h) small calanoid copepods and Cladocera were the most abundant

in herring diets. Juvenile herring were significantly more selective from 0000 to 0759h than from 0800 to 1559h or from 1600 to 2300h.

Though similar times were sampled each year to avoid bias due to light levels, depth distribution of herring changed over the study. The monthly average fish depth in 1996 decreased from 32 m in March to 10 m in August, and then increased from 32 m to 38 m in the winter (Fig. 23). The monthly average fish depths in 1997 were deeper than in the summer of 1996, increasing from an average of 48 m in March to 28 m in August. Evenness of prey taxa in diets was higher for fish caught deeper in the water column than shallower suggesting that herring may be less selective in deeper water where light levels are lower.

Discussion

Zooplankton availability varies seasonally and annually among and within bays in PWS (Foy 2000). Zooplankton species composition and abundance are dependent on multiple biological and environmental factors. The seasonal variability in zooplankton density encountered in this project was typical given the strong seasonal production cycles in PWS. The decline in zooplankton density and number of taxa between 1996 and the fall of 1997 was, however, not expected. There was also a shift in species composition in the zooplankton community occurring particularly in the fall between 1996 and 1997 (Foy 2000).

The decline in zooplankton abundance observed in the summer of 1997 coincides with increased temperatures that occurred at the same time (Foy 2000). Temperatures were 2°C warmer in the fall and winter of 1997, and may have been instrumental in indirectly reducing zooplankton density and composition due top predation and species succession. Temperature has been found to affect the availability of zooplankton prey for Bering Sea larval herring (Maksimenkov 1982). Although higher temperatures may enhance zooplankton production, we speculate that the higher temperatures may have increased the herring demand on its prey population due to increased growth. These events combined with factors affecting stratification in the water column such as increased temperatures and freshwater runoff, may have limited nutrient input to the euphotic zone in the fall, inhibiting productivity that could support secondary production. Our zooplankton sampling did not continue into the winter of 1997-1998 to study the effects of a warmer than normal winter in PWS.

Diel variability in the amount of feeding was encountered at multiple scales. Increased feeding from 1600 to 2359h is consistent with other studies of juvenile herring (Raid 1985; Arrhenius and Hansson 1994). Herring are visual feeders and they feed more in low light hours as they are vertically migrating to the surface (Blaxter *et al*. 1982). The increase in feeding on large calanoid copepods from 0000 to 0759h when there is most likely a large overlap of predator and prey distributions is suggestive of selective feeding due to the size of prey (Sandstrom 1980; Flinkman *et al*. 1991).

Seasonal species composition of prey in the diets was closely related to the species composition of zooplankton found in the nearshore PWS in 1996 and 1997 (Foy 2000) and in this region of the Northeast Pacific (Vogel and McMurray 1982; Cooney 1988). More feeding during the summer months was expected as a response to increased

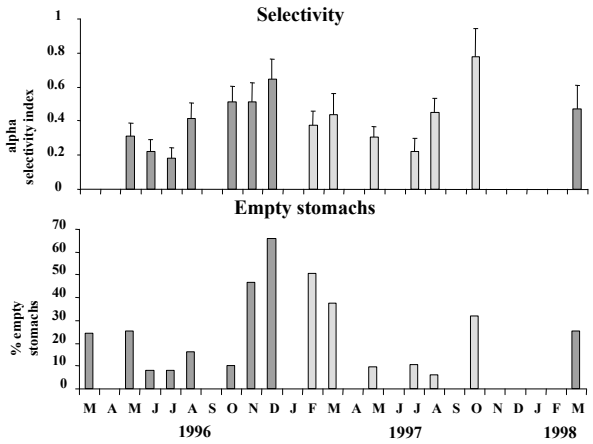

Fig. 22 Average (with standard error) selectivity index (alpha) of prey in juvenile herring diets (top), and the percentage of juvenile herring stomachs empty (bottom) from March 1996 to March 1998, in four Prince William Sound bays. Blank spaces represent months that were not sampled.

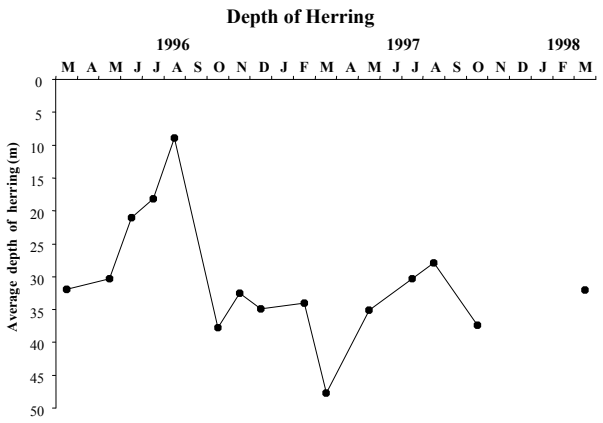

Fig. 23 Average depth of capture of juvenile herring used in the diet analyses from March 1996 through March 1998.

zooplankton availability (Foy and Norcross 1999b, Foy 2000) following increased primary production during the spring in PWS (Goering *et al*. 1973). The species succession of prey in 1996 juvenile herring diets from spring (small Calanoida and invertebrate eggs) through summer (small Calanoida and Cladocera) was similar to the Baltic Sea herring diets (Mehner 1993, Arrhenius 1996), suggesting that the zooplankton species composition is similar at upper taxonomic levels in the nearshore areas of these two systems. In May 1997, species composition of prey found in the diets was similar to May 1996, but large changes in species abundance and composition occurred in July 1997 and subsequent months. Regression analyses suggest that increased temperature decreased the availability of prey and caused the fish to remain deeper in the fall, all of which may have influenced this change in diet composition. Similar trends in species composition were noted in the zooplankton community and speculated to be due to the increased temperatures (Foy 2000). The change in the depth of the fish (Fig. 23) may be due to either a direct response by the juvenile herring to the warmer temperatures or to the lack of available prey in the upper water column during the summer and fall of 1997.

The reduced incidence of feeding and fewer prey taxa ingested by juvenile herring in 1997 may be a response to the lower zooplankton availability. Food composition changed from being dominated by Larvaceans and small calanoid copepods in the fall of 1996 to only small calanoids in 1997. If the densities of prey had been higher in 1997, having only small copepods (with higher energy density) to eat may have been positive for the condition of herring prior to overwintering. Studies estimating the assimilation rates given *in situ* prey compositions found that the smallest juvenile herring are liable to fall below basal metabolic demands in a year with temperatures similar to 1996 (Foy and Norcross 1999a). Warmer temperatures in the fall of 1997 increased growth rates of juvenile herring (Stokesbury *et al*. 1999). Consequently, herring predation pressure on the zooplankton community increased and led to lower prey concentrations in the fall. Lower feeding occurrence in the fall caused the herring to have a lower fall weight at length than in previous years (Stokesbury *et al*. 1999). Despite this, herring were in better energetic condition in the fall of 1997 than in 1996 (Paul and Paul 1998), and consequently, a larger number of smaller fish survived through the winter of 1997-1998 than in 1996-1997. The average length and weight of the fish that survived the 1997-1998 winter were smaller and lower than in previous years (Stokesbury pers. comm.), providing evidence that the smallest fish did not die from starvation during the winter as has been speculated in previous years (Paul *et al*. 1998; Foy and Paul 1999).

In conclusion, important mechanisms in the trophic relationship between herring and zooplankton and the environment exist in PWS. On seasonal scales, juvenile herring relied heavily on prey availability, with greater feeding, diet diversity, and opportunistic feeding in the spring when zooplankton were abundant. Seasonal and spatial fluctuations in temperature and its influence on zooplankton were important at this time. On diel scales, juvenile herring relied on vertical migration for greater prey overlap and higher diet diversity from 1600 to 2359h when the light levels were decreased. Juvenile herring switched to selective feeding from 0000 to 0759h when large calanoid copepods were present in the water column. Furthermore, we suggest that lower prey availability affects the feeding dynamics of juvenile herring. Evidence suggests that environmental conditions may have affected the prey resource base for herring in 1997.

Consequently, herring growth rates increased and the energy density of herring was high by fall 1997. However, we hypothesize that a combination of lower feeding in the fall and warm winter temperatures meant that the average condition of surviving fish in the spring was lower than previous years.

Acknowledgements

This project was funded by the Exxon Valdez Oil Spill Trustee Council through the Sound Ecosystem Assessment project. The findings presented are the authors' and not necessarily the Trustee Council's position. This paper is based on three papers by the authors:

Foy, R.J., and Norcross, B.L. Temperature effects on zooplankton assemblages and juvenile herring feeding in Prince William Sound, Alaska. Proc. Herring 2000, Alaska Sea Grant (in press).

Foy R.J., and Norcross, B.L. Seasonal zooplankton composition and abundance in Prince William Sound, Alaska. J. Planktology (in review).

Foy R.J., and Norcross, B.L. Feeding characteristics of juvenile Pacific herring: Trends in prey availability and environmental conditions in the nearshore subarctic. Can. J. Fish. Aquat. Sci.(in review).

References

Arrhenius, F. 1996. Diet composition and food selectivity of 0-group herring (*Clupea harengus* L.) and sprat (*Sprattus sprattus* (L.)) in the northern Baltic Sea. ICES J. Mar. Sci. 53: 701-712.

Arrhenius, F., and Hansson, S. 1994. In situ food consumption by young-of-the-year Baltic Sea herring *Clupea harengus*: a test of predictions from a bioenergetics model. Mar. Ecol. Prog. Ser. 110: 145-149.

Blaxter, J.H.S., and Holliday, F.G. 1963. The behaviour and physiology of herring and other clupeids. Adv. Mar. Biol. 1: 261-393.

Blaxter, J.H.S., Russell, S.F.S., and Yonge, S.M. 1982. The biology of clupeoid fishes. Adv. Mar. Biol. 20: 1-223.

Chesson, J. 1978. Measuring preference in selective predation. Ecology. 59: 211-215.

Chesson, J. 1983. The estimation and analysis of preference and its relationship to foraging models. Ecology. 64: 1297-1304.

Cooney R.T. 1988. Distribution and ecology of zooplankton in the Gulf of Alaska: a synopsis. Bulletin of the Ocean Research Institute, University of Tokyo, pp. 27-41.

Flinkman J., Vuorinen, I., and Aro, E. 1991. Planktivorous Baltic herring (*Clupea harengus*) prey selectivity on reproducing copepods and cladocerans. Can J Fish Aquat. Sci 48: 73-77.

Foy, R.J. 2000. Juvenile Pacific herring (*Clupea pallasi*) feeding ecology in Prince William Sound, Alaska. Ph.D. thesis, University of Alaska Fairbanks, Fairbanks, Alaska.

Foy, R.J., and Norcross, B.L. 1999a. Spatial and temporal differences in the diet of juvenile Pacific herring (*Clupea pallasi*) in Prince William Sound, Alaska. Can. J. Zool. 77: 697-706.

Foy, R.J., and Norcross, B.L. 1999b. Feeding behavior of herring (*Clupea pallasi*) associated with zooplankton availability in Prince William Sound, Alaska. Proceedings of Ecosystem Considerations in Fisheries Management. 16th Lowell Wakefield Fisheries Symposium. Anchorage, Alaska. September 30 – October 3, 1999. University of Alaska Sea Grant College Program Report No. 99-01. pp. 129-135.

Foy, R.J., and Paul, A.J. 1999. Winter feeding and changes in somatic energy content for age 0 Pacific herring in Prince William Sound, Alaska. Trans. Am. Fish. Soc. 128: 1193-1200.

Goering, J.J., Shiels, W.E., and Patton, C.J. 1973. Primary production. *In* Environmental studies of Port Valdez. *Edited by* D.W. Hood, W.E. Shiels and E.J. Kelley. Institute of Marine Science, Fairbanks.

Maksimenkov, V.V. 1982. Correlation of abundance of food (for herring larvae) zooplankton and water temperature in the Korf-Karaginsk region of Bering Sea. Sov. J. Mar. Biol. 8: 132-136.

Mehner, T. 1993. Distribution and diet composition of 0+ herring (*Clupea harengus* L.) and perch (*Perca fluviatilis* L.) in a shallow estuary of the Southern Baltic. Arch. Hydrobiol. 128: 309-316.

Niebauer, H.J., Royer, T.C., and Weingartner, T.J. 1994. Circulation of Prince William Sound. J. Geophys. Res. 99: 14,113-14,126.

Paul, A.J., and Paul, J.M. 1998. Spring and summer whole-body energy content of Alaskan juvenile Pacific herring. Alaska Fish. Res. Bull. 5: 131-136.

Paul, A.J., Paul, J.M., and Brown, E.D. 1998. Fall and spring somatic energy content for Alaskan Pacific herring (*Clupea pallasi*) relative to age, size and sex. J. Exp. Mar. Biol. Ecol. 223: 133-142.

Raid, T. 1985. The reproduction areas and ecology of Baltic herring in the early stages of development found in the Soviet zone of the Gulf of Finland. Finnish Fisheries Research 6: 20-34.

Sandstrom, O. 1980. Selective feeding by Baltic herring. Hydrobiologia 69: 199-207.

Stokesbury, K.D.E., Foy, R.J., and Norcross, B.L. 1999. Spatial and temporal variability in juvenile Pacific herring, *Clupea pallasi*, growth in Prince William Sound, Alaska. Environ. Biol. Fish. 56: 409-418.

Vogel, A.H., and McMurray, G. 1982. Seasonal population density distribution of copepods, euphausiids, amphipods and other holoplankton on the Kodiak shelf. National Ocean Service, Wilsonville, Oregon.

Dynamics of Sakhalin-Hokkaido herring growth rate and zooplankton biomass (Sea of Japan)

Elsa R. Ivshina
Sakhalin Research Institute of Fisheries and Oceanography (SakhNIRO), Yuzhno-Sakhalinsk, Russia.
E-mail: elsa@tinro.sakhalin.ru

The Sakhalin-Hokkaido herring population has been in low abundance for several decades (Fig. 24). Fish growth rates, including herring, are closely connected with the state of population. A negative relationship between fish size and population abundance has been observed for Sakhalin-Hokkaido herring (Kitahama 1955; Motoda and Hirano, 1963).

On the whole, relatively low growth rates of Sakhalin-Hokkaido herring were recorded from 1955-1970 and 1990-1998, and much higher growth rates from 1970-1990. A comparison of the parameters of regression equations for linear growth of feeding herring during 1955-1959 and 1991 did not show certain differences (at P=0.05). Such regularity was marked both for immature and adult fish. The increase in growth rate during the 1970-1980s seemed to be due to a great decrease in abundance, but in the 1990s, a decrease in mean length and a further reduction of herring abundance and their main food competitors (walleye pollock, sardine) were recorded.

Fish growth is dependent on many factors including zooplankton abundance. The mean length fluctuations for Sakhalin-Hokkaido herring during 1955-1998, appeared to correspond to fluctuations of total zooplankton biomass in the area of feeding along southwestern Sakhalin coast. Herring growth rate did not vary much with year-class strength, but seemed to follow in parallel with fluctuations of total zooplankton biomass (Figs. 25 and 26). A supply with food organisms is perhaps one of the factors limiting herring growth in periods of low abundance.

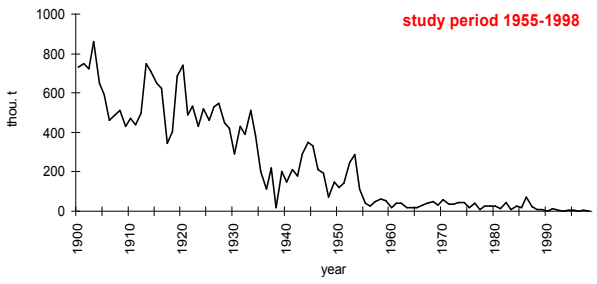

Fig. 24 Catch of Sakhalin-Hokkaido herring.

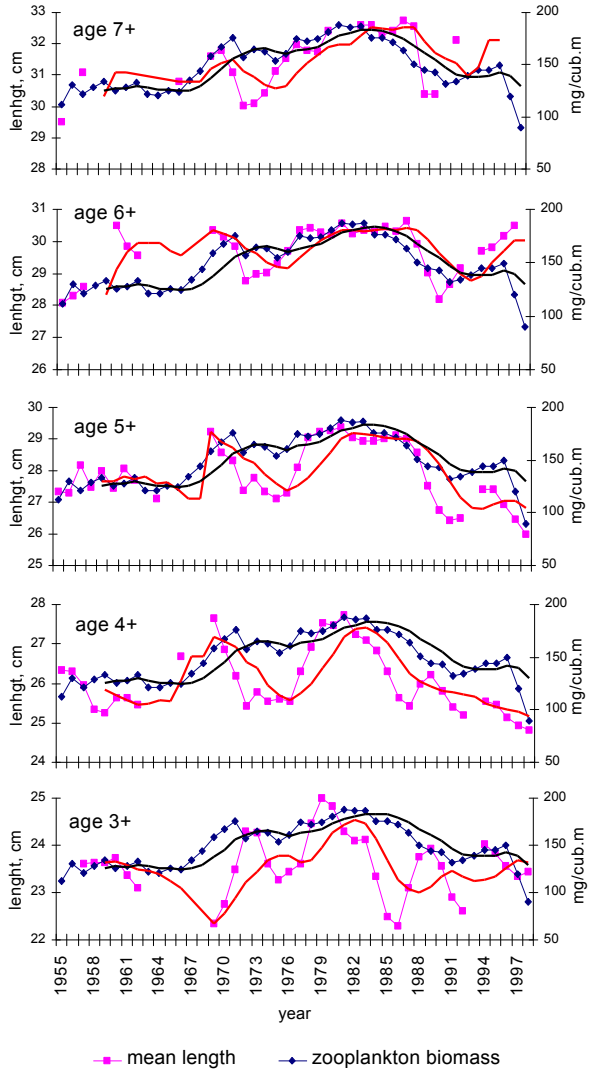

Fig. 25 Total zooplankton biomass and mean length of ages 3-7 herring. Smoothed lines indicate 5 year running averages.

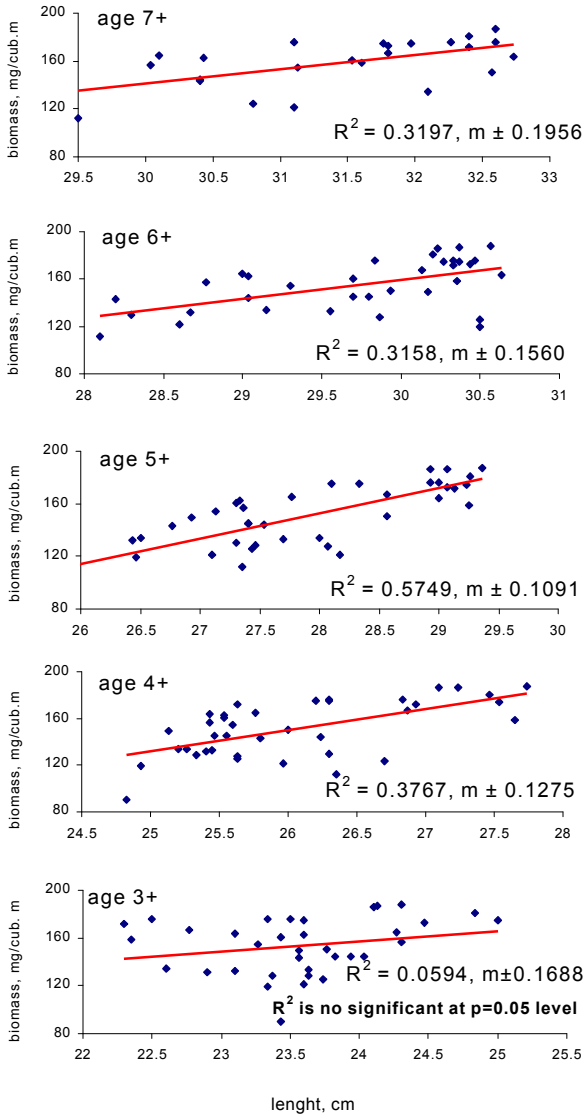

Fig. 26 Linear regression of total zooplankton biomass versus mean length by age.

Euphausiids as indicators of changing ocean conditions in the Oregon upwelling zone

William T. Peterson, Leah R. Feinberg and Julie E. Keister
National Marine Fisheries Service and Cooperative Institute for Marine Resource Studies, Hatfield Marine Science Center, 2030 S. Marine Science Drive, Newport, OR 97365, U.S.A. E-mail: bill.peterson@noaa.gov

We have been sampling off Newport Oregon on a biweekly basis since 1996, at stations located 1 and 5, 10 and 15 miles from shore. At each station, a CTD profile is taken, surface seawater samples are collected with a bucket for later analysis of chlorophyll and nutrients, and a vertical plankton tow is taken with a 1/2 m diameter 202 mesh nets. From these samples, we

have counted all zooplankton including euphausiid larval stages. In this brief paper, we discuss the data on euphausiid furcilia larvae from the station five miles (9 km) from shore. This station is designated as NH05 on the figures shown below.

Two species dominate the euphausiid assemblage off Oregon, *Euphausia pacifica* and *Thysanoessa spinifera.* Under "normal" ocean conditions, *E. pacifica* dominates offshore waters and *T. spinifera* shelf waters. We have found that this pattern of dominance varies depending upon physical conditions –*T. spinifera* dominates nearshore waters only during years of strong upwelling; during summers of weak upwelling, *E. pacifica* moves into shelf waters in significant numbers. Figure 27 illustrates this pattern for the May-September growth season. Weak upwelling years were 1996, 1997 and 1998; strong upwelling years were 1999 and 2000. During 1996, though *T. spinifera* dominated, there were significant numbers of *E. pacifica* furcilia present in shelf waters. During 1997, abundances of furcilia larvae of *T. spinifera* and *E. pacifica* were equal but in 1998, during the El Niño, *E. pacifica* was the dominant species.

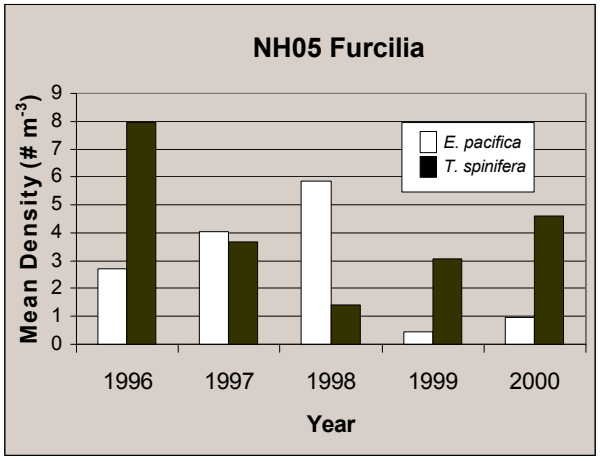

Fig. 27 Time series of euphausiid furcilia densities at a NH05 (a station 5 miles off Newport, Oregon). Note that *Euphausia pacifica*, an oceanic species, were abundant from 1996-1998, and were the dominant species during the 1997-98 El Niño period. From spring 1999 until present, the coastal species, *Thysanoessa spinifera*, is the dominant form.

Also apparent in the data in Figure 27 is the long-term trend in declining abundances of *T. spinifera* from 1996-1998, followed by a trend toward increasing numbers in 1999 and 2000. *E. pacifica* showed the opposite pattern of increasing numbers from 1996-1998, then a decline to very low levels in 1999 and 2000. The same data are shown as a time series in Figure 28.

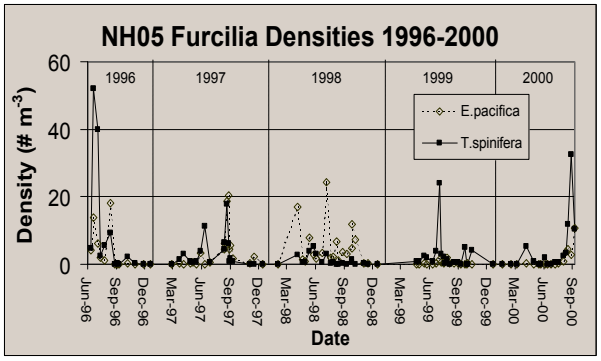

Fig. 28 Mean densities of euphausiid furcilia during the May-September upwelling season. Dominance shifts to *Euphausia pacifica* during the El Niño period, and returns to *Thysanoessa spinifera* in 1999.

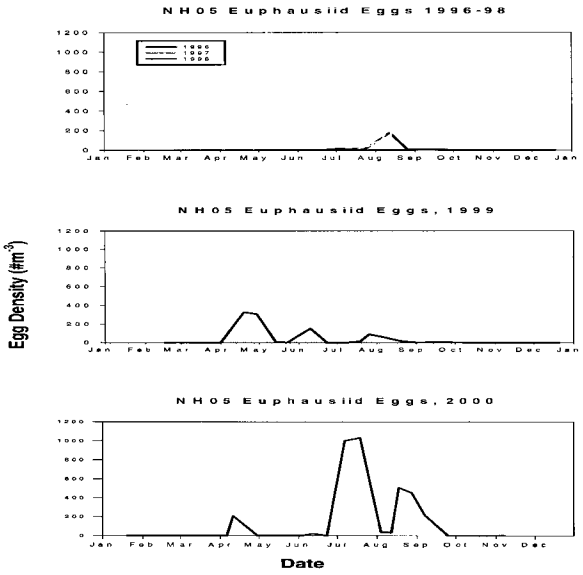

Fig. 29 Changes in spawning season of euphausiids at a station five miles off Newport, Oregon. In 1996-1998, spawning occurred only in late summer. Spawning times in 1999 and 2000 were greatly expanded and included major spawning in the spring and early summer months as well.

Another feature of euphausiid ecology that has shown significant change in the past five years is the length of the spawning season. We have found that the spawning season at NH05 in 1996-1998 was very short, lasting only a few weeks in July and August (Fig. 29). Beginning in 1999, the spawning season was extended from April through September. Euphausiid egg densities averaged over the summer also increased greatly and by 2000, numbers greater than 300 per cubic meter on average were seen. This compared to 1996-1998, when average abundances were approximately 20, 40 and 2 per cubic meter respectively. We do not know which species of which euphausiid produced these eggs because we have only recently been able to identify the eggs to species. We do know that the eggs in 2000 were *T. spinifera* but we will have to re-count the other samples to determine the relative abundances of *T. spinifera* and *E. pacifica* eggs. Given the inter-annual variability in dominance, we expect to find a dominance of *T. spinifera* eggs in 1996 and 1999, and *E. pacifica* eggs in 1997 and 1998.

Modeling environmental and predation-induced variability in euphausiid recruitment: Its dependence and impact on herring trophodynamics

Scott M. Rumsey
Oregon State University, U.S. Geological Survey, 3200 SW Jefferson Way, Corvallis, OR 97330, U.S.A.
E-mail: Scott_Rumsey@usgs.gov

The interaction between predation and zooplankton recruitment processes in determining the availability of euphausiid prey for adult Pacific herring, *Clupea pallasi*, was investigated. Variability in euphausiid recruitment is influenced by the magnitude of spawning input, environmentally induced variability in larval survivorship and development, as well as by predation on early life-history stages. Previous life-history modelling of euphausiid larval development has underscored how heterogeneity in the developmental environment can have more pronounced effects during particular stages of the euphausiid larval ontogeny and disproportionately influence subsequent recruitment (Rumsey and Franks 1999).

In this modelling work, however, I focus on the role of herring predation in determining variability in euphausiid abundances. Herring predation can impact euphausiid demography directly through consumption. Additionally, predation effects on euphausiids can be delayed, or indirect, by affecting adult abundance through predation on developing larvae, and by impacting larval euphausiids through predation on adults and subsequently diminishing the magnitude of spawning. Furthermore, I investigate the potential feedback on juvenile and adult herring of changes in their zooplankton prey preferences. Although copepods often dominate the diets of juvenile Pacific herring in the Eastern Pacific (Ivashina and Bragina 1999; Radchenko and Dulepova 1999), juvenile and larval euphausiids are often represented in stomach contents, and thus juvenile prey could potentially impact adult herring food availability.

A simple ecosystem model was developed to evaluate the impact of herring prey preferences on zooplankton dynamics, as well as that of juvenile (0+ age class) and adult (>3+ age class) herring. Juvenile herring prey consisted of varying proportions of copepod larvae, copepod adults, and euphausiid larvae. Adult herring prey were comprised of adult copepods and/or euphausiids (Fig. 30). The effect of predation was investigated by manipulating juvenile and adult herring prey-preference values, and monitoring the impact on the model state variables (e.g. the abundances of copepod, euphausiid and herring adults and larvae/juveniles). Additionally, the impact on state variables of variations in the initial values of model parameters was determined, and compared with the manipulations of herring prey preference. This comparison provides insights into how predation mediated changes in state variables compare with environmentally forced changes. The results of these analyses are reported as

elasticities, or proportional effect on a given state variable for a given proportional manipulation of a model parameter. Elasticity values facilitate the comparison of parameters that differ in their units of measure and/or magnitude. Additionally, elasticities provide a robust statistic for the analysis of model results in spite of poorly constrained parameter values.

The response of zooplankton and herring abundances was most pronounced for manipulations of the initial values of model parameters (e.g. Bollens 1988). This observation suggests a greater impact of varying environmental conditions (especially primary productivity) on herring-zooplankton population dynamics than that of herring predation and prey preferences (Fig. 31).

Although not as pronounced as the initial value elasticities, elasticity values for varying herring prey preference produced as much as a 30% variation in the output of modeled zooplankton populations. The influence of herring predation on modeled adult euphausiid abundance was primarily the result of direct predation by adult herring. The abundance of larval euphausiids, however, was controlled indirectly through predation on adult euphausiids and subsequent impacts on reproductive output (Fig. 32). Similar to the results for adult euphausiids, modelled copepod abundance was influenced directly by herring predation (Fig. 33).

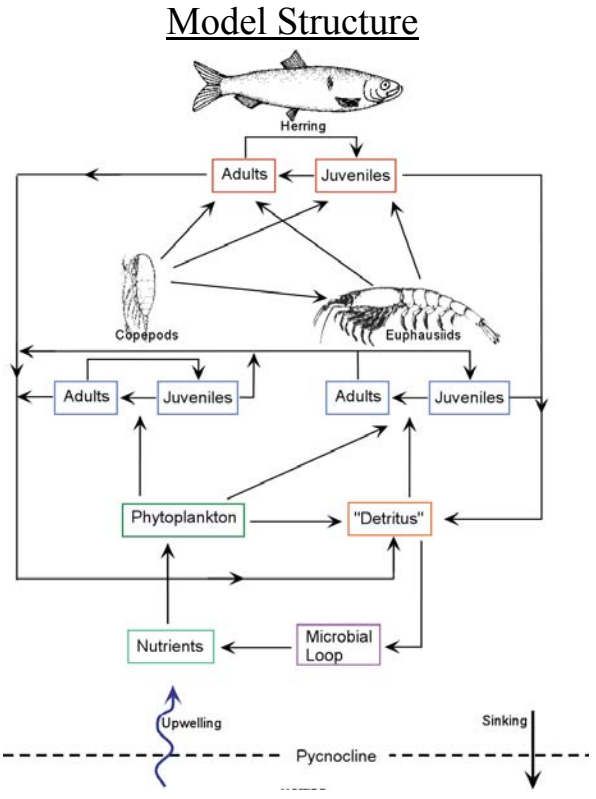

Fig. 30 General model structure herring-eupahausiid-copepod trophodynamic model.

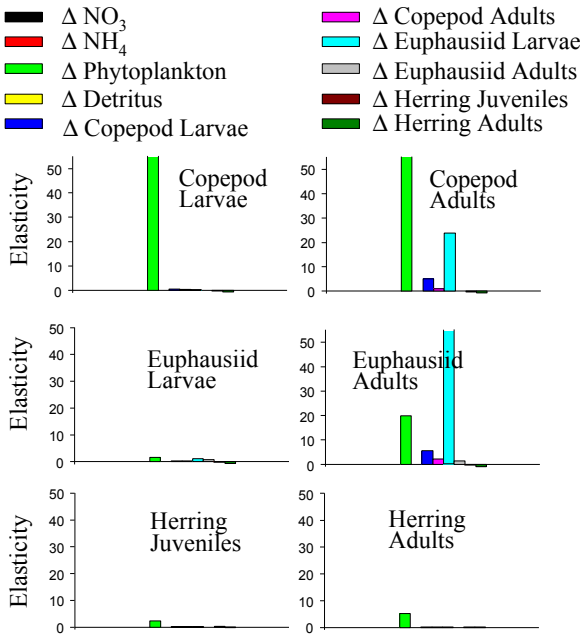

Fig. 31 Elasticity of the state variable response to the manipulation of the initial values of model parameters.

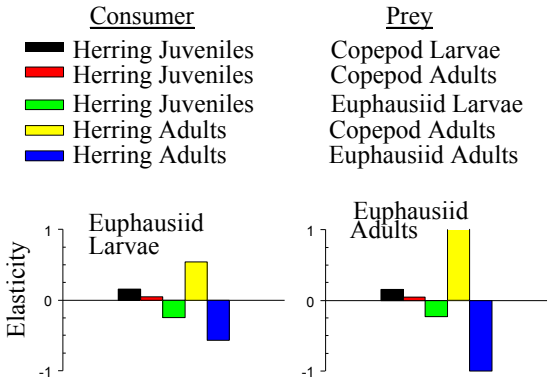

Fig. 32 Elasticity of the euphausiid response to the manipulation of prey-preference parameters.

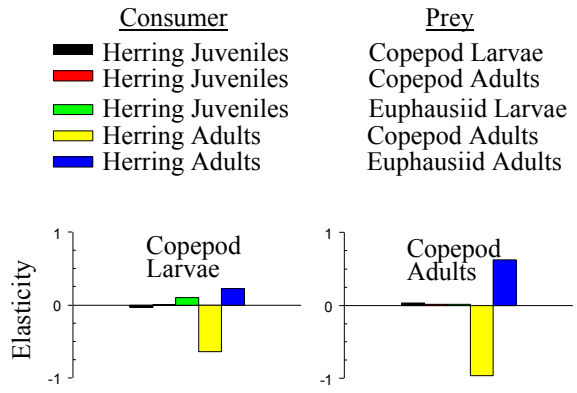

Fig. 33 Elasticity of the copepod response to the manipulation of prey-preference parameters.

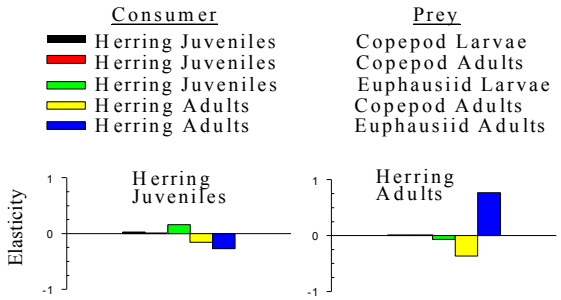

Fig. 34 Elasticity of the herring response to the manipulation of prey-preference parameters.

Increased prey preference for copepod prey resulted in diminished adult herring abundance, indicating a cost associated with broader diet choice (Fig. 34, left). No such cost, however, was associated with changing prey preferences for juvenile herring (Fig. 34, right). Although juvenile herring benefited by increased predation on euphausiid larvae, there appears to be little indirect impact on adult herring through the reduction of their adult euphausiid prey (e.g. McGurk *et al*. 1993).

References

Bollens, S. M. 1988. A model of the predatory impact of larval marine fish on the population dynamics of their zooplankton prey. J. Plank. Res. 10: 887-906.

Ivashina, E.R., and Bragina, I.Y. 1999. On relationship between crustacean zooplankton (Euphausiidae and Copepods) and Sakhalin-Hokkaido herring (Tatar Strait, Sea of Japan). Rep. 1999 REX Task Team Workshop.

McGurk, M.D., Paul, A.J., Coyle, K.O., Ziemann, D.A., and Haldorson, L.J. 1993. Relationships between prey concentration and growth, condition, and mortality of Pacific herring, *Clupea pallasi*, larvae in an Alaskan subarctic embayment. Can. J. Fish Aquat. Sci. 50: 163-180.

Radchenko, V.L., and Dulepova, E.P. 1999. Shall we expect the Korf-Karaginsky herring migrations into the offshore western Bering Sea? PICES Sci. Rep. 15: 115-123.

Rumsey, S., and Franks, P. 1999. Influence of variability in larval development on recruitment success in the euphausiid *Euphausia pacifica*: elasticity and sensitivity analyses. Mar. Biol. 133: 283-291.

Recent state of Japanese herring populations

Tokimasa Kobayashi and Keizo Yabuki
Hokkaido National Fisheries Research Institute, 116 Katsurakoi, Kushiro, Hokkaido, Japan. 085-0802
E-mail: tokikoba@hnf.affrc.go.jp

Judging from the fluctuation of the catch data, the stock condition of herring populations around Japan are in different phases. Hokkaido-Sakhalin population spawn in high salinity shallow waters, the life span is longer than 15 years, and migration range is wide within these populations. Annual catch had been maintained at more than three hundred thousand tons from the 1880s to the mid-1930s, with a historical peak of about one million tons in 1897. However the catch declined since the mid-1940s, and has been still at quite a low level since 1955, except the appearance of the 1983 year-class which was caught totally about one hundred thousand tons. The Mangoku-Ura

population spawn in high salinity waters but migration range is smaller and life span is shorter than the Hokkaido-Sakhalin population. Its annual catch increased gradually from 1977, and reached about six hundred tons in 1984. But it decreased since 1987 due to the small recruitment relating to the rise of water temperature in the spawning season. For the Lake-Furen population which spawn in brackish lake, the annual catch had fluctuated below ten tons before 1984. Since 1985, it gradually increased and reached about seven hundred tons in 1997, but it decreased below fifty tons in 1999 and 2000, due to the weak year-classes of 1997 and 1998. Different phases of stock condition observed among each population may be deeply related to the inherent ecological and physiological abilities of adaptation to the number of oceanic condition factors.

Oil, disease and fishing as factors in the multiple collapses of the Prince William Sound herring population

Gary L. Thomas and Richard E. Thorne
Prince William Sound Science Center, P.O. Box 705, Cordova, AK 99574, U.S.A. E-mail: loon@pwssc.gen.ak.us

In 1993, the largest biomass of Pacific herring in history was predicted to return to Prince William Sound to spawn. Instead, there was a record low return. In the fall of 1993, we conducted an echointegration-purse seine assessment of the stock that confirmed the stock collapse to 20,000 metric tons (MT). After a fall 1993 fishery, acoustic surveys showed that the population further collapsed to 13,000 MT. With a moratorium on fishing, the population rebuilt to 23,000 MT and 38,000 MT in the falls of 1995 and 1996, respectively. However, the acoustic surveys in the springs of 1998 and 1999, after reopening the commercial fishery, showed the population to have collapsed again to about 17,000 MT. After test fishing in the spring of 1999, management cancelled the fishery. The spring survey 2000 showed the population to have fallen to a new, all-time low of 9,000 MT. Co-occurring with the collapses of the herring population in 1993 and 1997, were outbreaks of viral hemorrhagic septicemia. This suggests that the herring have a low immunity to disease after handling by fishing operations. Researchers have suggested the possibility of immune-system damage due to oil exposure in 1989. We present infrared observations of herring surfacing at night to replace air in their gas bladder as a plausible mechanism for oil exposure.

Temporal comparisons of juvenile and adult growth: Implications for changes in trophic conditions in shelf versus nearshore waters

Douglas E. Hay
Pacific Biological Station, Nanaimo, B.C., Canada. V9R 5K6 E-mail: hayd@pac.dfo-mpo.gc.ca

Many herring populations in the North Pacific had relatively high levels of abundance in the 1990s, but many populations also experienced a decline in growth rates (length-at-age) since the 1980s. This statement is based on data presented at the 1999 PICES REX Workshop in Vladivostok, and the 2000 Alaska Herring Symposium in Anchorage.

Size-at-age has decreased in BC herring populations since 1980. As an example, Figure 35 shows the length-at-age of samples taken by purse seine, between February and April, in the same location in the Strait of Georgia, BC (near Denman Island). The mean lengths for each age and year are estimated from measurements of over 146,000 fish with about 6000 measurements used

each year. Note that age 2 fish do not follow the declining trend. This pattern is seen in other herring populations, in the Pacific and Atlantic. Close inspection of many data presentations, such as the one shown here for the Strait of Georgia, indicates that the temporal decline in size-at-age is seen mainly in the older age groups - and it may not occur, or is much less pronounced and in the recruits or juveniles.

In 1977, there was a strong cohort of herring (and some other species) in much of Alaska and all northern BC populations (Fig. 36). In 1980, when the 1977 year class was age 3, the size-at-age was normal or slightly above average in most populations. In later years, at ages 5 and older, the size-at-age of this cohort decreased. Figure 37 shows the mean length-at-age of the 1977 cohort class (dark circle with lateral line) relative to those of other year classes from 1980 to 1996 from the Prince Rupert Region of northern BC.

A project requiring detailed analyses of scale growth started in 1999. A major objective was to examine and compare growth rates of the juvenile stages and the adult stages: between years, and areas. (In part, this project started as an outcome of a special PICES WG 3 meeting in 1995, in La Jolla, that recommended examination and comparison of early growth rates among North Pacific pelagic species.) In this project, the length of lateral scales, from the focus to the edge in a strait line, parallel to the midline of the fish (i.e. from nose to tail), was measured to the nearest 0.01 mm using a digital camera on a microscope (Fig. 38). Measurements on digital images were made using Sigmascan© software.

The scale-length - body-length relationship in herring is approximately linear (Fig. 39), and it is very consistent, both within and between various populations that have different growth rates. Therefore the length of annual growth increments on scales provides an index of past growth rates.

Temporal patterns of scale size-at-age, based on scale measurements between the focus and annuli, show temporal changes with time (Fig. 40), similar to those seen in Figure 1, except the scale measurements show growth patterns from ages 1-5 herring, (and not ages 2-8 as shown in Figure 35).

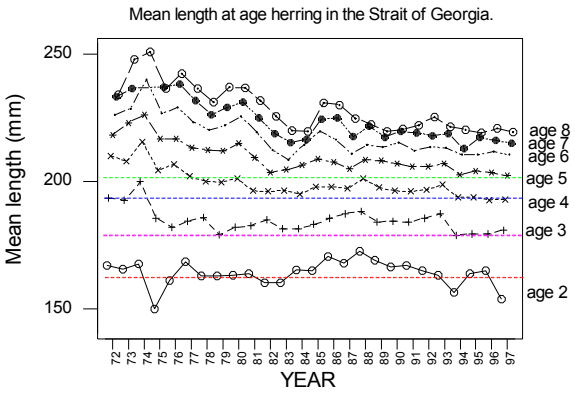

Fig. 35 Mean length of herring by age (≤ age 8). For ages 4 through age 8, mean length has decreased with age since 1972. The mean size of age 2 and 3 herring varied, and had a slight increasing trend in the 1980's, followed by a decrease in the 1990's.

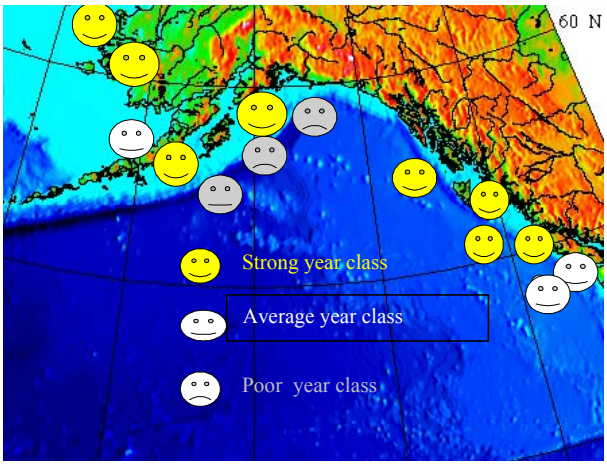

Fig. 36 Distribution of herring populations with strong 1977 cohorts.

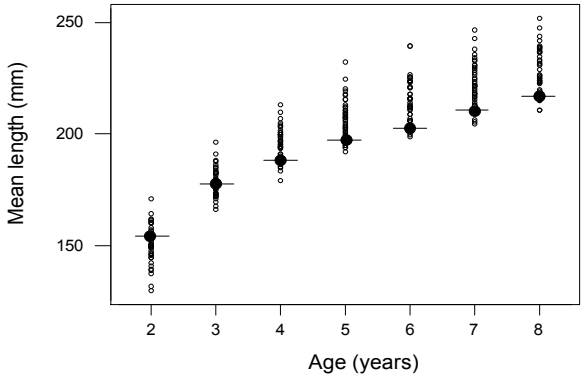

Fig. 37 Changes in relative length of the 1977 year-class.

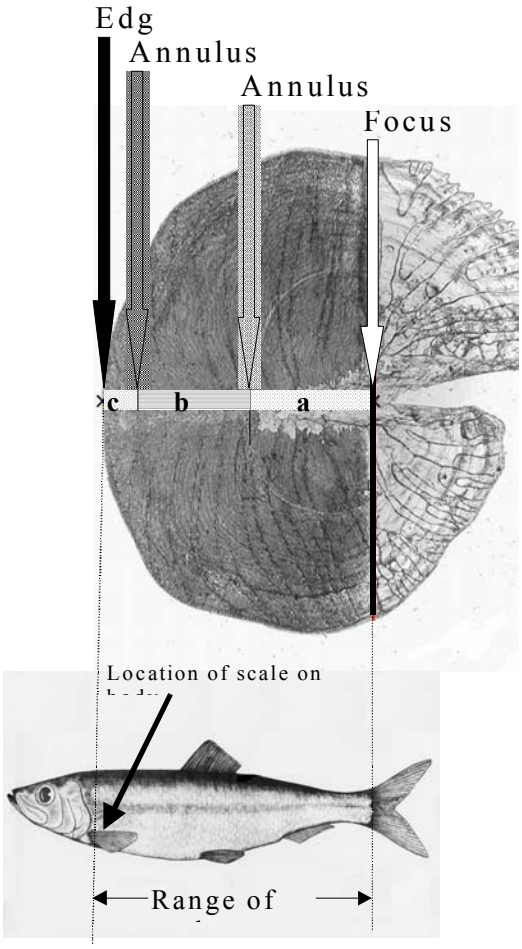

Fig. 38 Herring scale, showing the position of the focus, annuli (a, b, c), and the relationship of scale growth to the length of a herring.

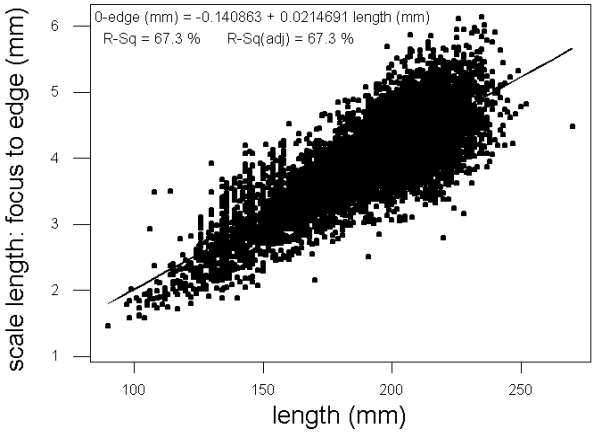

Fig. 39 The relationship between scale length (focus to outer edge) and fish length (standard length, from nose to end of the hypural plate).

Note that the long-term decrease in (scale) size-at-age is seen for measurements from annuli 4-5, similar to that in Figure 35.

Temporal differences in juvenile growth are seen most clearly by a comparison of the inter-annuli distances on scales, with the first measurement as the distance between the focus and first annulus (Fig. 41). The top line in Figure 41 is the distance (mm) between the focus and first annulus, and represents the first year growth. First year growth increased in the 1980s (see arrow A in Figure 41) followed by a decrease in the 1990s (arrow B). Trends in second year growth were nearly the opposite, with a decrease in the 1980s (arrow C) and increase in the 1990s (arrow D). Adult growth also deceased in the 1990s (arrow E).

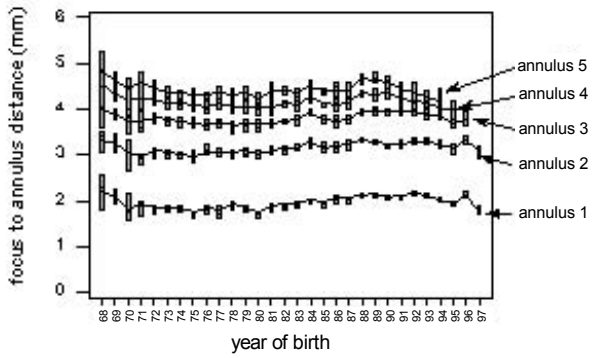

Fig. 40 Comparison of scale growth by time; data taken from Strait of Georgia.

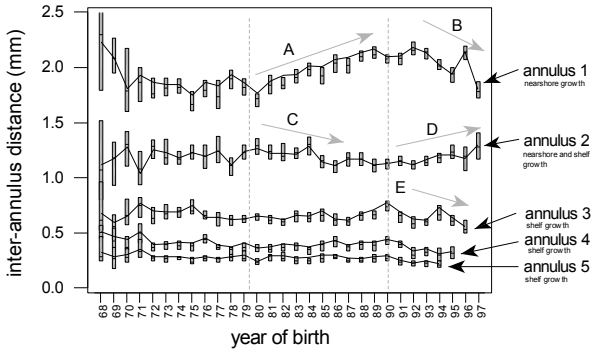

Fig. 41 Inter-annulus comparison of growth, by age and year, from samples taken from the Strait of Georgia. Each bar represents a 95% CI about the mean. The arrows and letters depict periods of growth change (see text).

Biological implications

Juvenile herring surveys in the Strait of Georgia (SOG), conducted since 1990, indicate that age 0+ juveniles (< 12 months) spend the first year in SOG. In September, or about the end of their second summer, most age 1+ juveniles have left SOG, and few herring remain resident in SOG after their second year, except for some resident populations, which are usually found in specific locations. Consequently, age 0+ and age 1+ herring occupy different habitats, and may be subject to different trophic limitations and opportunities, that may affect their growth rates differently.

The causes of the recent (post 1980) declines in size-at-age of adult herring (mainly age 3 and older as depicted in Figure 35) could have several explanations. The size-at-age of adult herring represents the cumulative increments of growth from previous years. It is interesting to note that the relative contributions of growth from the first and second years of life may vary. In particular, the increasing rate of age 0+ growth in the 1980s was not accompanied by increases in later years, and in general, size at age of older age classes declined at this time (Fig. 35). This may indicate that feeding conditions for age 0+ herring, in the inside waters of SOG, were good, but that feeding conditions for age 1+ juveniles and older age classes, which feed mainly on shelf waters, was poorer in the 1980s than during other decades. If so, these results are consistent with the observation that the strong 1977 year class had normal or good size-at-age for juveniles and young fish recruiting at age 3, followed by slower growth and reduced size-at-age for older age classes.

In summary, the detailed reconstruction of past growth rates of Strait of Georgia herring may have implications for other populations. Specifically we observed that first year growth rates varied with time, but appeared to increase in the 1980's, when growth rates of older age groups were in decline. This difference indicates that the processes that limited growth of adult fish in shelf waters may have been separate, and different than those which controlled the growth of age 0+ juveniles in inshore waters.

BASS/MODEL WORKSHOP ON HIGHER TROPHIC LEVEL MODELING

(Co-convenors: Gordon A. McFarlane, Andrei S. Krovnin, Bernard A. Megrey and Akihiko Yatsu)

The PICES BASS/MODEL Workshop to examine the feasibility of using ECOPATH/ECOSIM as a tool to model higher trophic level components of the Subarctic gyre systems, was held March 5-6, 2001, in Honolulu, U.S.A. The participants are listed in BASS Endnote 1. Objectives of the workshop were to:

1. Synthesize all trophic level data in a common format;
2. Examine trophic relationships in both the Eastern Subarctic Gyre (ESA) and Western Subarctic Gyre (WSA) using ECOPATH/ECOSIM; and
3. Examine methods of incorporating the PICES NEMURO lower trophic level model into the analysis.

Overview of ECOPATH/ECOSIM

Kerim Aydin gave a brief overview of ECOPATH/ECOSIM. An ECOPATH model creates a quantitative food web using the principle of mass-balance. Each "box" in an ECOPATH model may represent a single species or a species guild. The units may vary from model to model. The following quantities were used as input for the initial ESA and WSA models:

- Biomass (t/km^2)
- Production per unit biomass ($year^{-1}$)
- Consumption per unit biomass ($year^{-1}$)
- Fisheries catch ($t/km^2/year$)
- Diet matrix for each predator (% of diet by weight, shown here as trophic level)

From this information, ECOPATH calculates an "Ecotrophic Efficiency" for each box, which represents the ratio between the production of each box and the amount of biomass "demanded" by the predators and fisheries on a box. An Ecotrophic Efficiency greater than 1 indicates that, according to the model, more is being demanded of a box than is being produced. This quantity is a useful diagnostic tool for examining the quality of data between boxes.

The inputs used for each box in the ESA and WSA models are shown in Tables 1 and 2. No fishing was included in the model as befits the subarctic North Pacific in the early 1990s. These values represent the model as it existed at the end of the workshop and incorporate adjustments made over the course of the workshop. This model was "mass-balanced" in that all Ecotrophic Efficiency values were less than 1.

Data quality was categorized as follows (Tables 1 and 2):

- Acceptable: generally considered to be "reasonable" estimates for model use
- General: consistent with known patterns for the species in question, but may be improved through re-examination of existing data, or further consultation with other researchers
- Poor: little information for these species, or the information available to the workshop was known to be potentially inaccurate (collected outside the model domain)
- N/A: no data available: estimates were derived from ECOPATH model

There is considerable room for improving the estimates, and every attempt should be made to upgrade most of the estimates from "General" to "Acceptable" before the model is considered "functional". It was felt that much improvement in data quality could be accomplished by re-reviewing existing data using this preliminary model as a framework. Final data quality is a combination of two properties: the quality of each datum, and the sensitivity of the model to that input.

Overview of NEMURO

Bernard Megrey gave a brief review of the NEMURO lower trophic level model focusing on recent improvement to NEMURO. Topics included the addition of diagnostic calculations, validation to Station P data, addition of

Table 1 ECOPATH biomass estimates used in eastern/western subarctic gyre models.

Group	Eastern Gyre t	Eastern Gyre t/km^2	Western Gyre t	Western Gyre t/km^2	Data Quality
Sperm whales	3,364	0.000929	2,014	0.000929	Acceptable
Toothed whales (orca)	100	0.000028	2,168	0.001000	General
Fin	100,992	0.027883	60,450	0.027883	Poor
Sei	21,379	0.005902	12,796	0.005902	Not. Avail.
Minke	-	-	2,168	0.001000	
Northern fur seals	890	0.000246	533	0.000246	
Elephant seals	1,558	0.000430	-	-	
Dall's porpoise	21,683	0.005986	12,978	0.005986	
Pacific white sided dolphin	14,352	0.003962	8,591	0.003962	
Northern right whale dolphin	14,116	0.003897	8,449	0.003897	
Common dolphin	-	-	2,168	0.001000	
Albatross	143	0.000040	3,361	0.001550	
Shearwaters	1,449	0.000400	2,681	0.001237	
Storm Petrels	203	0.000056	340	0.000157	
Kittiwakes	189	0.000052	249	0.000115	
Fulmars	269	0.000074	328	0.000151	
Puffins	209	0.000058	698	0.000322	
Skuas	195	0.000054	174	0.000080	
Jaegers	137	0.000038	132	0.000061	
Sharks (Blue & Salmon)	181,100	0.050000	53,550	0.024700	
Dogfish	181,100	0.050000	53,550	0.024700	
Daggertooth	18,110	0.005000	2,003	0.000924	
Large gonatid squid	108,660	0.030000	102,330	0.047200	
Clubhook squid	43,464	0.012000	160,432	0.074000	
Flying squid	1,629,900	0.450000	47,696	0.022000	
Sockeye	324,733	0.089656	6,721	0.003100	
Chum	196,080	0.054136	32,954	0.015200	
Pink	84,272	0.023267	427,746	0.197300	
Coho	16,131	0.004453	12,574	0.005800	
Chinook	33,696	0.009303	8,455	0.003900	
Steelhead	33,696	0.009303	8,455	0.003900	
Pomfret	760,620	0.210000	115,121	0.053100	
Saury	1,629,900	0.450000	102,546	0.047300	
Japanese anchovy	-	-	381,250	0.175853	
Pacific sardine	-	-	37,207	0.017162	
Misc. Forage (Stickleback)	3,763,258	1.039000	897,552	0.414000	
Micronektonic squid	3,462,632	0.956000	1,903,504	0.878000	
Mesopelagic fish	16,299,000	4.500000	14,092,000	6.500000	
Lg. Jellyfish	14,488,000	4.000000	1,017,264	0.469217	
Ctenophores	32,960,200	9.100000	21,680,000	10.000000	
Salps	28,976,000	8.000000	21,680,000	10.000000	
Chaetognaths	23,905,200	6.600000	115,737,135	53.384287	
Sergestid shrimp	18,110,000	5.000000	17,634,512	8.134000	
Oth. Lg. Zoop. (Larv., Poly)	18,359,194	5.068800	17,634,512	8.134000	
Amphipods (most. Hyp)	36,718,387	10.137600	18,449,680	8.510000	
Pteropods	36,718,387	10.137600	35,269,024	16.268000	
Euphausiids	91,795,968	25.344000	88,172,560	40.670000	
Copepods	126,219,456	34.848000	101,267,280	46.710000	
Microzooplankton	126,219,456	34.848000	49,232,701	22.708810	
Bacteria	75,880,000	35.000000	355,601,864	164.023000	
Large phytoplankton	252,453,400	69.700000	148,386,592	68.444000	
Small phytoplankton	275,272,000	76.000000	187,694,600	86.575000	
DNH3	-	-	-	-	
DNO3	-	-	-	-	
PON	-	-	-	-	

Table 2 Life history and diet parameters of eastern and western subarctic gyre ECOPATH Models.

Group	Prod./Bio. ($year^{-1}$)	Cons./Bio. ($year^{-1}$)	Trophic Level East	Trophic Level West	Data Quality
Sperm whales	0.060	6.608	5.4	5.4	Acceptable
Toothed whales (orca)	0.025	11.157	5.3	5.3	General
Fin	0.020	4.562	4.1	4.3	Poor
Sei	0.020	6.152	4.1	4.3	Not. Avail.
Minke	0.020	7.782	-	4.4	
Northern fur seals	0.235	39.030	5.2	5.2	
Elephant seals	0.368	11.078	5.2	-	
Dall's porpoise	0.100	27.471	5.3	5.2	
Pacific white sided dolphin	0.140	25.828	5.2	5.2	
Northern right whale dolphin	0.160	24.138	5.3	5.2	
Common dolphin	0.100	24.983	-	5.2	
Albatross	0.050	81.586	5.9	5.5	
Shearwaters	0.100	100.127	4.7	4.8	
Storm Petrels	0.100	152.083	4.6	4.7	
Kittiwakes	0.100	123.000	4.6	4.7	
Fulmars	0.100	100.256	4.9	5.1	
Puffins	0.100	104.333	4.7	4.8	
Skuas	0.075	96.600	4.8	4.9	
Jaegers	0.075	96.600	4.8	4.9	
Sharks (Blue & Salmon)	0.200	10.950	5.4	5.3	
Dogfish	0.200	10.950	4.9	5.0	
Daggertooth	1.000	10.000	5.0	5.0	
Large gonatid squid	2.555	7.300	4.2	4.4	
Clubhook squid	2.555	7.300	4.9	5.1	
Flying squid	2.555	6.205	5.3	5.1	
Sockeye	1.265	10.132	4.3	4.4	
Chum	1.932	14.507	3.7	3.9	
Pink	3.373	18.494	4.2	4.1	
Coho	2.472	16.548	4.9	4.8	
Chinook	0.800	5.333	4.9	4.9	
Steelhead	0.800	5.333	4.9	4.8	
Pomfret	0.750	3.750	4.8	5.0	
Saury	1.600	7.900	3.8	3.5	
Japanese anchovy	1.500	5.000	-	3.8	
Pacific sardine	0.400	3.000	-	3.2	
Misc. Forage (Stickleback)	1.500	5.000	3.9	4.1	
Micronektonic squid	3.000	15.000	3.9	4.1	
Mesopelagic fish	0.900	3.000	3.9	3.9	
Lg. Jellyfish	3.000	10.000	3.6	3.7	
Ctenophores	4.000	110.000	2.7	2.7	
Salps	9.000	30.000	2.7	2.7	
Chaetognaths	2.555	12.045	3.5	3.5	
Sergestid shrimp	2.555	12.045	3.5	3.5	
Oth. Lg. Zoop. (Larv., Poly)	2.555	12.045	3.5	3.5	
Amphipods (most. Hyp)	2.555	12.045	3.1	3.1	
Pteropods	2.555	12.045	3.1	3.1	
Euphausiids	2.555	12.045	3.1	3.1	
Copepods	23.725	112.420	2.4	2.4	
Microzooplankton	48.910	233.235	2.3	2.3	
Bacteria	18.450	25.000	2.0	2.0	
Large phytoplankton	42.340	-	1.0	1.0	
Small phytoplankton	129.575	-	1.0	1.0	
DNH3	-	-	1.0	1.0	
DNO3	-	-	1.0	1.0	
PON	-	-	1.0	1.0	

zooplankton vertical migration, examining the effects of including a microbial loop approximation, and performing a sensitivity analysis and data assimilation

Diagnostic calculations

In order to perform regional comparisons of model performance, several diagnostic calculations were added to NEMURO. These included Production/ Biomass (P/B) ratios for phytoplankton and zooplankton, Food Consumption/Biomass (C/B) ratios for small, large and predatory zooplankton, and Ecotrophic Efficiency (a measure of how much primary production transfers up the food web to the zooplankton species and ultimately to higher trophic level species) calculations.

Comparison of model output and field measurements

NEMURO was parameterized for Ocean Station P and output was compared to data collected from that site. Results were favourable. The C/B and P/C ratios are both reasonable. Annual primary production from the model (149 $gC/m^2/yr$) is only 6% higher than the best current estimate (140 $gC/m^2/yr$). An f-ratio (assuming that the production of the large phytoplankton is primarily fuelled by "new" nitrogen was 0.23.

Vertical migration

At Station P, during spring, the large zooplankton component (ZP) should be dominated by *Calanus/Neocalanus* spp. which undergo a strong ontogenetic vertical migration. Thus, the model population should increase in biomass in the early spring independently of food availability/grazing. Later in the year, the population should decrease by some amount to simulate the descent of the large zooplankton to deeper depths. NEMURO was modified to reflect this situation.

Results without migration of predatory zooplankton (ZP) show a large diatom bloom around day 73. The prevailing view is that there is no spring bloom at Station P. Thus the bloom is an artifact of the "box" nature of the model. With ZP migration, values of PL drop by a factor of 2 and generate more reasonable diagnostics. The estimates of Ecotropic Efficiency are not significantly affected.

Microbial loop approximation

Climate change patterns that produce warmer water and greater rainfall enhance stratification of the water column. This lowers primary production by reducing or eliminating the mixing that is needed to propel nutrients into the surface photic zone. Data from Ocean Station P show decreased nitrogen and reduced primary production with warmer temperatures over a period of about 25 years. These conditions change the quantity of phytoplankton as well as the phytoplankton assemblage. With high nutrient concentrations, large phytoplankton that are eaten by copepods dominate the phytoplankton assemblage (i.e. the pelagic food chain). This energy is transferred to larval and adult planktivorous fishes. With low nutrient concentrations, the phytoplankton assemblage is altered, with the microbial loop food chain being favoured over the pelagic food chain. Small nanoplankton are favoured, which are eaten by protozoans like rotifers, with secondary production generally becoming unavailable to fish.

A pragmatic approach to including the microbial food web is through the variable BetaZS (growth efficiency of Small Zooplankton, ZS)

$$BetaZS = 0.3\ (1+ PhySn/(PhySn+PhyLn))$$

This means that the gross growth efficiency of the small zooplankton can vary between 0.3 and 0.09, and will probably average about 0.16 over the year at Station P. For the base model run, a constant BetaZS=0.3 was used.

Including a microbial loop had only a small impact on the standing stocks of small and large zooplankton. Predatory zooplankton were reduced by about one half reducing potentially available biomass for fish production. These differences are due to the decreased net trophic efficiency of the system, which results when a large portion of the primary production passes through a microbial community before entering the zooplankton community.

Sensitivity analysis

A Monte Carlo analysis of the WSA with 600 replications randomly varied the input parameters and initial values by ±10% using a uniform error distribution. Principal component analysis (PCA) reduced the 600 sets of output of biological parameters and initial values. The PCA indicated that four factors explained 22% of variance in the data. The first principal component, was clearly related to photosynthesis of PL. It accounted for 10% of variance and was correlated with the variables VmaxS, VmaxL, and PL, $N0_3$, NH_4. The second principal component was related to the zooplankton state variables, ZL and ZS.

Based on the sensitivity analysis, the parameters selected to estimate from the observed data were V_{maxS}, V_{maxL}, λ_P, MorZP0 and VD2N0. Data from the A-line (off Hokkaido, Japan - outside the Oyashio region) was used with a conjugate gradient method to calculate the local minimum of the cost function, which is defined as the squared differences between observed and simulated data. After estimating these parameters, the time-dependent features of each compartment of the NEMURO/FORTRAN Box model were calculated.

The boundary areas selected for the two ECOPATH models coincide with PICES' definitions of the Western Subarctic (WSA) and the Eastern Subarctic (ESA), namely the regions above 45°N, bounded by the shelf breaks and divided by 165°W. The total areas for the WSA and the ESA are 2 168 000 km^2 and 3 622 000 km^2 respectively.

BASS Endnote 1

Participation List

Canada
- Richard J. Beamish
- Jacqueline R. King
- Gordon A. McFarlane
- Daniel M. Ware

China
- Qi-Sheng Tang

Japan
- Makoto Kashiwai
- Michio J. Kishi
- Hiroyuki Sakano
- Lan Smith
- Akihiko Yatsu

Russia
- Andrei S. Krovnin

U.S.A.
- Kerim Y. Aydin
- Bernard A. Megrey
- Jeffrey J. Polovina